

N66 29082

(ACCESSION NUMBER)

247

(PAGES)

CR-54963

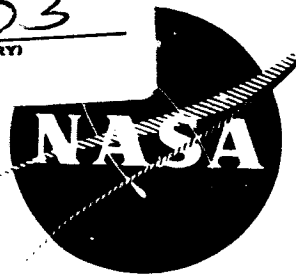
(NASA CR OR TMX OR AD NUMBER)

(THRU)

(CODE)

03

(CATEGORY)



Report No.

NASA-CR-54963

Westinghouse

WAED 66.13E**PART. 1****IMPROVED MAGNETIC COMPONENTS
FOR STATIC INVERTERS AND CONVERTERS****CONTRACT NO. NAS 3-2792****AMENDMENT NO. 2****EIGHTH QUARTERLY REPORT FOR THE PERIOD
MARCH 31, 1965 TO AUGUST 31, 1965**

by

R. E. McVay et al**PREPARED FOR THE NATIONAL AERONAUTICS AND SPACE ADMINISTRATION****Technical Management, NASA-Lewis Research Center
Space Power Systems Division, Francis Gourash****Westinghouse Electric Corporation
AEROSPACE ELECTRICAL DIVISION
LIMA, OHIO**

GPO PRICE \$

CFSTI PRICE(S) \$

Hard copy (HC) **6.00**Microfiche (MF) **1.50**

PART 1

IMPROVED MAGNETIC COMPONENTS

FOR

STATIC INVERTERS AND CONVERTERS

NAS 3-2792, Amendment 2

Prepared by R. E. McVay, Project Engineer

Approved by:



R. M. Frost
Project Manager



N. W. Bucci, Jr.
Engineering Manager
Systems Research & Development

WESTINGHOUSE ELECTRIC CORPORATION
AEROSPACE ELECTRICAL DIVISION
LIMA, OHIO

PREFACE

The following Westinghouse AED personnel have supported this program.
Their cooperation is gratefully acknowledged.

O. E. Watkins

N. K. Harpster

ABSTRACT

29082

All of the sine current screening CCFR and sine flux screening core loss tests have been completed. The square wave CCFR tests at 400, 800, 1600, and 3200 cps have been completed.

The square wave a-c core loss and apparent power at 400, 800, 1600, and 3200 cps, on all the materials at room ambient temperature and -55°C have been obtained. The magnetic test results are shown in tables and curves.

The CCFR calibration traces and test pictures are shown.

The materials tested were Supermendur (magnetic field annealed), Cubex (regular and magnetic field annealed), Magnesil, Orthosil, Hy-Ra-80, Square Permalloy 80, Hipernik V, and Square Orthonol.

Author

TABLE OF CONTENTS

<u>Section</u>	<u>Page</u>
List of Figures	v
List of Tables	xvii
I INTRODUCTION	1
II MATERIAL TEST RESULTS AND DISCUSSION	2
III CORE DESCRIPTIONS	5
IV TESTING PROCEDURES	6
V GENERAL PROGRESS AND PLANS FOR FUTURE WORK	8
VI APPENDIX A- SYMBOLS AND DEFINITIONS	169
PART I	
A. Symbols Used in Magnetic Testing	170
B. Definitions of Terms Used in Magnetic Testing....	171
PART II	
A. Symbols Used in CCFR Testing of Toroidal Mag- netic Amplifier Cores	173
B. Definitions Used in CCFR Testing of Toroidal Mag- netic Amplifier Cores	174
PART III	
General Definition of Terms	176

LIST OF FIGURES

<u>Figure</u>	<u>Title</u>	<u>Page</u>
1	Calibration Traces and CCFR Test Pictures for Core..... No. 14 of 0.002 Inch Hipernik V Tape Wound Cores in Core .. Boxes at Room Ambient Temperature	16
2	Calibration Traces and CCFR Test Pictures for Core No 23 of 0.002 Inch Hy-Ra 80 Tape Wound Cores in Core Boxes .. at Room Ambient Temperature	17
3	Calibration Traces and CCFR Test Pictures for Core No..... 28 of 0.002 Inch Magnesil Tape Wound Cores in Core Boxes.. at Room Ambient Temperature	18
4	Calibration Traces and CCFR Test Pictures for Core No..... 32 of 0.002 Inch Supermendur Tape Wound Cores in Core Boxes at Room Ambient Temperature	19
5	Calibration Traces and CCFR Test Pictures for Core No 74 of 0.002 Inch Cubex Tape Wound Cores, Magnetic Field .. Annealed, in Core Boxes at Room Ambient Temperature	20
6	Calibration Traces and CCFR Test Pictures for Core No 80 of 0.002 Inch Cubex Tape Wound Cores in Core Boxes at Room Ambient Temperature	21
7	Tape Wound Cores Damaged by Failure of Aluminum Ortho-... phosphate During Stress Relief Annealing at Magnetics, Inc...	22
8	Rowland Ring Lamination Drawing	23
9	Cubex Double Window Lamination Drawing.....	24
10	P_c, sq - Total Core Loss, 0.002 Inch Cubex Toroid, Core .. 74, Magnetic Field Annealed, Room Ambient.....	25
11	P_a, sq - Apparent Power, 0.002 Inch Cubex Toroid, Core .. 74, Magnetic Field Annealed, Room Ambient	26

LIST OF FIGURES (Cont'd)

<u>Figure</u>	<u>Title</u>	<u>Page</u>
12	P _C , sq - Total Core Loss, 0.002 Inch Cubex Toroid, Core .. 74, Magnetic Field Annealed, -55°C	27
13	P _a , sq - Apparent Power, 0.002 Inch Cubex Toroid, Core .. 74, Magnetic Field Annealed, -55°C	28
14	P _C , sq - Total Core Loss, 0.002 Inch Cubex Toroid, Core .. 75, Magnetic Field Annealed, Room Ambient	29
15	P _a , sq - Apparent Power, 0.002 Inch Cubex Toroid, Core .. 75, Magnetic Field Annealed, Room Ambient	30
16	P _C , sq - Total Core Loss, 0.002 Inch Cubex Toroid, Core .. 75, Magnetic Field Annealed, -55°C	31
17	P _a , sq - Apparent Power 0.002 Inch Cubex Toroid, Core.... 75, Magnetic Field Annealed, -55°C	32
18	P _C , sq - Total Core Loss, 0.002 Inch Cubex Toroid, Core .. 76, Magnetic Field Annealed, Room Ambient	33
19	P _a , sq - Apparent Power, 0.002 Inch Cubex Toroid, Core .. 76, Magnetic Field Annealed, Room Ambient	34
20	P _C , sq - Total Core Loss, 0.002 Inch Cubex Toroid, Core .. 76, Magnetic Field Annealed, -55°C	35
21	P _a , sq - Apparent Power, 0.002 Inch Cubex Toroid, Core .. 76, Magnetic Field Annealed, -55°C	36
22	P _C , sq - Total Core Loss, 0.002 Inch Cubex Toroid, Core .. 79, Stress Relief Annealed, Room Ambient	37
23	P _a , sq - Apparent Power, 0.002 Inch Cubex Toroid, Core .. 79, Stress Relief Annealed, Room Ambient	38

LIST OF FIGURES (Cont'd)

<u>Figure</u>	<u>Title</u>	<u>Page</u>
24	$P_{C, sq}$ - Total Core Loss, 0.002 Inch Cubex Toroid, Core .. 79, Stress Relief Annealed, -55°C	39
25	$P_{a, sq}$ - Apparent Power, 0.002 Inch Cubex Toroid, Core .. 79, Stress Relief Annealed, -55°C	40
26	$P_{C, sq}$ - Total Core Loss 0.002 Inch Cubex Toroid, Core .. 80, Stress Relief Annealed, Room Ambient	41
27	$P_{a, sq}$ - Apparent Power, 0.002 Inch Cubex Toroid, Core .. 80, Stress Relief Annealed, Room Ambient	42
28	$P_{C, sq}$ - Total Core Loss, 0.002 Inch Cubex Toroid, Core .. 80, Stress Relief Annealed, -55°C	43
29	$P_{a, sq}$ - Apparent Power, 0.002 Inch Cubex Toroid, Core .. 80, Stress Relief Annealed, -55°C	44
30	$P_{C, sq}$ - Total Core Loss, 0.002 Inch Cubex Toroid, Core .. 81, Stress Relief Annealed, Room Ambient	45
31	$P_{a, sq}$ - Apparent Power, 0.002 Inch Cubex Toroid, Core .. 81, Stress Relief Annealed, Room Ambient	46
32	$P_{C, sq}$ - Total Core Loss, 0.002 Inch Cubex Toroid, Core .. 81, Stress Relief Annealed, -55°C	47
33	$P_{a, sq}$ - Apparent Power, 0.002 Inch Cubex Toroid, Core .. 81, Stress Relief Annealed, -55°C	48
34	$P_{C, sq}$ - Total Core Loss, 0.006 Inch Cubex Double Window Core 1, Magnetic Field Annealed, Room Ambient	49
35	$P_{a, sq}$ - Apparent Power, 0.006 Inch Cubex Double Window Core 1, Magnetic Field Annealed, Room Ambient.....	50
36	$P_{C, sq}$ - Total Core Loss, 0.006 Inch Cubex Double Window Core 1, Magnetic Field Annealed, -55°C	51

LIST OF FIGURES (Cont'd)

<u>Figure</u>	<u>Title</u>	<u>Page</u>
37	P_a, sq - Apparent Power, 0.006 Inch Cubex Double Window Core 1, Magnetic Field Annealed, $-55^{\circ}C$	52
38	P_c, sq - Total Core Loss, 0.006 Inch Cubex Double Window Core 3, Magnetic Field Annealed, Room Ambient	53
39	P_a, sq - Apparent Power, 0.006 Inch Cubex Double Window Core 3, Magnetic Field Annealed, Room Ambient	54
40	P_c, sq - Total Core Loss, 0.006 Inch Cubex Double Window Core 3, Magnetic Field Annealed, $-55^{\circ}C$	55
41	P_a, sq - Apparent Power, 0.006 Inch Cubex Double Window Core 3, Magnetic Field Annealed, $-55^{\circ}C$	56
42	P_c, sq - Total Core Loss, 0.006 Inch Cubex Double Window Core 4, Stress Relief Annealed, Room Ambient	57
43	P_a, sq - Apparent Power, 0.006 Inch Cubex Double Window Core 4, Stress Relief Annealed, Room Ambient	58
44	P_c, sq - Total Core Loss, 0.006 Inch Cubex Double Window Core 4, Stress Relief Annealed, $-55^{\circ}C$	59
45	P_a, sq - Apparent Power, 0.006 Inch Cubex Double Window Core 4, Stress Relief Annealed, $-55^{\circ}C$	60
46	P_c, sq - Total Core Loss 0.006 Inch Cubex Double Window Core 6, Stress Relief Annealed, Room Ambient	61
47	P_a, sq - Apparent Power, 0.006 Inch Cubex Double Window Core 6, Stress Relief Annealed, Room Ambient	62
48	P_c, sq - Total Core Loss, 0.006 Inch Cubex Double Window Core 6, Stress Relief Annealed, $-55^{\circ}C$	63
49	P_a, sq - Apparent Power, 0.006 Inch Cubex Double Window Core 6, Stress Relief Annealed, $-55^{\circ}C$	64

LIST OF FIGURES (Cont'd)

<u>Figure</u>	<u>Title</u>	<u>Page</u>
50	P_c, sq - Total Core Loss, 0.002 Inch Orthonol Toroid, Core 7, Room Ambient	65
51	P_a, sq - Apparent Power, 0.002 Inch Orthonol Toroid Core 7, Room Ambient	66
52	P_c, sq - Total Core Loss, 0.002 Inch Orthonol Toroid Core 7, -55°C	67
53	P_a, sq - Apparent Power, 0.002 Inch Orthonol Toroid Core 7, -55°C	68
54	P_c, sq - Total Core Loss, 0.002 Inch Orthonol Toroid Core 9, Room Ambient	69
55	P_a, sq - Apparent Power, 0.002 Inch Orthonol Toroid..... Core 9, Room Ambient	70
56	P_c, sq - Total Core Loss, 0.002 Inch Orthonol Toroid Core 9, -55°C	71
57	P_a, sq - Apparent Power, 0.002 Inch Orthonol Toroid Core 9, -55°C	72
58	P_c, sq - Total Core Loss, 0.004 Inch Orthonol Toroid Core 11, Room Ambient	73
59	P_a, sq - Apparent Power, 0.004 Inch Orthonol Toroid Core 11, Room Ambient	74
60	P_c, sq - Total Core Loss, 0.004 Inch Orthonol Toroid Core 11, -55°C.....	75
61	P_a, sq - Apparent Power, 0.004 Inch Orthonol Toroid Core 11, -55°C.....	76
62	P_c, sq - Total Core Loss, 0.004 Inch Orthonol Toroid Core 12, Room Ambient	77

LIST OF FIGURES (Cont'd)

<u>Figure</u>	<u>Title</u>	<u>Page</u>
63	P_a, sq - Apparent Power, 0.004 Inch Orthonol Toroid, ... Core 12, Room Ambient	78
64	P_c, sq - Total Core Loss, 0.004 Inch Orthonol Toroid, ... Core 12, -55°C	79
65	P_a, sq - Apparent Power, 0.004 Inch Orthonol Toroid, ... Core 12, -55°C	80
66	P_c, sq - Total Core Loss, 0.002 Inch Hipernik V Toroid, .. Core 14, Room Ambient	81
67	P_a, sq - Apparent Power, 0.002 Inch Hipernik V Toroid, .. Core 14, Room Ambient	82
68	P_c, sq - Total Core Loss 0.002 Inch Hipernik V Toroid, .. Core 14, -55°C	83
69	P_a, sq - Apparent Power, 0.002 Inch Hipernik V Toroid, .. Core 14, -55°C	84
70	P_c, sq - Total Core Loss, 0.002 Inch Hipernik V Toroid, .. Core 15, Room Ambient	85
71	P_a, sq - Apparent Power, 0.002 Inch Hipernik V Toroid, .. Core 15, Room Ambient	86
72	P_c, sq - Total Core Loss, 0.002 Inch Hipernik V Toroid, .. Core 15, -55°C	87
73	P_a, sq - Apparent Power, 0.002 Inch Hipernik V Toroid, .. Core 15, -55°C	88
74	P_c, sq - Total Core Loss, 0.004 Inch Hipernik V Toroid, .. Core 17, Room Ambient	89
75	P_a, sq - Apparent Power, 0.004 Inch Hipernik V Toroid, .. Core 17, Room Ambient	90

LIST OF FIGURES (Cont'd)

<u>Figure</u>	<u>Title</u>	<u>Page</u>
76	$P_{c, sq}$ - Total Core Loss, 0.004 Inch Hipernik V Toroid, . Core 17, -55°C	91
77	$P_{a, sq}$ - Apparent Power, 0.004 Inch Hipernik V Toroid, . Core 17, -55°C	92
78	$P_{c, sq}$ - Total Core Loss, 0.004 Inch Hipernik V Toroid, . Core 18, Room Ambient	93
79	$P_{a, sq}$ - Apparent Power, 0.004 Inch Hipernik V Toroid, . Core 18, Room Ambient	94
80	$P_{c, sq}$ - Total Core Loss, 0.004 Inch Hipernik V Toroid, . Core 18, -55°C	95
81	$P_{a, sq}$ - Apparent Power, 0.004 Inch Hipernik V Toroid, . Core 18, -55°C	96
82	$P_{c, sq}$ - Total Core Loss, 0.002 Inch Magnesil Toroid, .. Core 28, Room Ambient	97
83	$P_{a, sq}$ - Apparent Power, 0.002 Inch Magnesil Toroid, .. Core 28, Room Ambient	98
84	$P_{c, sq}$ - Total Core Loss, 0.002 Inch Magnesil Toroid, .. Core 28, -55°C	99
85	$P_{a, sq}$ - Apparent Power, 0.002 Inch Magnesil Toroid, .. Core 28, -55°C	100
86	$P_{c, sq}$ - Total Core Loss, 0.002 Inch Magnesil Toroid, .. Core 30, Room Ambient	101
87	$P_{a, sq}$ - Apparent Power, 0.002 Inch Magnesil Toroid, .. Core 30, Room Ambient	102
88	$P_{c, sq}$ - Total Core Loss, 0.002 Inch Magnesil Toroid, .. Core 30, -55°C	103

LIST OF FIGURES (Cont'd)

<u>Figure</u>	<u>Title</u>	<u>Page</u>
89	P_a, sq - Apparent Power, 0.002 Inch Magnesil Toroid, ... Core 30, -55°C	104
90	P_c, sq - Total Core Loss, 0.004 Inch Magnesil Toroid, ... Core 26, Room Ambient	105
91	P_a, sq - Apparent Power, 0.004 Inch Magnesil Toroid, ... Core 26, Room Ambient	106
92	P_c, sq - Total Core Loss, 0.004 Inch Magnesil Toroid, ... Core 26, -55°C	107
93	P_a, sq - Apparent Power, 0.004 Inch Magnesil Toroid, ... Core 26, -55°C	108
94	P_c, sq - Total Core Loss, 0.004 Inch Magnesil Toroid, ... Core 27, Room Ambient	109
95	P_a, sq - Apparent Power, 0.004 Inch Magnesil Toroid, ... Core 27, Room Ambient	110
96	P_c, sq - Total Core Loss, 0.004 Inch Magnesil Toroid, ... Core 27, -55°C	111
97	P_a, sq - Apparent Power, 0.004 Inch Magnesil Toroid, ... Core 27, -55°C	112
98	P_c, sq - Total Core Loss, 0.002 Inch Supermendur Toroid, Core 12, Magnetic Field Annealed, Room Ambient	113
99	P_a, sq - Apparent Power, 0.002 Inch Supermendur Toroid, Core 32, Magnetic Field Annealed, Room Ambient	114
100	P_c, sq - Total Core Loss, 0.002 Inch Supermendur Toroid, Core 32, Magnetic Field Annealed, -55°C	115
101	P_a, sq - Apparent Power, 0.002 Inch Supermendur Toroid, Core 32, Magnetic Field Annealed, -55°C	116

LIST OF FIGURES (Cont'd)

<u>Figure</u>	<u>Title</u>	<u>Page</u>
102	$P_{c, sq}$ - Total Core Loss, 0.002 Inch Supermendur Toroid, Core 33, Magnetic Field Annealed, Room Ambient	117
103	$P_{a, sq}$ - Apparent Power, 0.002 Inch Supermendur Toroid, Core 33, Magnetic Field Annealed, Room Ambient	118
104	$P_{c, sq}$ - Total Core Loss, 0.002 Inch Supermendur Toroid, Core 33, Magnetic Field Annealed, -55°C	119
105	$P_{a, sq}$ - Apparent Power, 0.002 Inch Supermendur Toroid, Core 33, Magnetic Field Annealed, -55°C	120
106	$P_{c, sq}$ - Total Core Loss, 0.002 Inch Supermendur Toroid, Core 34, Magnetic Field Annealed, Room Ambient	121
107	$P_{a, sq}$ - Apparent Power, 0.002 Inch Supermendur Toroid, Core 34, Magnetic Field Annealed, Room Ambient	122
108	$P_{c, sq}$ - Total Core Loss, 0.002 Inch Supermendur Toroid, Core 34, Magnetic Field Annealed, -55°C	123
109	$P_{a, sq}$ - Apparent Power, 0.002 Inch Supermendur Toroid, Core 34, Magnetic Field Annealed, -55°C	124
110	$P_{c, sq}$ - Total Core Loss, 0.004 Inch Supermendur Toroid, Ring Core 35, Magnetic Field Annealed, Room Ambient ...	125
111	$P_{a, sq}$ - Apparent Power, 0.004 Inch Supermendur Rowland Ring, Core 35, Magnetic Field Annealed, Room Ambient ...	126
112	$P_{c, sq}$ - Total Core Loss, 0.004 Inch Supermendur Rowland Ring, Core 35, Magnetic Field Annealed, -55°C	127
113	$P_{a, sq}$ - Apparent Power, 0.004 Inch Supermendur Rowland Ring, Core 35, Magnetic Field Annealed, -55°C	128
114	$P_{c, sq}$ - Total Core Loss, 0.004 Inch Supermendur Rowland Ring, Core 36, Magnetic Field Annealed, Room Ambient ...	129

LIST OF FIGURES (Cont'd)

<u>Figure</u>	<u>Title</u>	<u>Page</u>
115	P_a, sq - Apparent Power, 0.004 Inch Supermendur Rowland Ring, Core 36, Magnetic Field Annealed, Room Ambient ...	130
116	P_c, sq - Total Core Loss, 0.004 Inch Supermendur Rowland Ring, Core 36, Magnetic Field Annealed, -55°C	131
117	P_a, sq - Apparent Power, 0.004 Inch Supermendur Rowland Ring, Core 36, Magnetic Field Annealed, -55°C	132
118	P_c, sq - Total Core Loss, 0.004 Inch Supermendur Rowland Ring, Core 37, Magnetic Field Annealed, Room Ambient ...	133
119	P_a, sq - Apparent Power, 0.004 Inch Supermendur Rowland Ring, Core 37, Magnetic Field Annealed, Room Ambient ...	134
120	P_c, sq - Total Core Loss, 0.004 Inch Supermendur Rowland Ring, Core 37, Magnetic Field Annealed, -55°C	135
121	P_a, sq - Apparent Power, 0.004 Inch Supermendur Rowland Ring, Core 37, Magnetic Field Annealed, -55°C	136
122	P_c, sq - Total Core Loss, 0.002 Inch Hy-Ra 80 Toroid, ... Core 23, Room Ambient	137
123	P_a, sq - Apparent Power, 0.002 Inch Hy-Ra 80 Toroid, ... Core 23, Room Ambient	138
124	P_c, sq - Total Core Loss, 0.002 Inch Hy-Ra 80 Toroid, ... Core 23, -55°C	139
125	P_a, sq - Apparent Power, 0.002 Inch Hy-Ra 80 Toroid, ... Core 23, -55°C	140
126	P_c, sq - Total Core Loss, 0.002 Inch Hy-Ra 80 Toroid, ... Core 24, Room Ambient	141
127	P_a, sq - Apparent Power, 0.002 Inch Hy-Ra 80 Toroid, ... Core 24, Room Ambient	142

LIST OF FIGURES (Cont'd)

<u>Figure</u>	<u>Title</u>	<u>Page</u>
128	$P_{c, sq}$ - Total Core Loss, 0.002 Inch Hy-Ra 80 Toroid, ... Core 24, -55°C	143
129	$P_{a, sq}$ - Apparent Power, 0.002 Inch Hy-Ra 80 Toroid, ... Core 24, -55°C	144
130	$P_{c, sq}$ - Total Core Loss, 0.004 Inch Hy-Ra 80 Toroid, ... Core 19, Room Ambient	145
131	$P_{a, sq}$ - Apparent Power, 0.004 Inch Hy-Ra 80 Toroid, ... Core 19, Room Ambient	146
132	$P_{c, sq}$ - Total Core Loss, 0.004 Inch Hy-Ra 80 Toroid, ... Core 19, -55°C	147
133	$P_{a, sq}$ - Apparent Power, 0.004 Inch Hy-Ra 80 Toroid, ... Core 19, -55°C	148
134	$P_{c, sq}$ - Total Core Loss, 0.004 Inch Hy-Ra 80 Toroid, ... Core 20, Room Ambient	149
135	$P_{a, sq}$ - Apparent Power, 0.004 Inch Hy-Ra 80 Toroid, ... Core 20, Room Ambient	150
136	$P_{c, sq}$ - Total Core Loss, 0.004 Inch Hy-Ra 80 Toroid, ... Core 20, -55°C	151
137	$P_{a, sq}$ - Apparent Power, 0.004 Inch Hy-Ra 80 Toroid, ... Core 20, -55°C	152
138	$P_{c, sq}$ - Total Core Loss, 0.002 Inch Permalloy 80 Toroid, Core 2, Room Ambient	153
139	$P_{a, sq}$ - Apparent Power, 0.002 Inch Permalloy 80 Toroid, Core 2, Room Ambient	154
140	$P_{c, sq}$ - Total Core Loss, 0.002 Inch Permalloy 80 Toroid, Core 2, -55°C	155

LIST OF FIGURES (Cont'd)

<u>Figure</u>	<u>Title</u>	<u>Page</u>
141	$P_{a, sq}$ - Apparent Power, 0.002 Inch Permalloy 80 Toroid, Core 2, -55°C	156
142	$P_{c, sq}$ - Total Core Loss, 0.002 Inch Permalloy 80 Toroid, Core 3, Room Ambient	157
143	$P_{a, sq}$ - Apparent Power, 0.002 Inch Permalloy 80 Toroid, Core 3, Room Ambient	158
144	$P_{c, sq}$ - Total Core Loss, 0.002 Inch Permalloy 80 Toroid, Core 3, -55°C	159
145	$P_{a, sq}$ - Apparent Power, 0.002 Inch Permalloy 80 Toroid, Core 3, -55°C	160
146	$P_{c, sq}$ - Total Core Loss, 0.004 Inch Permalloy 80 Toroid, Core 5, Room Ambient	161
147	$P_{a, sq}$ - Apparent Power, 0.004 Inch Permalloy 80 Toroid, Core 5, Room Ambient	162
148	$P_{c, sq}$ - Total Core Loss, 0.004 Inch Permalloy 80 Toroid, Core 5, -55°C	163
149	$P_{a, sq}$ - Apparent Power, 0.004 Inch Permalloy 80 Toroid, Core 5, -55°C	164
150	$P_{c, sq}$ - Total Core Loss, 0.004 Inch Permalloy 80 Toroid, Core 6, Room Ambient	165
151	$P_{a, sq}$ - Apparent Power, 0.004 Inch Permalloy 80 Toroid, Core 6, Room Ambient	166
152	$P_{c, sq}$ - Total Core Loss, 0.004 Inch Permalloy 80 Toroid, Core 6, -55°C	167
153	$P_{a, sq}$ - Apparent Power, 0.004 Inch Permalloy 80 Toroid, Core 6, -55°C	168

LIST OF TABLES

<u>Number</u>	<u>Title</u>	<u>Page</u>
I	CCFR Properties of 0.002 Inch Supermendur, Magnesium Oxide Interlaminar Insulation	9
II	CCFR Properties of 0.004 Inch Supermendur, Aluminum Orthophosphate Interlaminar Insulation	10
III	CCFR Properties of 0.002 Inch Cubex, Regular Anneal and Magnetic Field Annealed, Aluminum Oxide Interlaminar Insulation	11
IV	CCFR Properties of 0.006 Inch Cubex, Aluminum Orthophosphate Interlaminar Insulation	12
V	CCFR Properties of 0.002 Inch and 0.004 Inch Magnesil, Magnesium Oxide Interlaminar Insulation	13
VI	CCFR Properties of 0.002 Inch and 0.004 Inch Hy-Ra 80, Magnesium Oxide Interlaminar Insulation	14
VII	Screening Core Loss Tests on 0.002 Inch and 0.006 Inch Cubex, Aluminum Oxide Interlaminar Insulation on Toroids and Aluminum Orthophosphate Interlaminar Insulation on Double Windows	15

SECTION I

INTRODUCTION

The objective of this contract is to obtain improved magnetic components for static inverters and converters.

The magnetic materials, electrical conductors and insulations, and inter-laminar insulations used in magnetic components specifically will be evaluated.

The literature is to be reviewed for pertinent data on materials for magnetic components. The environmental conditions to be considered are temperature, radiation, vacuum, shock, vibration, and noise. Operational conditions are to include sine wave and square wave excitation in the frequency range of 400 to 3200 cps. The magnetic materials to be evaluated are magnetic field annealed 49%Co-2%V-29%Fe; doubly grain-oriented, silicon steel (with and without a magnetic anneal); single grain-oriented, silicon steel; square loop 79%Ni-4%Mo-17%Fe; and oriented 50%Ni-50%Fe. The effects of processing are also to be evaluated.

The magnetic properties to be measured with square wave excitation are a-c core loss, a-c apparent core loss, a-c hysteresis, and constant current flux reset points (T, AT, DAT, SAT). The d-c magnetic properties to be measured are B versus H curves and d-c hysteresis major loops.

Optimum materials and processing for magnetic components are to be selected.

SECTION I I

MATERIAL TEST RESULTS AND DISCUSSION

TEST RESULTS

Tables I through VI show the CCFR (Constant Current Flux Reset) properties of 0.002 inch Supermendur (magnetic field annealed), 0.004 inch Supermendur (magnetic field annealed), 0.002 inch Cubex (regular and magnetic field annealed), and 0.006 inch Cubex (regular and magnetic field annealed), 0.002 inch and 0.004 inch Magnesil, and 0.002 inch and 0.004 inch Hy-Ra 80.

The 0.002 inch and 0.004 inch Supermendur and the 0.002 inch and 0.004 inch Hy-Ra 80 were screened using sinusoidal current at the conditions specified in Tables I through VI. The cores selected for further testing were screened on the basis of the highest G, gain, of two out of three cores except in certain cases where three cores were tested. The selected cores were tested for CCFR properties using square wave excitation.

In Table VII the screening core-loss tests at 10 kilogausses and 400 cps, sine flux, are shown for 0.002 inch and 0.006 inch Cubex.

The calibration traces and the CCFR test pictures for toroidal cores in core boxes are shown in Figures 1 through 6 inch Hipernik V, 0.002 inch Hy-Ra 80, 0.002 inch Magnesil, 0.002 inch Supermendur, 0.002 inch Cubex (magnetic field annealed), and 0.002 inch Cubex (regular annealed).

Figures 10 through 225 show the curves for a-c core loss and apparent power at 400, 800, and 3200 cps with a minimum of eight induction levels checked at each frequency.

All of the magnetic properties of individual materials can be located as follows:

<u>Material</u>	<u>Figures</u>
0.002 inch Cubex, Regular and Magnetic Field Annealed, Toroids	10 through 33
0.006 inch Cubex, Regular and Magnetic Field Annealed, Double Window Laminations in Core Boxes	34 through 49
0.002 inch and 0.004 inch Square Orthonol, Toroids	50 through 65
0.002 inch and 0.004 inch Hipernik V, Toroids	66 through 81
0.002 inch and 0.004 inch Magnesil, Toroids	82 through 97
0.002 inch Toroids and 0.004 inch Rowland Rings in Core Boxes, Magnetic Field Annealed Supermendur	98 through 121
0.002 inch and 0.004 inch Hy-Ra 80 Torids	122 through 137
0.002 inch and 0.004 inch Square Permalloy 80 Toroids	138 through 153

DISCUSSION

Of all the materials tested for CCFR properties, the 0.002 inch Square Permalloy 80 showed the highest average G (gain) 10.26×10^{-5} , using square wave current and the best T(squareness ratio), of 0.99 was exhibited by both the 0.004 inch Square Orthonol and the 0.004 inch Hipernik V.

The little loops at the tip of the CCFR loops in Figure 1-6, are caused by integrator drift during testing.

The erratic changes in gain of the 0.002 inch Supermendur in Table I, especially Core No. 33, cannot be explained. A recheck of the cores did not change the test values. The increase in the gain on core No. 79 in Table II at 800 cps, and the decrease in Bm of cores 1, 3, 4, and 6 at 3200 cps in Table IV cannot be satisfactorily explained.

The 0.004 inch Supermendur in Table II also exhibited an anomalous behavior with respect to its gain characteristics.

In Figure 7 the 0.004 inch Magnesil, 0.004 inch Square Orthonol, and 0.004 inch Square Permalloy 80 magnetic cores to be used in degradation testing

are shown. These were damaged by the failure of the aluminum orthophosphate interlaminar insulation to meet the high annealing temperature (800°C - 1160°C) required to relieve the stresses created by winding the cores. The coating of aluminum orthophosphate upon breakdown caused distortion and welding of the tape cores. The cores were coated heavier than normal to prevent sticking, but the annealing temperature was too high. The cores were replaced with new magnetic material, coated with magnesium oxide, and then stress relief annealed successfully.

The calculation of the a-c core loss and apparent power test values were partially performed by our computer facilities.

A Weston Inductronic Wattmeter was obtained in order to provide greater sensitivity for measuring square wave core loss at high levels and was used for core loss tests except as noted below.

The core loss on the 0.002 inch and 0.004 inch Hy-Ra 80 and 0.002 and 0.004 inch Square Permalloy 80 were obtained by using a John Fluke Model 102 (VAW) meter instead of a Weston Inductronic Wattmeter, Model 1483, since the sensitivity of the John Fluke was better for these materials when measuring low core loss.

The magnetic field anneal of the Cubex material shows an advantage over regular stress relief annealing in improving the magnetic properties under both sine voltage and square voltage conditions.

The a-c core loss increases with lowering the test temperature to -55°C from room ambient temperature.

The core loss curves and apparent power curves have been defined with new terms to reflect the conditions of square voltage testing rather than sine voltage testing. The core loss is represented by $P_{c, sq}$ to reflect the loss associated with the deliberate distortion of the sinusoidal wave form to a square wave form. The apparent power $P_{a, sq}$ reflects average exciting volt-amperes. Our flux voltage was measured with a Hewlett-Packard 400 H, Average Reading Voltmeter, rather than the normal average reading flux voltmeter that has a scale reading 1.11 times the average flux voltage. In square wave testing, the form factor is 1.00. The current was measured with a Hewlett-Packard, RMS Voltmeter, Model 3400A (true reading RMS) by using a shunt. The meter has very high sensitivity and fast response. However, the actual peak current caused by the fast rise time is not measured because of the small time interval when the current peaks. This peak current can create serious problems in components for aerospace static inverters and converters by causing failures in transistors and overloading capacitors.

SECTION I I I

CORE DESCRIPTIONS

The material used to make the tape wound toroids was coated with magnesium oxide for an interlaminar insulation, except for the 0.002 inch Cubex which was coated with aluminum oxide. The wound tape core has an outside diameter of 3.890 inches, an inside diameter of 3.256 inches, and a height of 1 inch.

The Rowland ring lamination drawing is shown in Figure 8. All Rowland rings were coated with aluminum orthophosphate for an interlaminar insulation.

The double window lamination drawing for 0.006 inch Cubex is shown in Figure 9. The laminations were coated with aluminum orthophosphate for an interlaminar insulation.

The cores described above are enclosed in anodized aluminum core boxes with a glass epoxy insert to provide a break in the electrical path. The cores were GVB epoxy insulated with a breakdown voltage of 1000 volts. The cores were silicone oil filled and hermetically sealed by the mechanical and epoxy seal.

SECTION IV

TESTING PROCEDURES

A fast sweep dual beam oscilloscope with a Polaroid camera attachment will be used to record the shock impulse and the a-c hysteresis loop in place of a single trace oscilloscope with a high speed camera to record the a-c hysteresis loop only. This recording of data is required in the shock testing of cores in the program.

The No. 3 position in the noise chamber at North American Aviation will be used for the acoustic noise tests.

Magnesium oxide was used in place of aluminum orthophosphate for the 0.004 inch Square Permalloy 80 square tape wound cores, the 0.004 inch Magnesil square tape wound cores, and the 0.004 inch Square Orthonol round tape wound cores to be used in the degradation testing.

The B_m , maximum induction, for each core for the a-c hysteresis loops is as follows at frequencies of 400, 800, 1600, and 3200 cps at room ambient temperature:

<u>Material</u>	<u>B_m, Maximum Induction (Kilogausses)</u>
2 and 4 mil Hy-Ra 80	7
2 and 4 mil Square Permalloy 80	7
2 and 4 mil Supremendur	20
2 mil Magnesil	18
4 mil Magnesil	19
2 and 4 mil Hipernik V	15
2 and 4 mil Square Orthonol	15

<u>Material</u>	<u>B_m, Maximum Induction (Kilogausses)</u>
2 mil Cubex, Regular and Magnetic Field Annealed	19
6 mil Cubex, Regular and Magnetic Field Annealed	15 (minimum)

The induction levels for each core for the a-c total core loss and apparent power at 400, 800, 1600, and 3200 cps and room ambient temperature are as follows:

<u>Material</u>	<u>B, Induction (Kilogausses)</u>
2 and 4 mil Hy-Ra 80	0.5, 1, 2, 3, 4, 5, 6, 7
2 mil Magnesil	1, 2, 3, 5, 10, 12, 15, 18
4 mil Magnesil	1, 2, 3, 5, 10, 12, 15, 19
2 and 4 mil Square Permalloy 80	0.6, 1, 2, 3, 4, 5, 6, 7
2 and 4 mil Supermendur	1, 3, 5, 9, 12, 14, 16, 20
2 and 4 mil Hipernik V	1, 3, 5, 8, 10, 11, 13, 15
2 and 4 mil Square Orthonol	1, 3, 5, 8, 10, 11, 13, 15
2 mil Cubex, Regular and Magnetic Field Annealed	1, 3, 5, 10, 12, 15, 17, 19
6 mil Cubex, Regular and Magnetic Field Annealed	1, 2, 3, 5, 10, 12

SECTION V

GENERAL PROGRESS AND PLANS FOR FUTURE WORK

All of the magnetic lamination material has been received. The metering sleeve for the 8 millisecond half sine pulse shock test has been received.

The following testing will be completed in the next quarter:

- 1) The testing of various samples for the effects of factory processing on the degradation of magnetic properties.
- 2) The test results of the effects of an exposure to a vacuum of 10^{-6} torr at 250°C for 1000 hours of the degradation samples as well as the Rowland rings and blanks.
- 3) The a-c hysteresis loops and d-c hysteresis loops at room ambient temperature and -55°C .
- 4) The d-c magnetization curves will be obtained at room ambient temperature, -55°C , and 250°C .

TABLE I. CCFR Properties of 0.002 Inch Supermendur, Magnesium Oxide Interlaminar Insulation*

Core No.	Material	Excitation Current	Frequency (cps)	T Squareness Ratio Br/Bm	Br Gausses	AT H ₁ (Oersteds)	DAT $\Delta H(H_2-H_1)$ (Oersteds)	SAT B _m (Gausses)	G Gain 10-5	H _m	
										SAT & T	Oersteds AT & DAT
32	0.002" Supermendur Magnetic Field Annealed	Sine	400	0.986	20,552	0.923	0.077	20,850	1.858	5.0	10.0
		Square	400	0.983	20,318	0.940	0.080	20,780	1.805	5.0	10.0
		Square	800	0.982	20,648	0.965	0.080	21,010	1.812	5.0	10.0
		Square	1600	0.979	20,423	1.062	0.093	20,850	1.565	5.0	10.0
33	0.002" Supermendur Magnetic Field Annealed	Square	3200	0.978	20,811	1.181	0.341	21,300	0.421	5.0	10.0
		Sine	400	0.987	20,443	0.982	0.098	20,750	1.432	5.0	10.0
		Square	400	0.975	19,900	0.964	0.078	20,400	1.768	5.0	10.0
		Square	800	0.976	19,915	1.035	0.083	20,400	1.685	5.0	10.0
34	0.002" Supermendur Magnetic Field Annealed	Square	1600	0.978	20,153	1.128	0.087	20,600	1.598	5.0	10.0
		Square	3200	0.980	20,680	1.260	0.075	21,100	1.890	5.0	10.0
		Sine	400	0.987	20,597	0.993	0.087	20,800	1.628	5.0	10.0
		Square	400	0.932	19,389	0.955	0.090	20,850	1.595	5.0	10.0
		Square	800	0.978	20,406	1.062	0.083	20,850	2.275	5.0	10.0
		Square	1600	0.979	20,428	1.130	0.095	20,850	1.505	5.0	10.0
		Square	3200	0.977	20,432	1.245	0.343	20,950	0.416	5.0	10.0

* 1) Tests run on toroids, tape wound cores, see page 5 for full description.

2) Tests run at room ambient temperature to AIEE No. 432, Test Procedure for Toroidal Magnetic Amplifier Cores, where applicable.

TABLE II. CCFR Properties of 0.004 Inch Supermendur, Aluminum Orthophosphate Interlaminar Insulation*

Core No.	Material	Excitation Current	Frequency (cps)	T Squareness Ratio B_r/B_m	B_r Gausses	H_i (Oersteds)	DAT $\Delta H(H_2-H_1)$ (Oersteds)	SAT B_m (Gausses)	G Gain 10-5	H_m	
										SAT & T	Oersteds AT & DAT
35	0.004" Supermendur Magnetic Field Annealed	Sine	400	0.944	16,850	0.56	0.102	17,850	1.255	5.0	10.0
		Square	400	0.946	16,832	0.576	0.110	17,800	1.42	5.0	10.0
		Square	800	0.944	16,805	0.607	0.119	17,800	1.06	5.0	10.0
		Square	1600	0.941	17,035	0.757	0.193	18,100	0.65	5.0	10.0
		Square	3200	0.921	16,715	0.946	0.439	18,150	0.299	5.0	10.0
36	0.004" Supermendur Magnetic Field Annealed	Sine	400	0.941	16,840	0.552	0.08	17,900	1.61	5.0	10.0
		Square	400	0.932	16,450	0.550	0.084	17,650	1.55	5.0	10.0
		Square	800	0.933	16,940	0.642	0.128	18,150	1.025	5.0	10.0
		Square	1600	0.935	17,200	0.779	0.242	18,400	0.545	5.0	10.0
		Square	3200	0.921	15,110	1.010	0.620	18,400	0.219	5.0	10.0
37	0.004" Supermendur Magnetic Field Annealed	Sine	400	0.948	17,540	0.562	0.108	18,500	1.192	5.0	10.0
		Square	400	0.945	16,960	0.541	0.044	17,950	2.86	5.0	10.0
		Square	800	0.946	16,928	0.616	0.114	17,900	1.11	5.0	10.0
		Square	1600	0.947	17,330	0.729	0.186	18,300	0.695	5.0	10.0
		Square	3200	0.946	17,500	0.900	0.310	18,500	0.434	5.0	10.0

* 1) Tests run on Rowland ring laminations sealed in core boxes, see page 5 for full description.

2) Tests run at room ambient temperature to AIEE NO. 432, Test Procedure for Toroidal Magnetic Amplifier Cores, where applicable.

TABLE III. CCFR Properties of 0.002 Inch Cubex, Regular Anneal and Magnetic Field Annealed, Aluminum Oxide Interlaminar Insulation*

Core No.	Material	Excitation Current	Frequency (cps)	T Squareness Ratio B_r/B_m	B_r Gausses	AT H_1 (Oersteds)	DAT $\Delta H(H_2-H_1)$ (Oersteds)	SAT B_m (Gausses)	G Gain 10 ⁻⁵	H_m	
										SAT & T	Oersteds AT & DAT
74	0.002" Cubex Magnetic Field Annealed	Square	400	0.974	16,270	0.506	0.086	16,700	1.71	3.0	6.0
		Square	800	0.972	16,135	0.576	0.082	16,600	1.24	3.0	6.0
		Square	1600	0.972	16,280	0.668	0.127	16,750	0.09	3.0	6.0
		Square	3200	0.975	16,083	0.805	0.141	16,500	1.025	3.0	6.0
75	0.002" Cubex Magnetic Field Annealed	Square	400	0.970	16,010	0.493	0.070	16,500	1.632	3.0	6.0
		Square	800	0.974	16,165	0.559	0.083	16,600	1.37	3.0	6.0
		Square	1600	0.974	16,266	0.660	0.115	16,700	1.0	3.0	6.0
		Square	3200	0.975	16,372	0.792	0.140	16,800	0.818	3.0	6.0
76	0.002" Cubex Magnetic Field Annealed	Square	400	0.967	16,175	0.501	0.071	16,700	1.632	3.0	6.0
		Square	800	0.971	16,310	0.572	0.10	16,800	1.16	3.0	6.0
		Square	1600	0.973	16,548	0.672	0.128	17,000	0.9	3.0	6.0
		Square	3200	0.975	16,472	0.796	0.153	16,900	0.774	3.0	6.0
79	0.002" Cubex Regular Anneal	Square	400	0.897	14,530	0.387	0.146	16,200	0.78	3.0	6.0
		Square	800	0.904	14,640	0.427	0.083	16,200	1.385	3.0	6.0
		Square	1600	0.913	14,930	0.484	0.221	16,350	0.523	3.0	6.0
		Square	3200	0.925	14,990	0.643	0.257	16,200	0.452	3.0	6.0
80	0.002" Cubex Regular Anneal	Square	400	0.901	14,550	0.392	0.153	16,150	0.744	3.0	6.0
		Square	800	0.909	14,810	0.4355	0.1765	16,300	0.646	3.0	6.0
		Square	1600	0.919	15,030	0.506	0.218	16,350	0.530	3.0	6.0
		Square	3200	0.929	15,000	0.620	0.240	16,150	0.479	3.0	6.0
81	0.002" Cubex Regular Anneal	Square	400	0.896	14,515	0.361	0.161	16,200	0.708	3.0	6.0
		Square	800	0.907	14,960	0.427	0.172	16,500	0.670	3.0	6.0
		Square	1600	0.916	15,205	0.497	0.215	16,600	0.534	3.0	6.0
		Square	3200	0.921	14,875	0.632	0.240	16,150	0.484	3.0	6.0

* 1) Tests run on toroids, tape wound cores, see page 5 for full description.

2) Tests run at room ambient temperature to AIEE No. 432, Test Procedure for Toroidal Magnetic Amplifier Cores, where applicable.

TABLE IV. CCFR Properties of 0.006 Inch Cubex, Aluminum Orthophosphate Interlaminar Insulation*

Core No.	Material	Excitation Current	Frequency (cps)	T Squareness Ratio B_r/B_m	B_r Gausses	AT H_1 (Oersteds)	DAT $\Delta H(H_2-H_1)$ (Oersteds)	SAT B_m (Gausses)	G Gain 10-5	H _m	
										SAT & T	Oersteds AT & DAT
1	0.006" Cubex Double Window Magnetic Field Annealed	Square	400	0.988	11,480	0.352	0.163	12,820	5.4	3.0	6.0
		Square	800	0.926	11,665	0.471	0.219	12,600	4.03	3.0	6.0
		Square	1600	0.929	10,220	0.636	0.289	11,000	3.08	3.0	6.0
		Square	3200	0.911	6,378	0.848	0.442	7,000	1.905	3.0	6.0
3	0.006" Cubex Double Window Magnetic Field Annealed	Square	400	0.928	11,420	0.394	0.134	12,309	6.4	3.0	6.0
		Square	800	0.932	11,515	0.591	0.200	12,350	4.31	3.0	6.0
		Square	1600	0.938	10,412	0.665	0.267	11,180	3.35	3.0	6.0
		Square	3200	0.905	6,585	0.858	0.302	7,280	2.74	3.0	6.0
4	0.006" Cubex Double Window	Square	400	0.883	10,980	0.3122	0.1918	12,100	4.4	3.0	6.0
		Square	800	0.909	10,820	0.436	0.154	11,900	5.53	3.0	6.0
		Square	1600	0.908	9,430	0.598	0.329	10,380	2.695	3.0	6.0
		Square	3200	0.890	5,965	0.812	0.418	6,700	1.945	3.0	6.0
6	0.006" Cubex Double Window	Square	400	0.840	10,420	0.273	0.224	12,406	3.93	3.0	6.0
		Square	800	0.858	10,120	0.387	0.289	11,800	2.94	3.0	6.0
		Square	1600	0.869	8,690	0.557	0.411	10,000	2.12	3.0	6.0
		Square	3200	0.837	5,460	0.752	0.633	6,520	1.288	3.0	6.0

* 1) Tests run on double window laminations sealed in core boxes, see page 5 for full description.

2) Tests run at room ambient temperature to AIEE No. 432, Test Procedure for Toroidal Magnetic Amplifier Cores, where applicable.

TABLE V. CCFR Properties of 0.002 Inch and 0.004 Inch Magnesi1, Magnesium Oxide Interlaminar Insulation*

Core No.	Material	Excitation Current	Frequency (cps)	T Squareness Ratio B_r/B_m	B _r Gausses	AT H _l (Oersteds)	DAT $\Delta H(H_2-H_1)$ (Oersteds)	SAT B _m (Gausses)	Gain 10-5	H _m	
										SAT & T	Oersteds AT & DAT
28	0.002" Magnesi1	Square	400	0.983	14,936	0.521	0.079	15,200	1.332	3.0	6.0
		Square	800	0.983	14,899	0.600	0.088	15,100	1.550	3.0	6.0
		Square	1600	0.983	14,994	0.662	0.086	15,250	1.622	3.0	6.0
		Square	3200	0.983	15,135	0.750	0.088	15,400	1.205	3.0	6.0
30	0.002" Magnesi1	Square	400	0.982	14,726	0.587	0.044	15,000	2.375	3.0	6.0
		Square	800	0.982	14,724	0.631	0.031	15,000	1.990	3.0	6.0
		Square	1600	0.982	14,776	0.671	0.087	15,050	1.202	3.0	6.0
		Square	3200	0.982	14,777	0.777	0.123	15,050	0.883	3.0	6.0
26	0.004" Magnesi1	Square	400	0.982	15,715	0.561	0.066	16,000	1.660	3.0	6.0
		Square	800	0.982	15,760	0.645	0.073	16,050	1.425	3.0	6.0
		Square	1600	0.983	15,728	0.759	0.106	16,000	1.042	3.0	6.0
		Square	3200	0.979	14,985	0.887	0.168	15,300	0.614	3.0	6.0
27	0.004" Magnesi1	Square	400	0.979	15,637	0.575	0.082	15,900	1.35	3.0	6.0
		Square	800	0.984	15,737	0.658	0.124	16,000	0.88	3.0	6.0
		Square	1600	0.983	15,630	0.772	0.112	15,900	0.978	3.0	6.0
		Square	3200	0.981	14,710	0.910	0.170	15,000	0.653	3.0	6.0

* 1) Tests run on toroids, tape wound cores, see page 5 for full description.

2) Tests run at room ambient temperature to AIEE No. 432, Test Procedure for Toroidal Magnetic Amplifier Cores, where applicable.

TABLE VI. CCFR Properties of 0.002 Inch and 0.004 Inch Hy-Ra 80, Magnesium Oxide Interlaminar Insulation*

Core No.	Material	Excitation Current	Frequency (cps)	T Squareness Ratio B_r/B_m	B_r Gausses	AT H_l (Oersteds)	DAT $\Delta H(H_2-H_1)$ (Oersteds)	SAT B_m (Gausses)	G Gain 10-5	H_m	
										SAT & T	Oersteds AT & DAT
22	0.002" Hy-Ra 80	Sine	400	0.931	6,627	0.0283	0.0050	6,730	9.15	0.5	1.0
		Square	400	0.929	6,270	0.0289	0.0061	6,740	7.7	0.5	1.0
		Square	800	0.931	6,190	0.0324	0.0083	6,650	5.65	0.5	1.0
		Square	1600	0.931	6,280	0.0388	0.015	6,750	3.14	0.5	1.0
		Square	3200	0.930	6,276	0.0502	0.024	6,750	1.97	0.5	1.0
23	0.002" Hy-Ra 80	Sine	400	0.928	6,208	0.0288	0.0048	6,680	9.52	0.5	1.0
		Square	400	0.932	6,324	0.0285	0.0055	6,789	8.5	0.5	1.0
		Square	800	0.928	6,245	0.0332	0.008	6,740	5.88	0.5	1.0
		Square	1600	0.927	6,218	0.0395	0.0127	6,710	3.89	0.5	1.0
		Square	3200	0.930	6,178	0.0500	0.0205	6,650	2.27	0.5	1.0
24	0.002" Hy-Ra 80	Sine	400	0.933	6,260	0.0282	0.0056	6,710	8.27	0.5	1.0
		Square	400	0.937	6,325	0.0291	0.0046	6,750	10.2	0.5	1.0
		Square	800	0.932	6,286	0.0336	0.0076	6,750	6.2	0.5	1.0
		Square	1600	0.928	6,210	0.0404	0.0126	6,700	3.74	0.5	1.0
		Square	3200	0.928	6,249	0.0528	0.0192	6,720	3.94	0.5	1.0
19	0.004" Hy-Ra 80	Sine	400	0.907	6,530	0.0263	0.0106	7,210	4.90	0.5	1.0
		Square	400	0.937	6,370	0.0268	0.0103	6,800	4.69	0.5	1.0
		Square	800	0.928	6,316	0.0368	0.0189	6,800	2.52	0.5	1.0
		Square	1600	0.933	6,346	0.0508	0.0392	6,800	1.23	0.5	1.0
		Square	3200	0.914	6,568	0.0668	0.0752	7,180	0.662	1.0	2.0
20	0.004" Hy-Ra 80	Sine	400	0.925	6,320	0.0263	0.0105	6,830	4.74	0.5	1.0
		Square	400	0.921	6,300	0.0268	0.0104	6,850	4.63	0.5	1.0
		Square	800	0.924	6,220	0.0357	0.0172	6,720	2.78	0.5	1.0
		Square	1600	0.936	6,327	0.0491	0.0323	6,770	1.47	0.5	1.0
		Square	3200	0.907	6,620	0.0668	0.0792	7,300	0.636	1.5	3.0

* 1) Tests run on toroids, tape wound cores, see page 5 for full description.

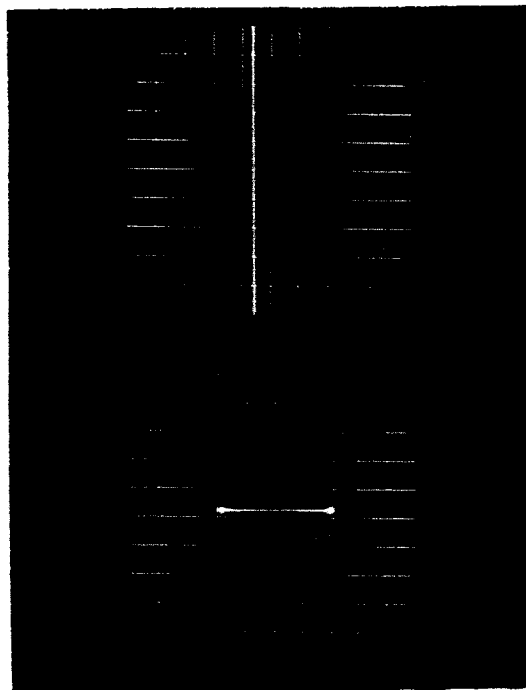
2) Tests run at room ambient temperature to AIEE No. 432, Test Procedure for Toroidal Magnetic Amplifier Cores, where applicable.

TABLE VII. Screening Core Loss Tests on 0.002 Inch and 0.006 Inch Cubex, Aluminum Oxide Interlaminar Insulation on Toroids and Aluminum Orthophosphate Interlaminar Insulation on Double Windows*

Core No. & Type	Material	Frequency (cps) (Sine Flux)	B _m (Gausses)	P _c Total Core Loss (Watts/lb.)
74, Toroid	0.002" Cubex, Magnetic Field Annealed	400	10,000	3.20
75, Toroid	0.002" Cubex, Magnetic Field Annealed	400	10,000	3.13
76, Toroid	0.002" Cubex, Magnetic Field Annealed	400	10,000	3.54
79, Toroid	0.002" Cubex	400	10,000	3.91
80, Toroid	0.002" Cubex	400	10,000	3.92
81, Toroid	0.002" Cubex	400	10,000	3.78
1, Double Window	0.006" Cubex, Magnetic Field Annealed	400	10,000	5.92
2, Double Window	0.006" Cubex, Magnetic Field Annealed	400	10,000	6.62
3, Double Window	0.006" Cubex, Magnetic Field Annealed	400	10,000	5.82
4, Double Window	0.006" Cubex	400	10,000	6.70
5, Double Window	0.006" Cubex	400	10,000	6.85
6, Double Window	0.006" Cubex	400	10,000	6.58

* 1) Core Loss Tests Run to ASTM A348-64.

2) See page 5 for full description of cores.



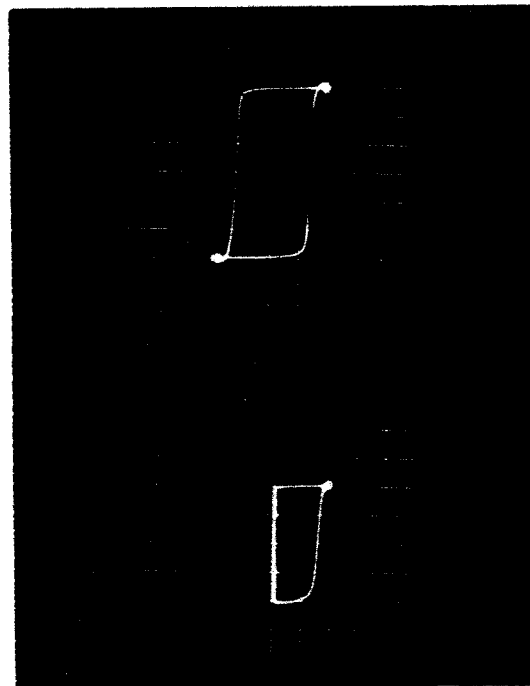
TOP TRACE

B = 50 KG TOTAL

BOTTOM TRACE

H = 2 Oersteds TOTAL

Calibration Trace For All CCFR Testing



TOP

A-C Hysteresis Loop,
Square Wave
Excitation

B_m = 15, 150KG

BOTTOM

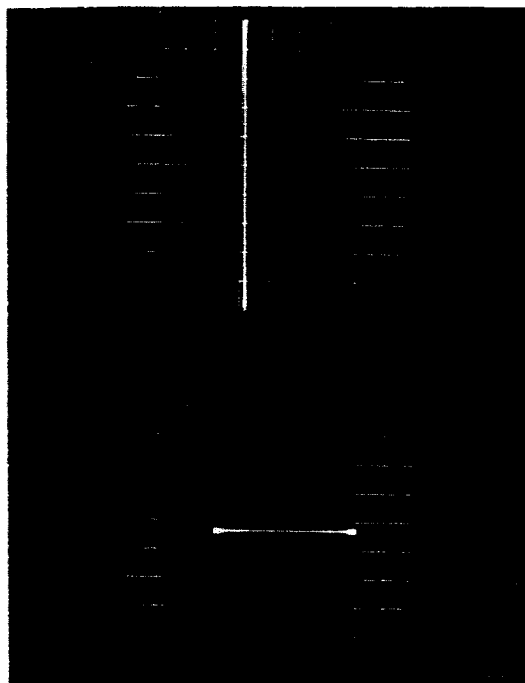
Half Square Wave
Excitation with d-c
Reset

H₂ = 0.203 Oersteds

CCFR Loops, 400 cps

FIGURE 1. Calibration Traces and CCFR Test Pictures for Core No. 14 of
0.002 Inch Hipernik V Tape Wound Cores in Boxes at Room
Ambient Temperature

WAED 66.13E-16



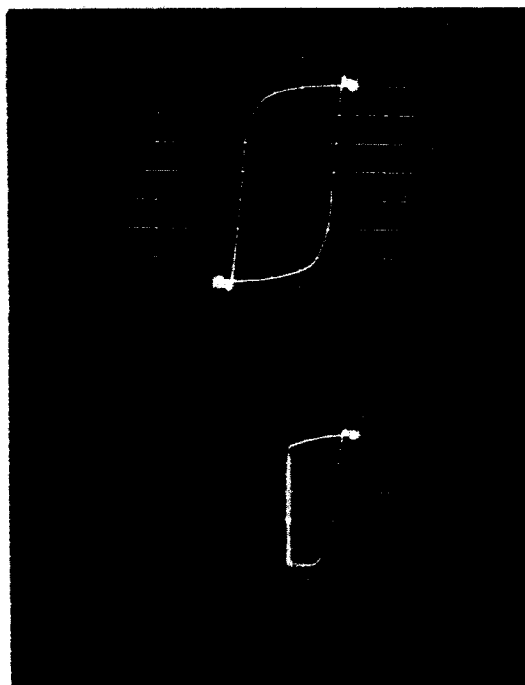
TOP TRACE

B = 20 KG TOTAL

BOTTOM TRACE

H = 0.5 Oersteds TOTAL

Calibration Trace For All CCFR Testing



TOP

A-C Hysteresis Loop,
Square Wave
Excitation

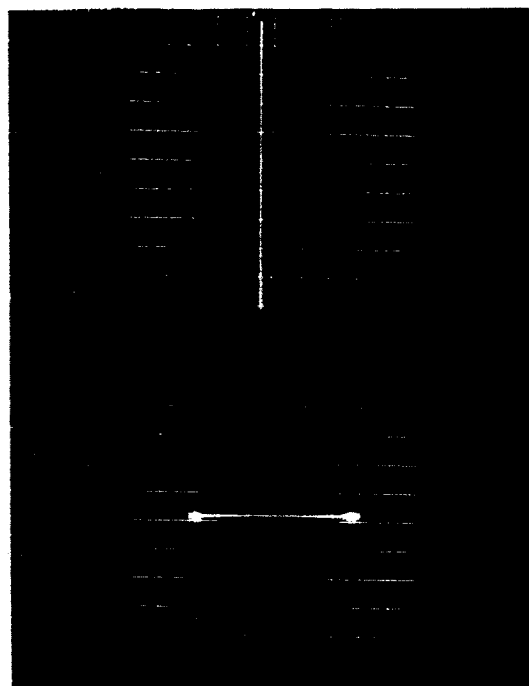
B_m = 6,789 KG

BOTTOM

Half Square Wave
Excitation with d-c
Reset
H₂ = 0.0339 Oersteds

CCFR Loops, 400 cps

FIGURE 2. Calibration Traces and CCFR Test Pictures for Core No. 23 of
0.002 Inch Hy-Ra 80 Tape Wound Cores in Core Boxes at
Room Ambient Temperature



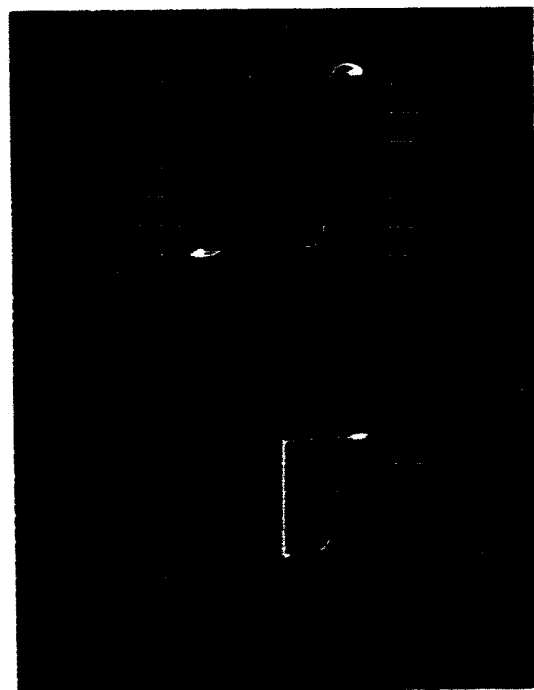
TOP TRACE

B = 50 KG TOTAL

BOTTOM TRACE

H = 6 Oersteds TOTAL

Calibration Trace For All CCFR Testing



TOP

A-C Hysteresis Loop,
Square Wave
Excitation

$B_m = 15,200\text{KG}$

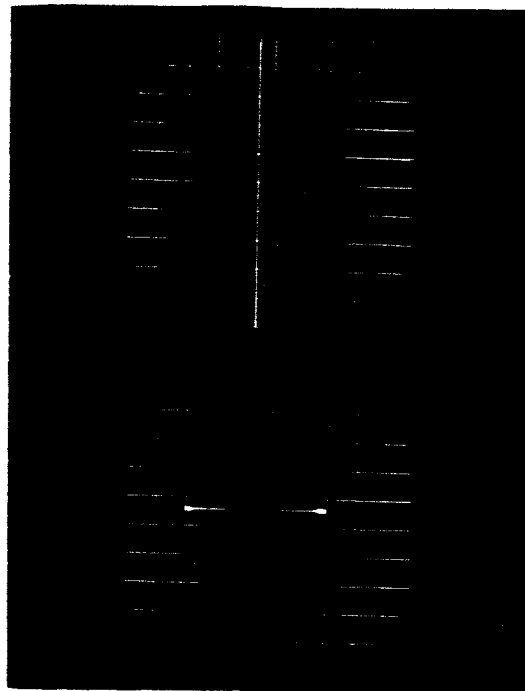
BOTTOM

Half Square Wave
Excitation with d-c
Reset
 $H_2 = 0.589$ Oersteds

CCFR Loops, 400 cps

FIGURE 3. Calibration Traces and CCFR Test Pictures for Core No. 28 of
0.002 Inch Magnesil Tape Wound Cores in Core Boxes at
Room Ambient Temperature

WAED 66. 13E- 18



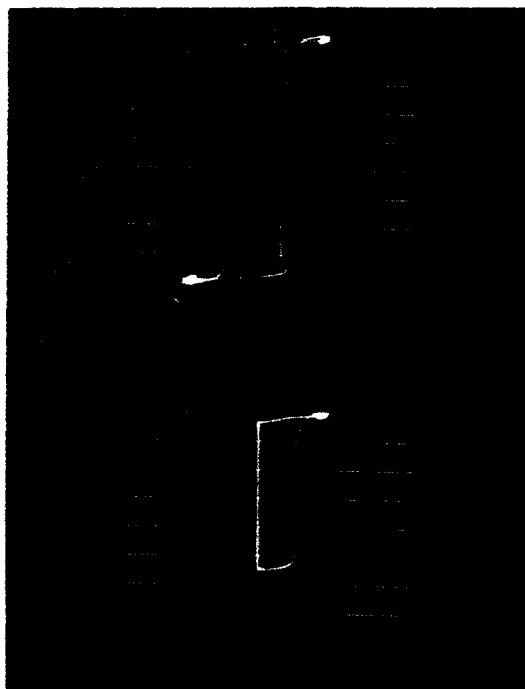
TOP TRACE

B = 50 KG TOTAL

BOTTOM TRACE

H = 10 Oersted TOTAL

Calibration Trace For All CCFR Testing



TOP

A-C Hysteresis Loop,
Square Wave
Excitation

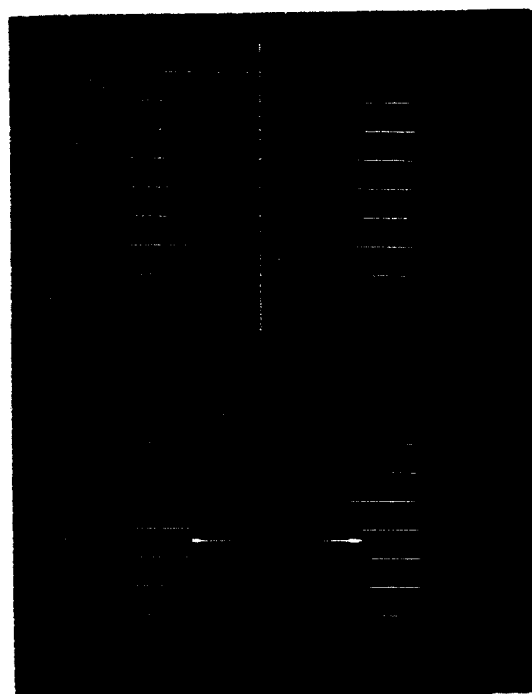
B_m = 20,780KG

BOTTOM

Half Square Wave
Excitation with d-c
Reset
H₂ = 1.01 Oersted

CCFR Loops, 400 cps

FIGURE 4. Calibration Traces and CCFR Test Pictures for Core No. 32 of 0.002 Inch Supermendur Tape Wound Cores in Core Boxes at Room Ambient Temperature



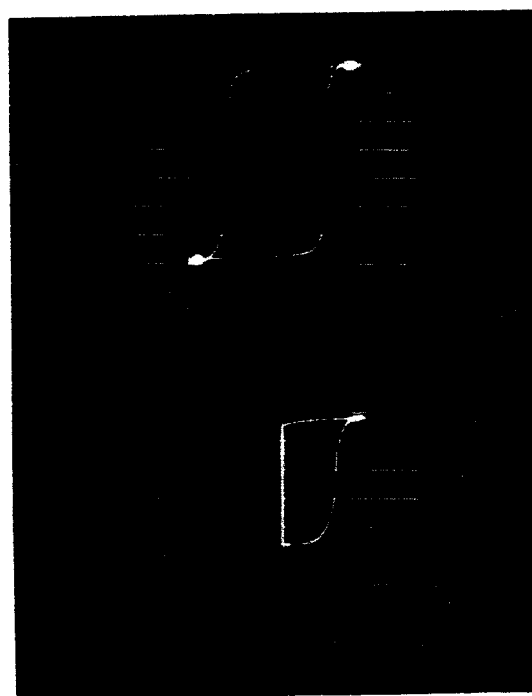
TOP TRACE

B = 50 KG TOTAL

BOTTOM TRACE

H = 6 Oersteds TOTAL

Calibration Trace For All CCFR Testing



TOP

A-C Hysteresis Loop,
Square Wave
Excitation

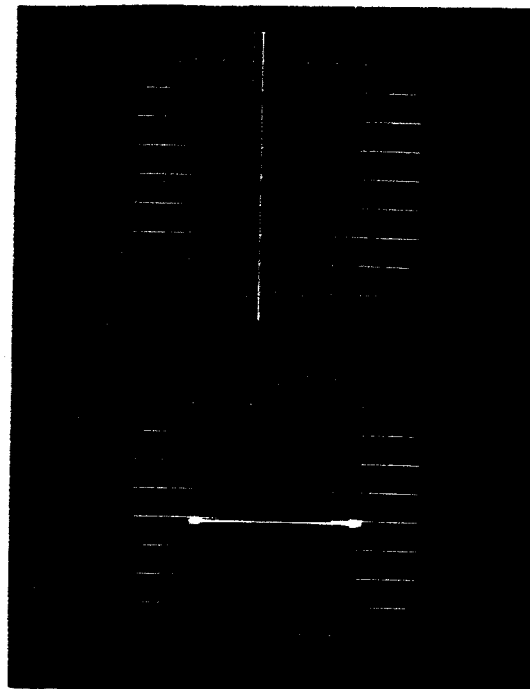
Bm = 16,700KG

BOTTOM

Half Square Wave
Excitation with d-c
Reset
 $H_2 = 0.559$ Oersteds

CCFR Loops, 400 cps

FIGURE 5. Calibration Traces and CCFR Test Pictures for Core No. 74 of 0.002 Inch Cubex Tape Wound Cores, Magnetic Field Annealed, in Core Boxes at Room Ambient Temperature



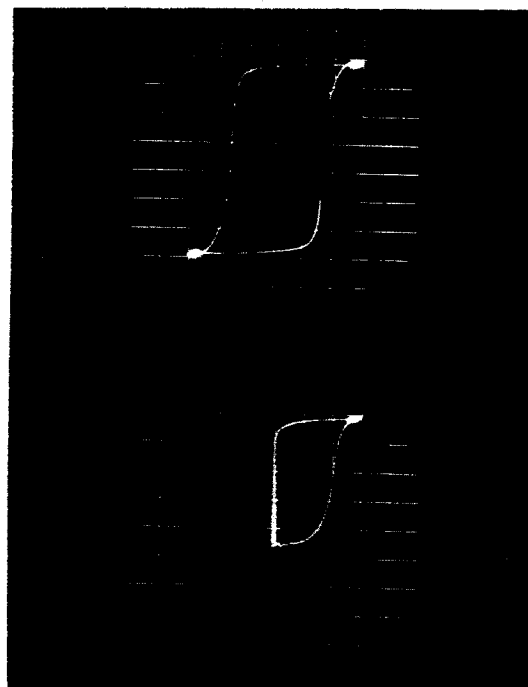
TOP TRACE

B = 50 KG TOTAL

BOTTOM TRACE

H = 6 Oersteds TOTAL

Calibration Trace For All CCFR Testing



TOP

A-C Hysteresis Loop,
Square Wave
Excitation

$B_m \approx 16, 150 \text{ KG}$

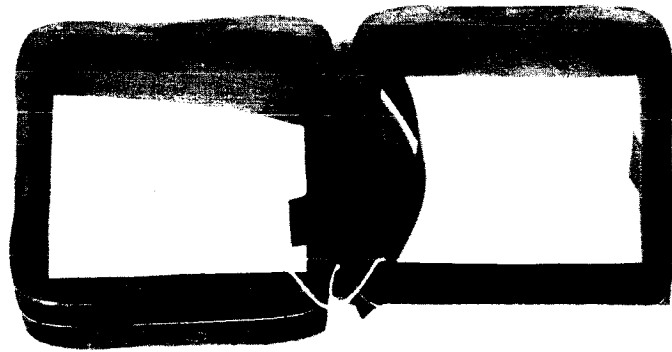
BOTTOM

Half Square Wave
Excitation with d-c
Reset
 $H_2 = 0.548 \text{ Oersteds}$

CCFR Loops, 400 cps

FIGURE 6. Calibration Traces and CCFR Test Pictures for Core No. 80 of
0.002 Inch Cubex Tape Wound Cores in Core Boxes at Room
Ambient Temperature

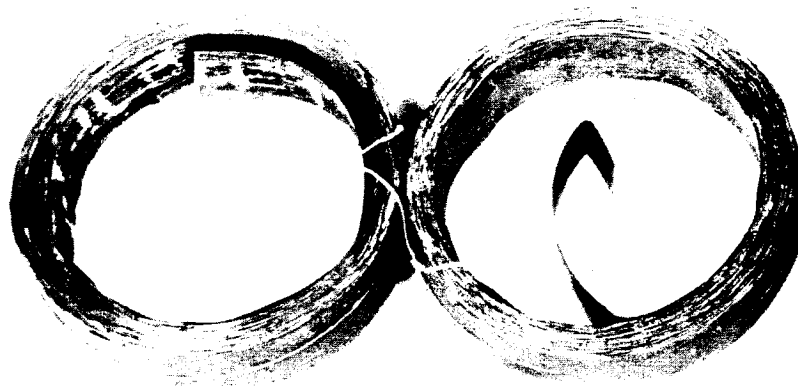
WAED 66. 13E-21



0.004" Magnasil
Alkophos Coat



0.004" Square Permalloy 80,
Alkophos Coat



0.004" Square Orthonol
Alkophos Coat

FIGURE 7. Tape Wound Cores Damaged by Failure of Aluminum
Orthophosphate During Stress Relief Annealing

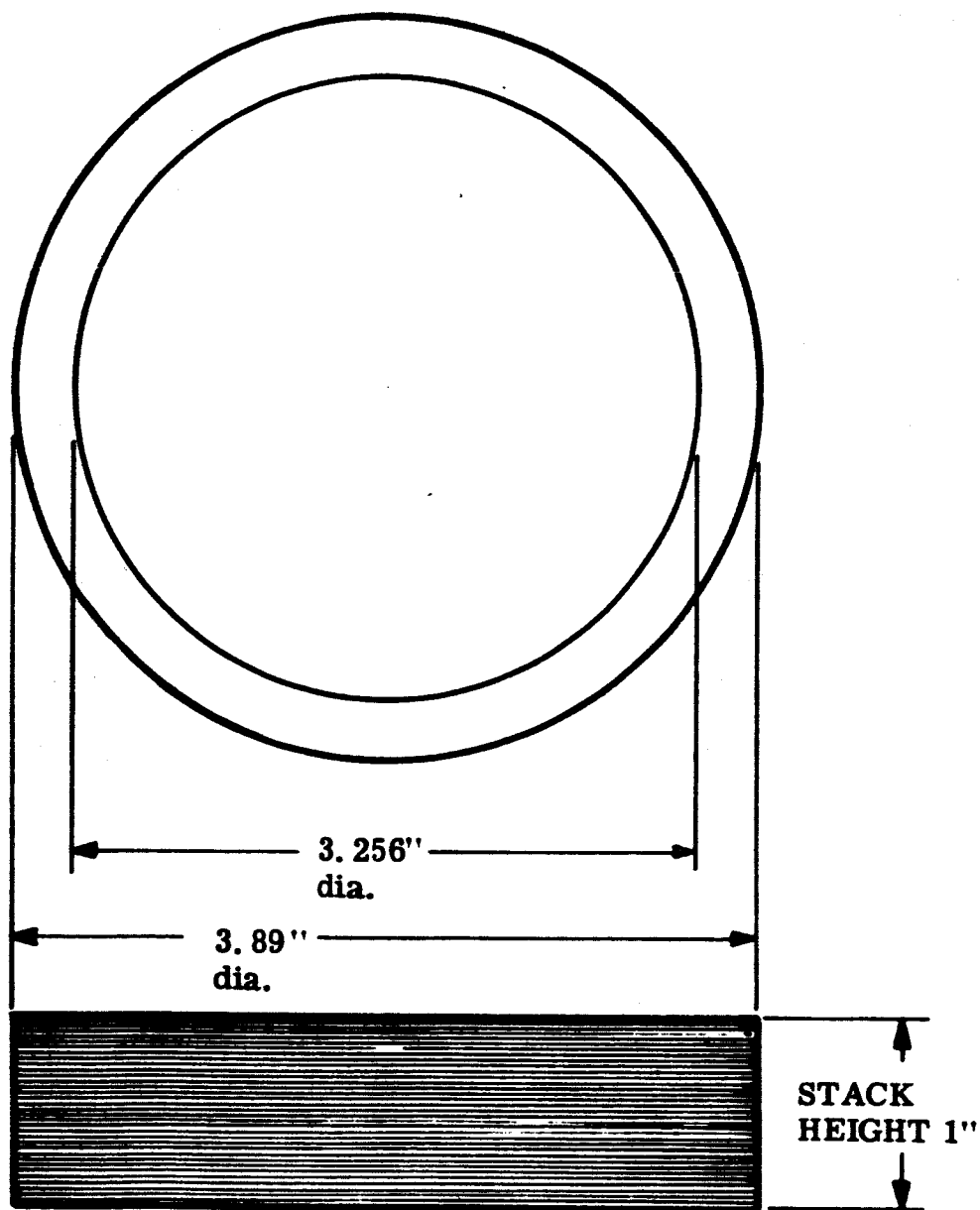


FIGURE 8. Rowland Ring Lamination Drawing

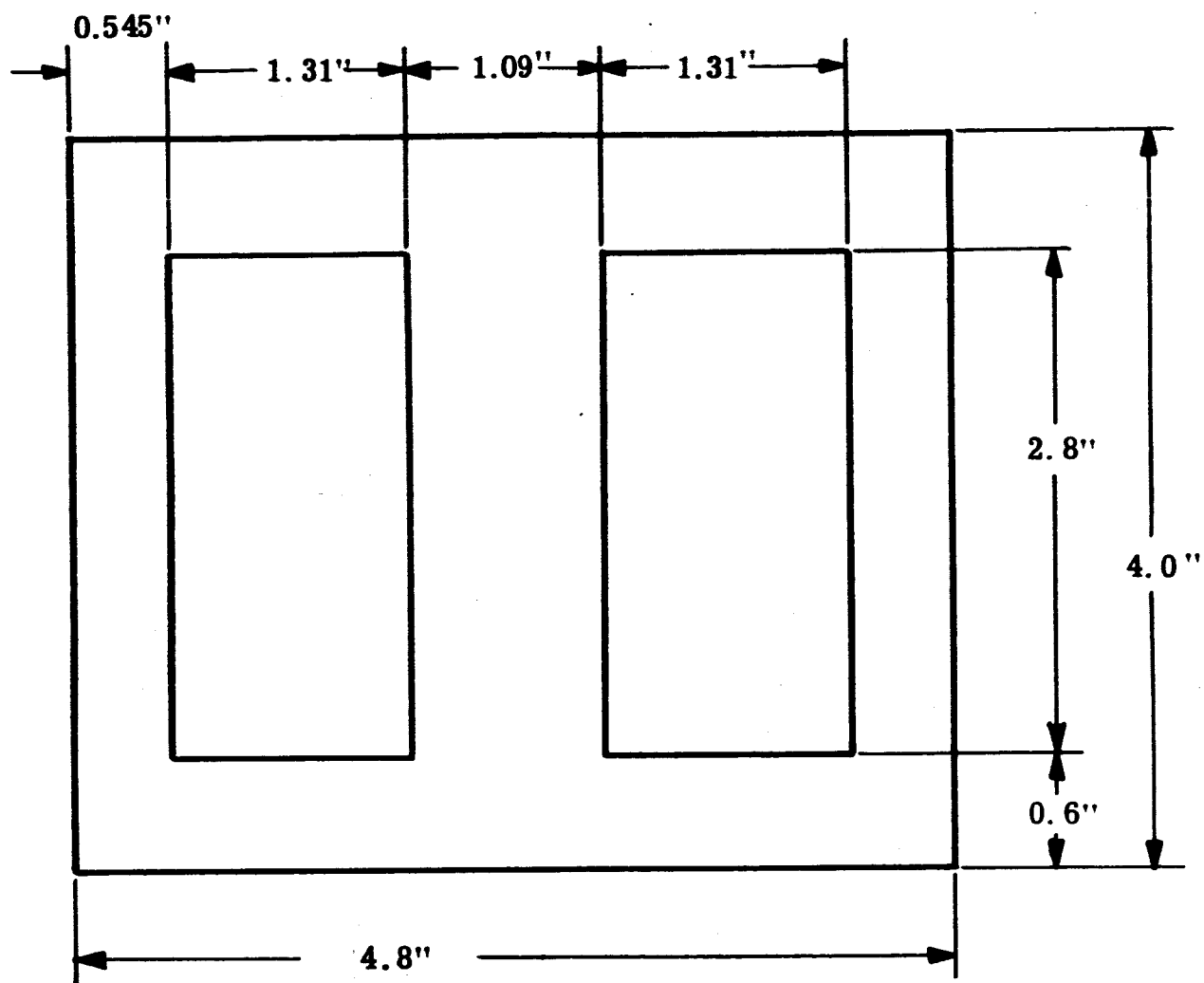


FIGURE 9. Cubex Double Window Lamination Drawing

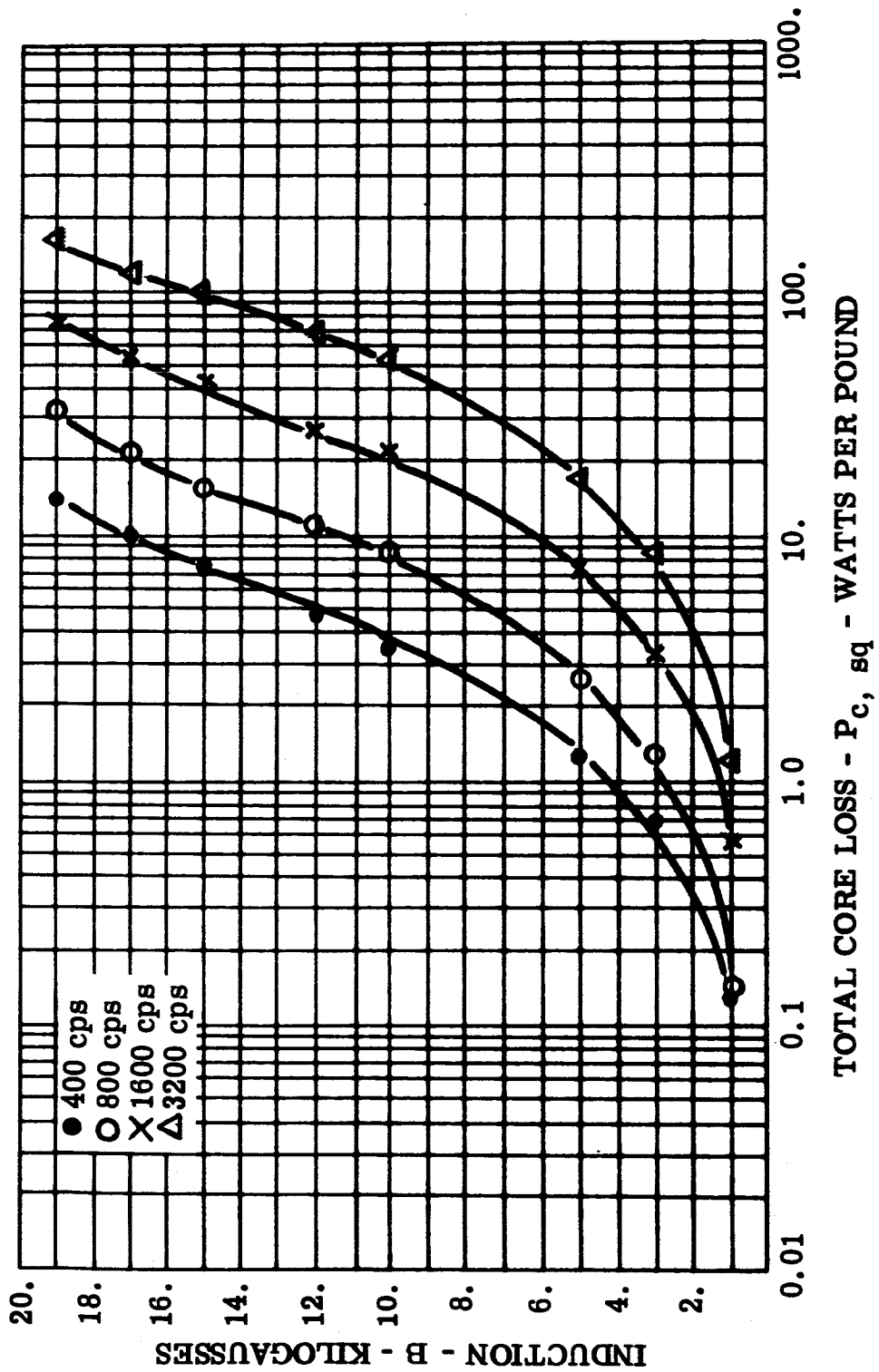


FIGURE 10. P_c , sq - Total Core Loss, 0.002 Inch Cubex Toroid, Core 74,
Magnetic Field Annealed, Room Ambient

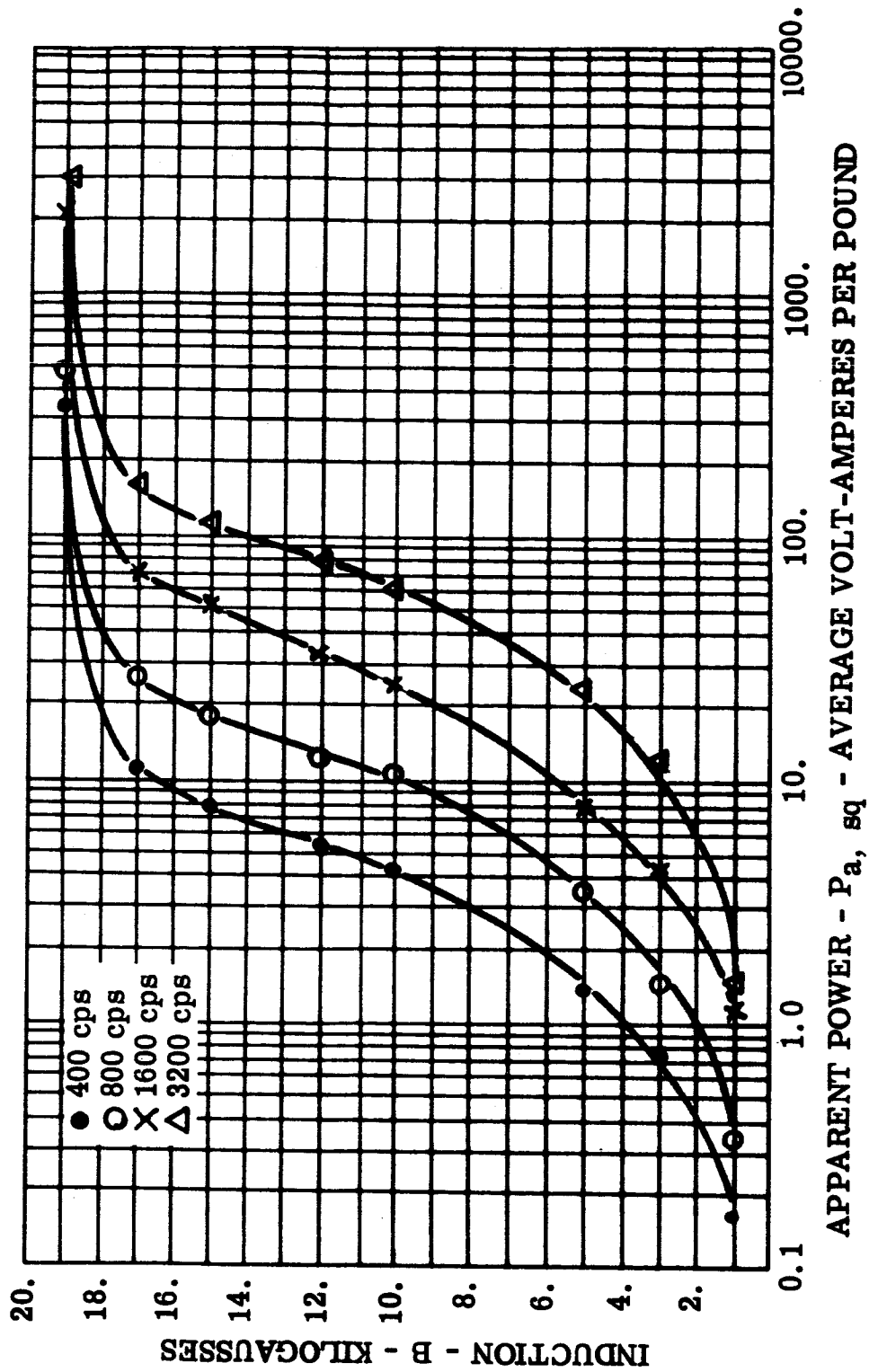


FIGURE 11. P_a, sq - Apparent Power, 0.002 Inch Cubex Toroid, Core 74, Magnetic Field Annealed, Room Ambient

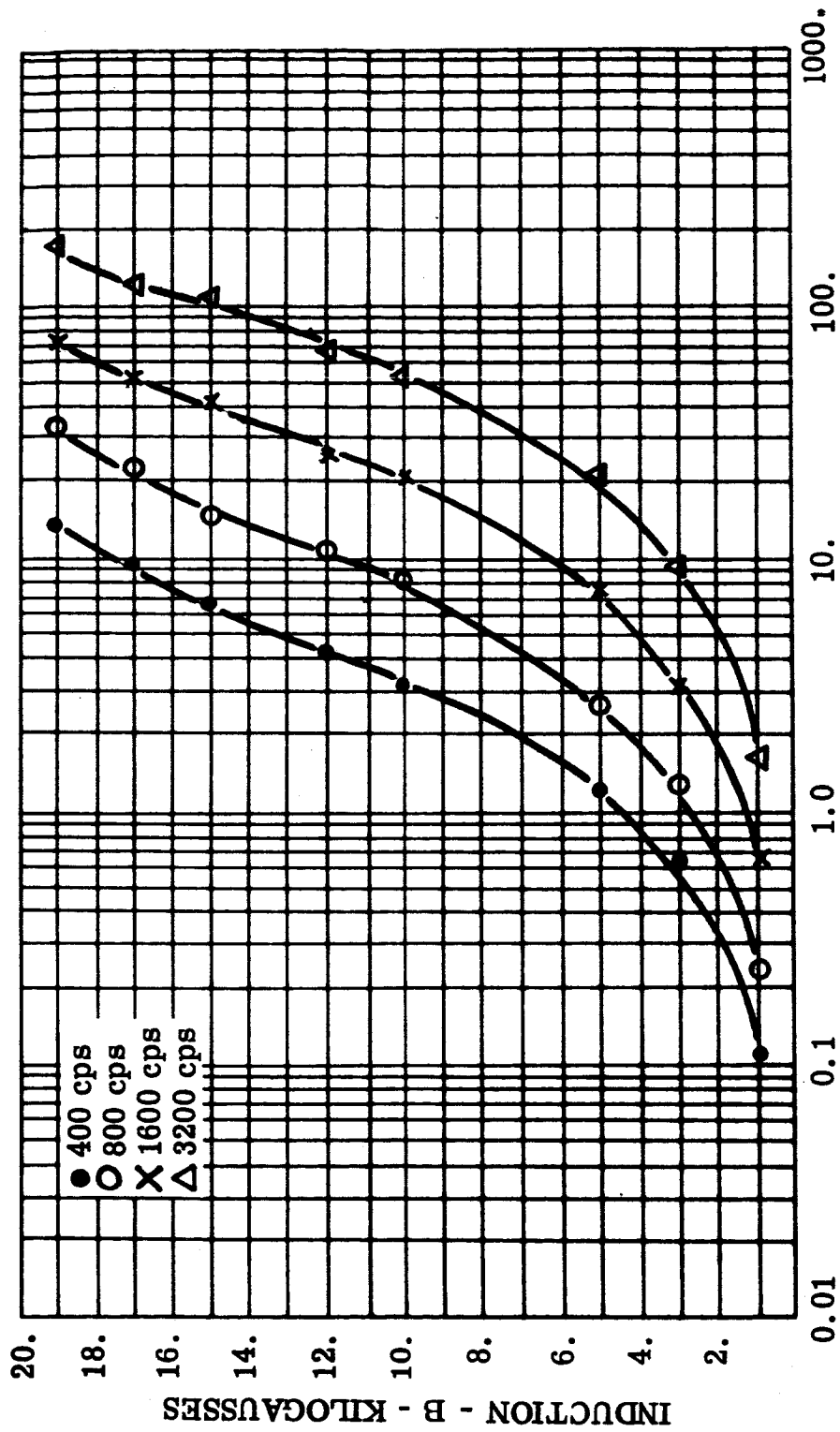


FIGURE 12 P_c , sq - Total Core Loss, 0.002 Inch Cubex Toroid, Core 74,
Magnetic Field Annealed, -55°C

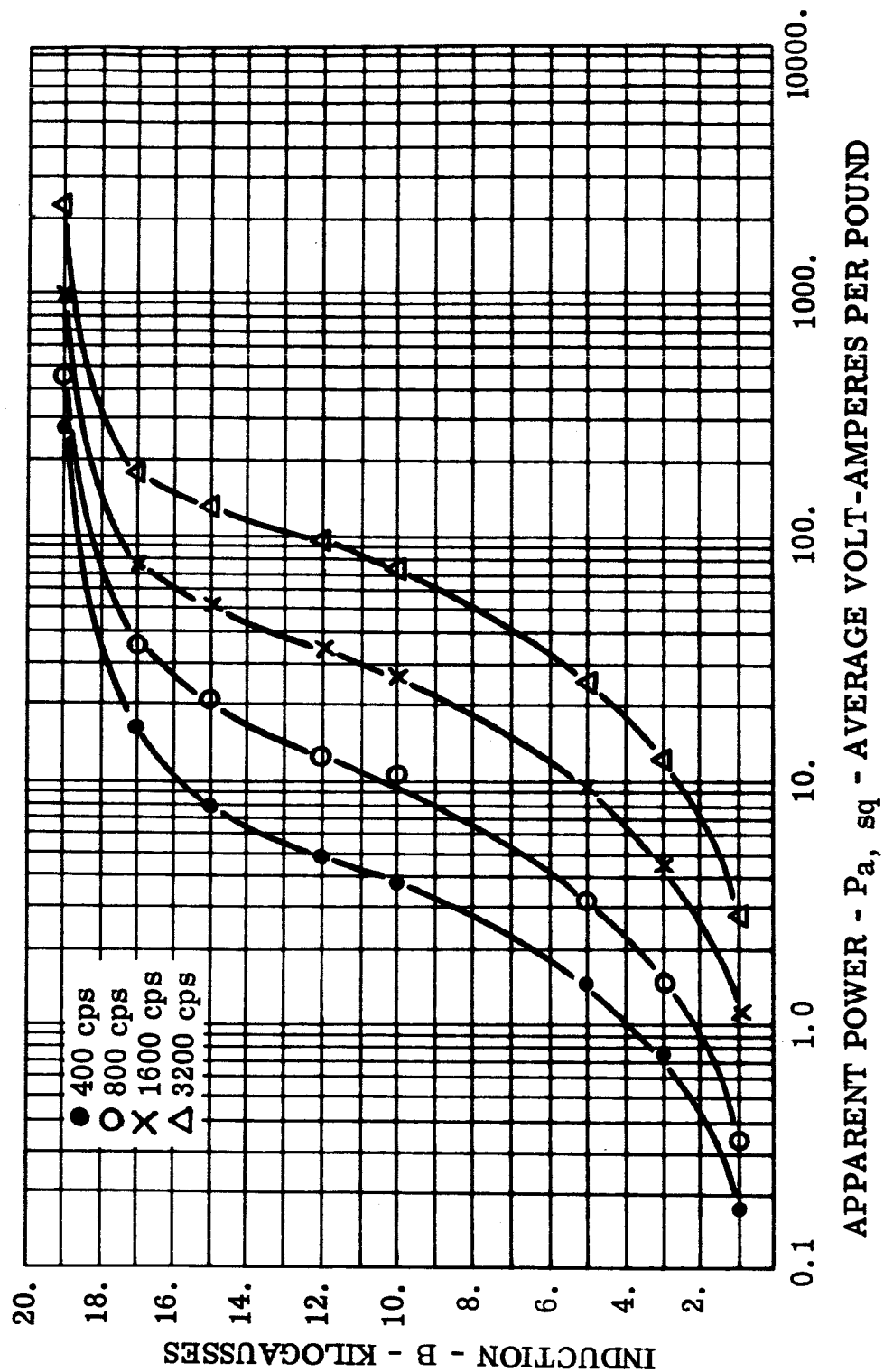


FIGURE 13 P_a, sq - Apparent Power, 0.002 Inch Cubex Toroid, Core 74,
Magnetic Field Annealed, -55°C

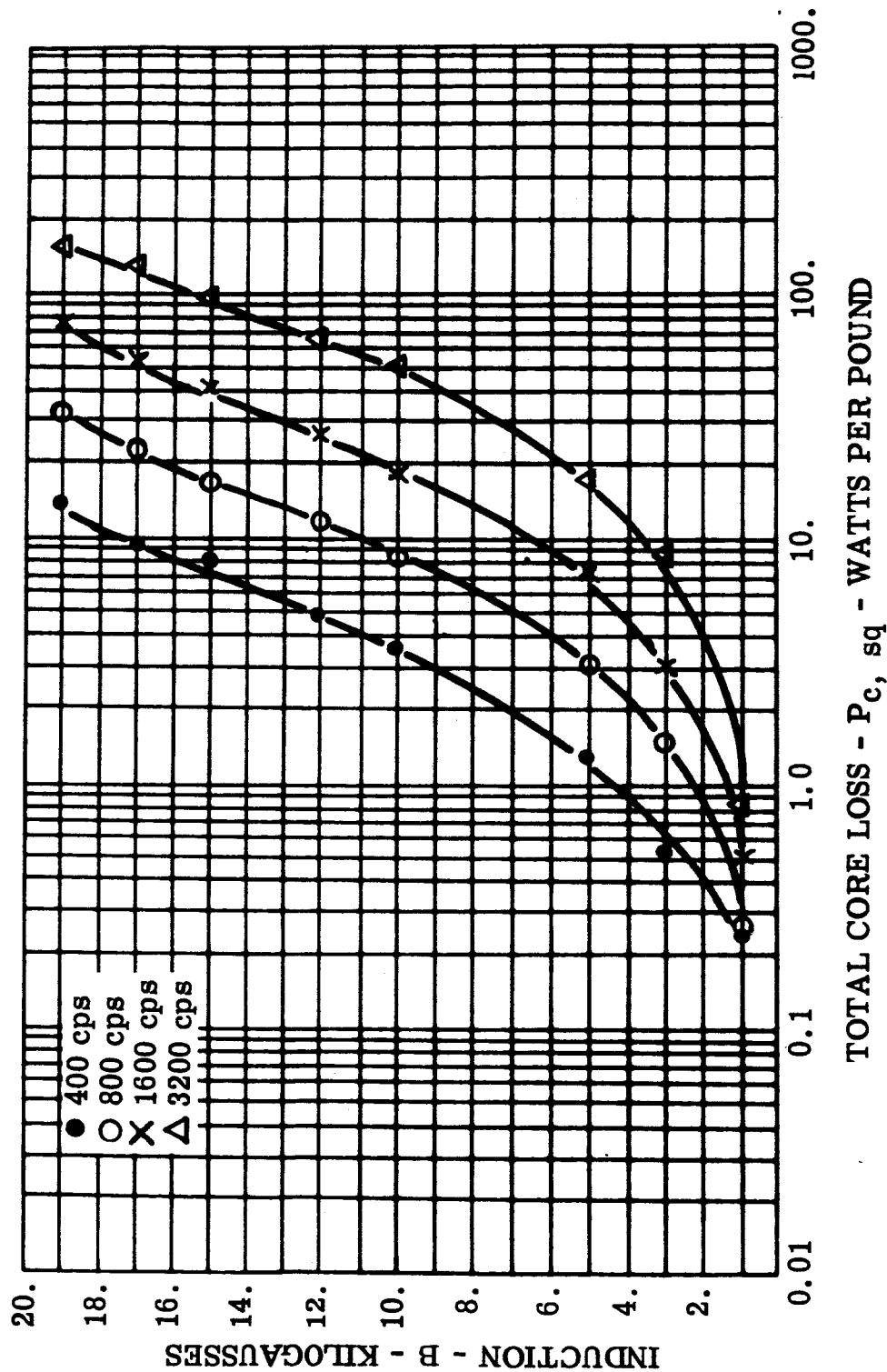


FIGURE 14 $P_{c, sq}$ - Total Core Loss, 0.002 Inch Cubex Toroid, Core 75,
Magnetic Field Annealed, Room Ambient

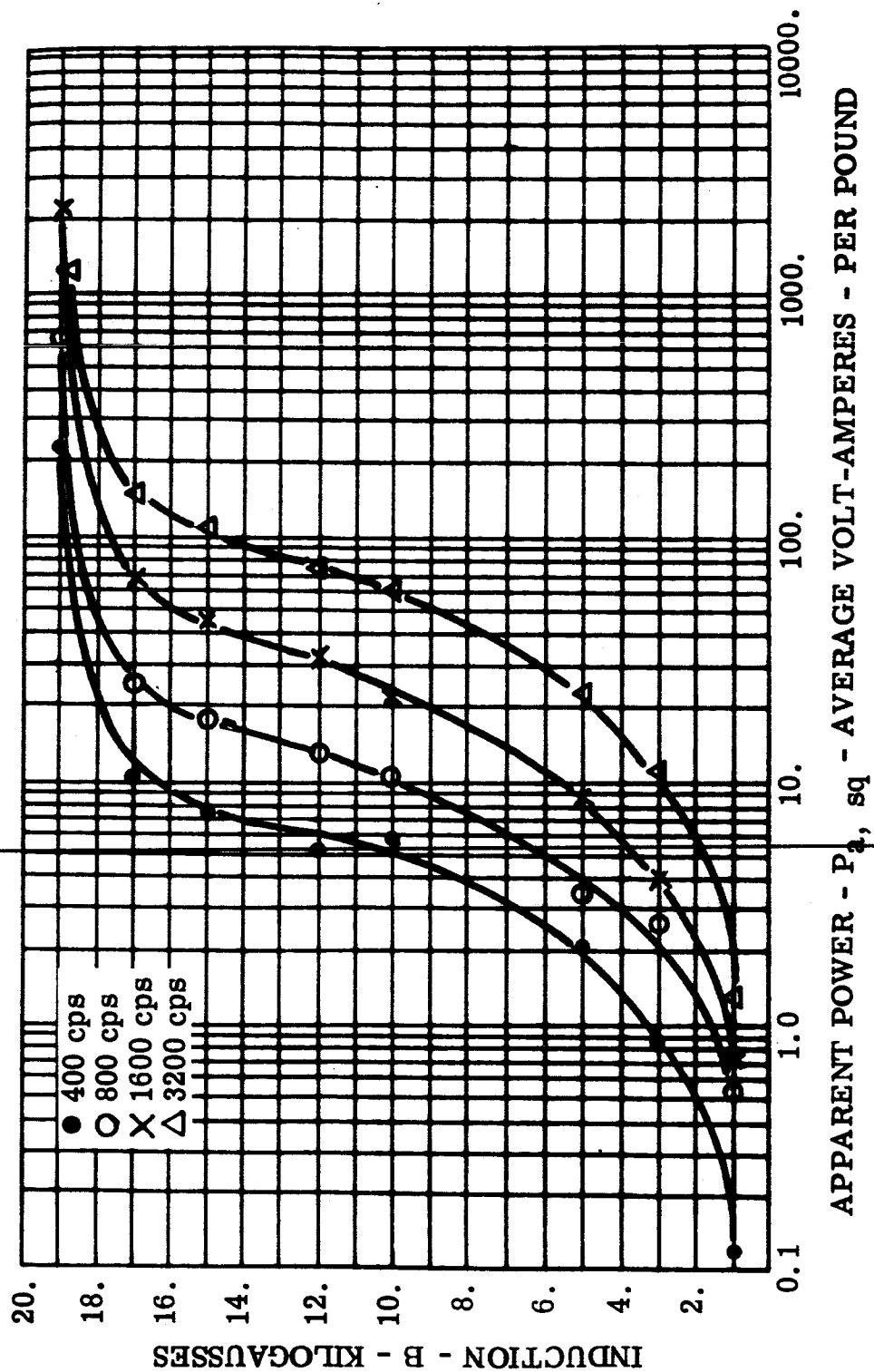


FIGURE 15 P_a, sq - Apparent Power, 0.002 Inch Cubex Toroid, Core 75, Magnetic Field Annealed, Room Ambient

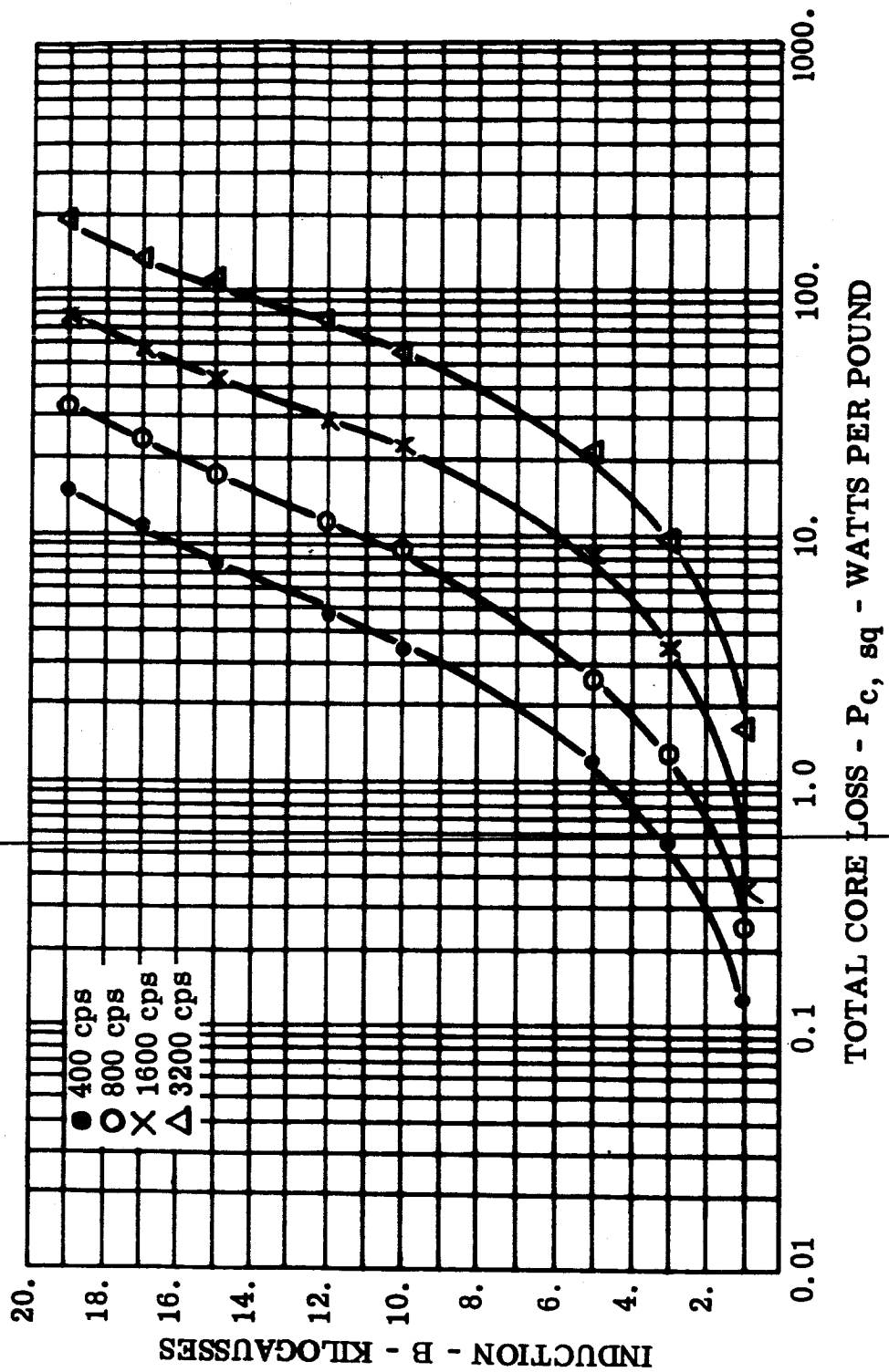


FIGURE 16 P_c , sq - Total Core Loss, 0.002 Inch Cubex Toroid, Core 75,
Magnetic Field Annealed, -55°C

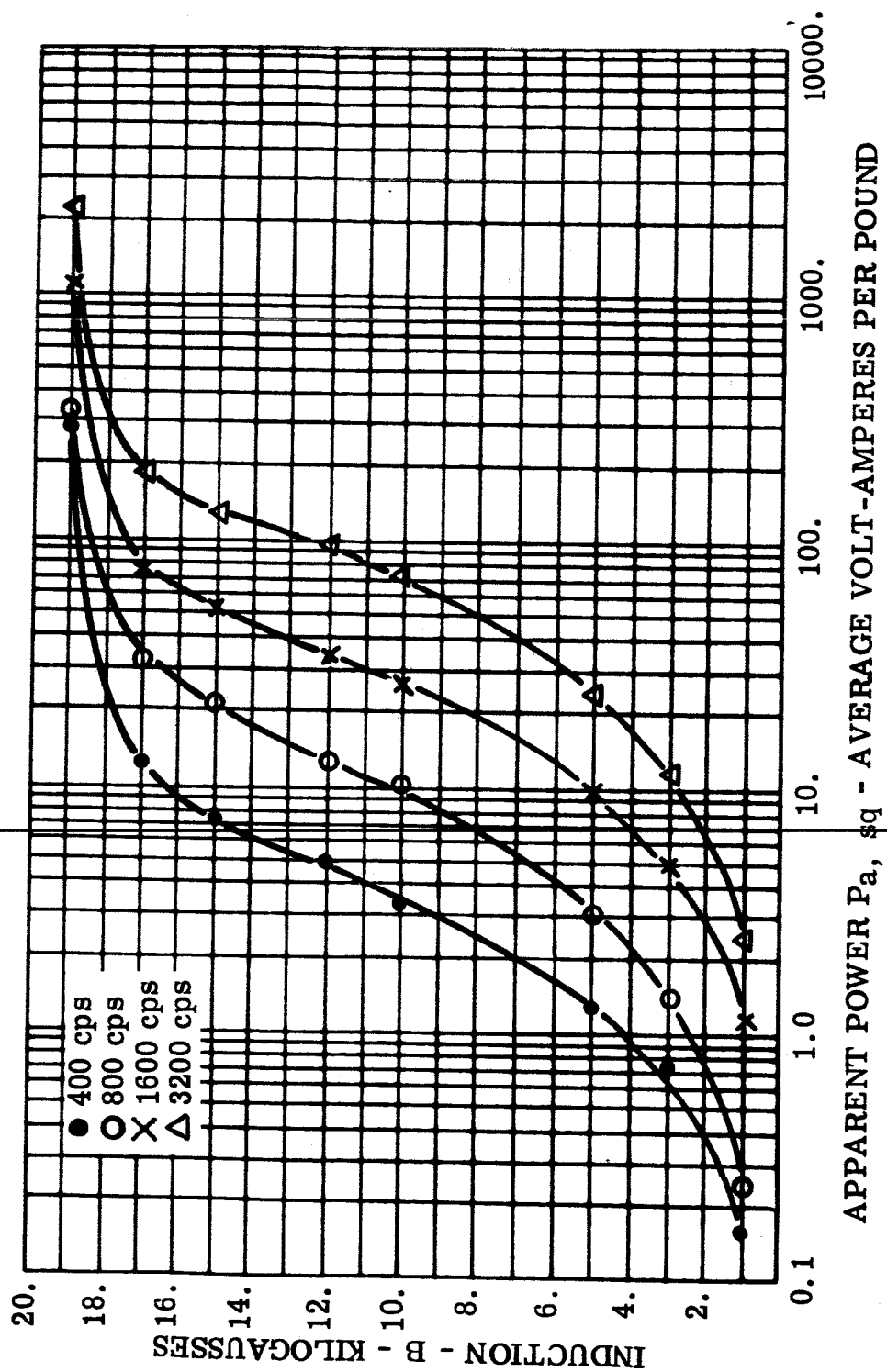


FIGURE 17 P_a, sq - Apparent Power, 0.002 Inch Cubex Toroid, Core 75,
Magnetic Field Annealed, $-55^{\circ}C$

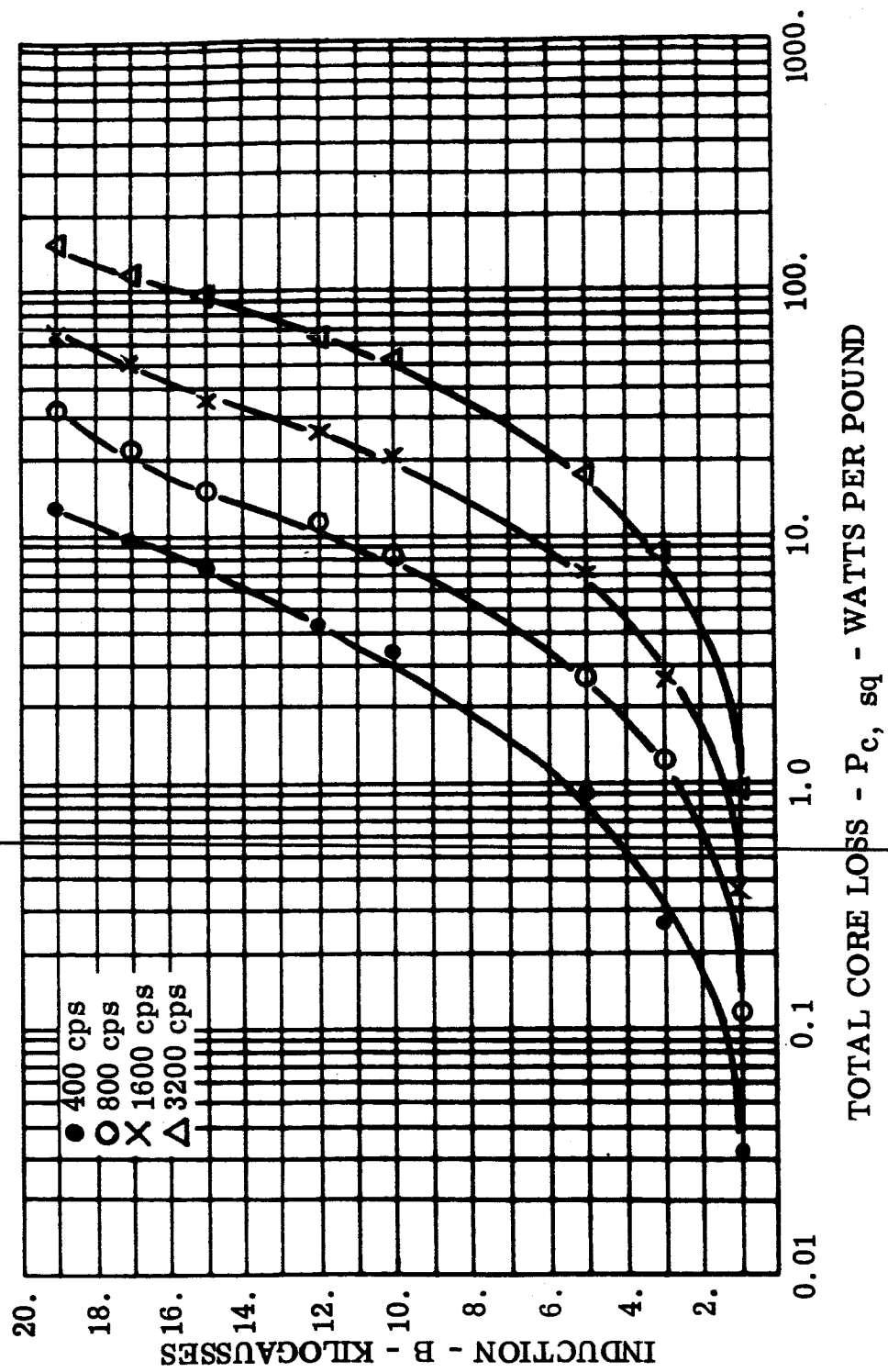
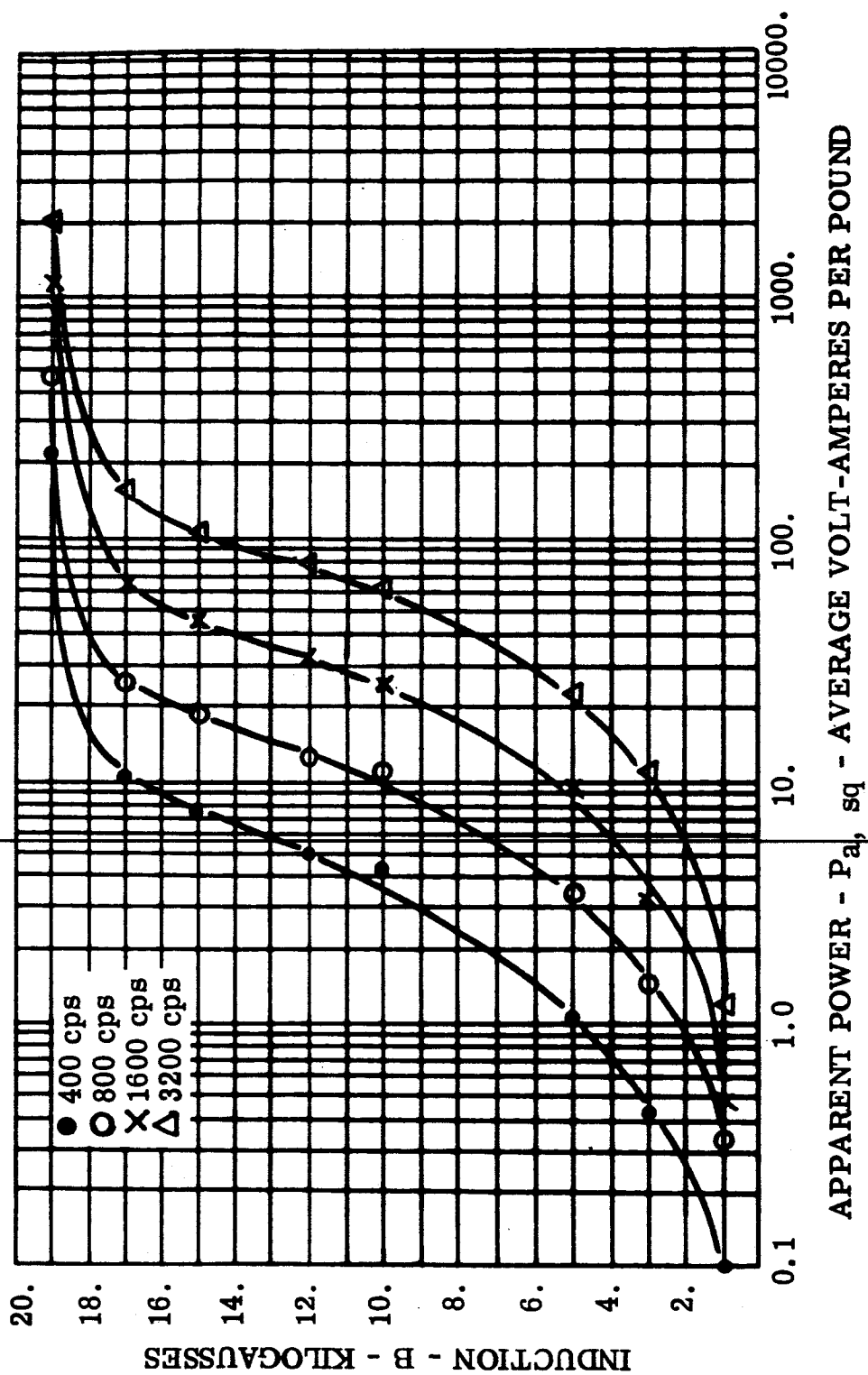


FIGURE 18 $P_{c, sq}$ - Total Core Loss, 0.002 Inch Cubex Toroid, Core 76,
Magnetic Field Annealed, Room Ambient



APPARENT POWER - $P_{a, sq}$ - AVERAGE VOLT-AMPERES PER POUND

FIGURE 19 $P_{a, sq}$ - Apparent Power, 0.002 Inch Cubex Toroid, Core 76, Magnetic Field Annealed, Room Ambient

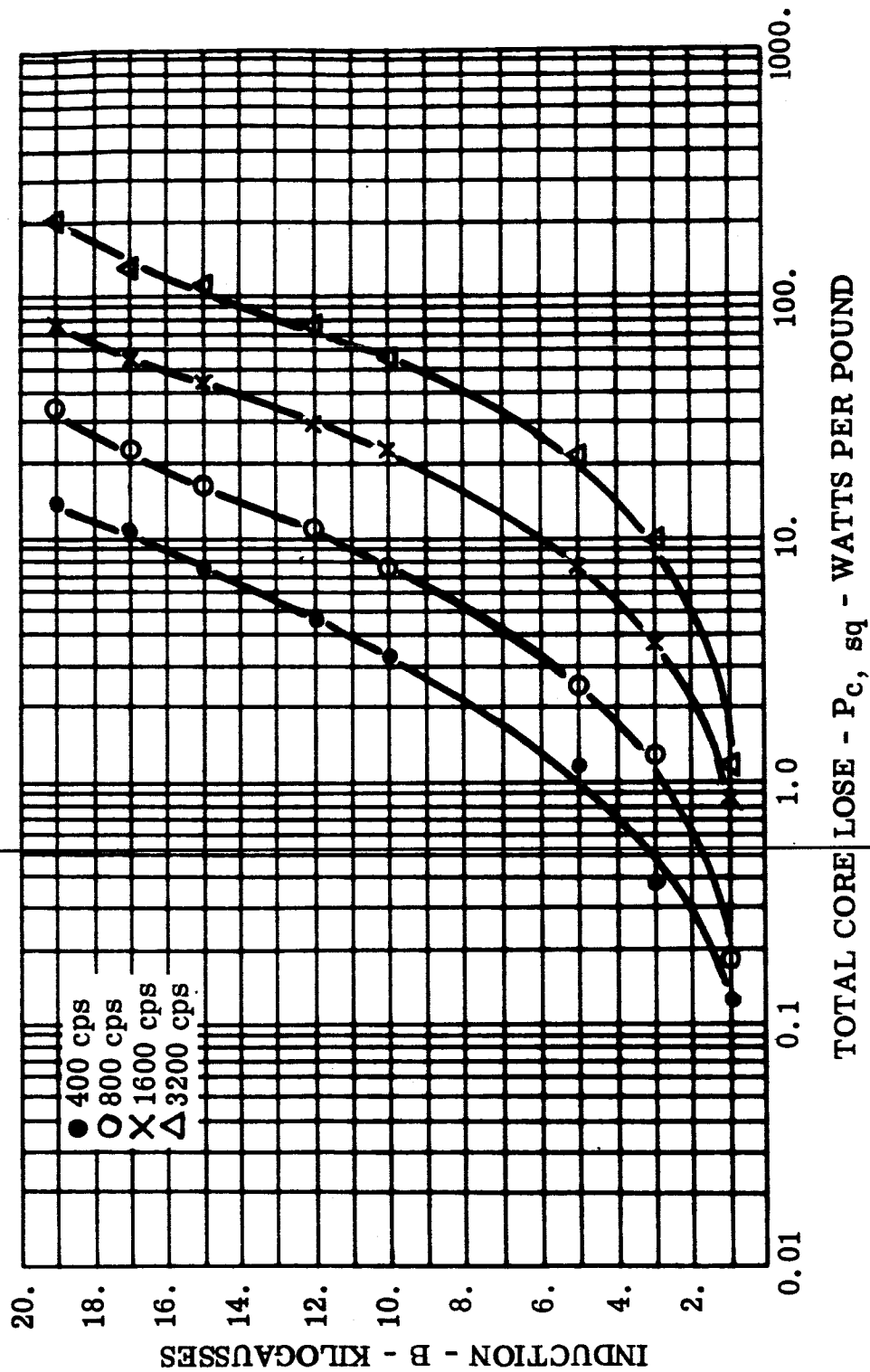


FIGURE 20 P_c , sq - Total Core Loss, 0.002 Inch Cubex Toroid, Core 76,
Magnetic Field Annealed, -55°C

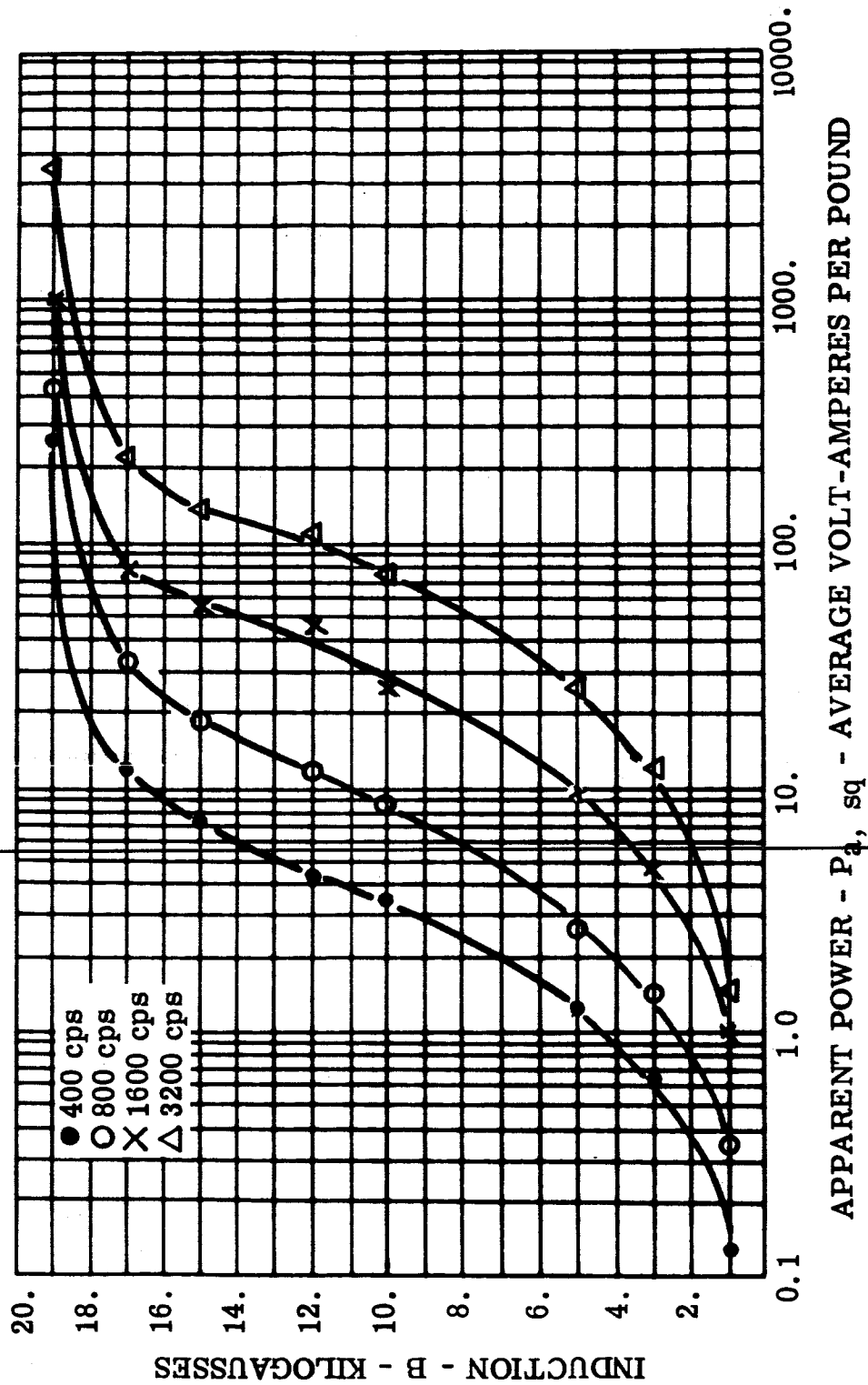


FIGURE 21 P_a , sq - Apparent Power, 0.002 Inch Cubex Toroid, Core 76, Magnetic Field Annealed, -55°C

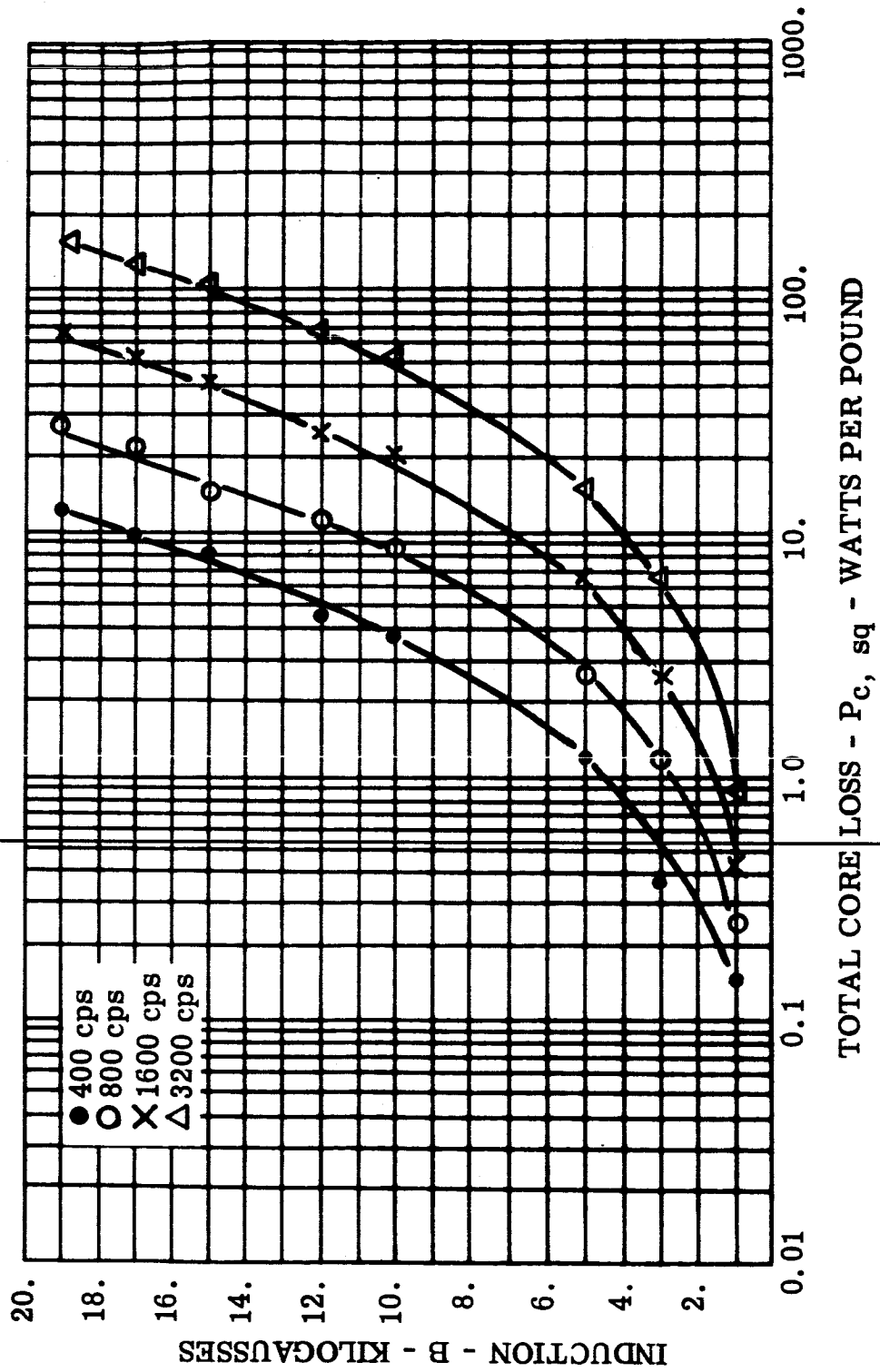


FIGURE 22 P_c , sq - Total Core Loss, 0.002 Inch Cubex Toroid, Core 79, Stress Relief Annealed, Room Ambient

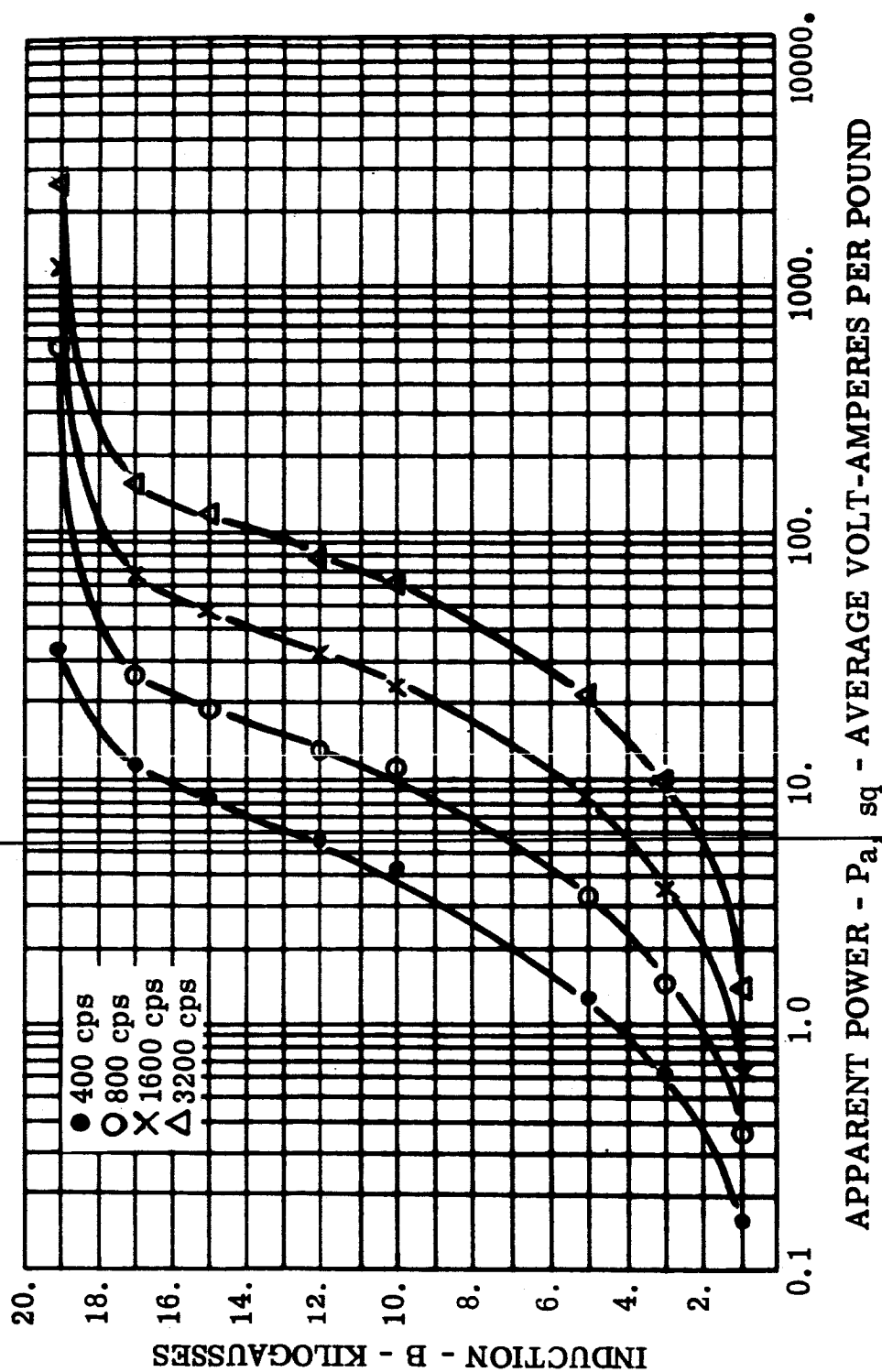


FIGURE 23 $P_{a, sq}$ - Apparent Power, 0.002 Inch Cubex Toroid, Core 79. Stress Relief Annealed, Room Ambient

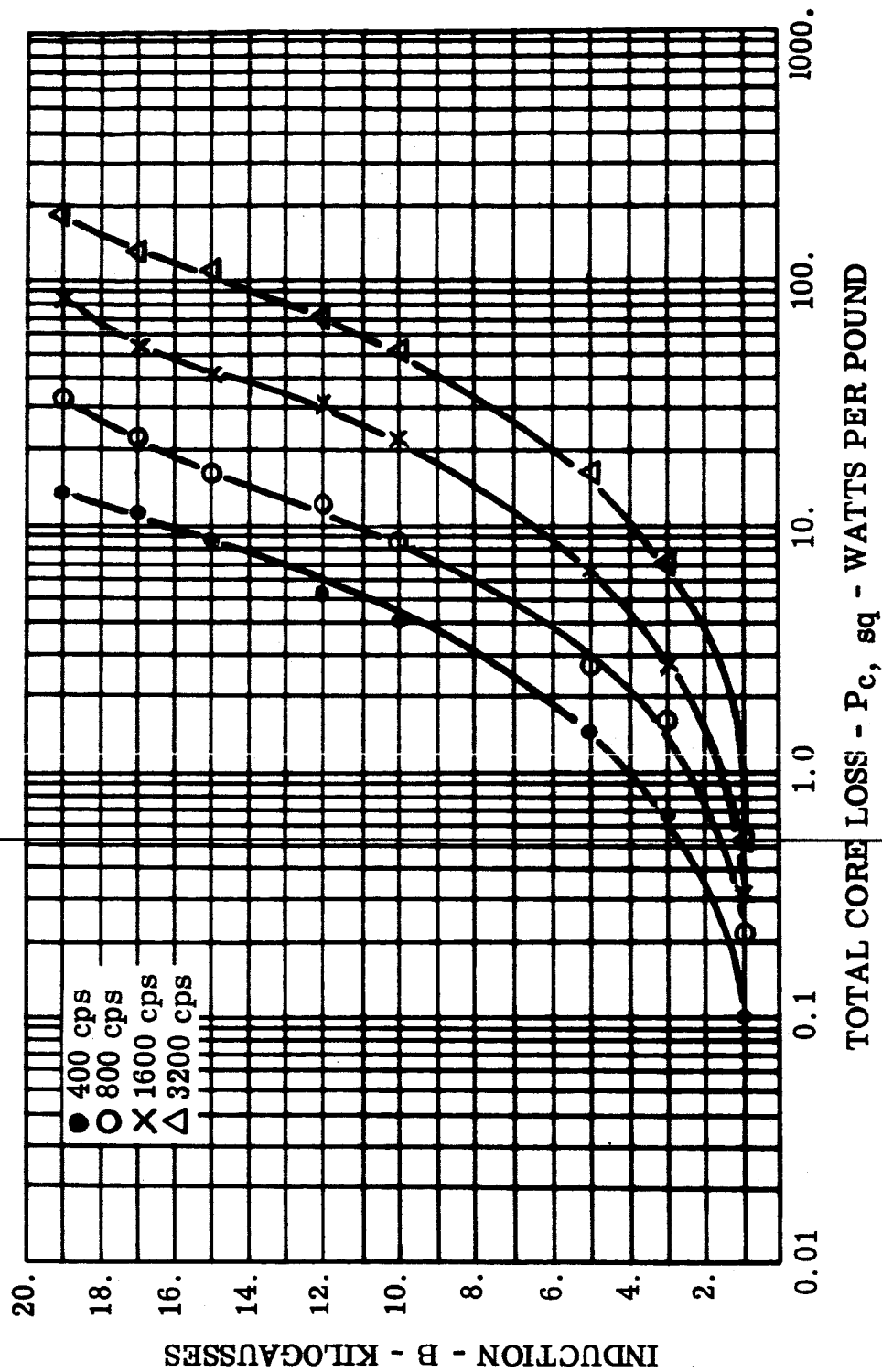
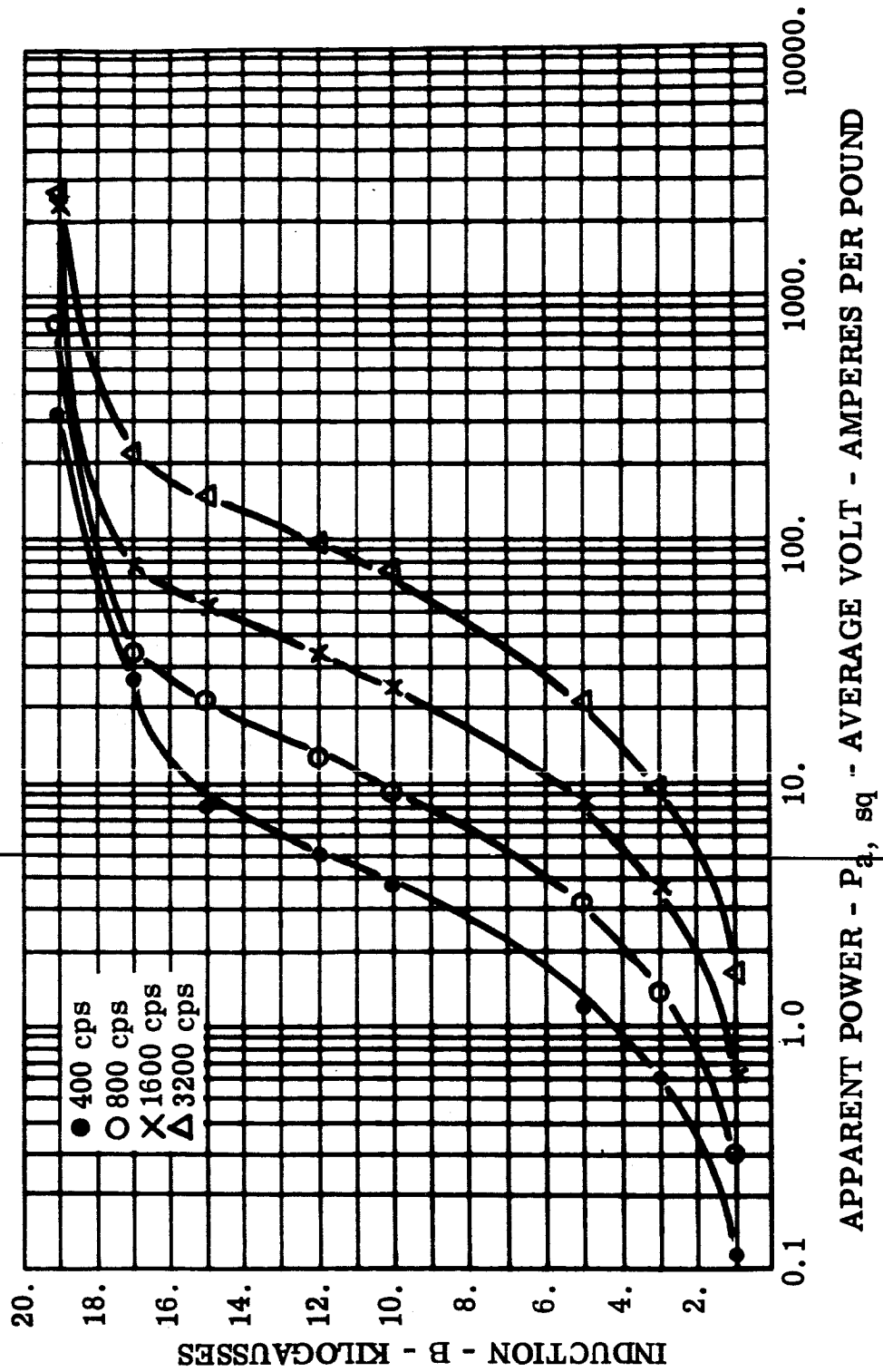


FIGURE 24 P_c , sq - Total Core Loss, 0.002 Inch Cubex Toroid, Core 79, Stress Relief Annealed, -55°C



APPARENT POWER - P_a , sq - AVERAGE VOLT - AMPERES PER POUND

FIGURE 25 P_a , sq - Apparent Power, 0.002 Inch Cubex Toroid, Core 79, Stress Relief Annealed, -55°C

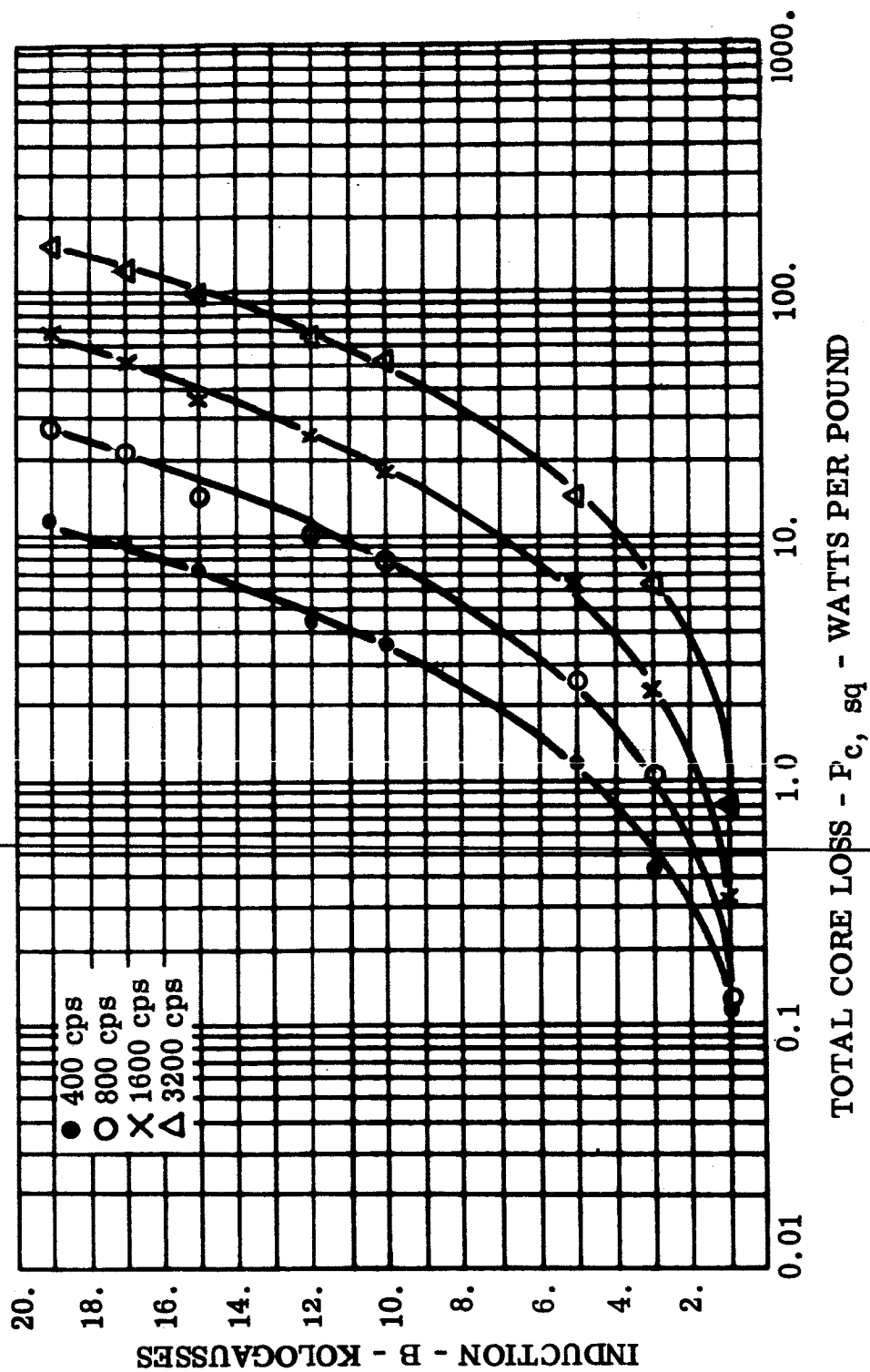


FIGURE 26 $P_{c, sq}$ - Total Core Loss, 0.002 Inch Cubex Toroid, Core 80, Stress Relief Annealed, Room Ambient

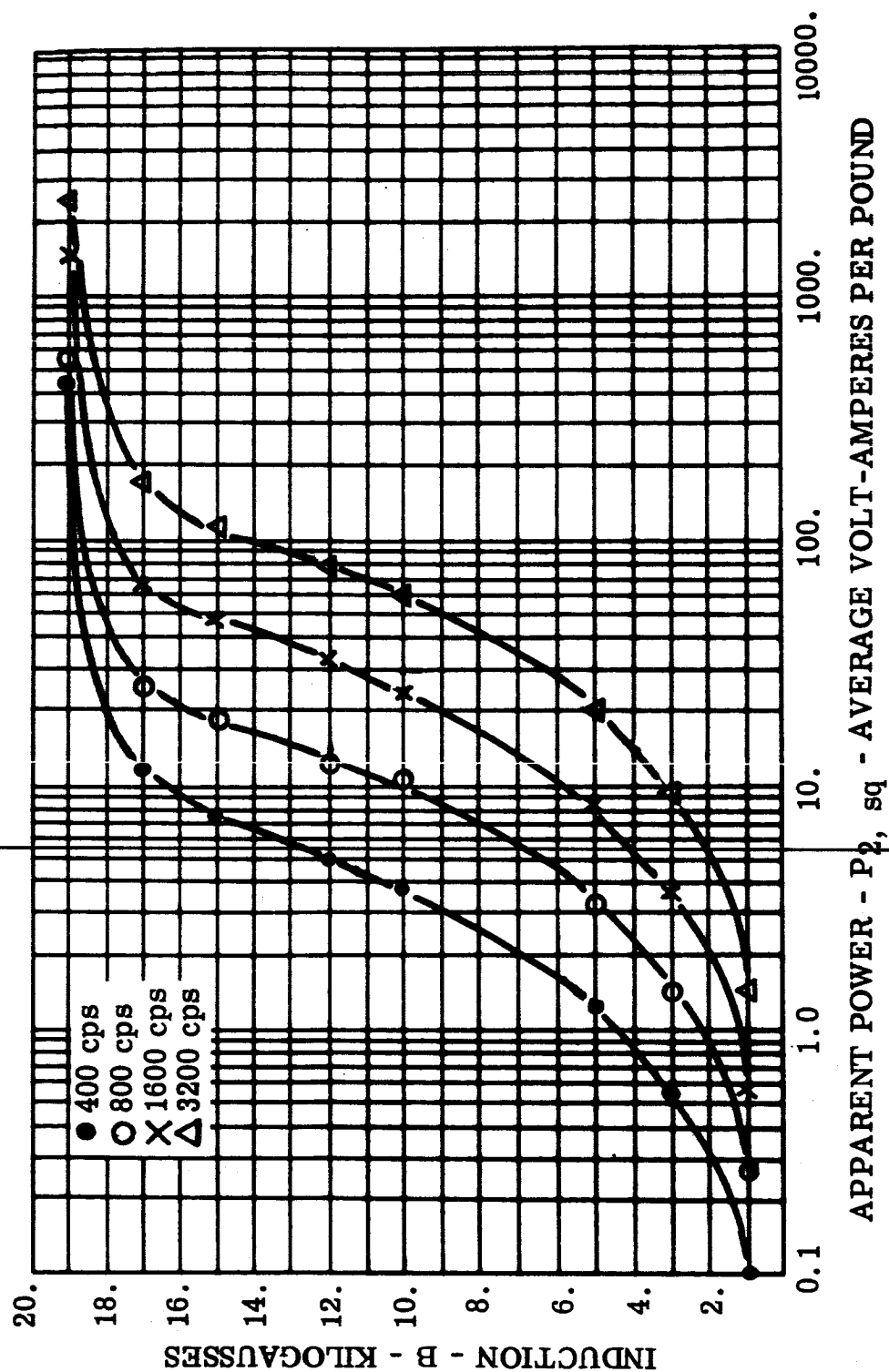


FIGURE 27 P_a , sq - Apparent Power, 0.002 Inch Cubex Toroid, Core 80,
Stress Relief Annealed, Room Ambient

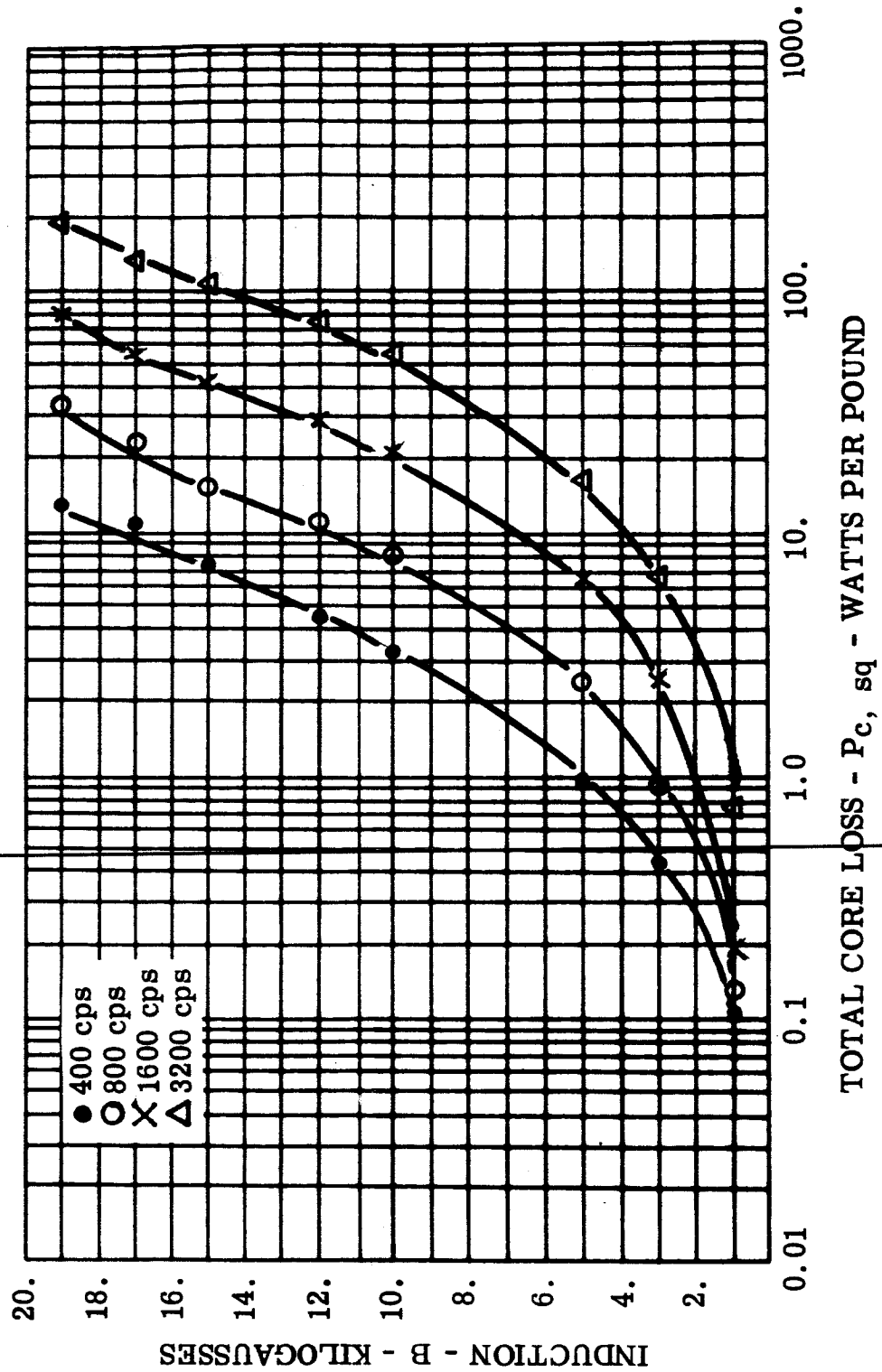


FIGURE 28 P_c , sq - Total Core Loss, 0.002 Inch Cubex Toroid, Core 80,
Stress Relief Annealed, -55°C

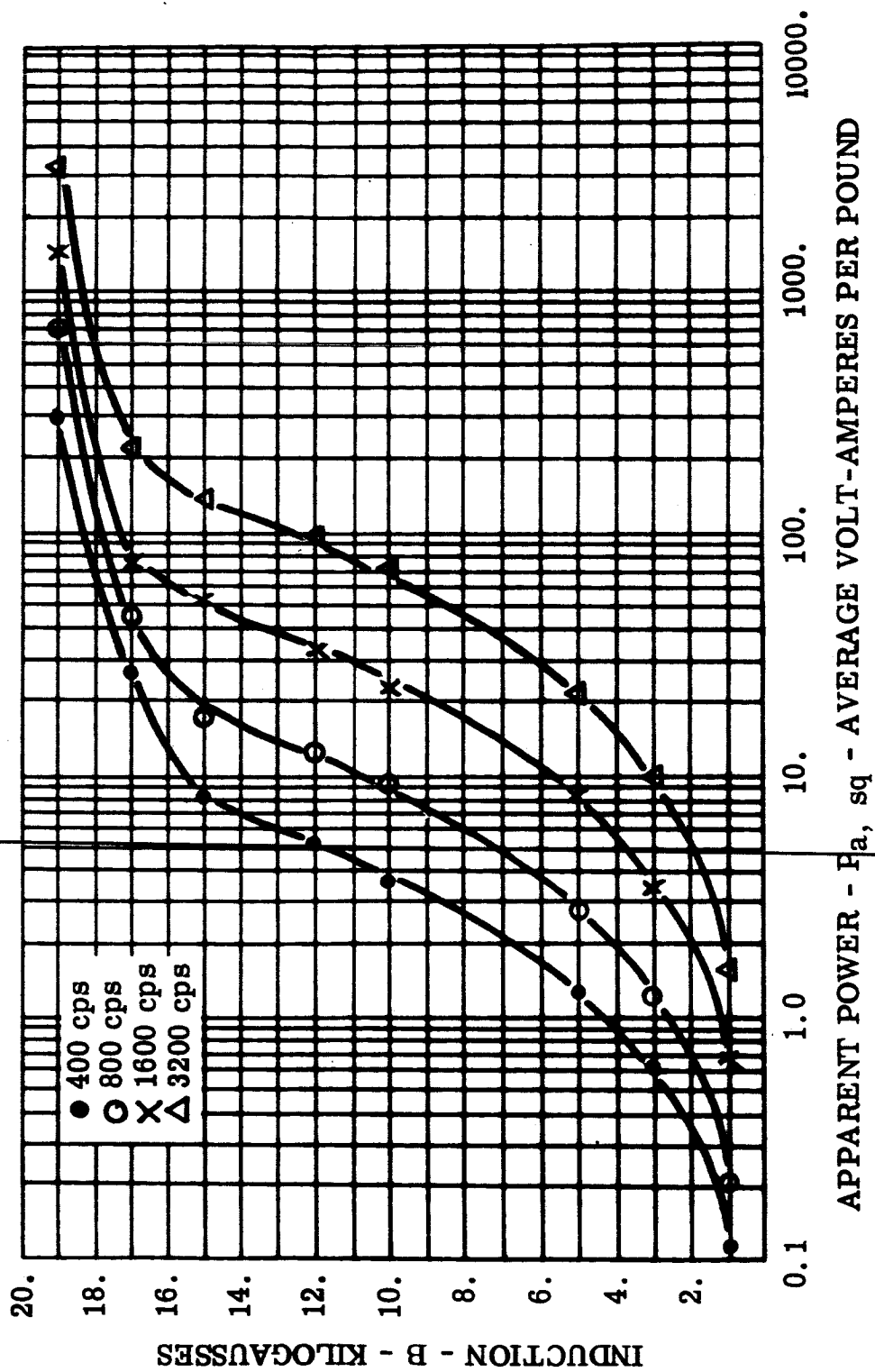


FIGURE 29 P_a, sq - Apparent Power, 0.002 Inch Cubex Toroid, Core 80,
Stress Relief Annealed, $-55^{\circ}C$

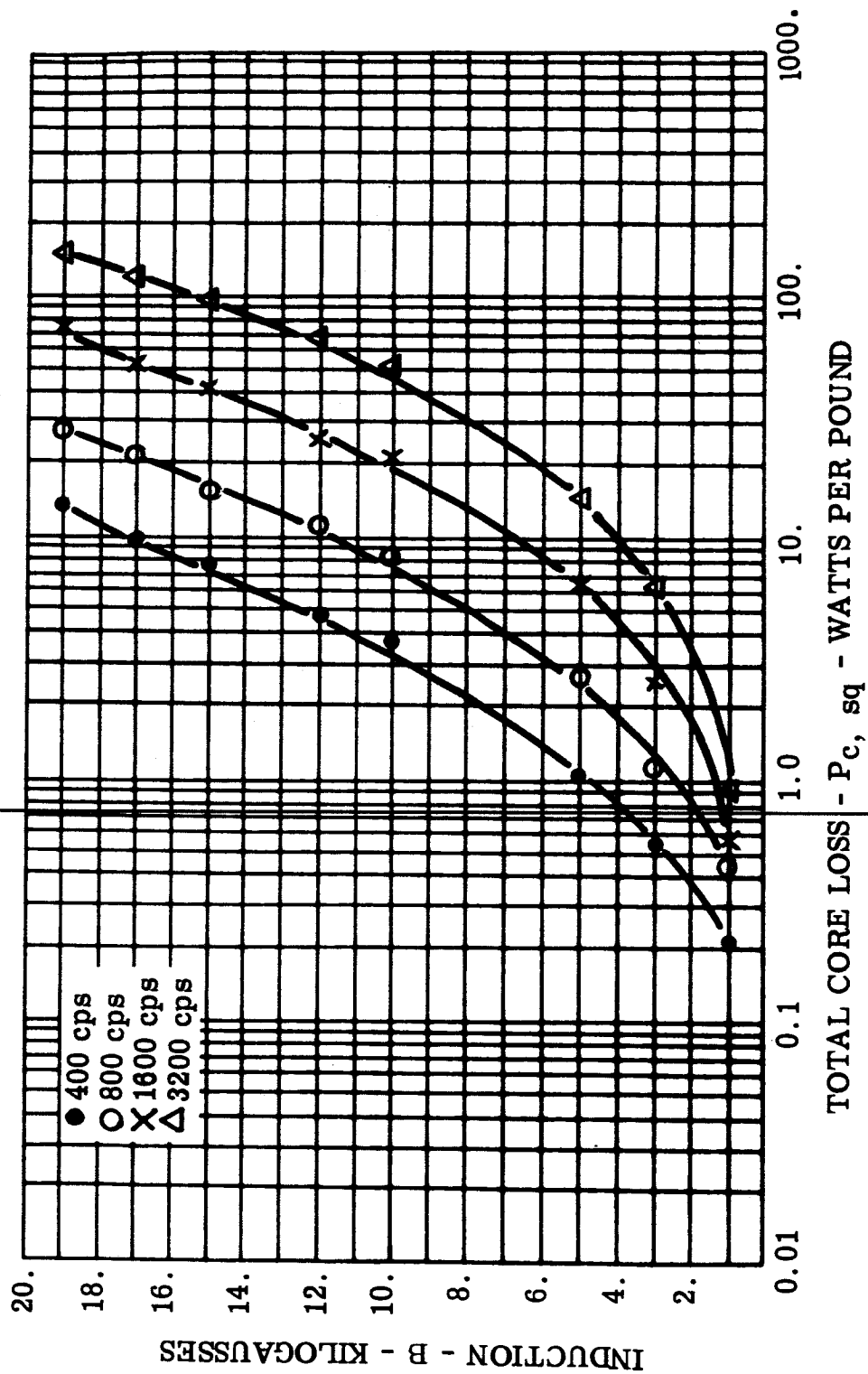


FIGURE 30 $P_{c, sq}$ - Total Core Loss, 0.002 Inch Cubex Toroid, Core 81, Stress Relief Annealed, Room Ambient

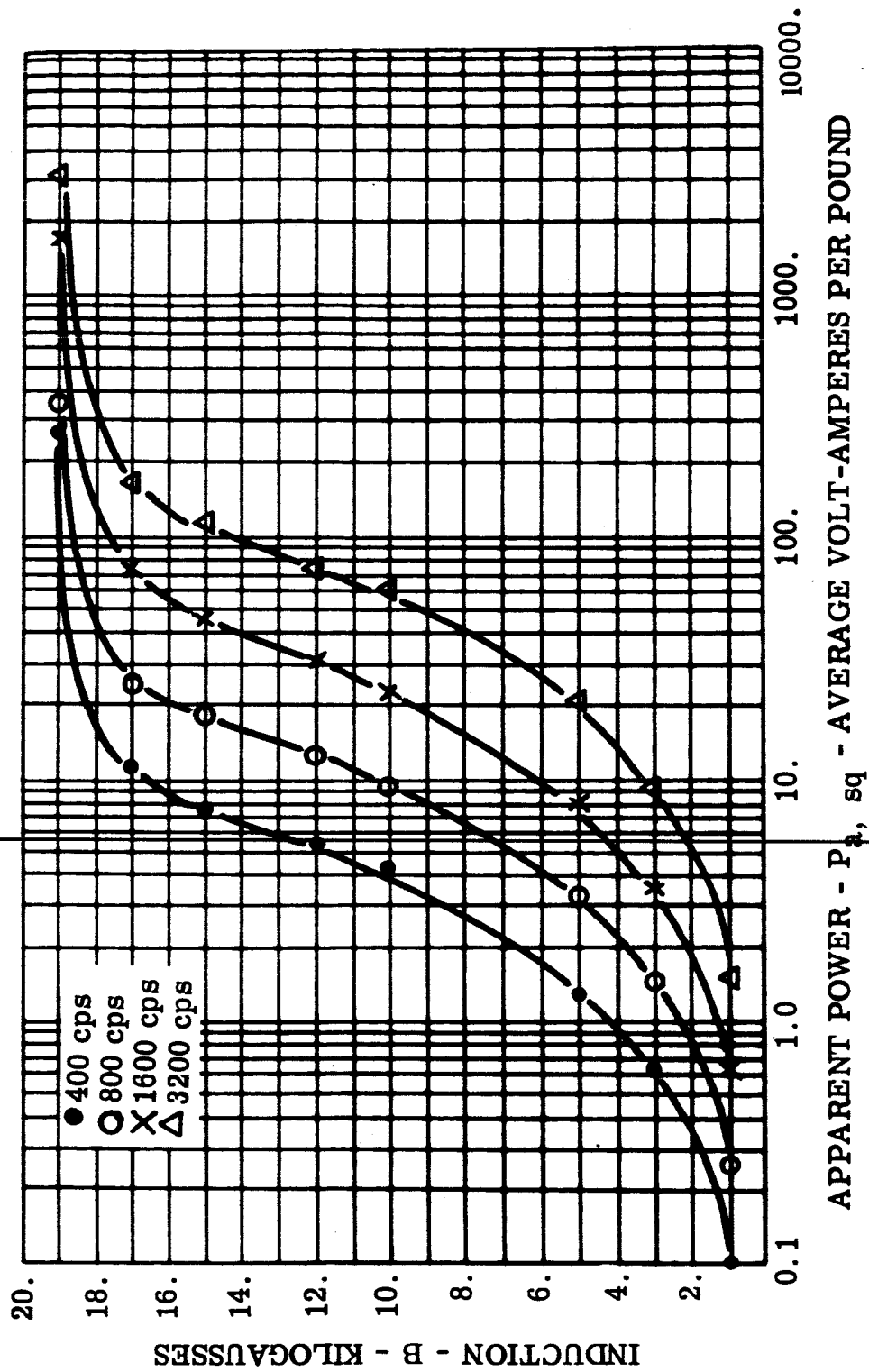


FIGURE 31 P_a, sq - Apparent Power, 0.002 Inch Cubex Toroid, Core 81, Stress Relief Annealed, Room Ambient

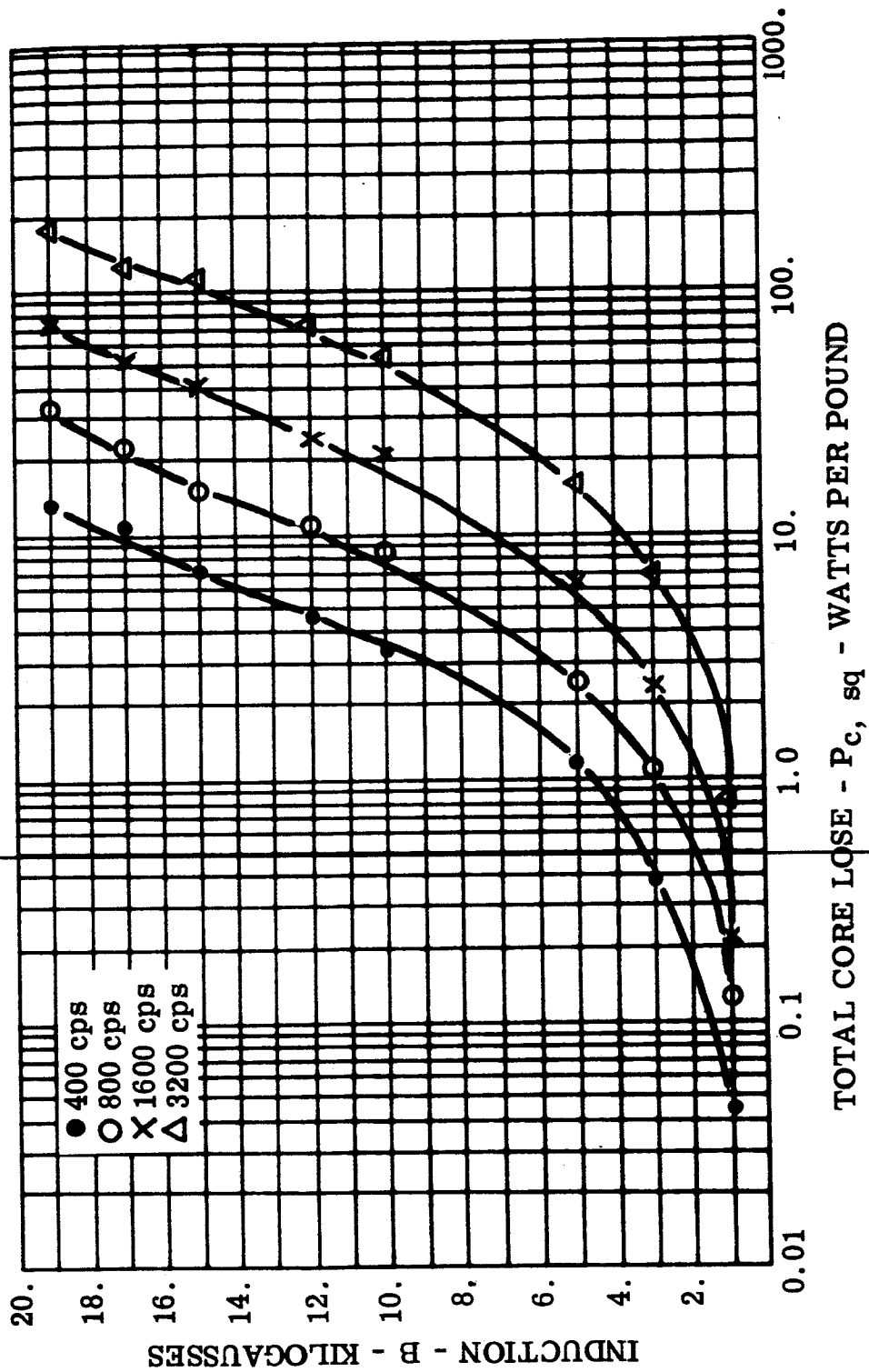


FIGURE 32 P_c , sq - Total Core Loss, 0.002 Inch Cubex Toroid, Core 81,
Stress Relief Annealed, -55°C

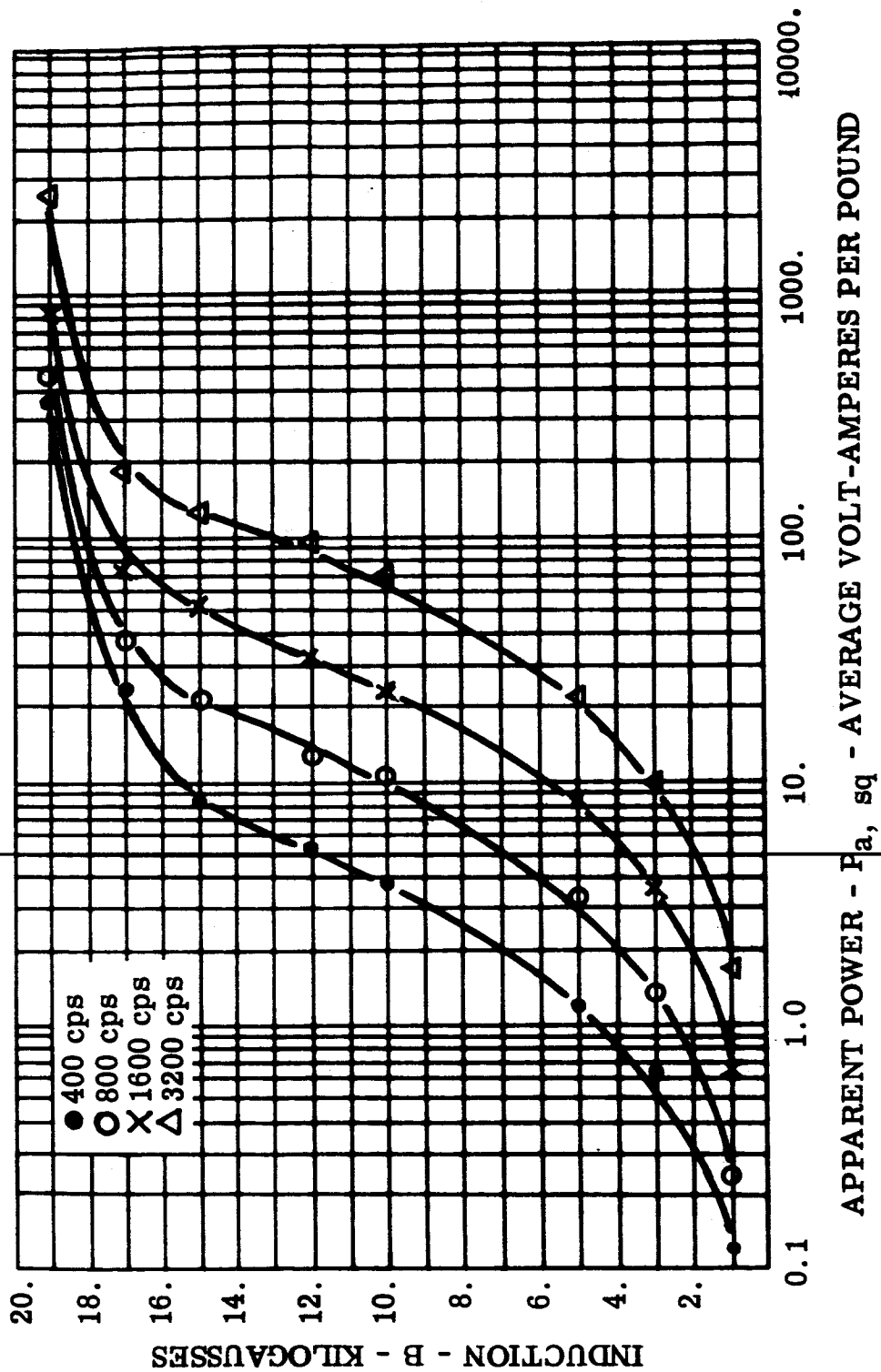


FIGURE 33 P_a , sq - Apparent Power, 0.002 Inch Cubex Toroid, Core 81,
Stress Relief Annealed, -55°C

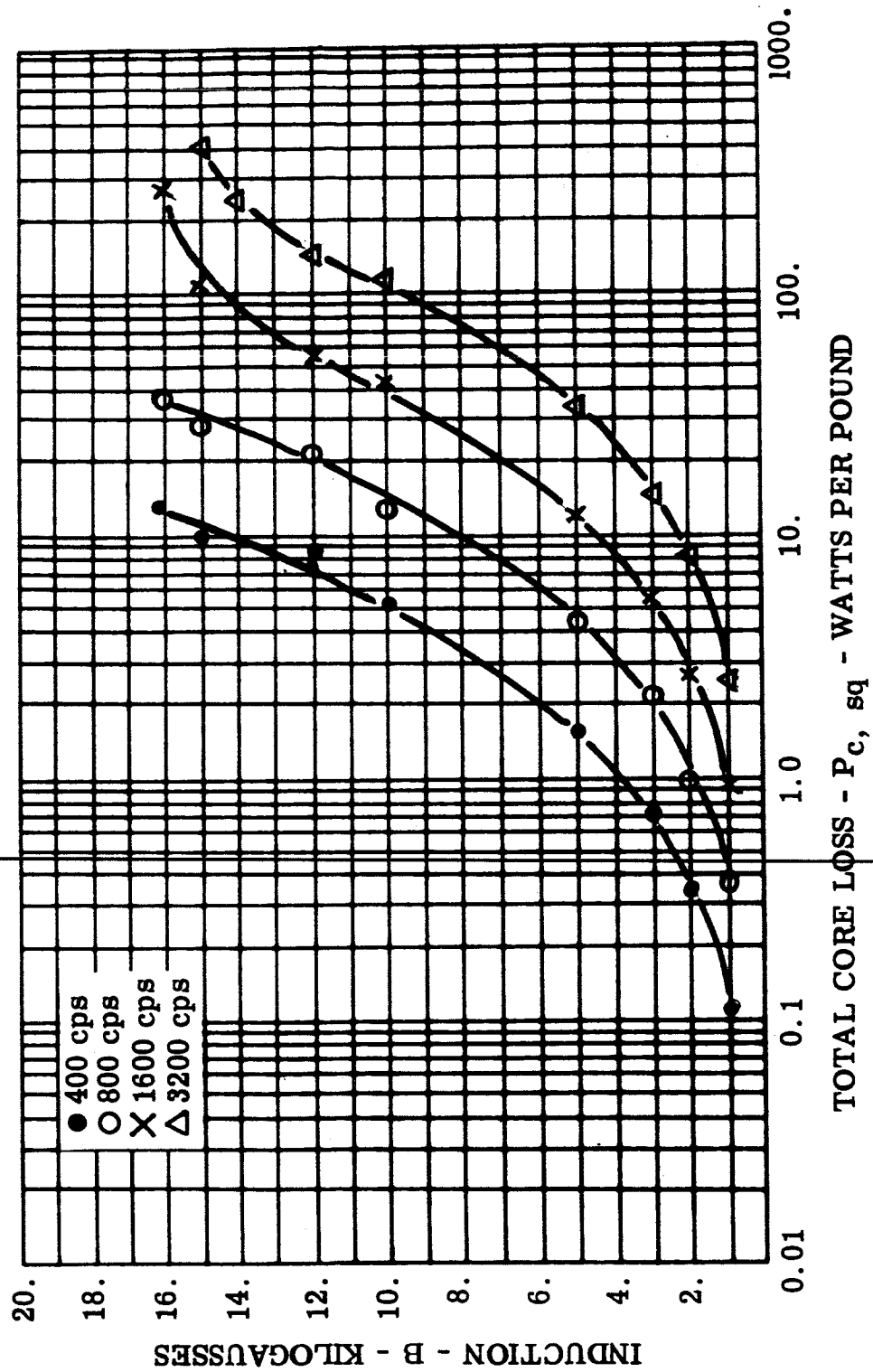
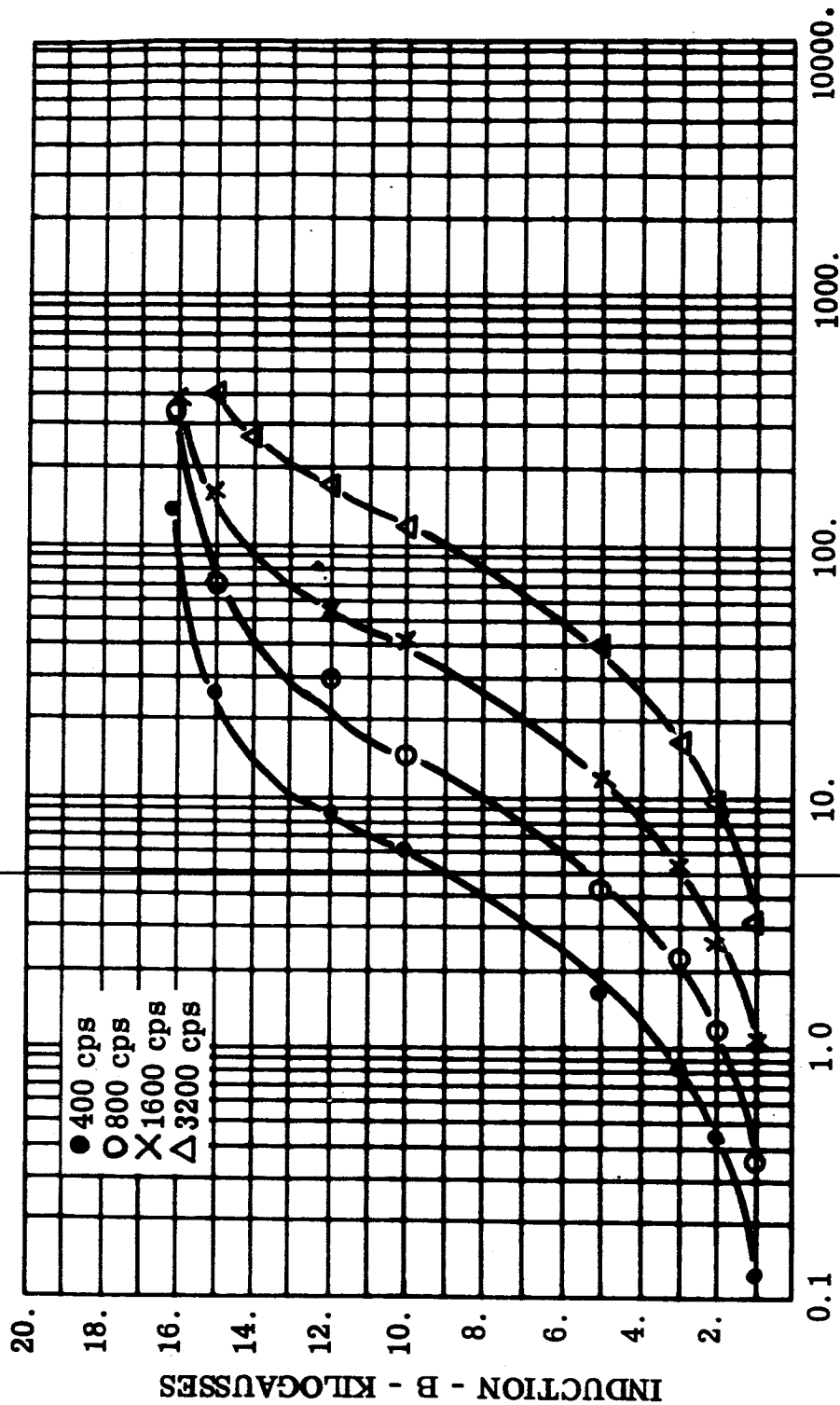


FIGURE 34 P_c , sq - Total Core Loss, 0.006 Inch Cubex Double Window, Core 1, Magnetic Field Annealed, Room Ambient



APPARENT POWER - P_a, sq - AVERAGE VOLT-AMPERES PER POUND

FIGURE 35 P_a, sq - Apparent Power, 0.006 Inch Cubex Double Window,
Core 1, Magnetic Field Annealed, Room Ambient

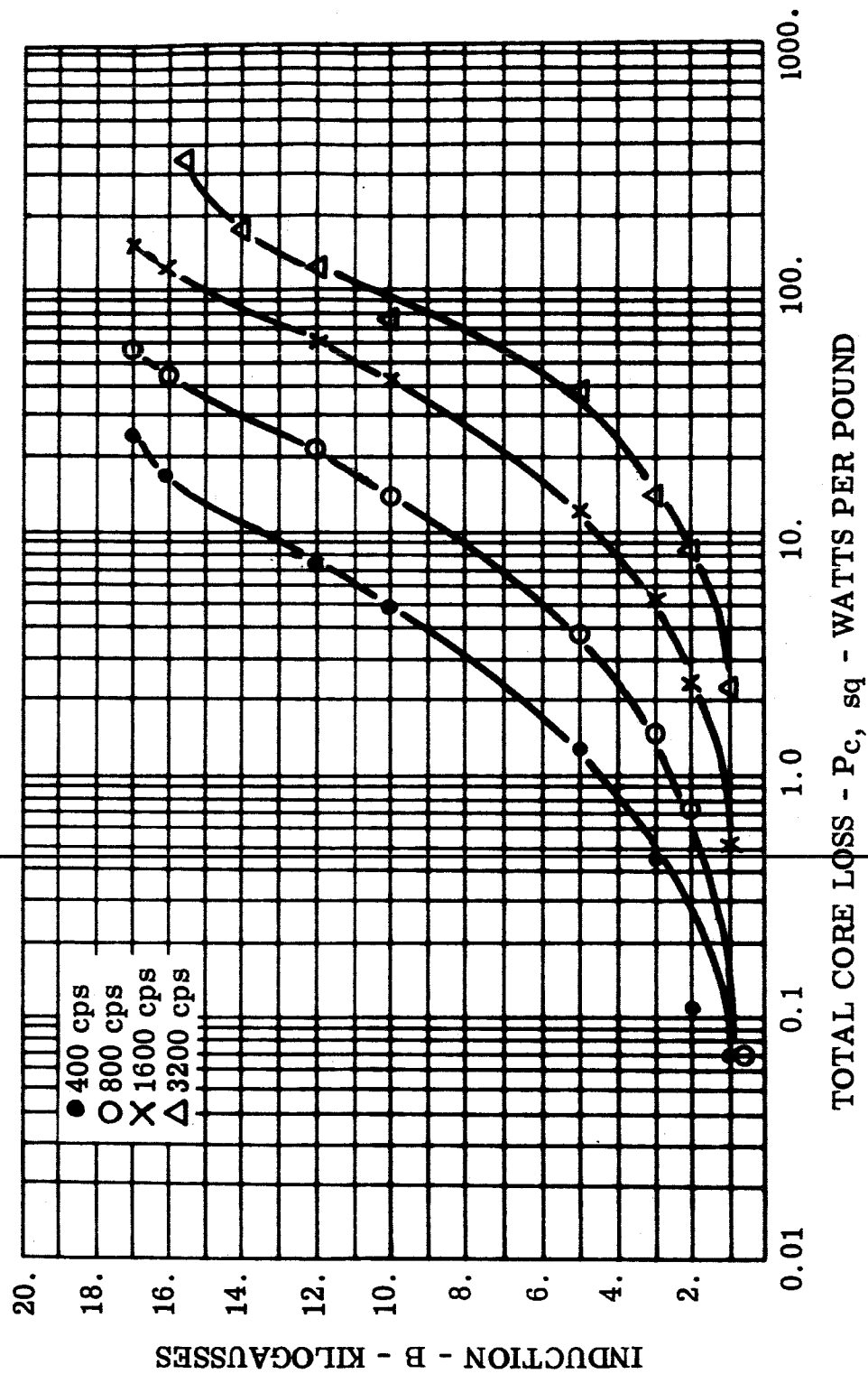


FIGURE 36 P_c , sq - Tdtal Core Loss, 0.006 Inch Cubex Double Window,
Core 1, Magnetic Field Annealed, -55°C

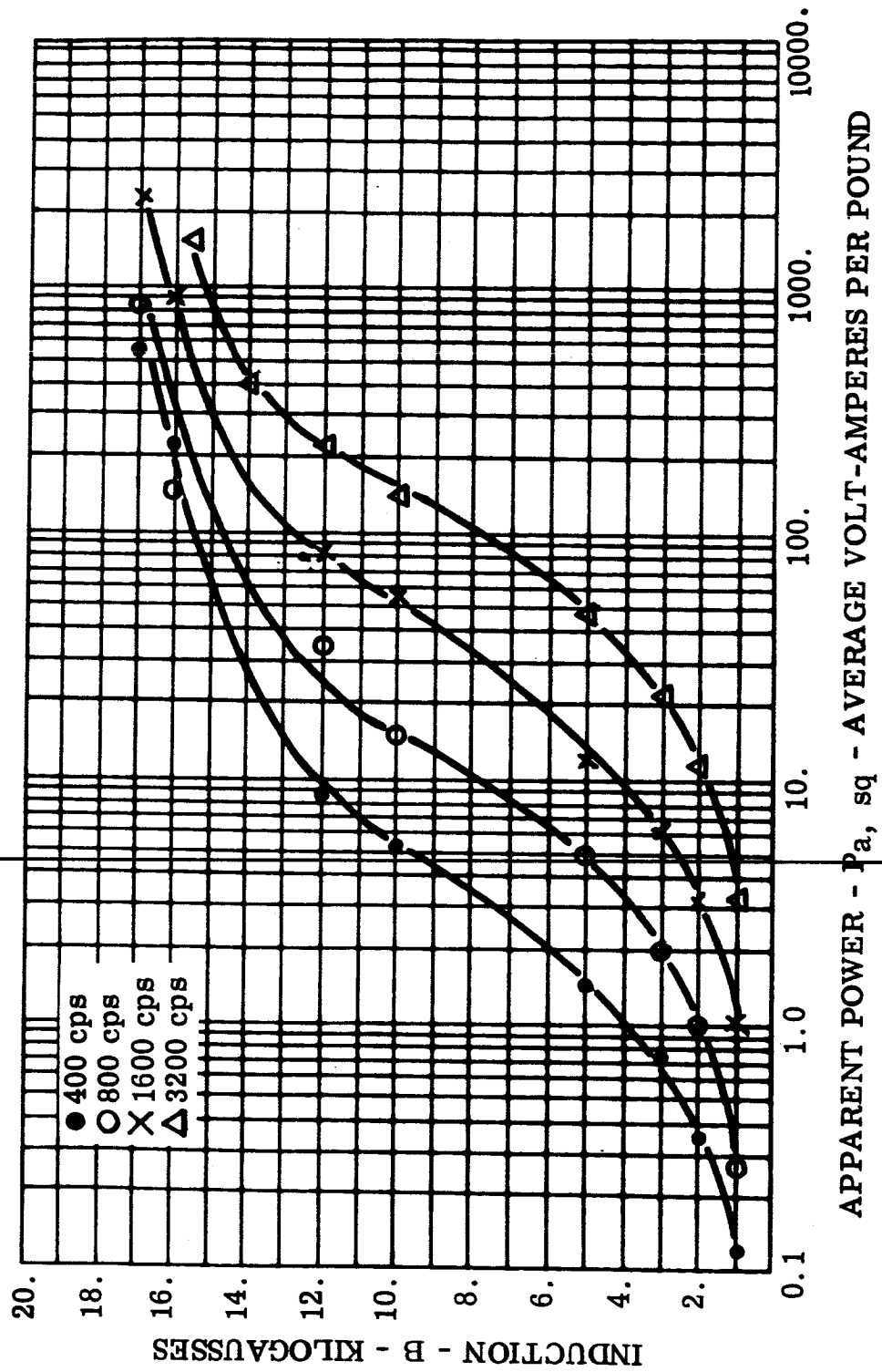


FIGURE 37 P_a, sq - Apparent Power, 0.006 Inch Cubex Double Window, Core 1, Magnetic Field Annealed, -55°C

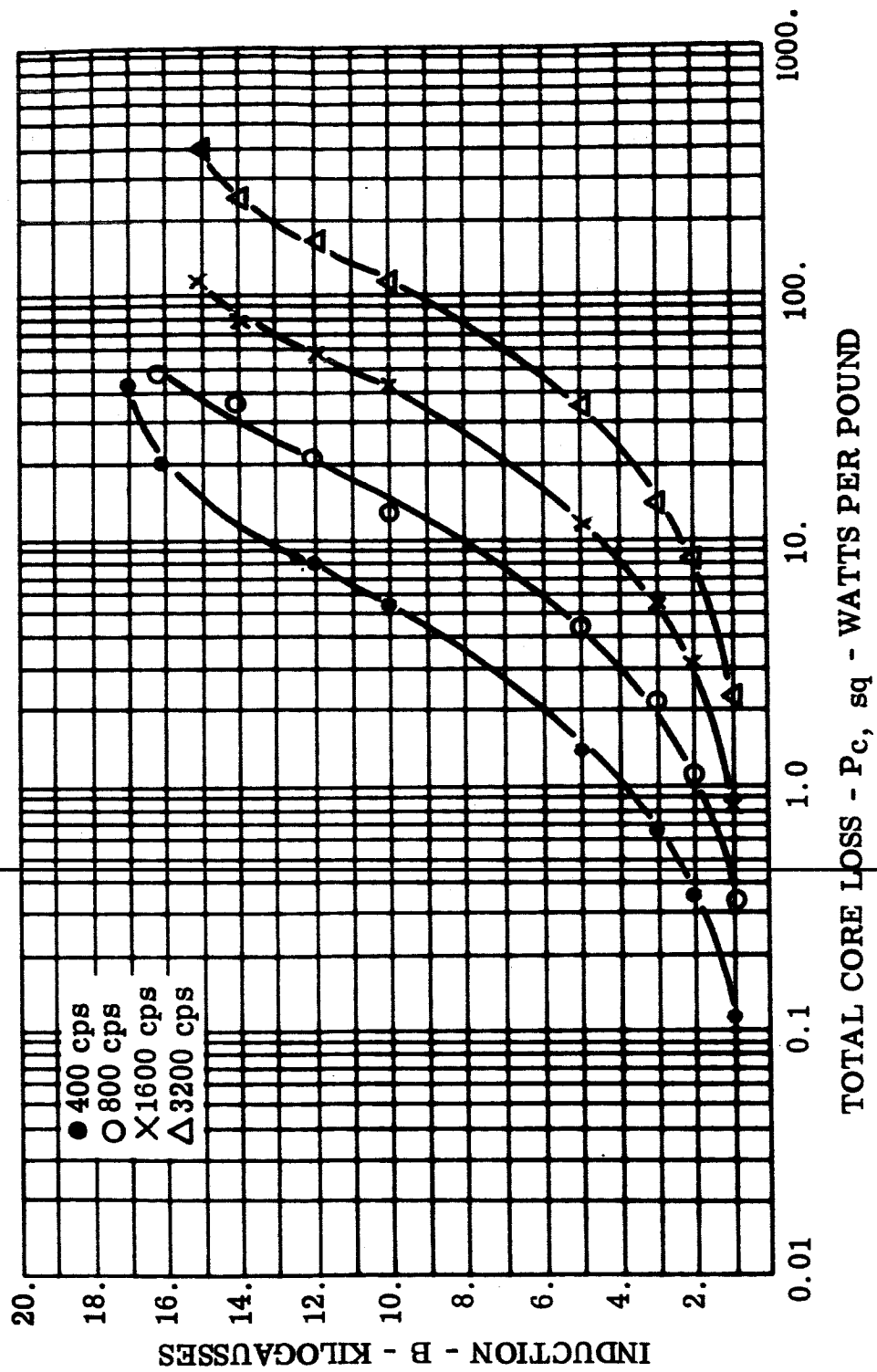


FIGURE 38 P_c , sq - Total Core Loss, 0.006 Inch Cubex Double Window
Core 3, Magnetic Field Annealed, Room Ambient

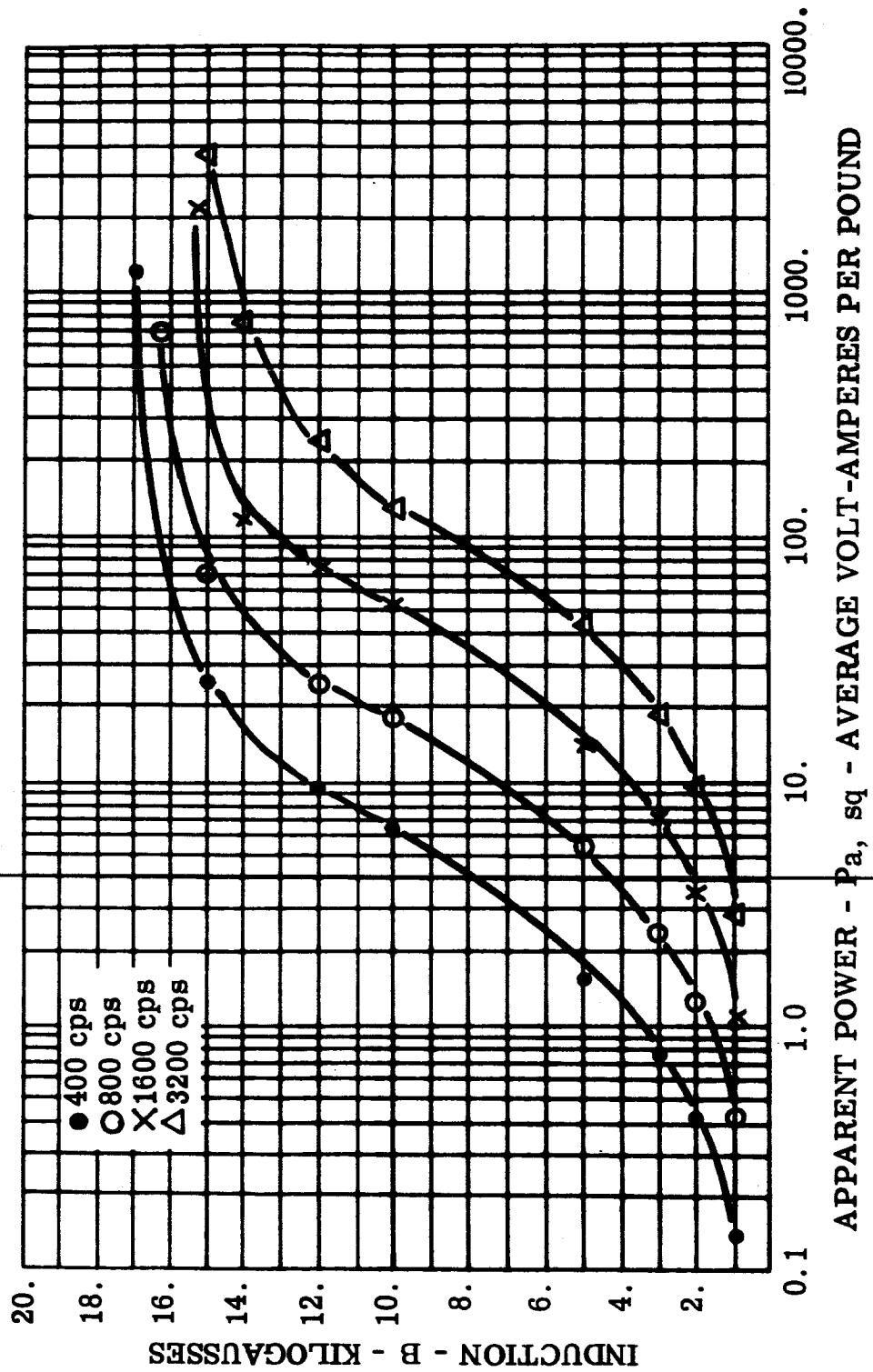


FIGURE 39 P_a, sq - Apparent Power, 0.006 Inch Cubex Dougle Window, Core 3, Magnetic Field, Annealed, Room Ambient

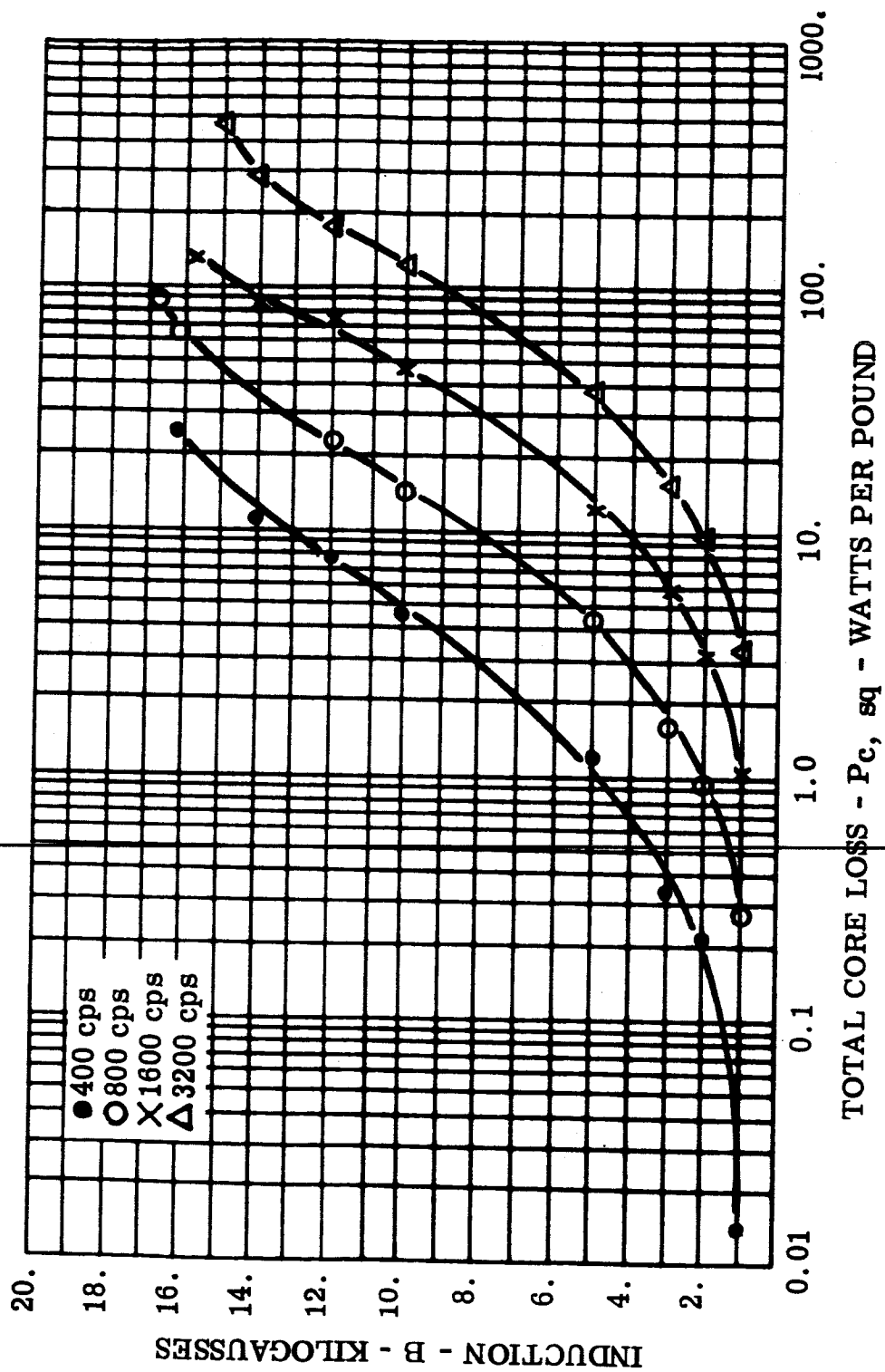
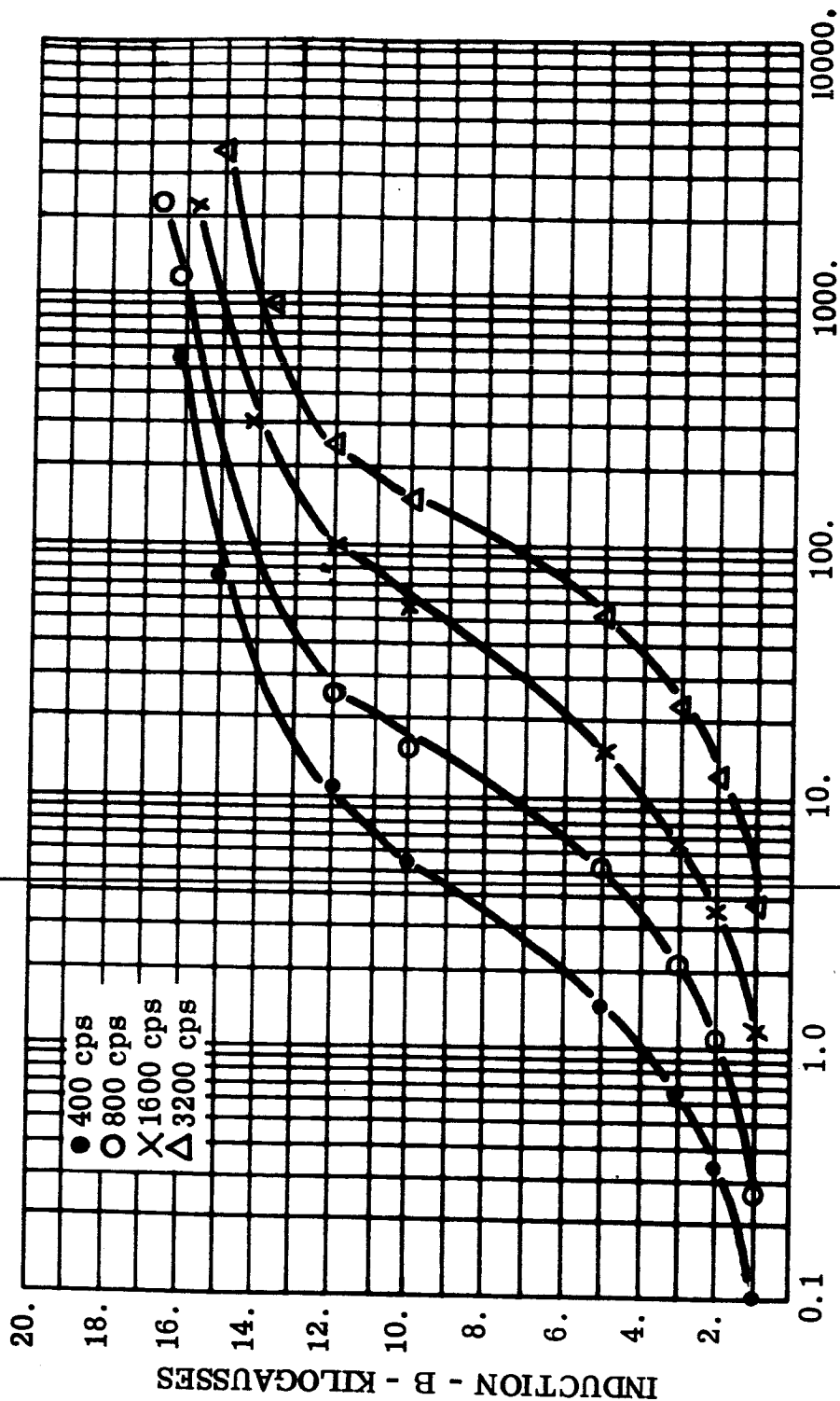


FIGURE 40 P_c , sq - Total Core Loss, 0.006 Inch Cubex Double Window,
Core 3, Magnetic Field Annealed, -55°C



APPARENT POWER - P_a, sq - AVERAGE VOLT-AMPERES PER POUND

FIGURE 41 P_a, sq - Apparent Power, 0.006 Inch Cubex Double Window,
Core 3, Magnetic Field Annealed, $-55^\circ C$

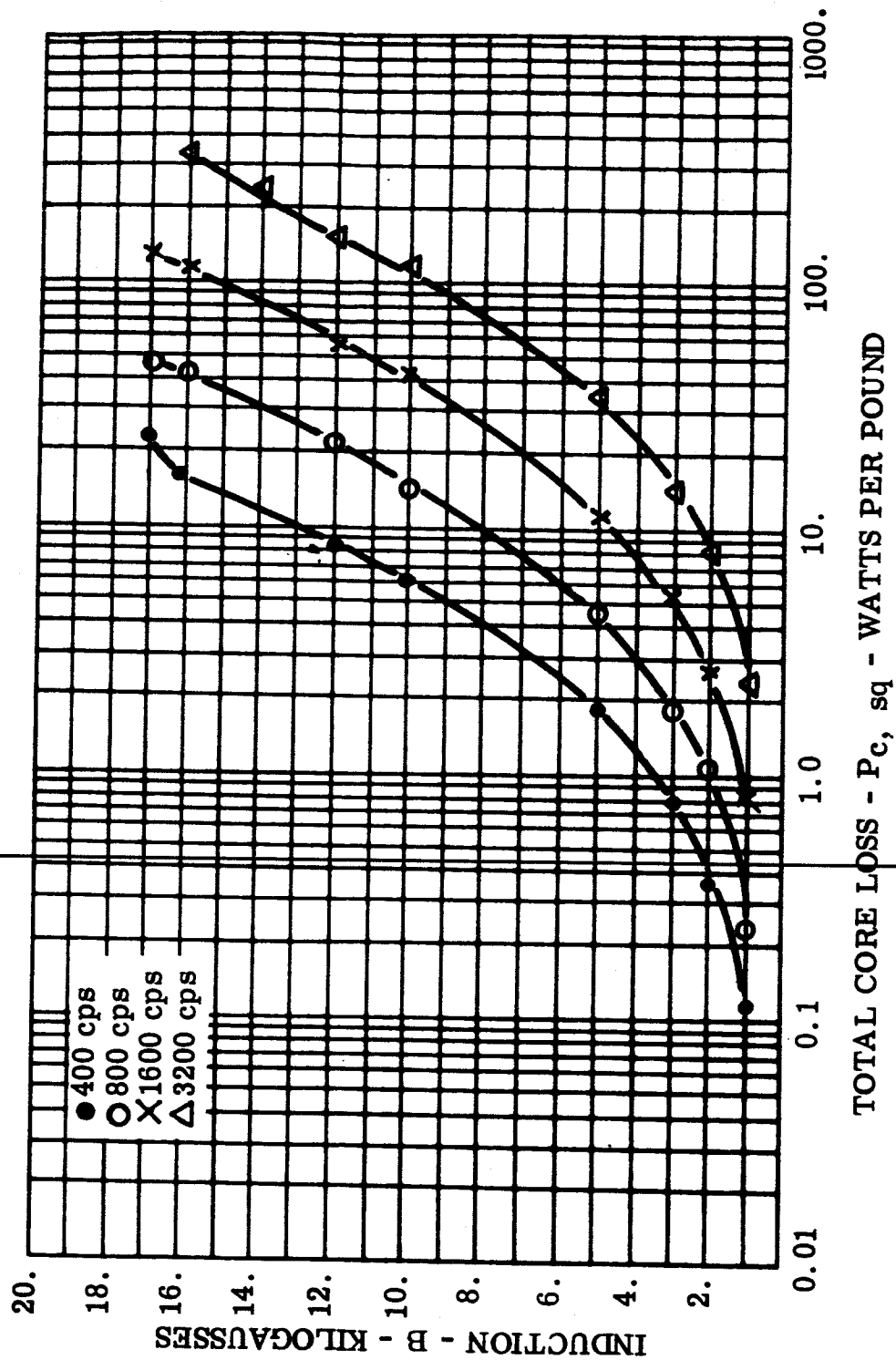


FIGURE 42 P_c , sq - Total Core Loss, 0.006 Inch Cubex Double Window, Core 4, Stress Relief Annealed, Room Ambient

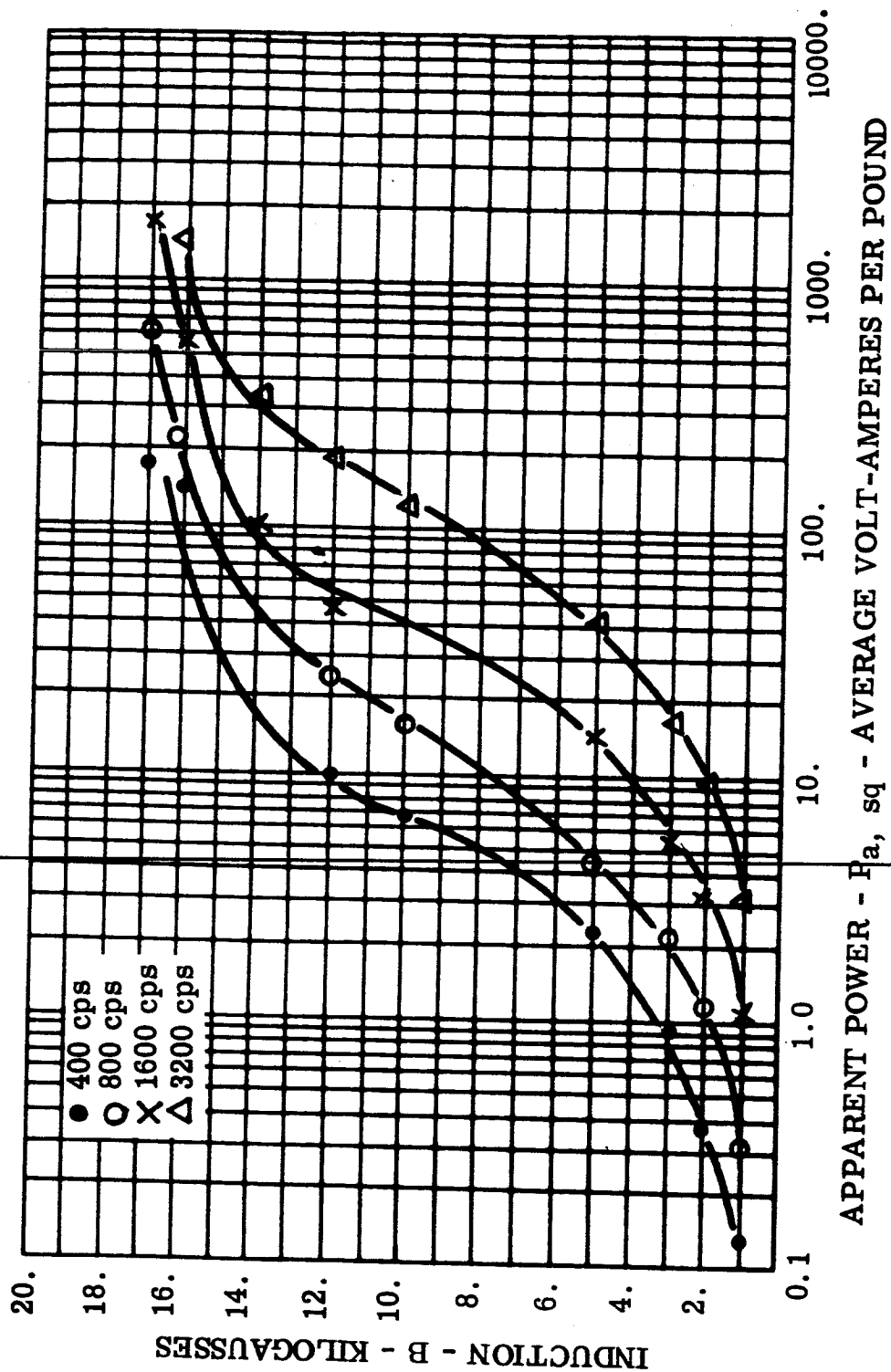


FIGURE 43 P_a, sq - Apparent Power, 0.006 Inch Cubex Double Window, Core 4, Stress Relief Annealed, Room Ambient

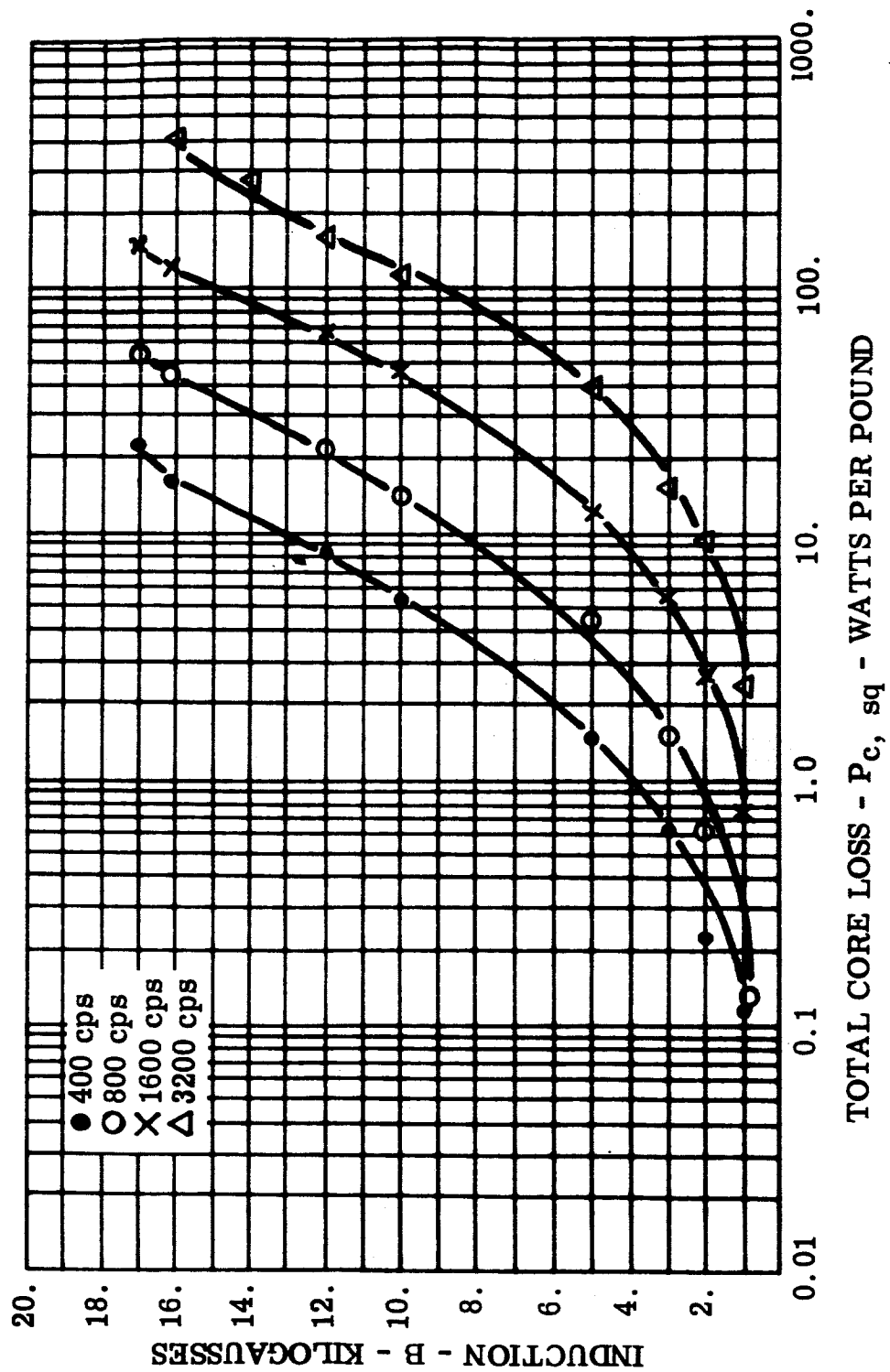


FIGURE 44 $P_{c, sq}$ - Total Core Loss, 0.006 Inch Cubex Double Window, Core 4, Stress Relief Annealed, -55°C

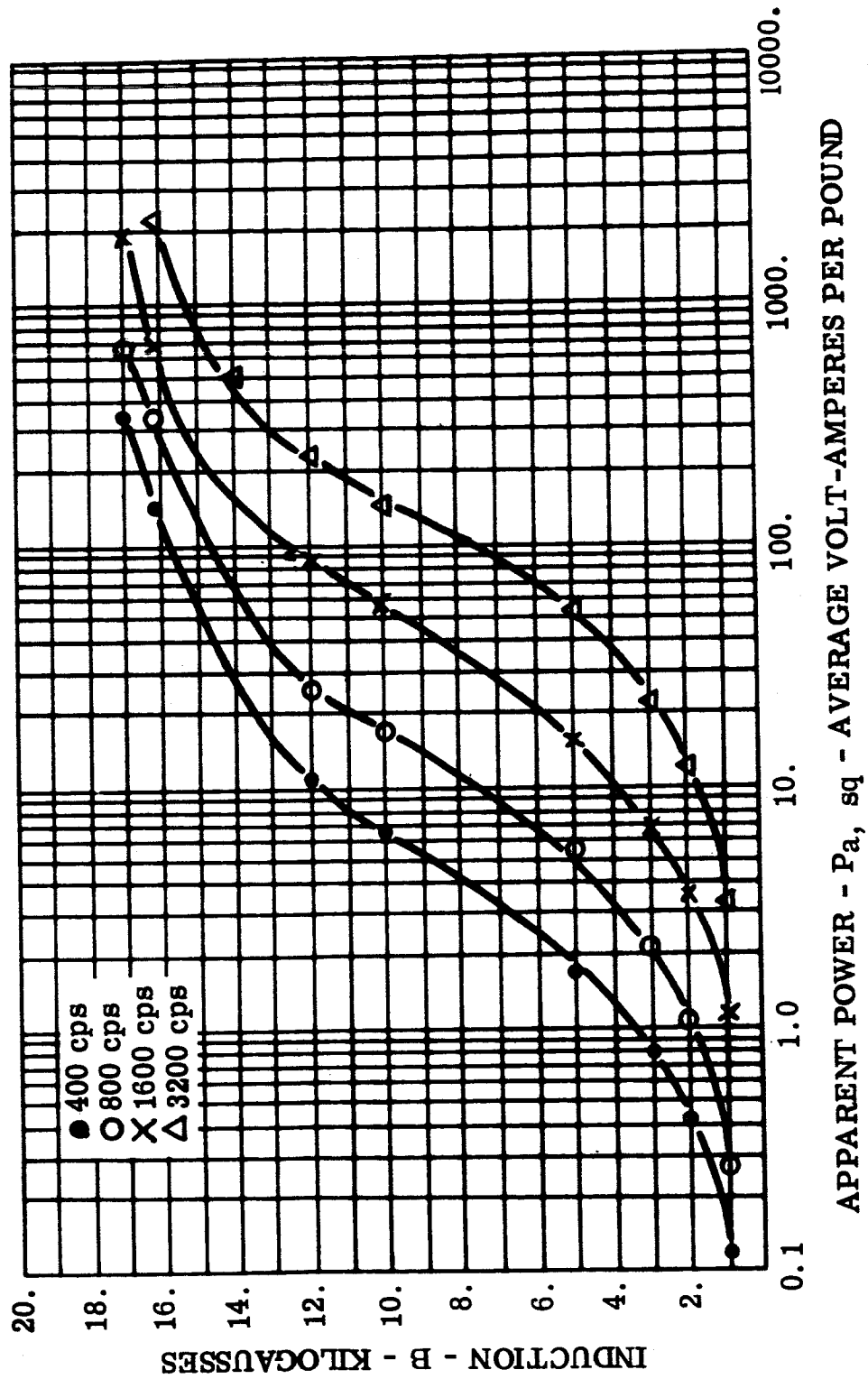


FIGURE 45 Pa, sq - Apparent Power, 0.006 Inch Cubex Double Window, Core 4, Stress Relief Annealed, -55°C

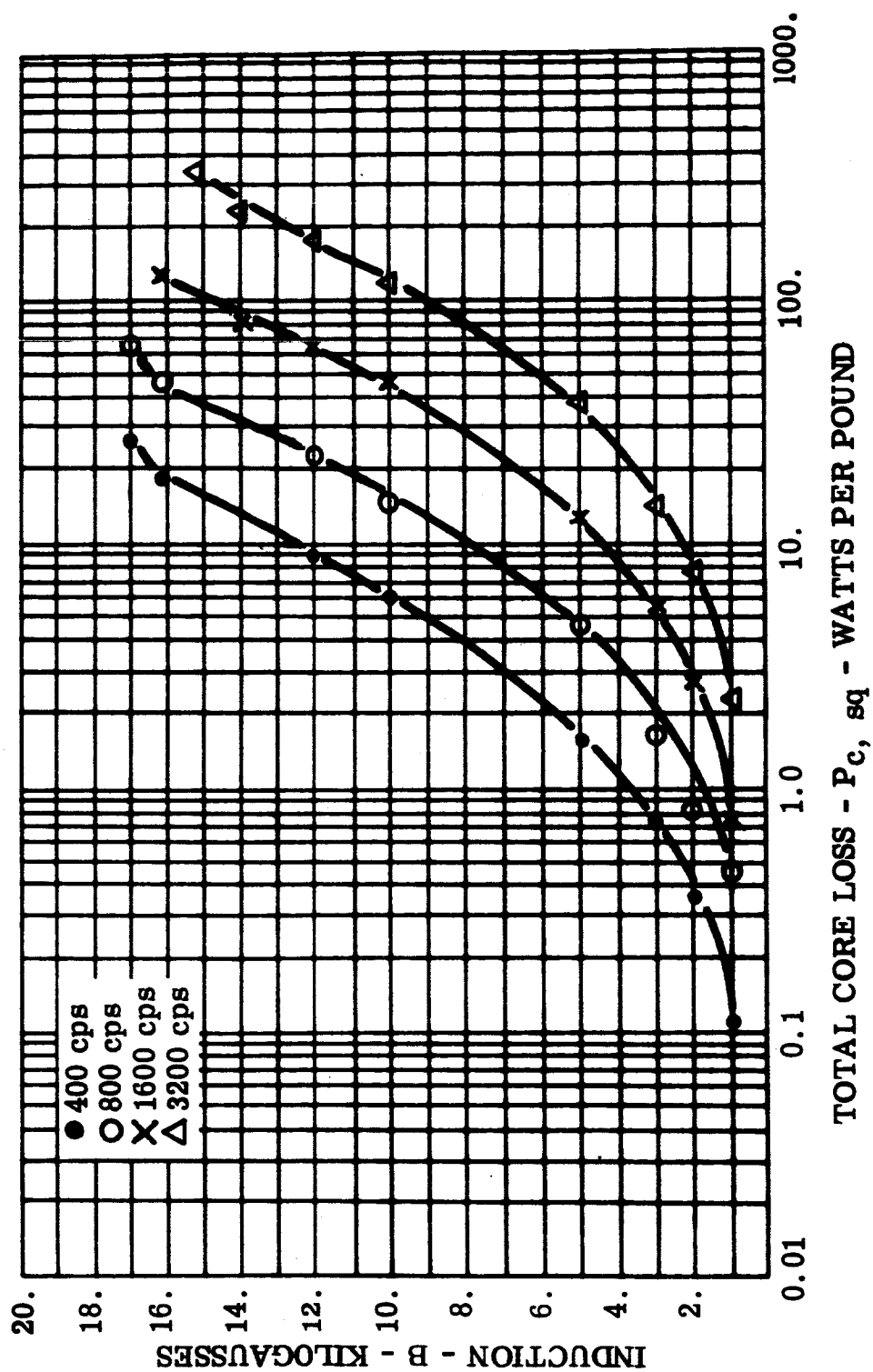


FIGURE 46 $P_{c, sq}$ - Total Core Loss, 0.006 Inch Cubex Double Window, Core 6, Stress Relief Annealed, Room Ambient

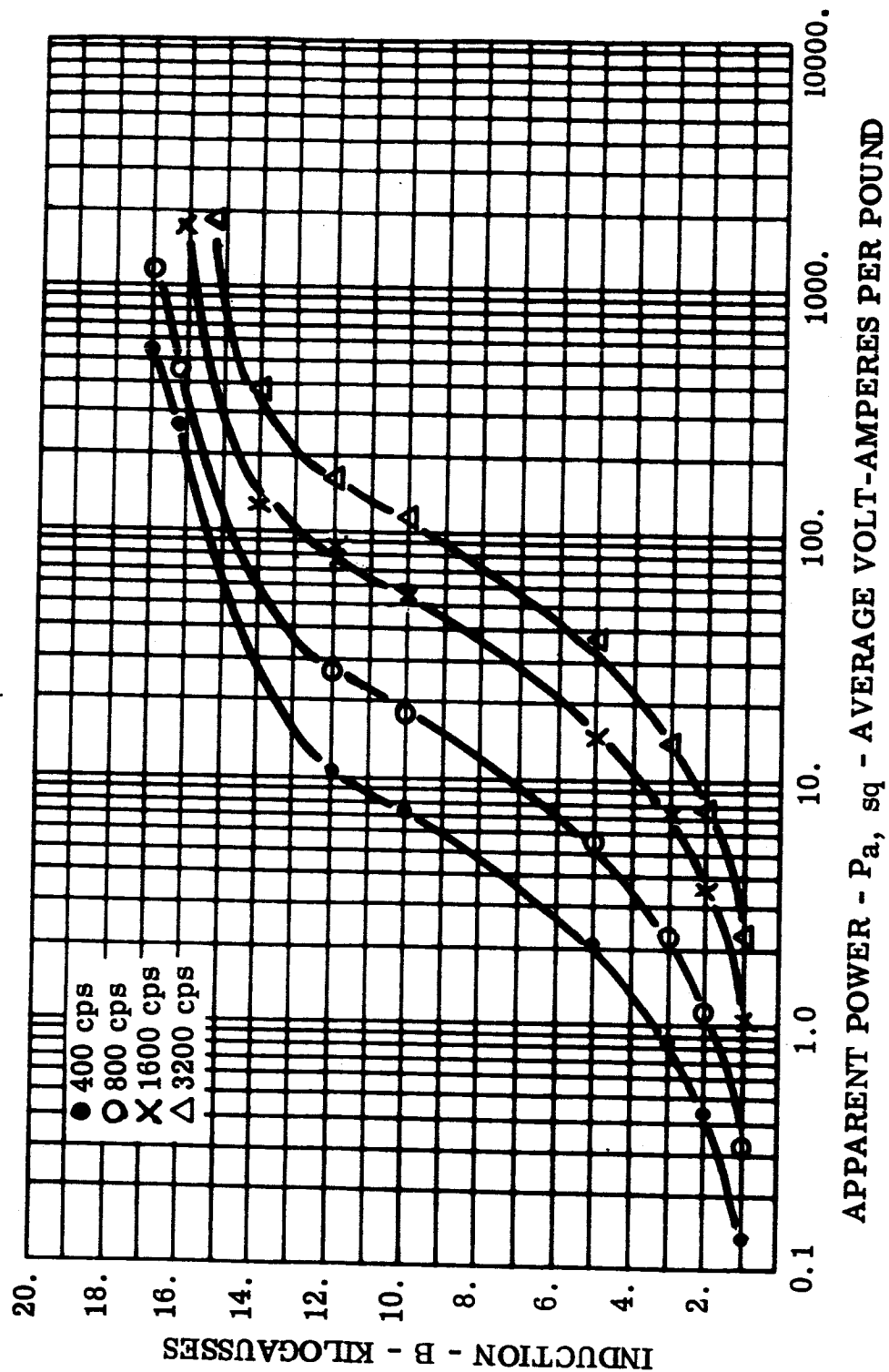


FIGURE 47 P_a, sq - Apparent Power, 0.006 Inch Cubex Double Window
Core 6, Stress Relief Annealed, Room Ambient

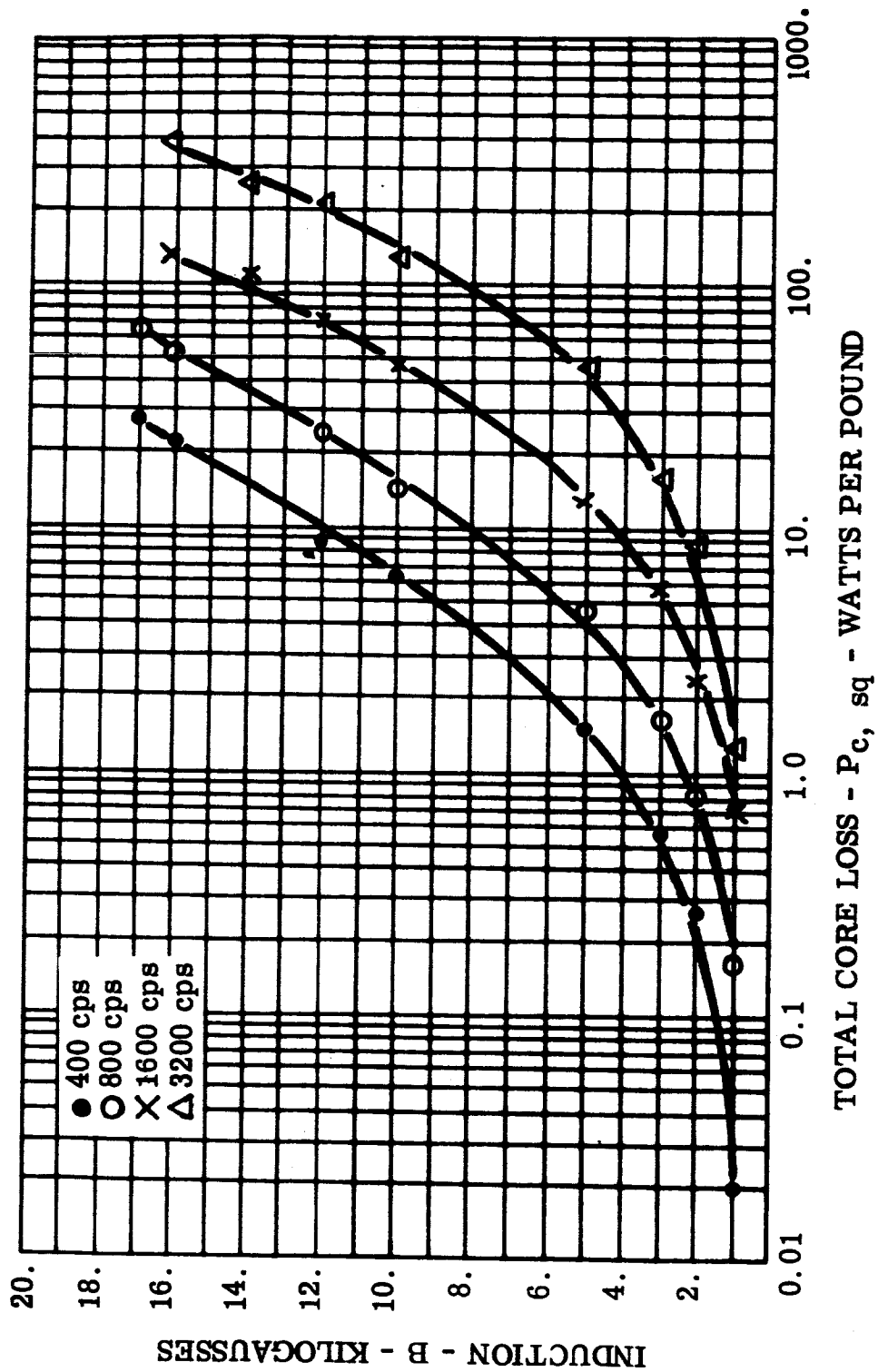


FIGURE 48 $P_{c, sq}$ - Total Core Loss, 0.006 Inch Cubex Double Window, Core 6, Stress Relief Annealed, -55°C

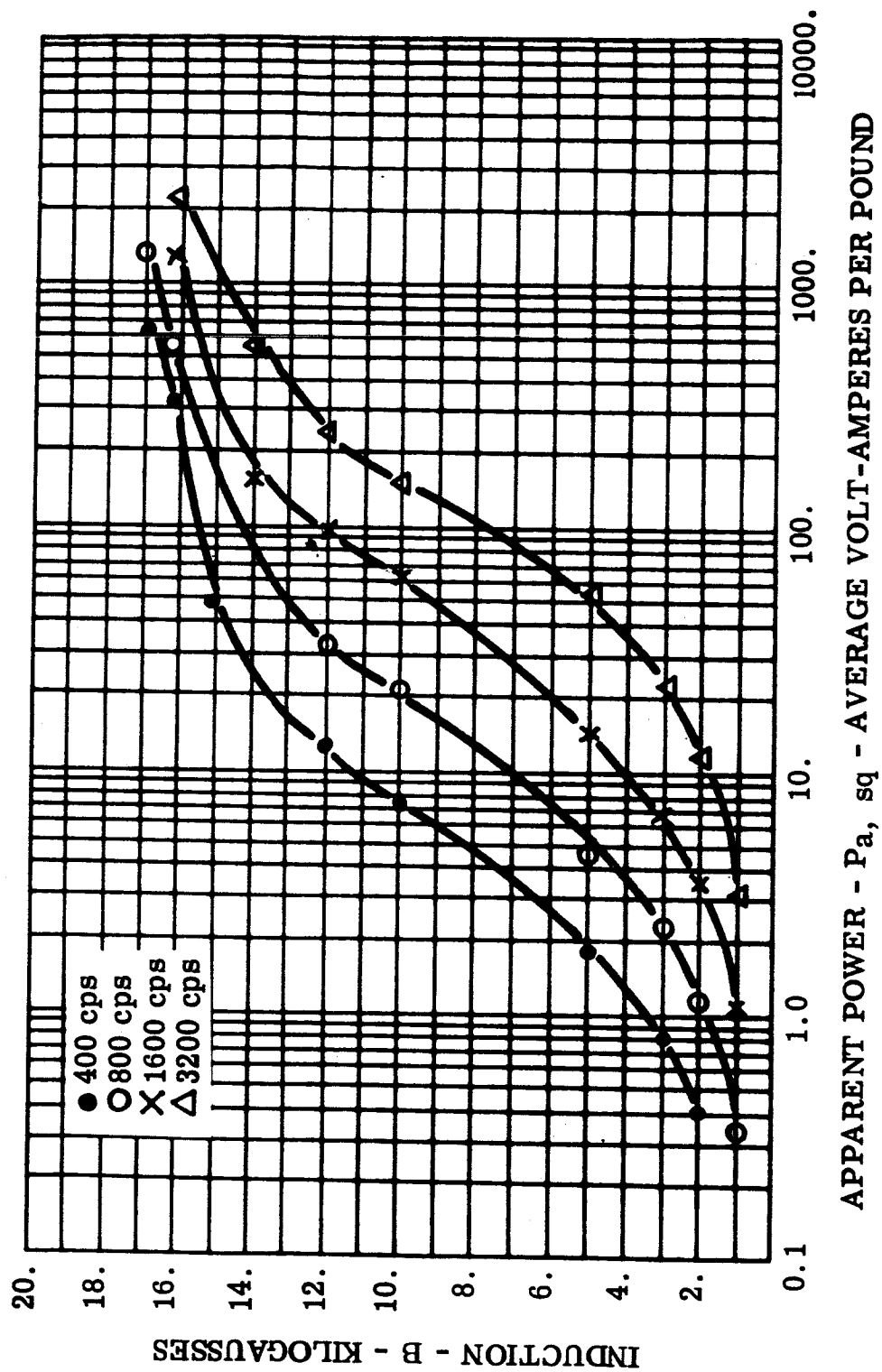


FIGURE 49 P_a , sq - Apparent Power, 0.006 Inch Cubex Double Window, Core 6, Stress Relief Annealed, -55°C

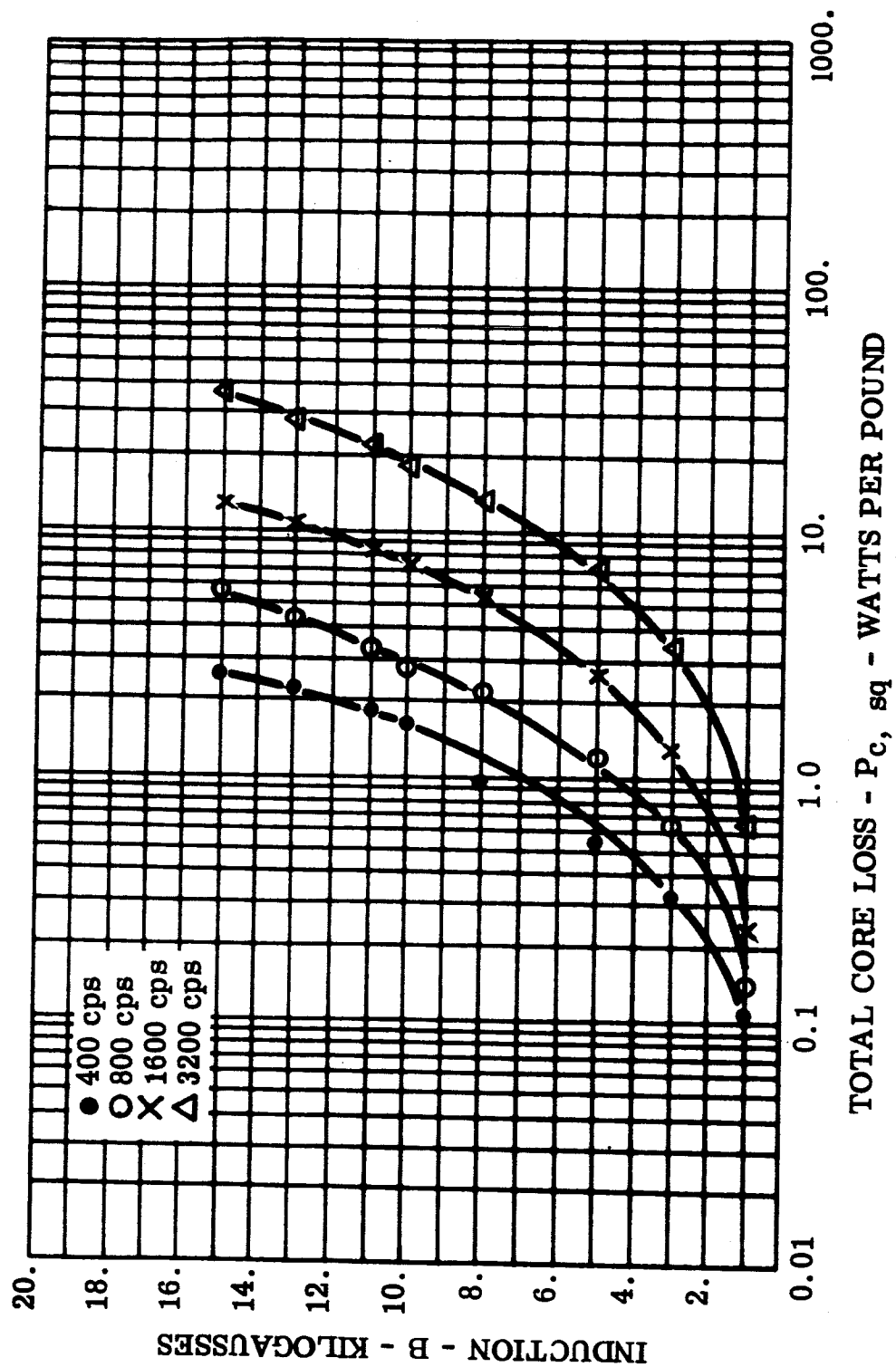


FIGURE 50 $P_{c, sq}$ - Total Core Loss, 0.002 Inch Orthonol Toroid, Core 7,
Room Ambient

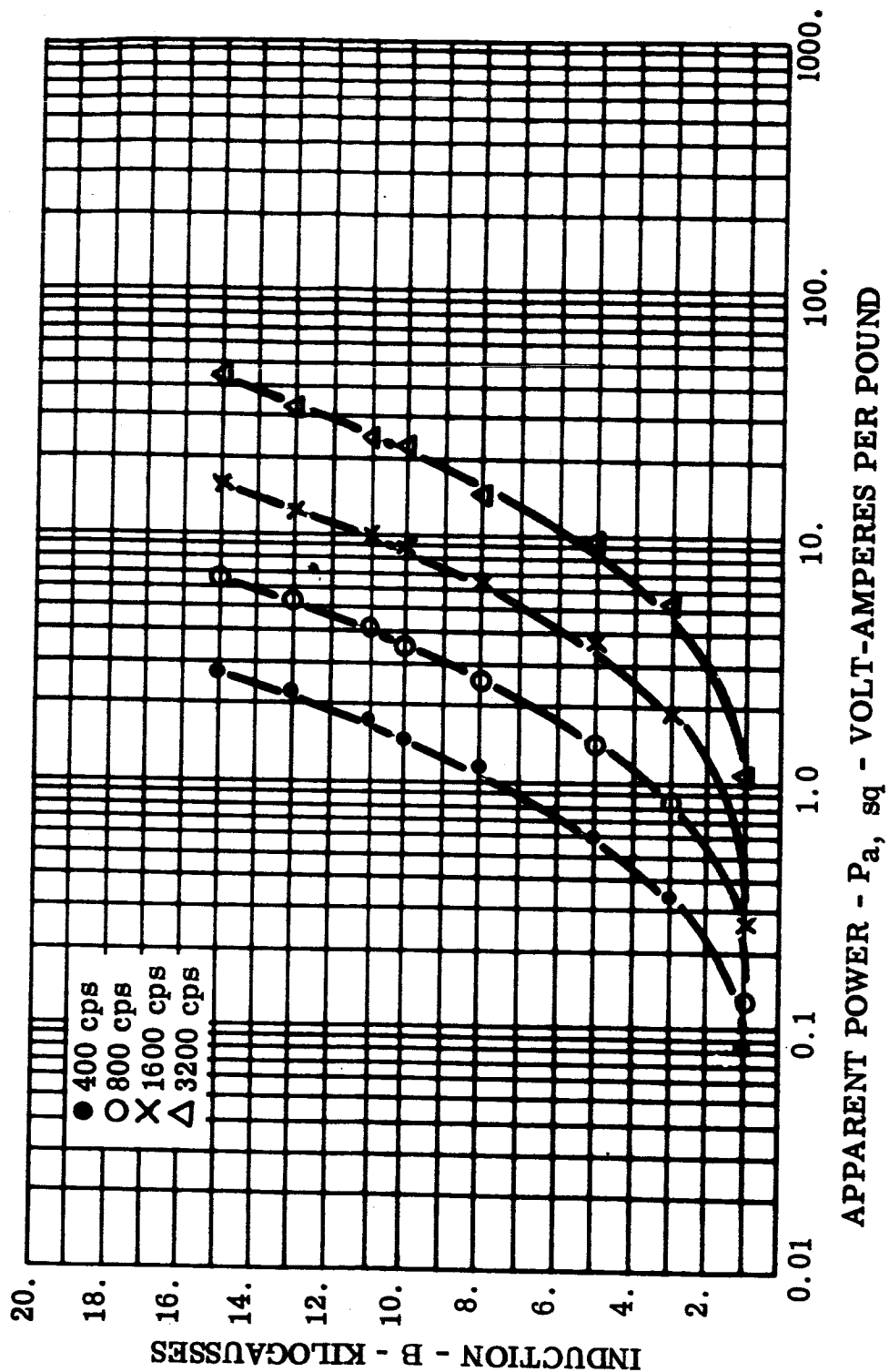


FIGURE 51 P_a, sq - Apparent Power, 0.002 Inch Orthonol Toroid, Core 7,
Room Ambient

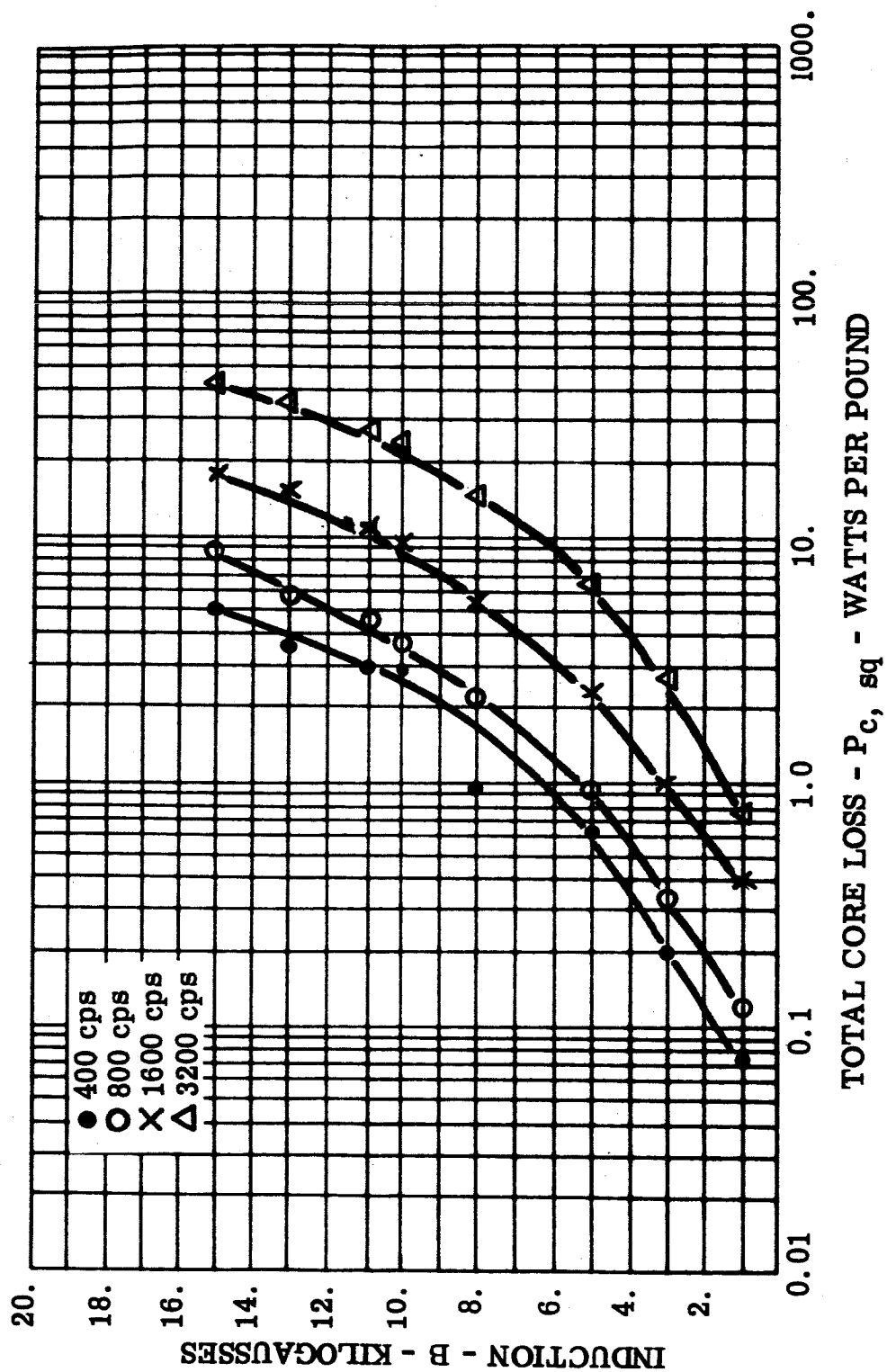


FIGURE 52 $P_{c, sq}$ - Total Core Loss, 0.002 Inch Orthonol Toroid, Core 7, -55°C .

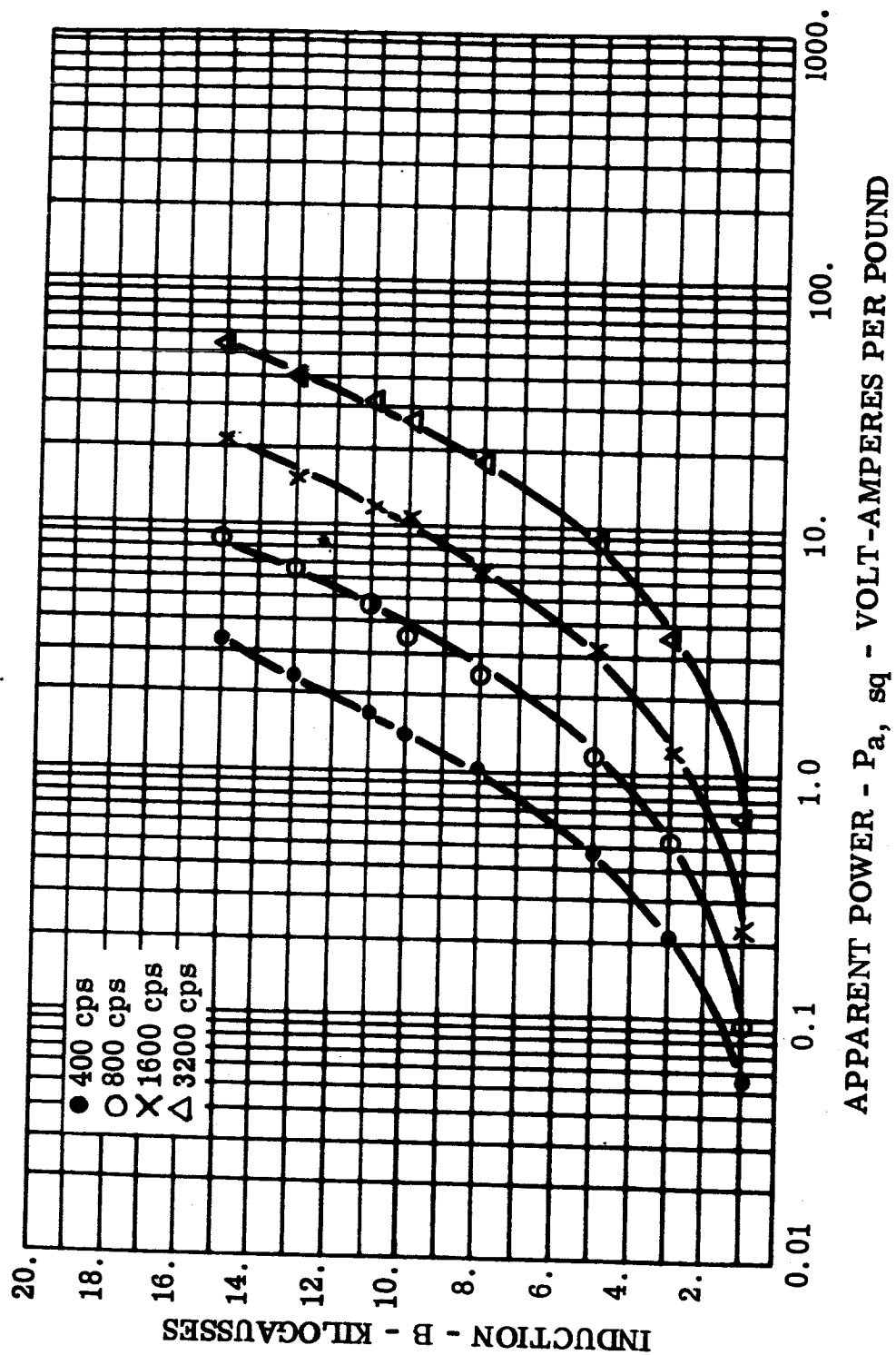


FIGURE 53 P_a , sq - Apparent Power, 0.002 Inch Orthonol Toroid, Core 7, -55°C

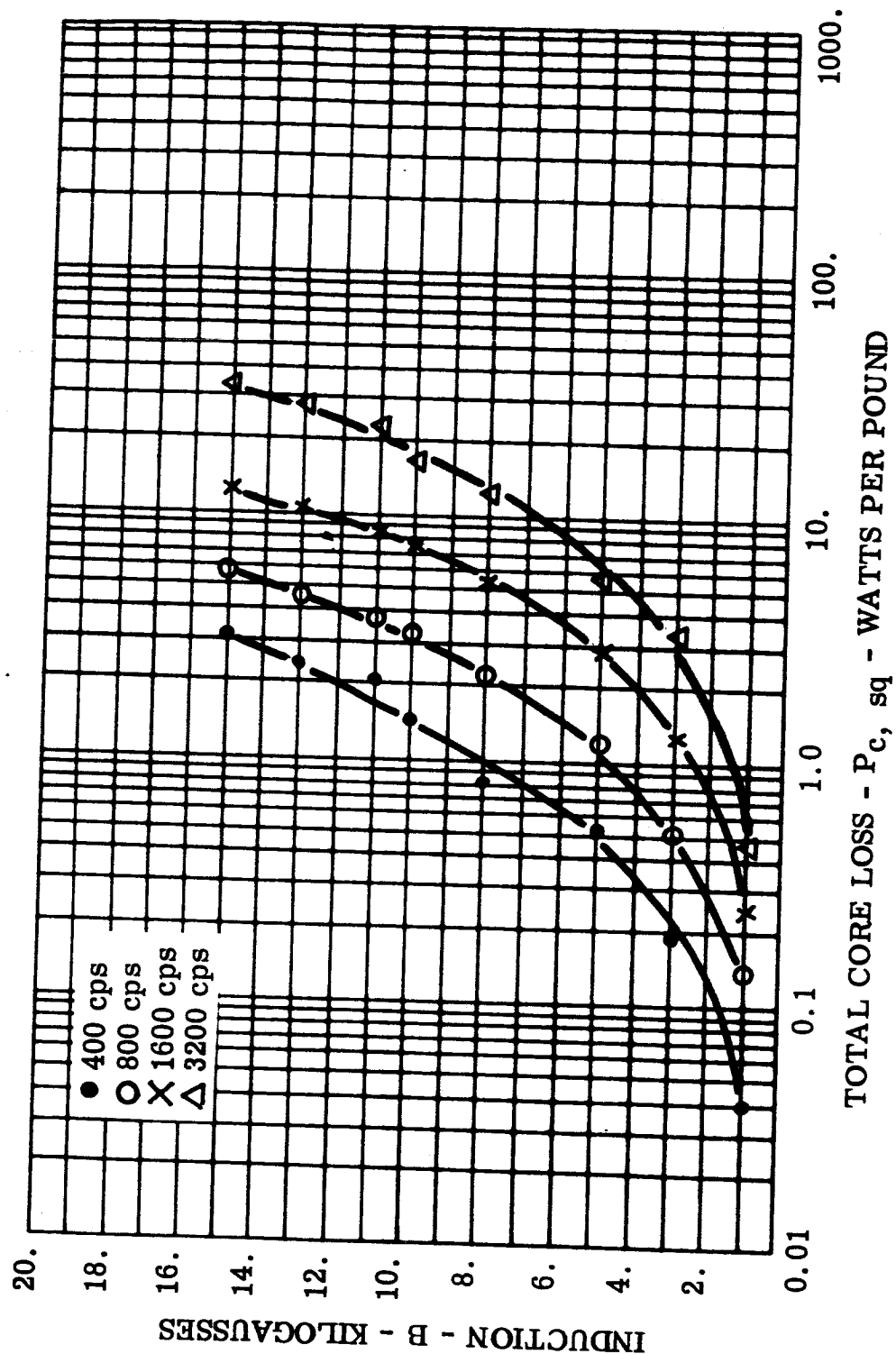


FIGURE 54 P_c , sq - Total Core Loss, 0.002 Inch Orthonol Toroid, Core 9,
Room Ambient

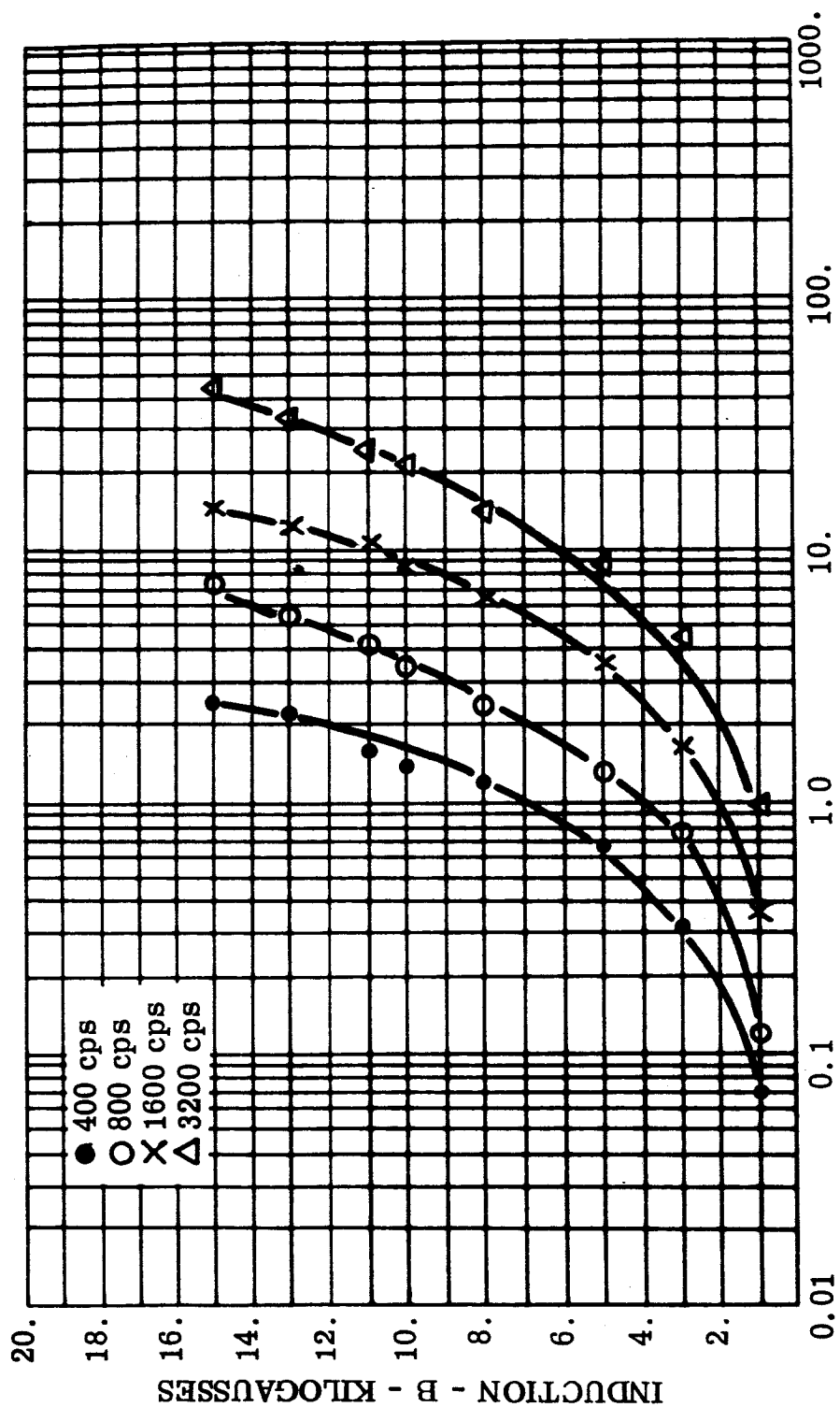


FIGURE 55 P_a , sq - Apparent Power, 0.002 Inch Orthonol Toroid, Core 9,
Room Ambient

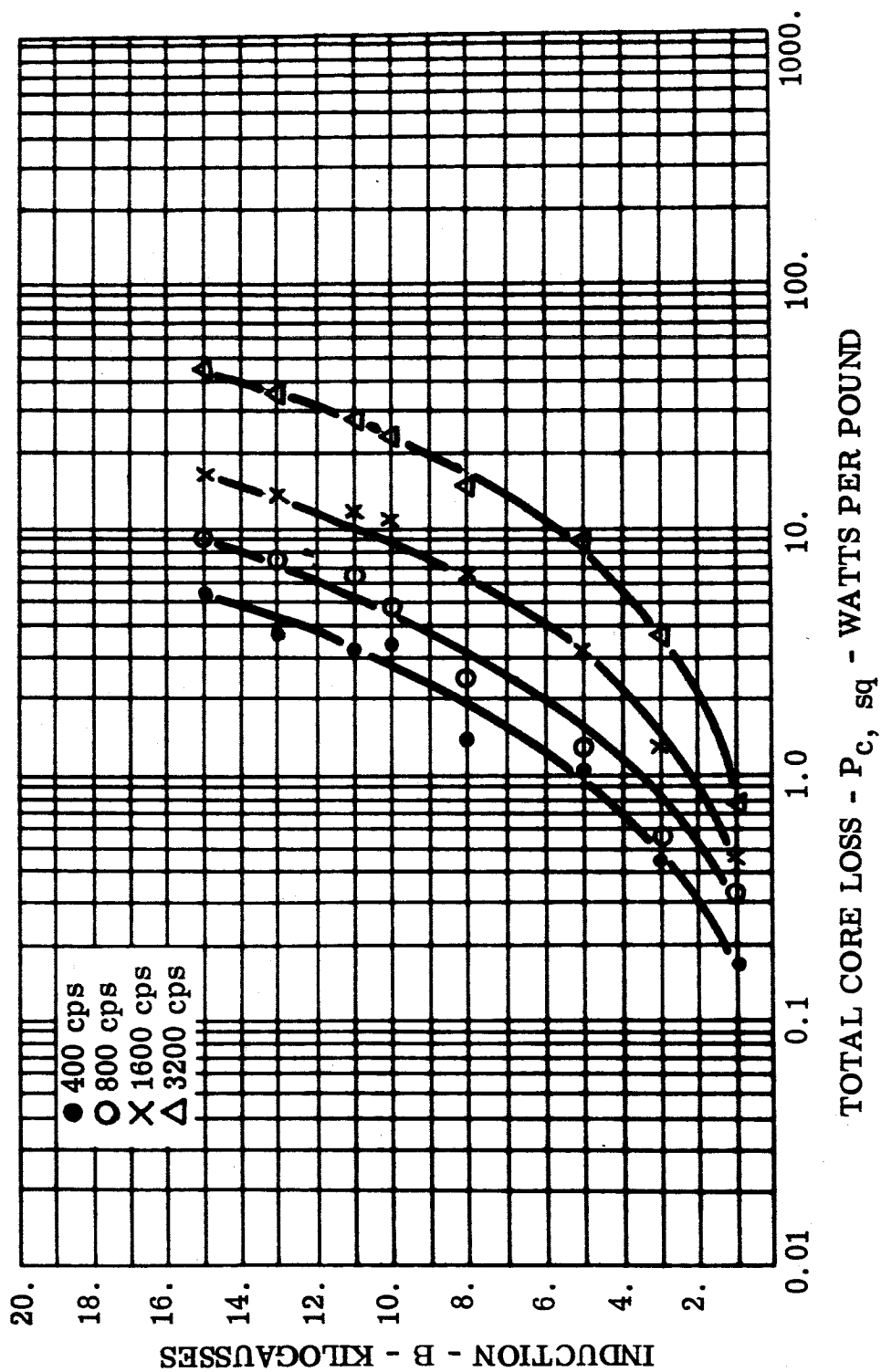
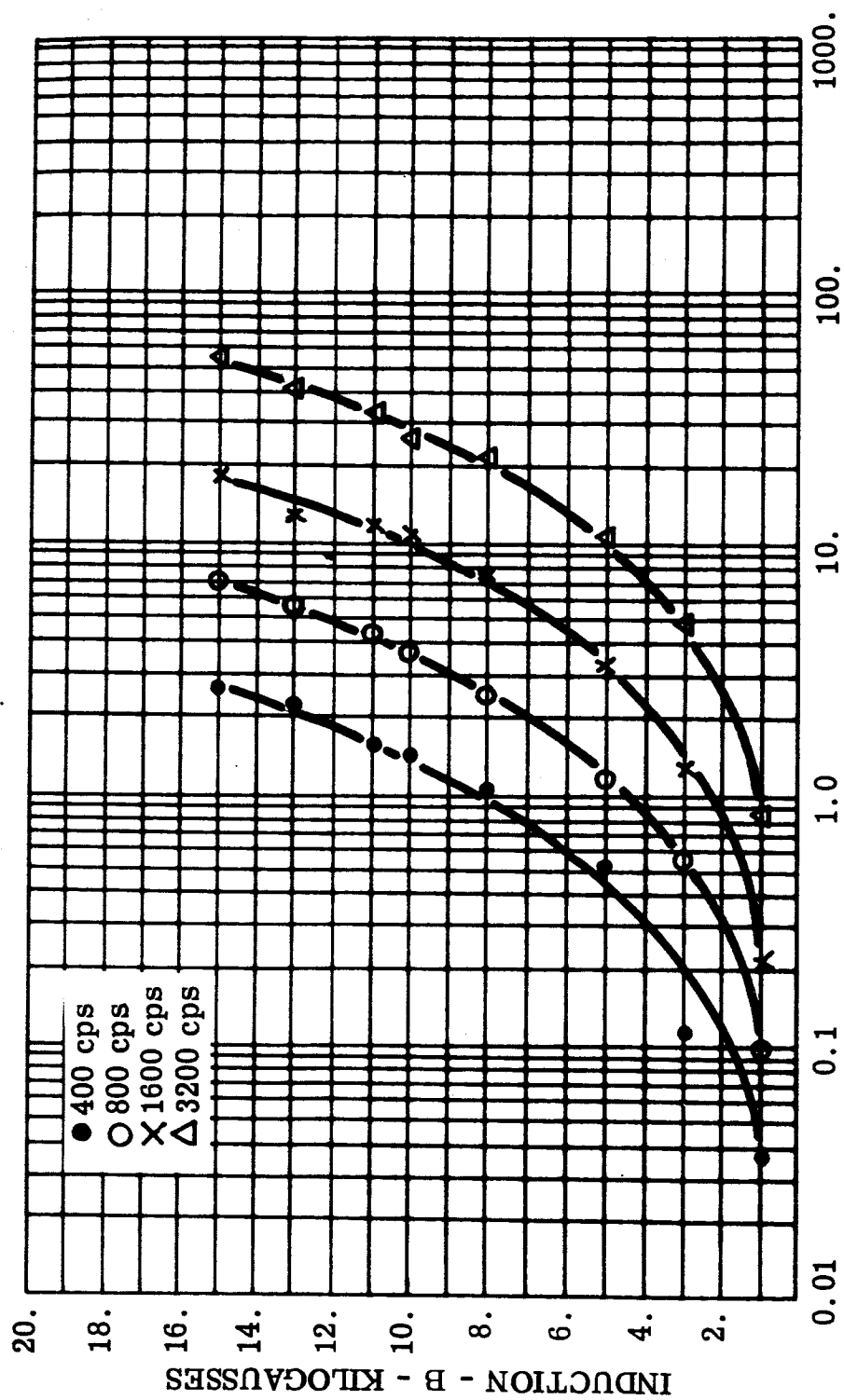


FIGURE 56 $P_{c, sq}$ - Total Core Loss, 0.002 Inch Orthonal Toroid, Core 9, -55°C



APPARENT POWER - P_a, sq - VOLT-AMPERES PER POUND

FIGURE 57 P_a, sq - Apparent Power, 0.002 Inch Orthonol Toroid, Core 9, $-55^\circ C$

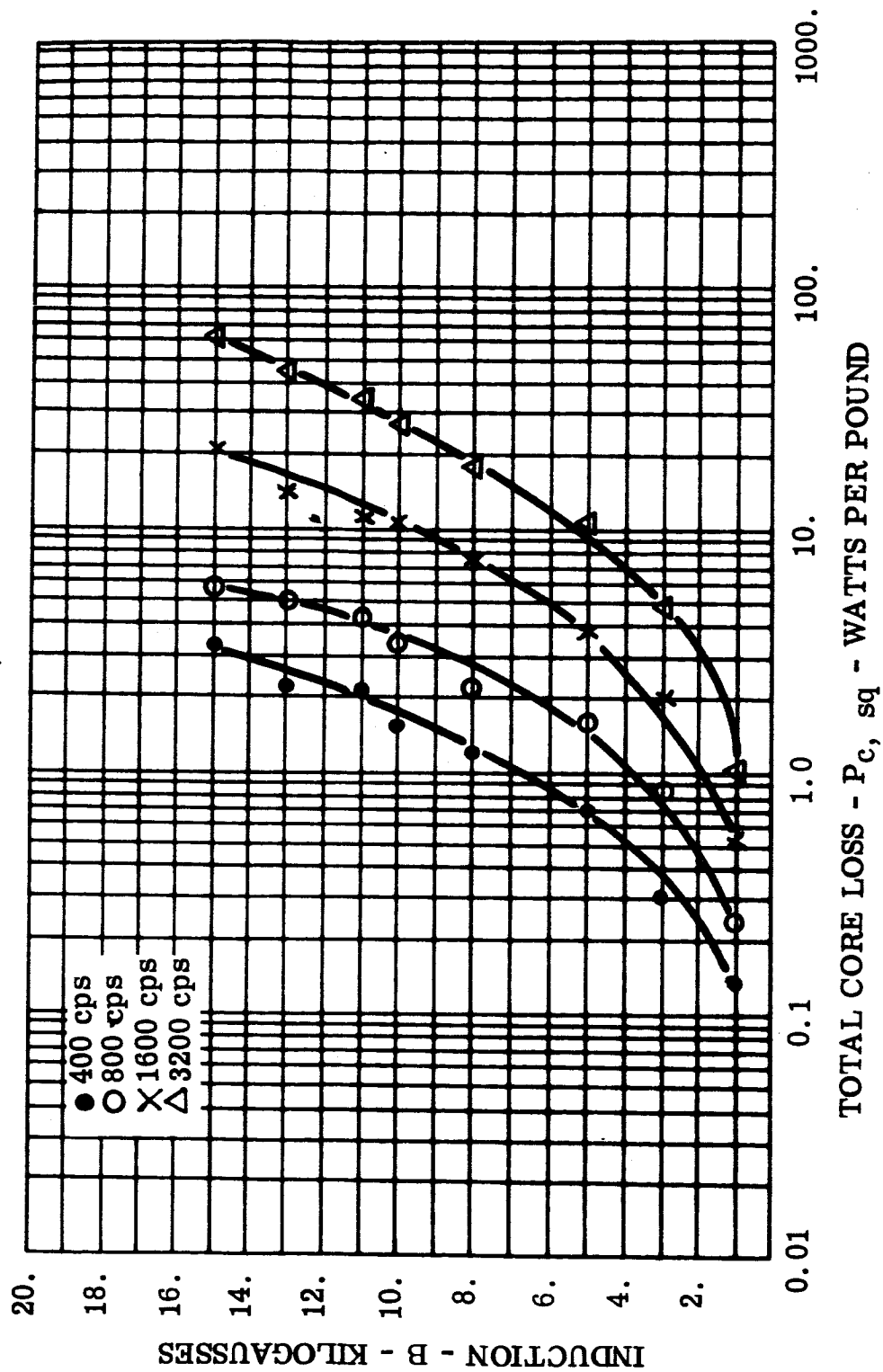


FIGURE 58 $P_{c, sq}$ - Total Core Loss, 0.004 Inch Orthonol Toroid, Core 11,
Room Ambient

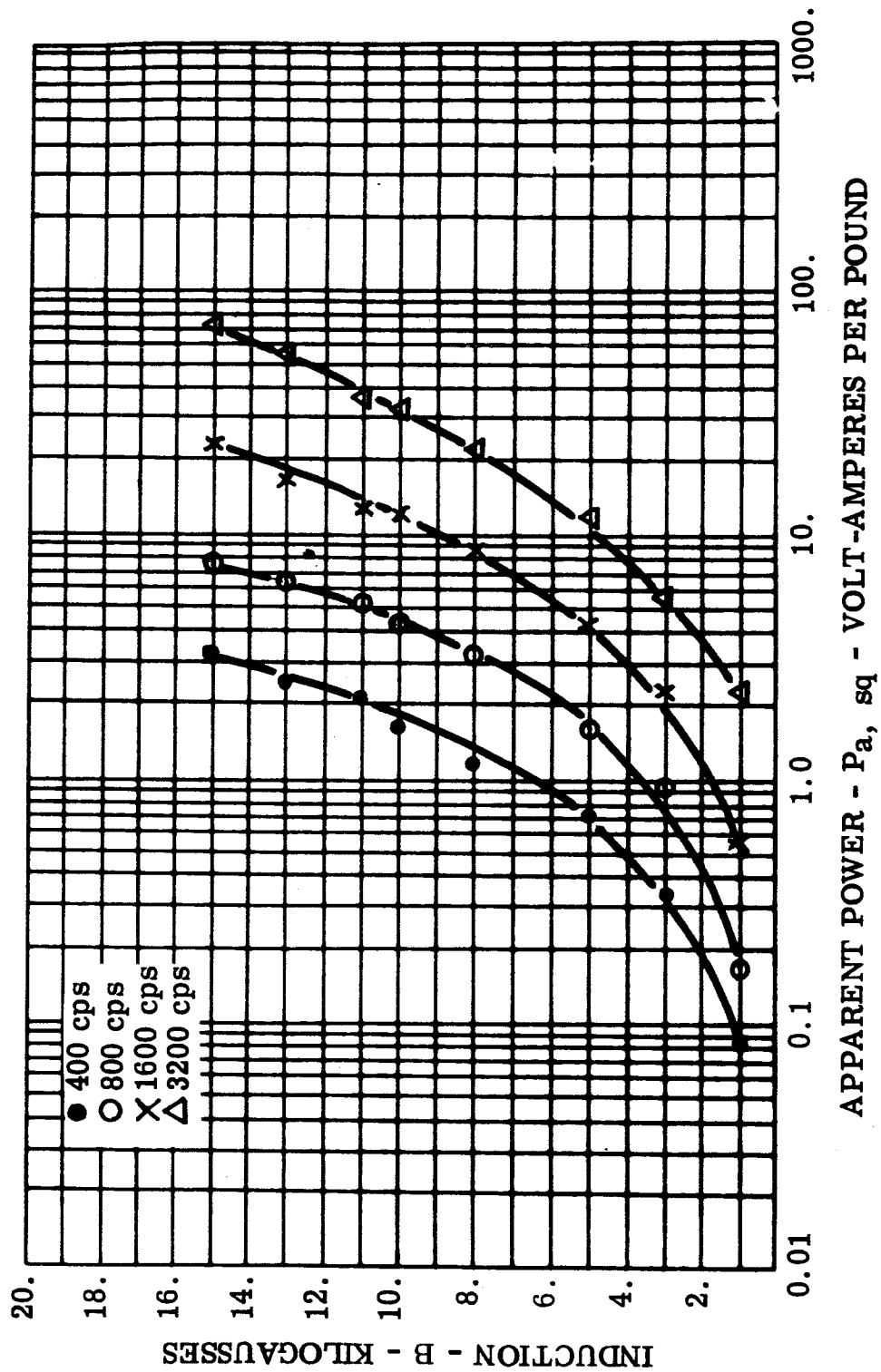


FIGURE 59 $P_{a, sq}$ - Apparent Power, 0.004 Inch Orthonol Toroid, Core 11,
Room Ambient

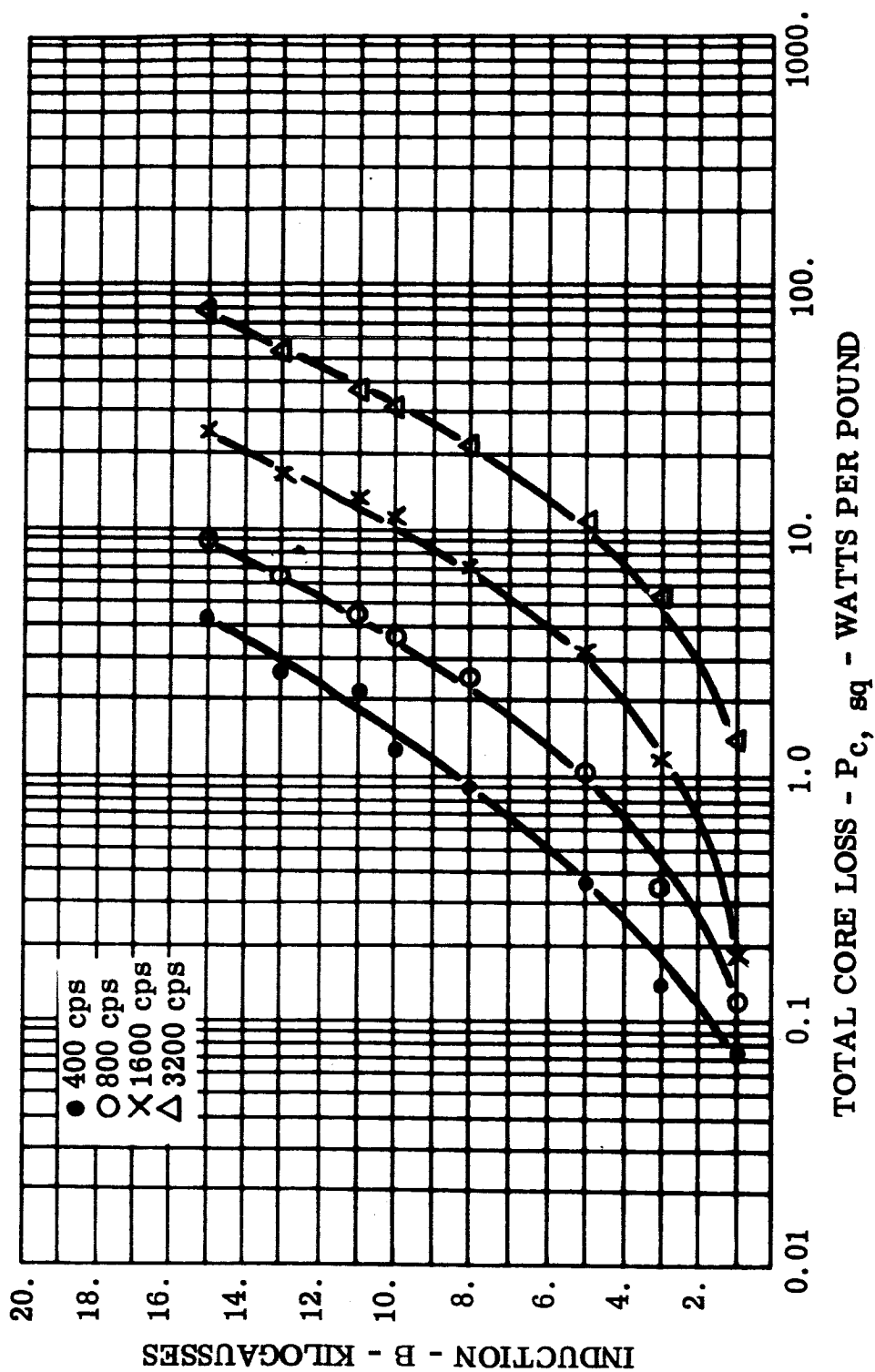


FIGURE 60 $P_{c, sq}$ - Total Core Loss, 0.004 Inch Orthonol Toroid, Core 11, -55°C

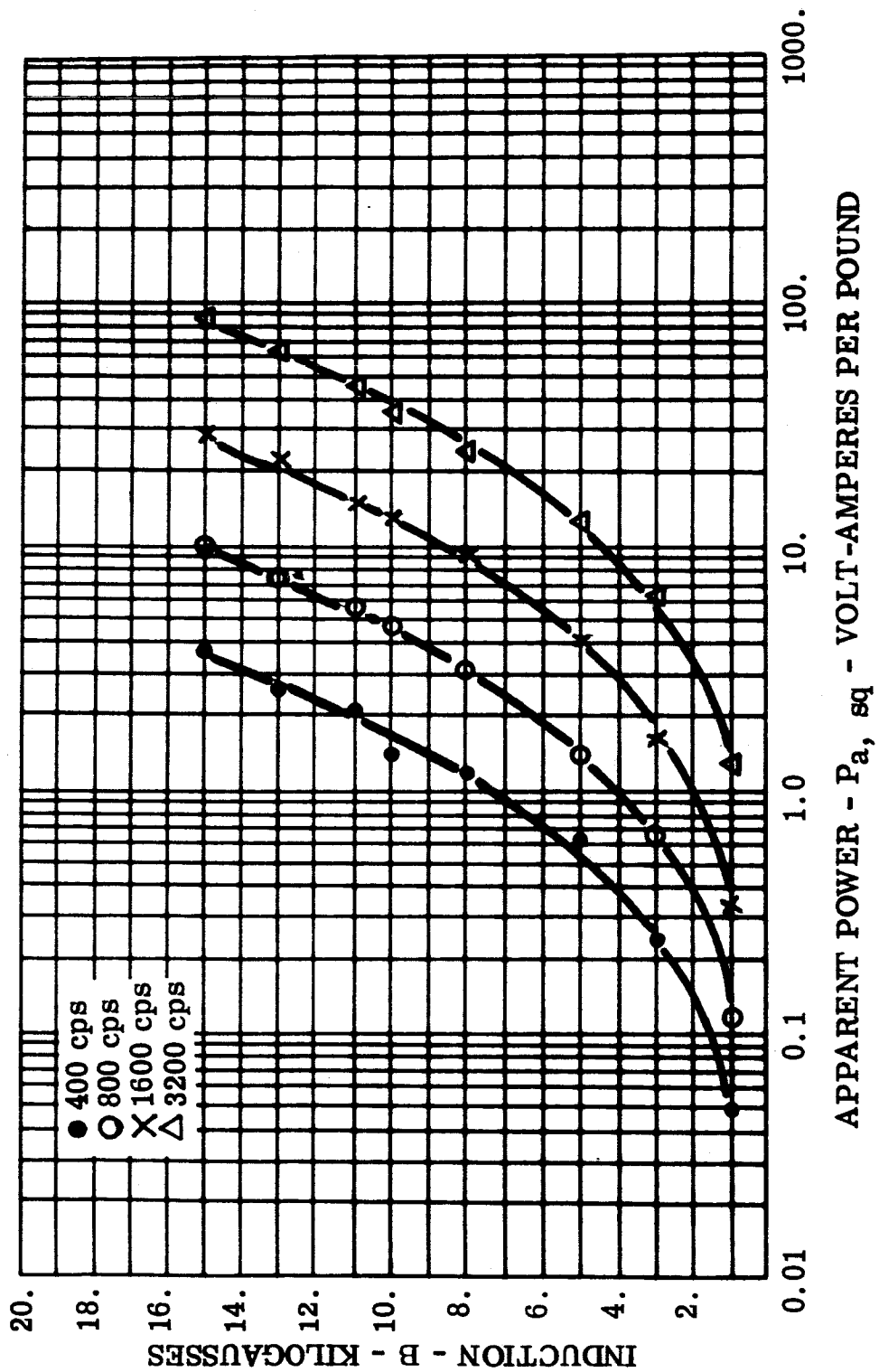


FIGURE 61 $P_{a, sq}$ - Apparent Power, 0.004 Inch Orthonol Toroid, Core 11, -55°C

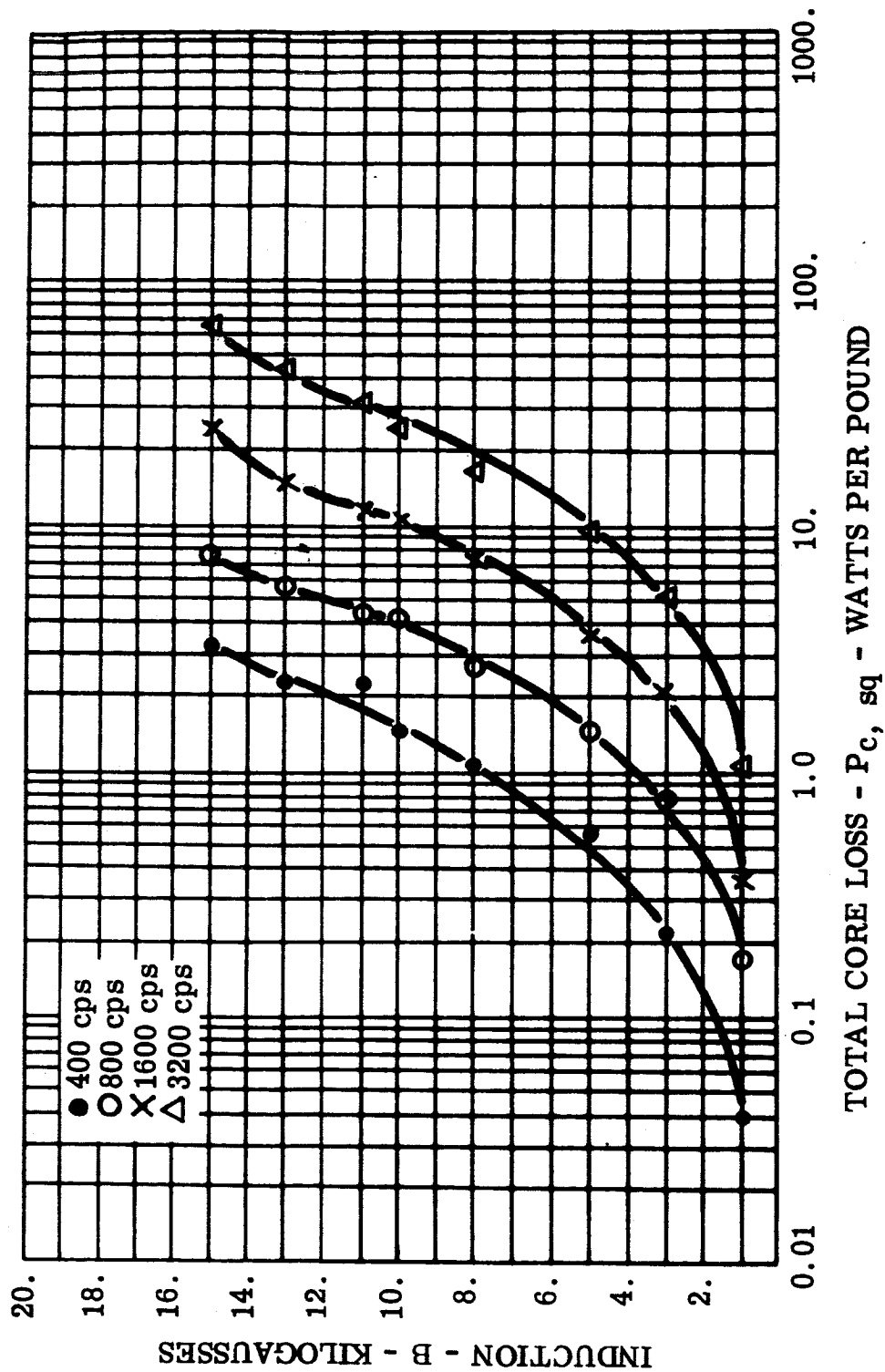


FIGURE 62 P_c , sq - Total Core Loss, 0.004 Inch Orthonal Toroid, Core 12, Room Ambient

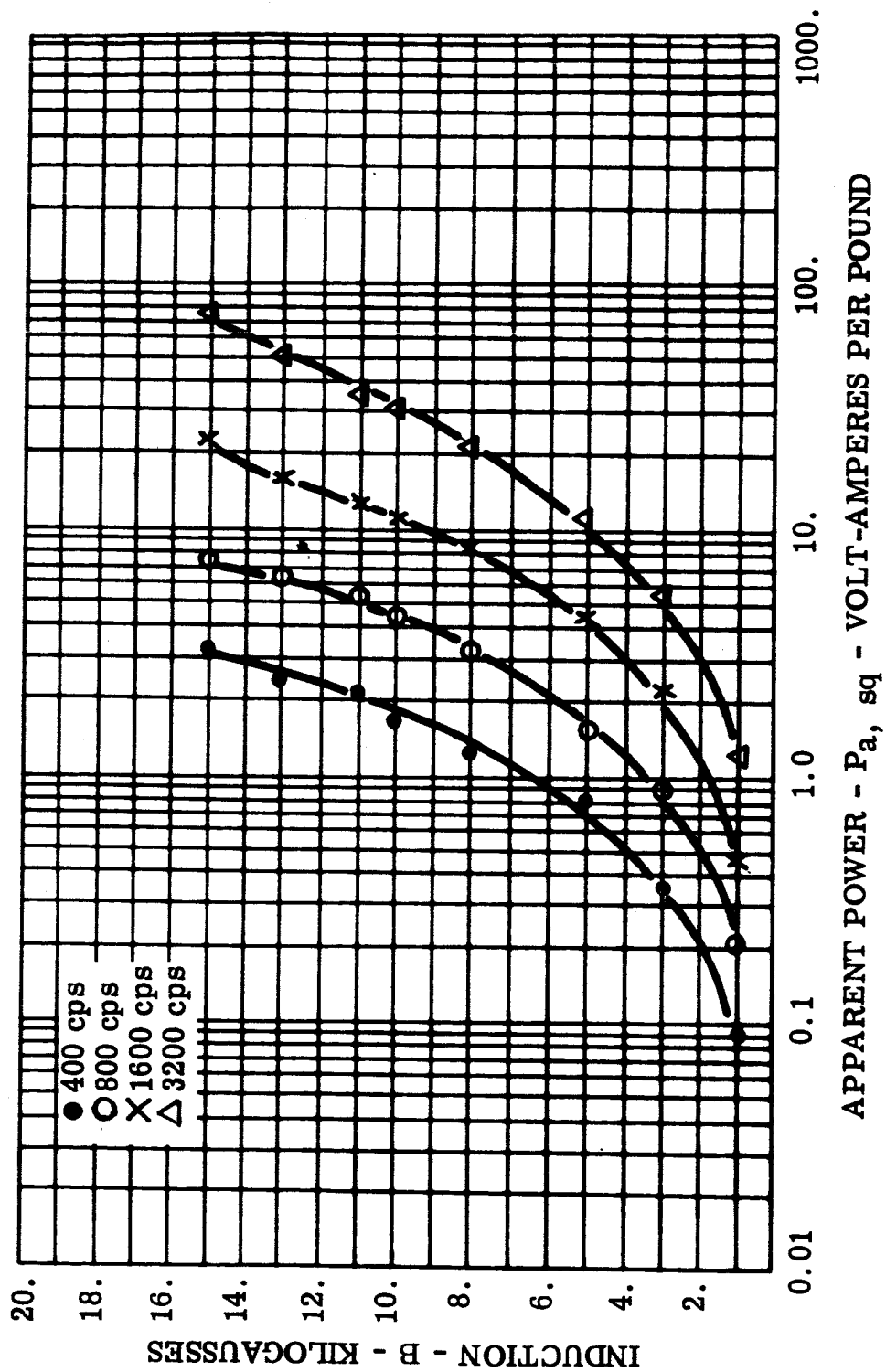


FIGURE 63 P_a, sq - Apparent Power, 0.004 Inch Orthonol Toroid, Core 12,
Room Ambient

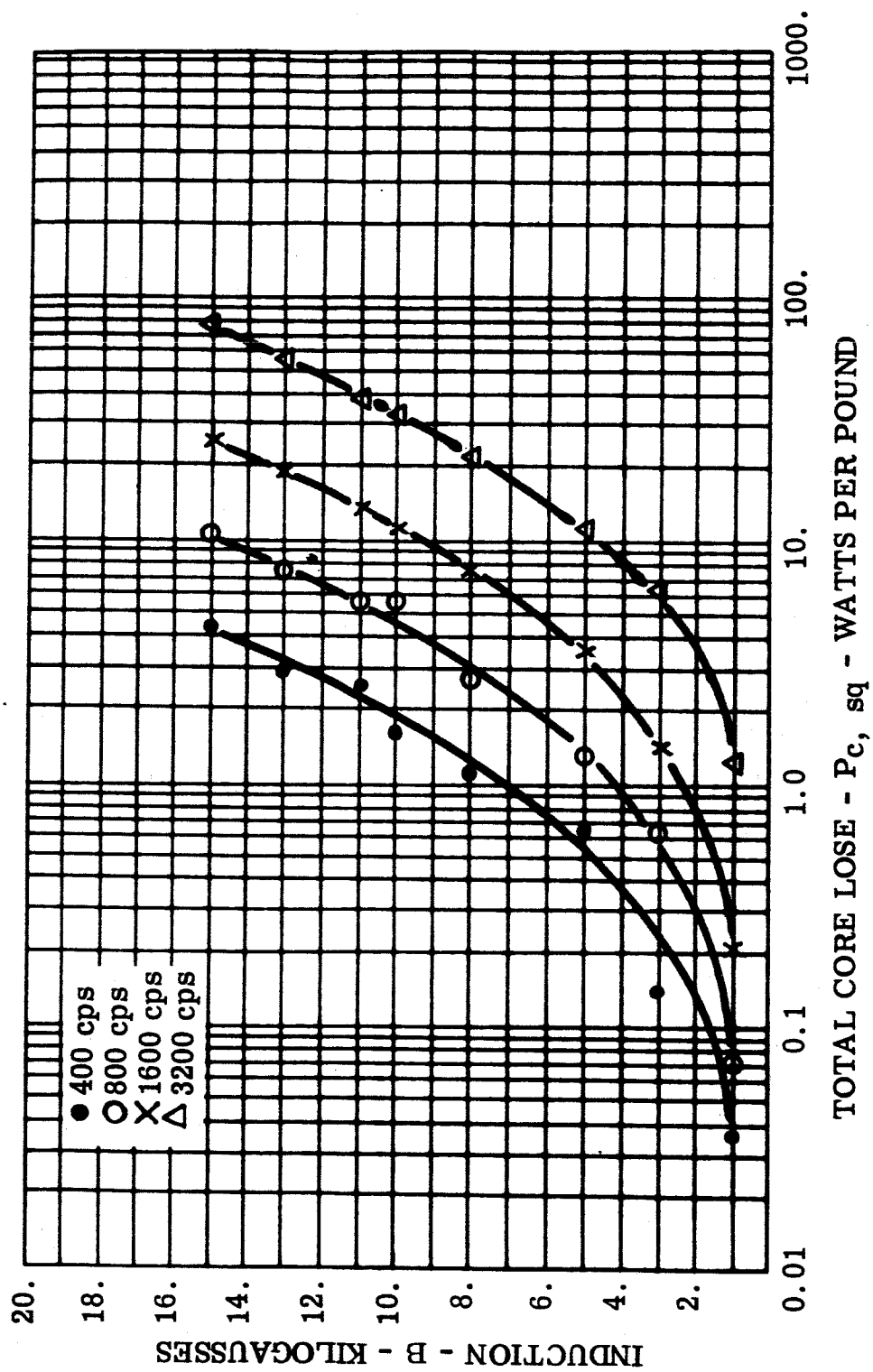


FIGURE 64 P_c , sq - Total Core Loss, 0.004 Inch Orthonol Toroid, Core 12, -55°C

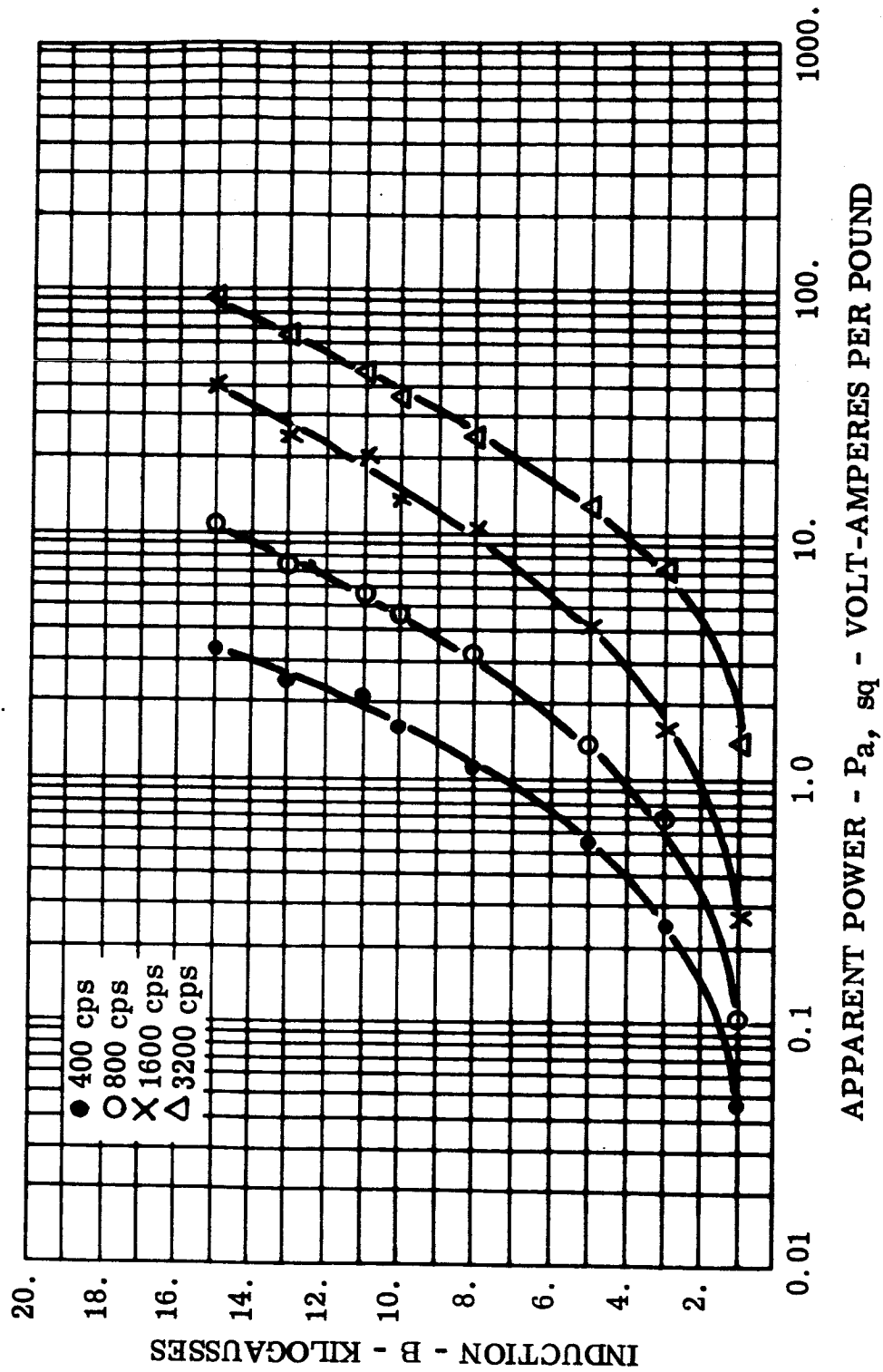


FIGURE 65 P_a , sq - Apparent Power, 0.004 Inch Orthonol Toroid, Core 12, -55°C

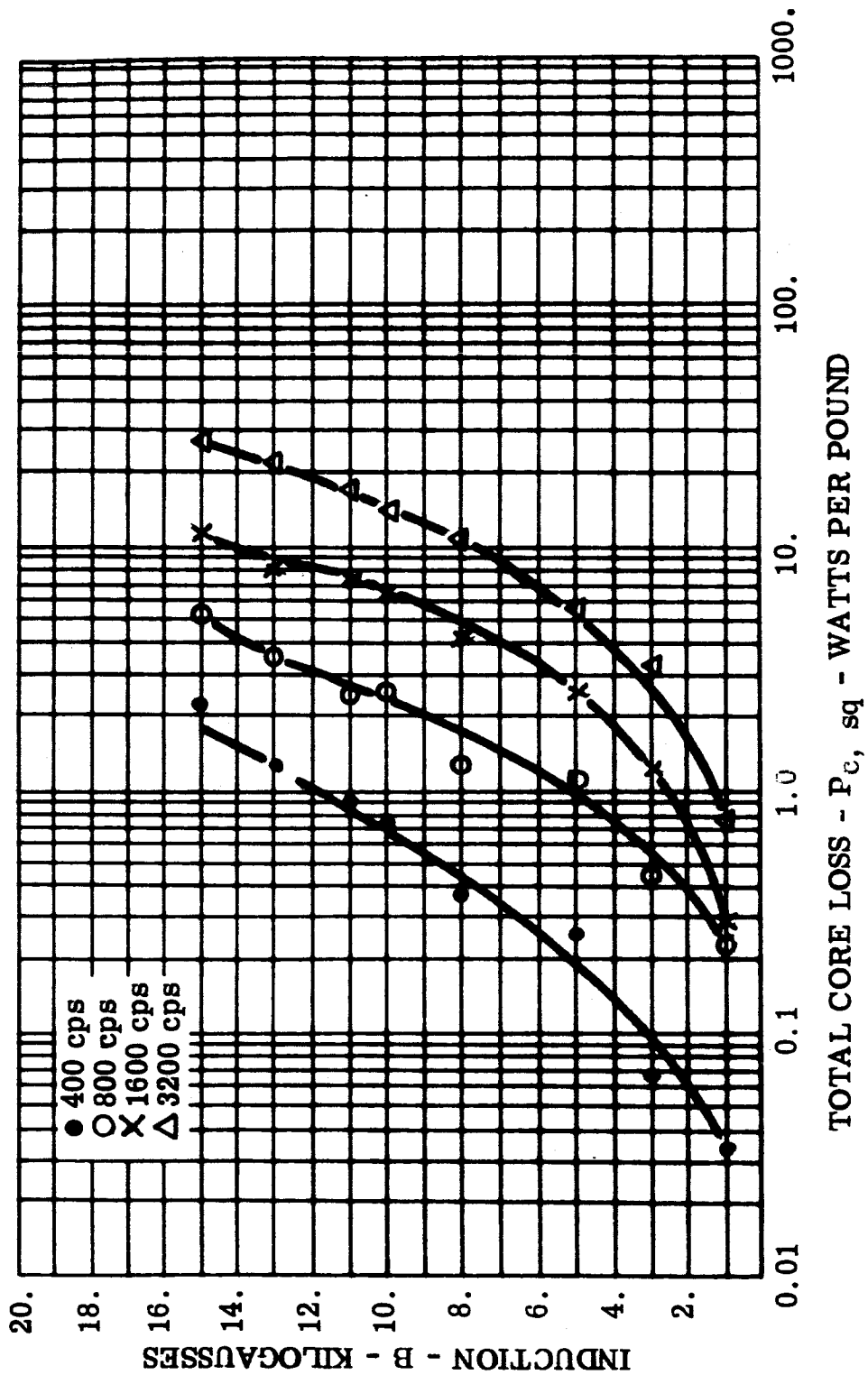


FIGURE 66 P_c , sq - Total Core Loss, 0.002 Inch Hipernik V Toroid, Core 14, Room Ambient

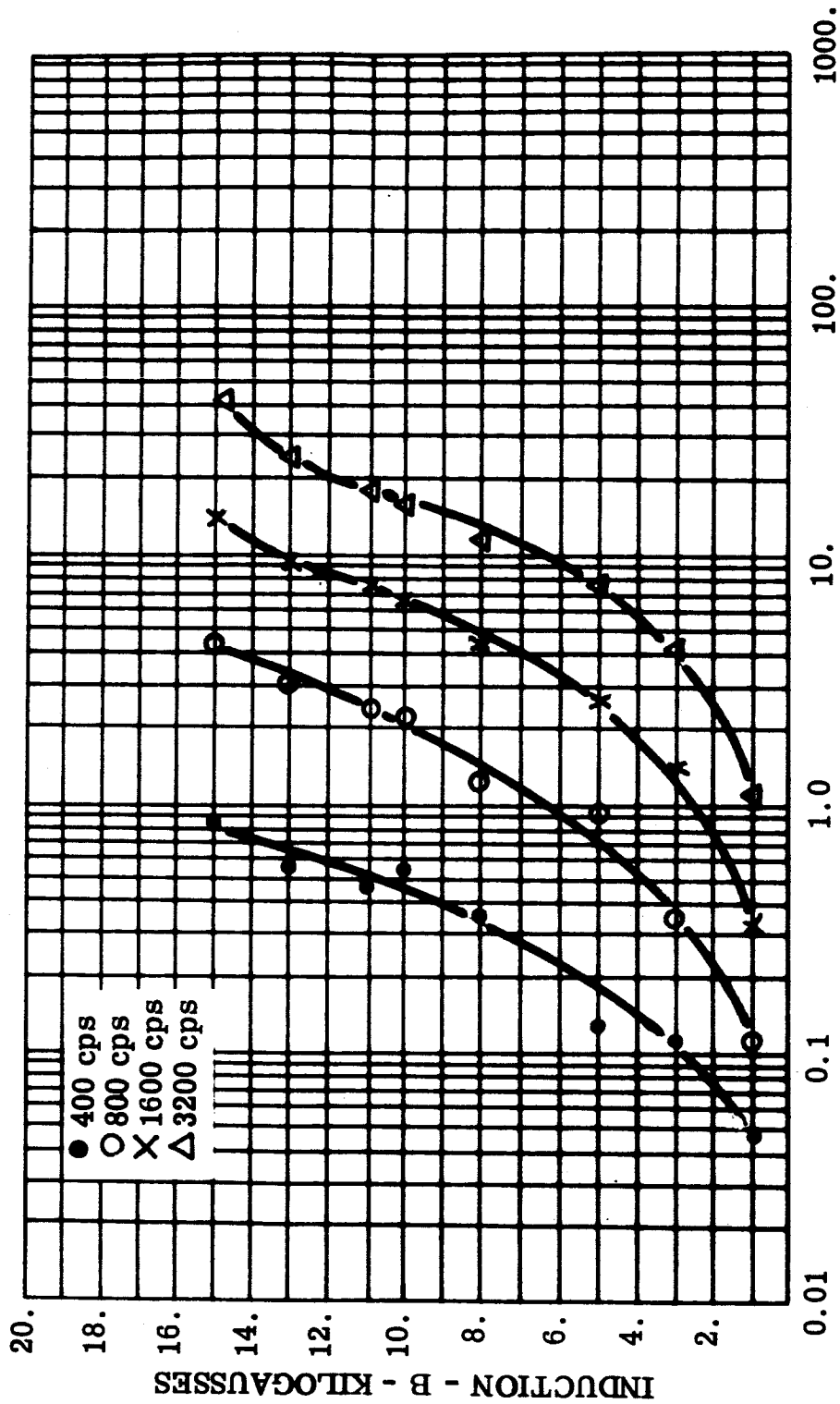


FIGURE 67 P_a , sq - Apparent Power, 0.002 Inch Hipernik V Toroid, Core 14,
Room Ambient

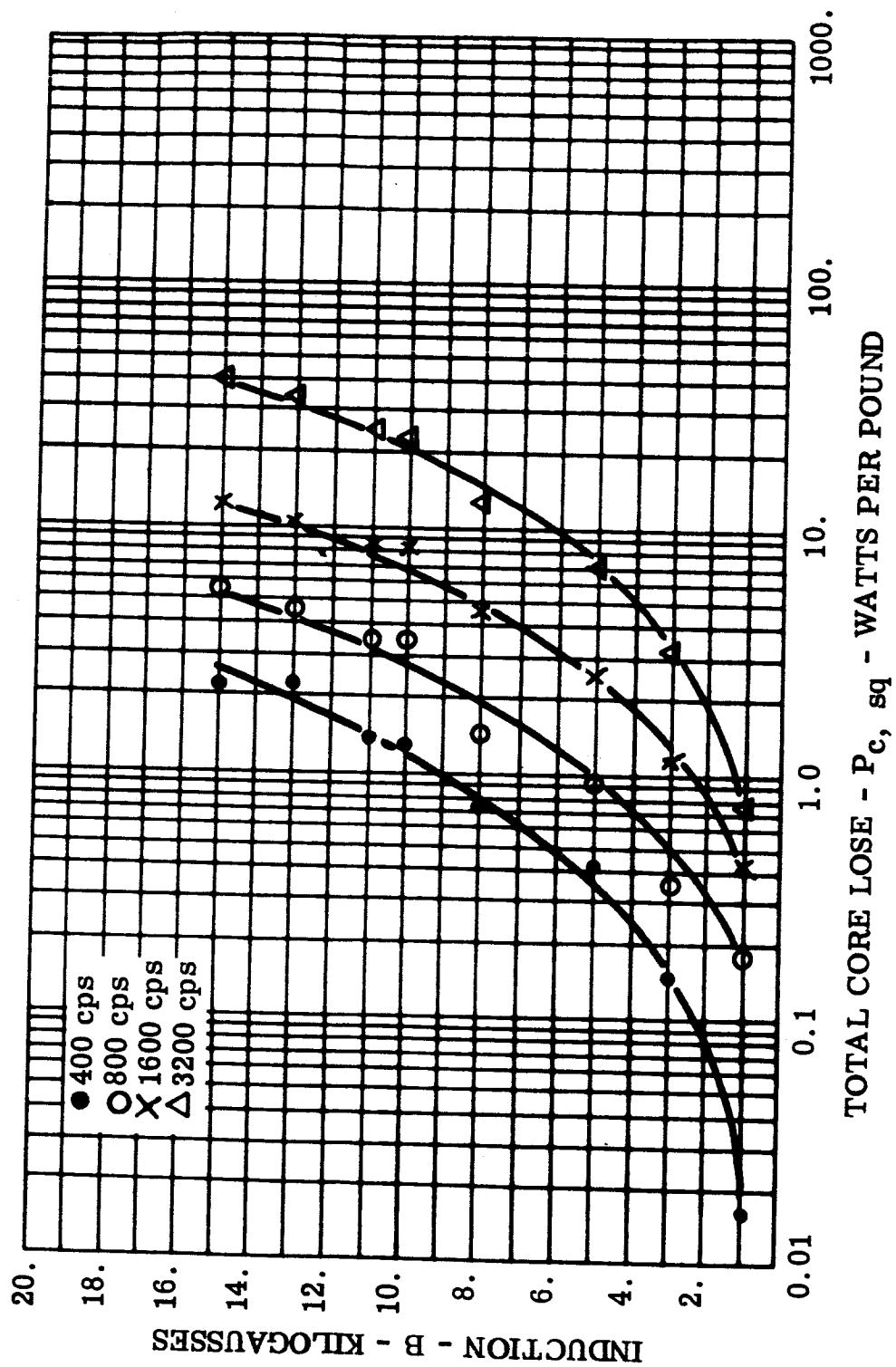
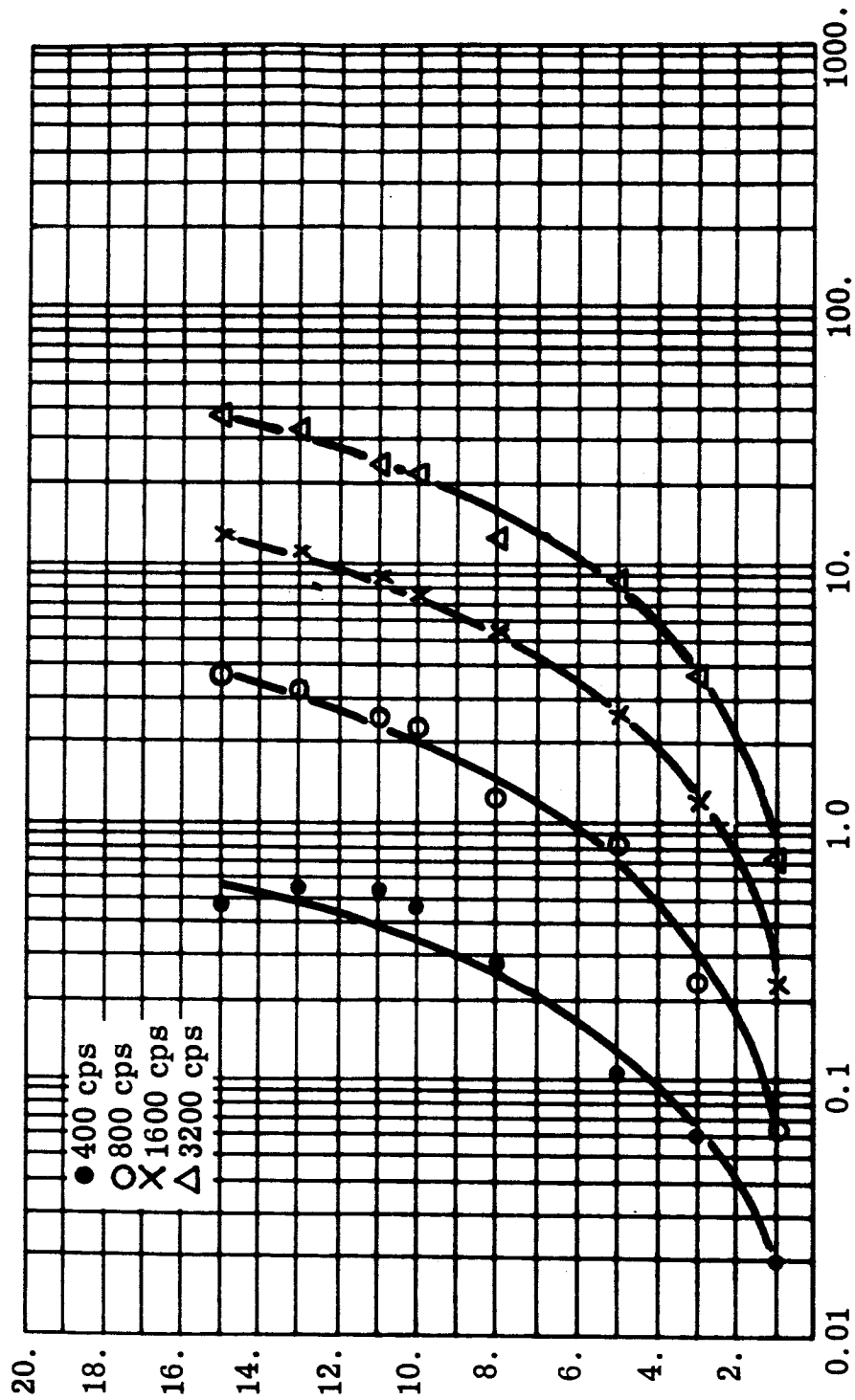


FIGURE 68 $P_{c, sq}$ - Total Core Loss, 0.002 Inch Hipernik V Toroid, Core 14, -55°C



APPARENT POWER - P_a , sq - VOLT-AMPERES PER POUND

FIGURE 69 Apparent Power, 0.002 Inch Hipernik V Toroid, Core 14, -55°C

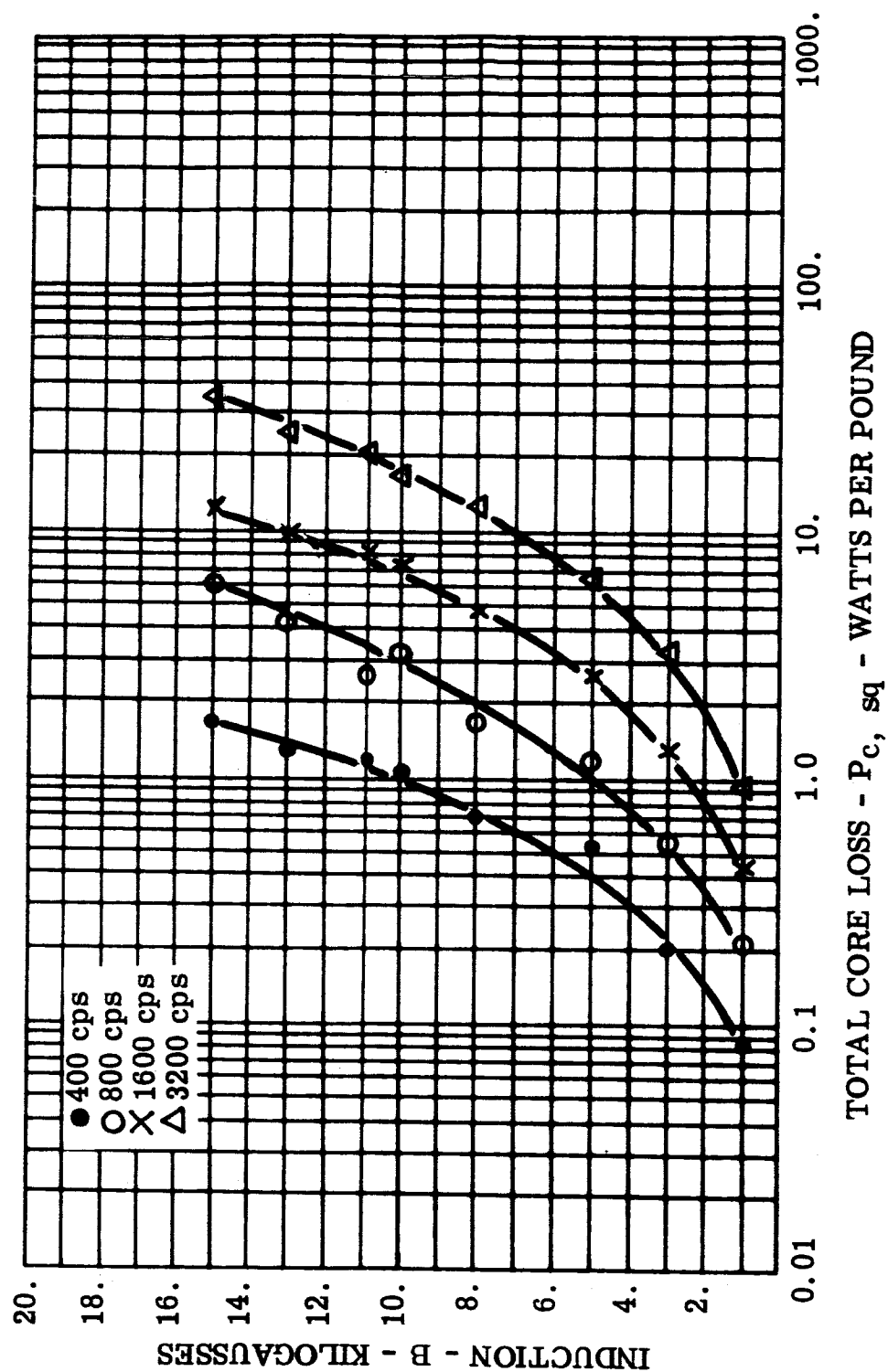


FIGURE 70 $P_{c, sq}$ - Total Core Loss, 0.002 Inch Hipernik V Toroid, Core 15,
Room Ambient

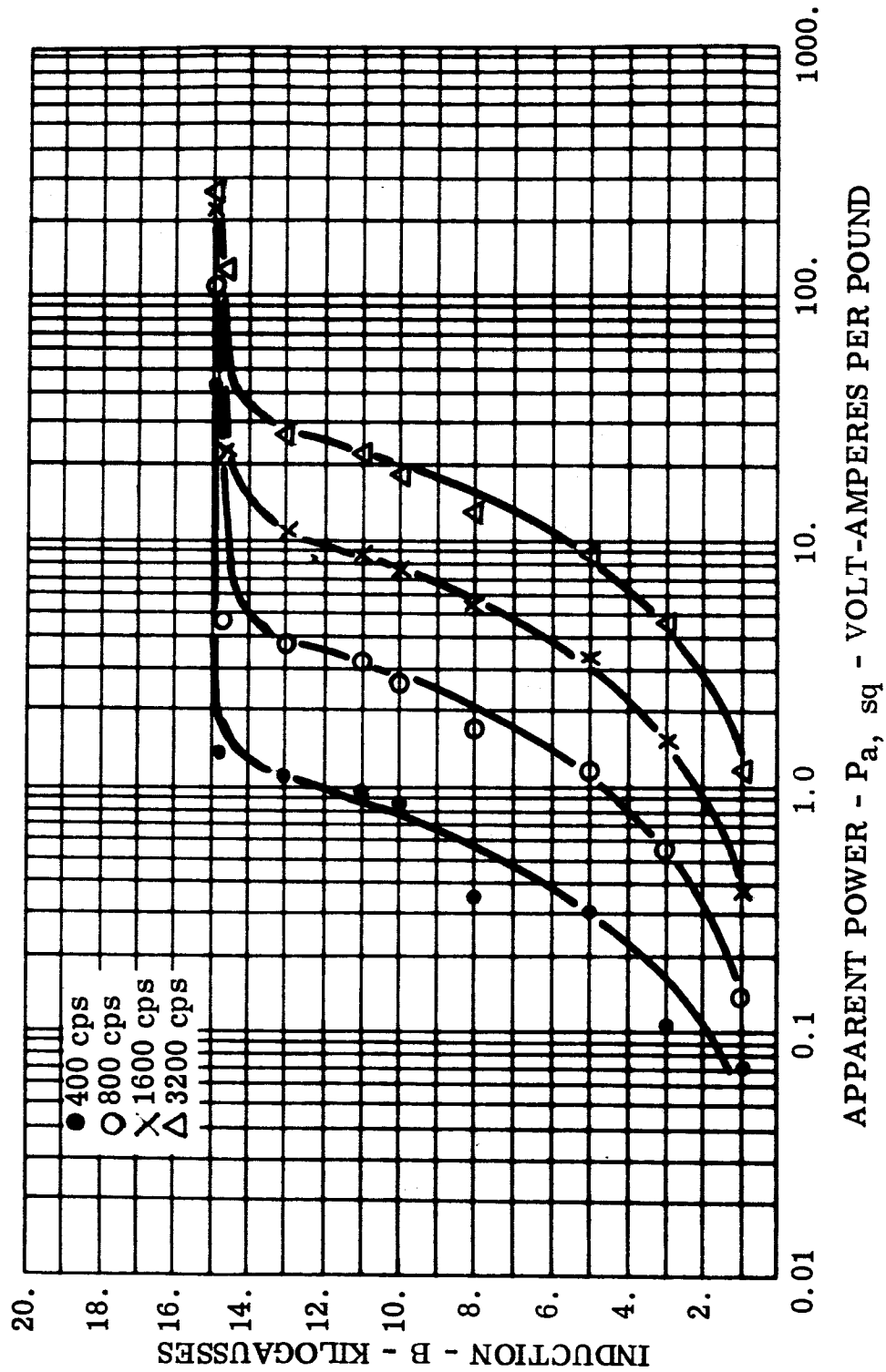


FIGURE 71 P_a, sq - Apparent Power, 0.002 Inch Hipernik V Toroid, Core 15,
Room Ambient

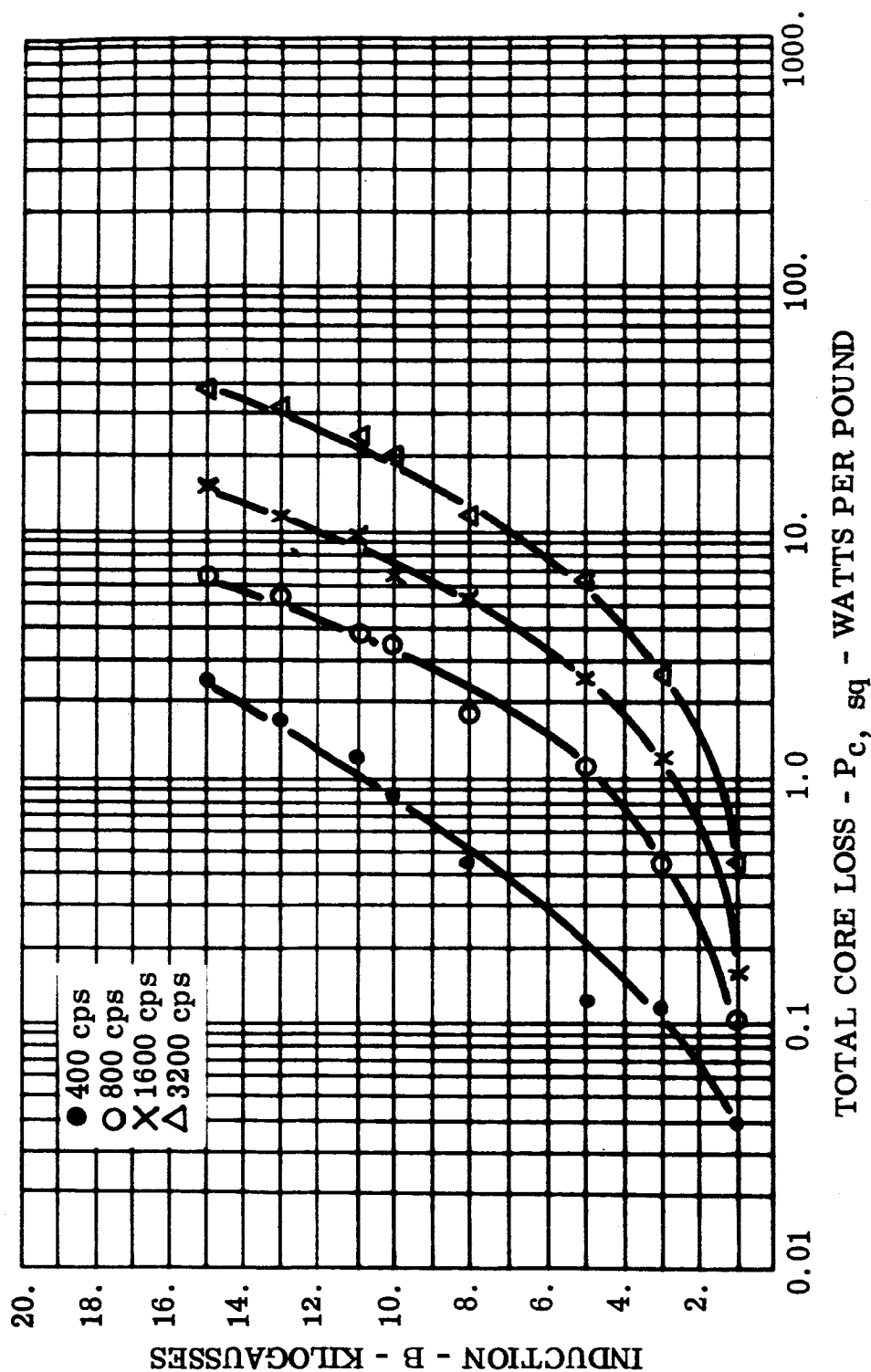


FIGURE 72 P_c , sq - Total Core Loss, 0.002 Inch Hipernik V Toroid, Core 15, -55°C

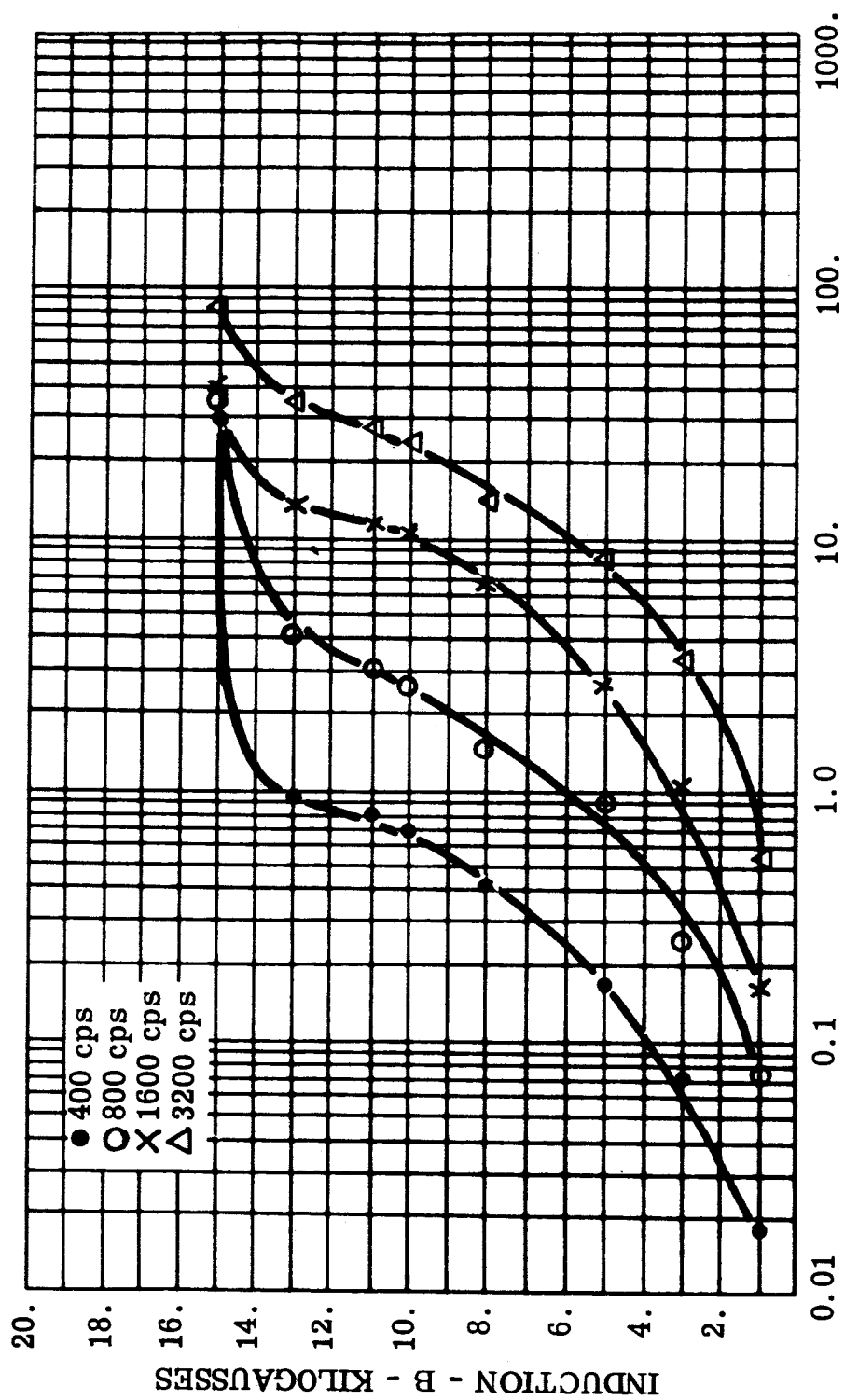
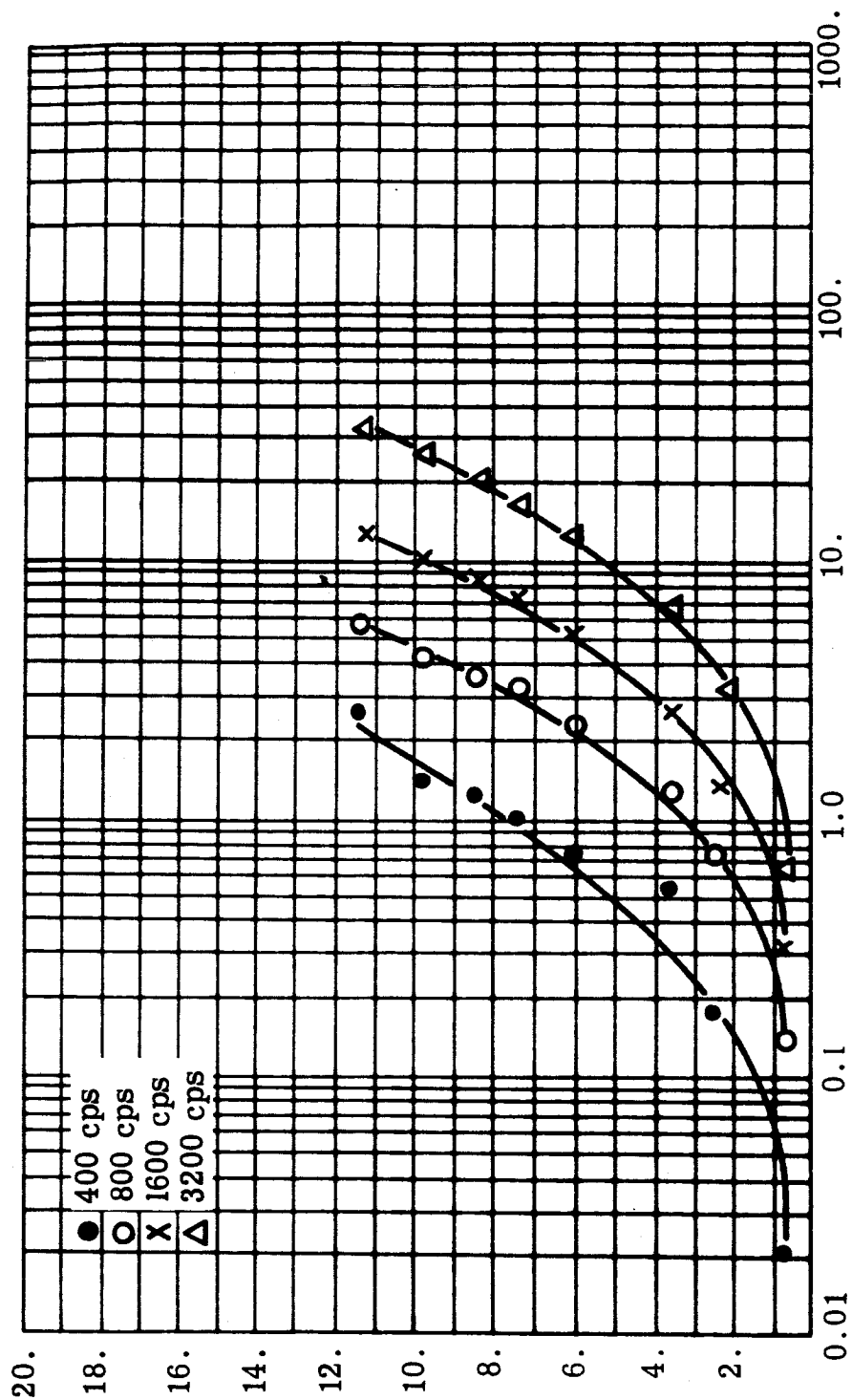
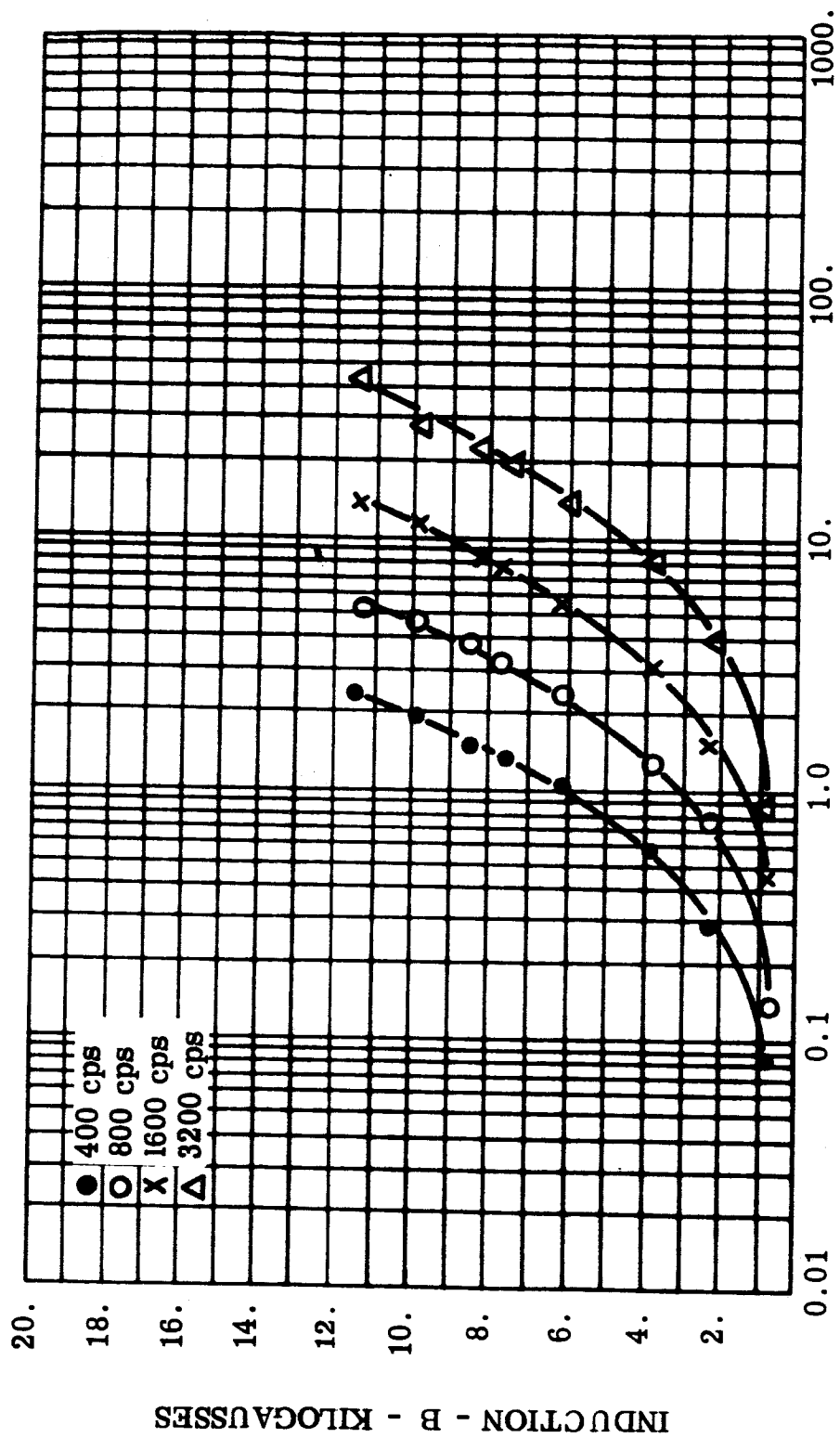


FIGURE 73 P_a, sq - Apparent Power, 0.002 Inch Hipernik V Toroid, Core 15, $-55^{\circ}C$



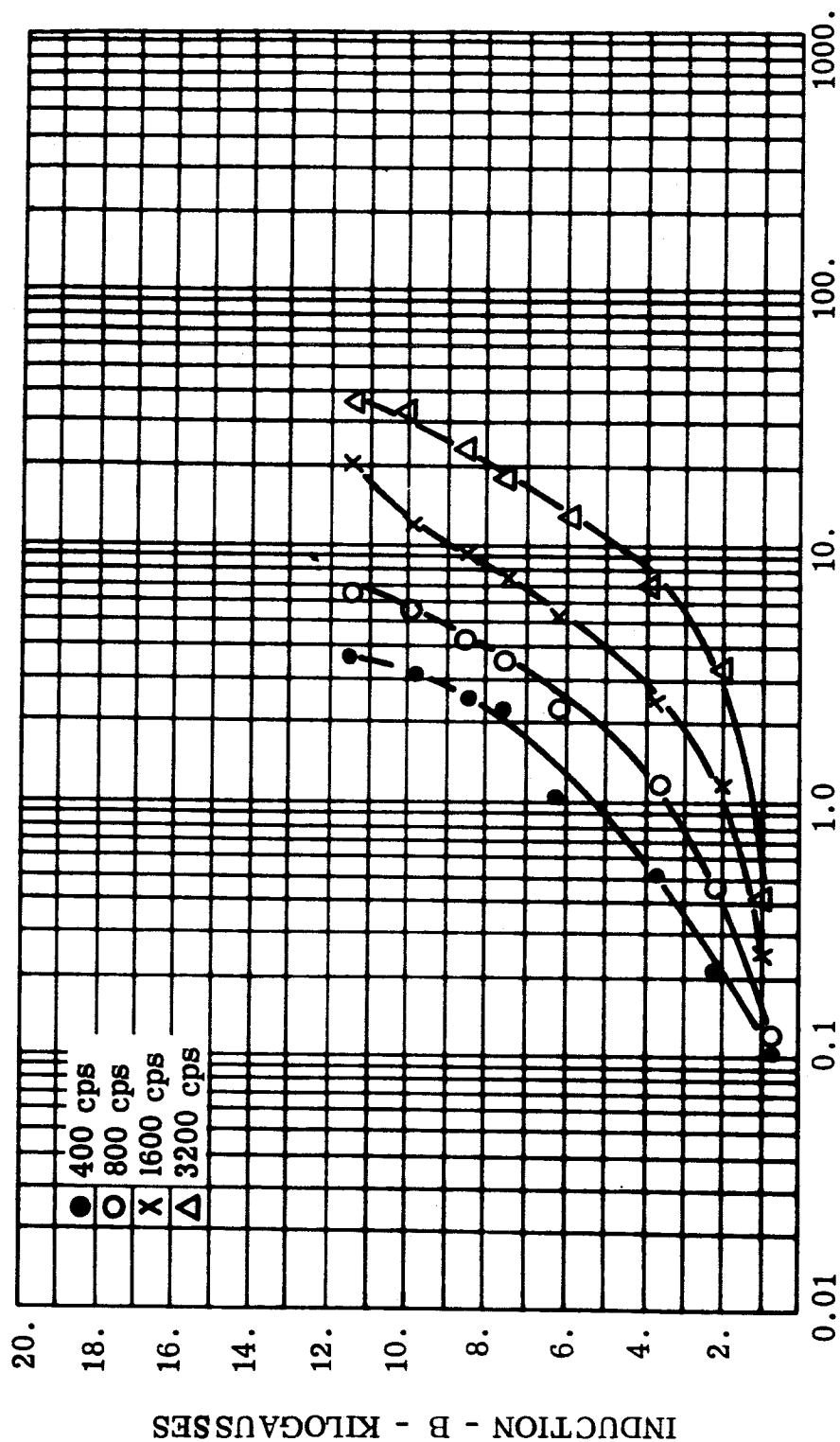
TOTAL CORE LOSS - $P_{c, sq}$ - WATTS PER POUND

FIGURE 74. $P_{c, sq}$ - Total Core Loss, 0.004 Inch Hipernik V Toroid, Core 17, Room Ambient



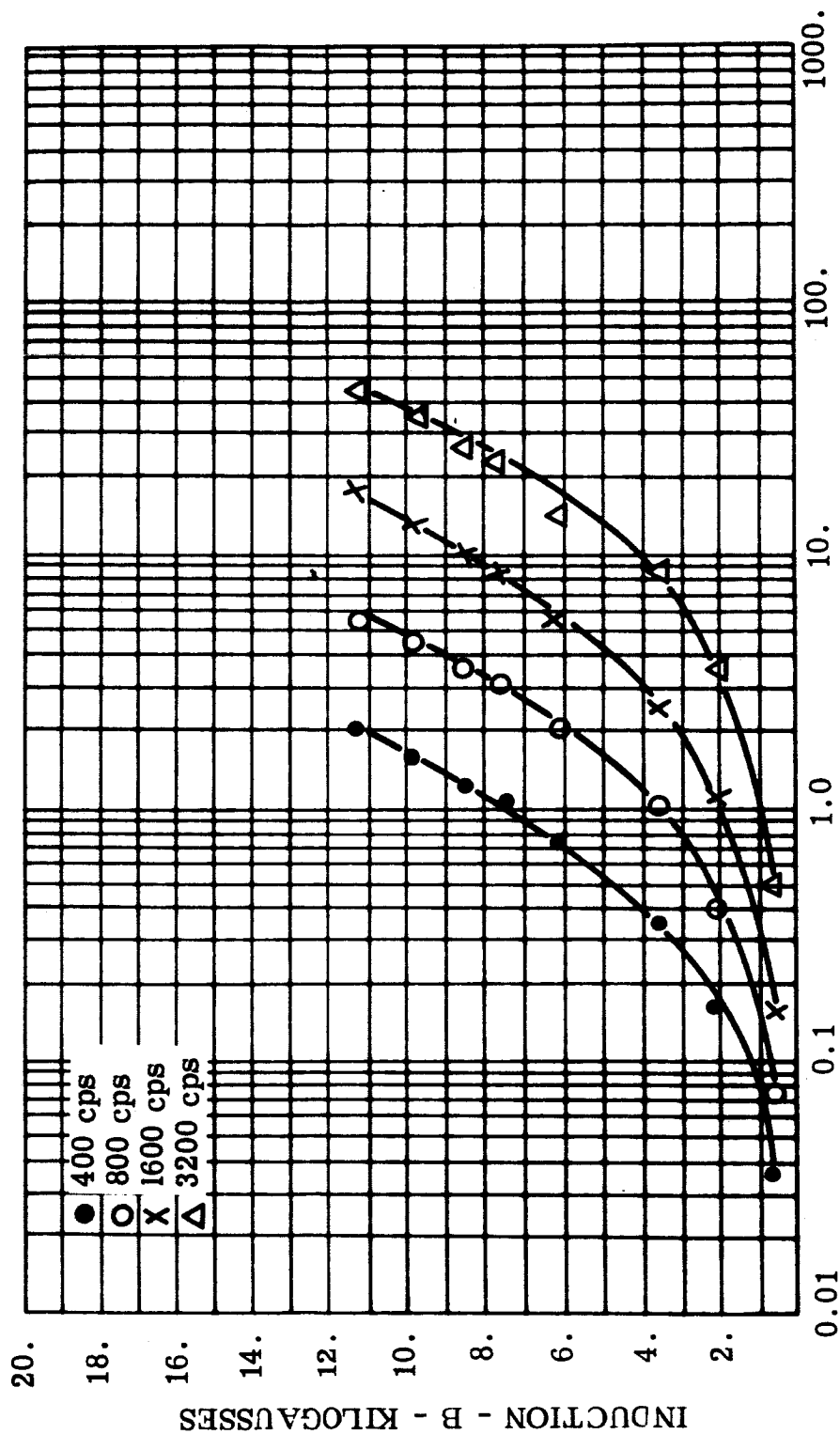
APPARENT POWER - P_a , sq - VOLT-AMPERES POUND

FIGURE 75. P_a , sq - Apparent Power, 0.004 Inch Hipernik V Toroid, Core 17, Room Ambient



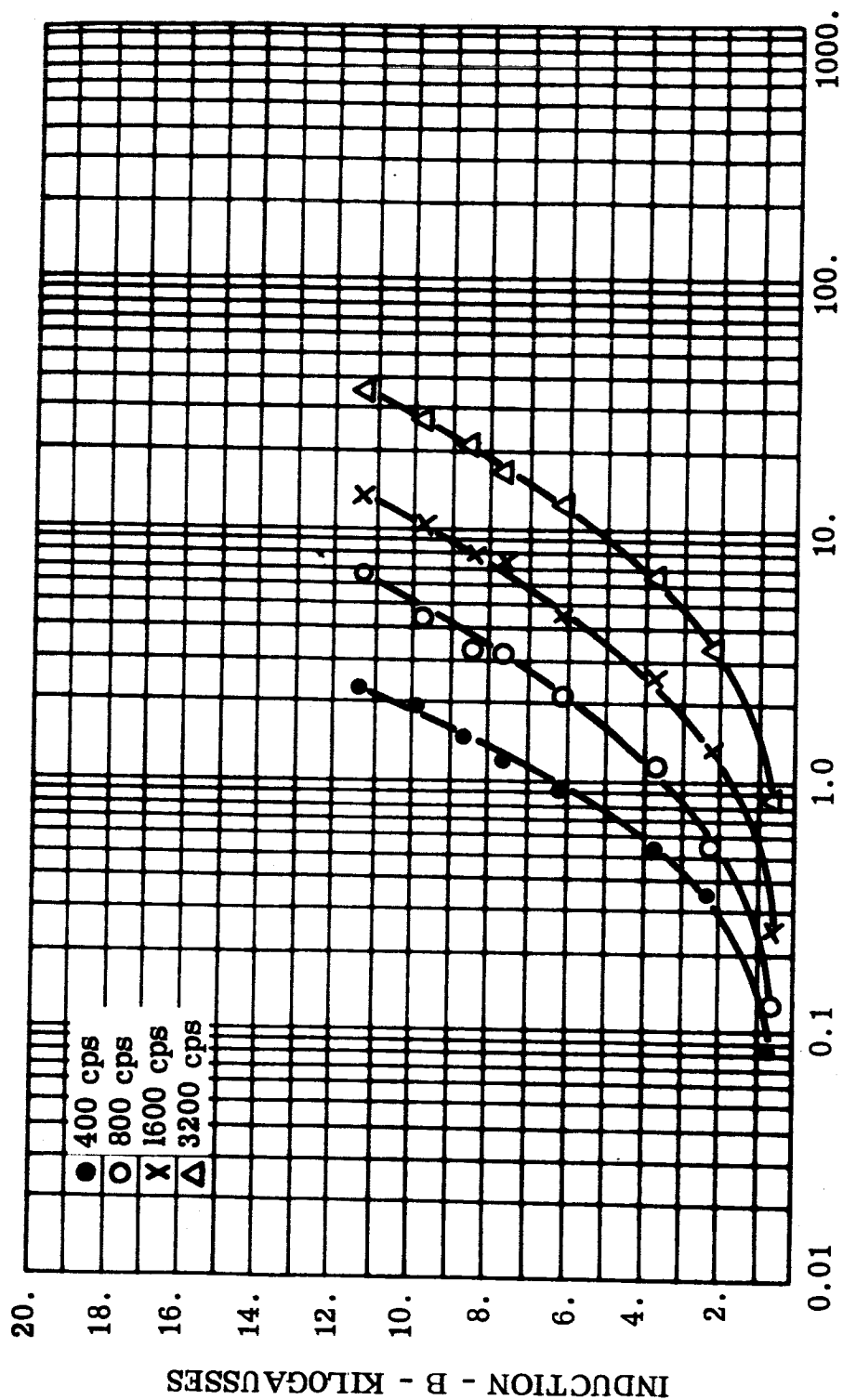
TOTAL CORE LOSS - $P_{c, sq}$ - WATTS PER POUND

FIGURE 76. $P_{c, sq}$ - Total Core Loss, 0.004 Inch Hipernik V Toroid, Core 17, -55°C



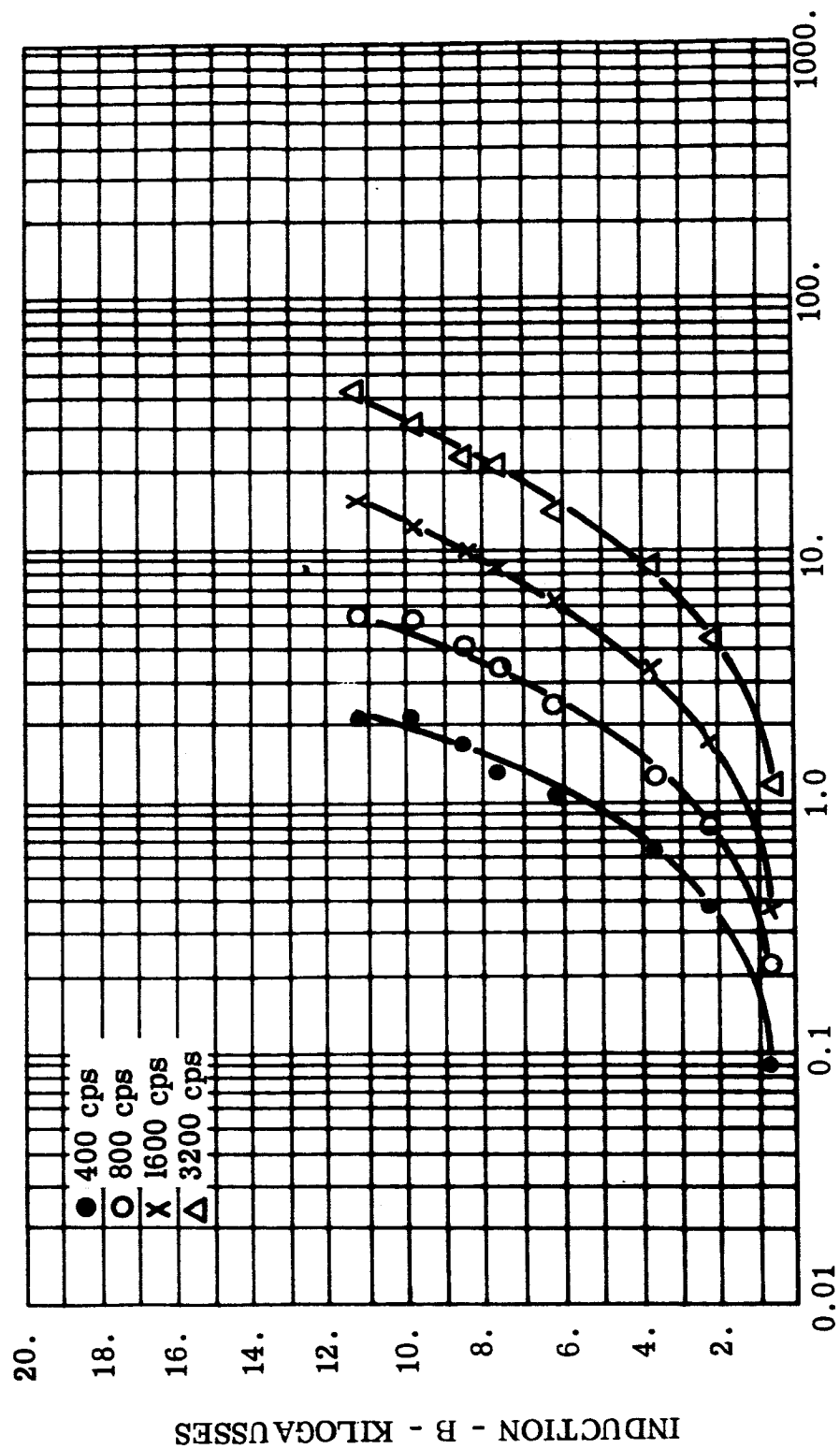
APPARENT POWER - P_a - VOLT AMPERES PER POUND

FIGURE 77. P_a , sq - Apparent Power, 0.004 Inch Hipernik V Toroid, Core 17, -55°C



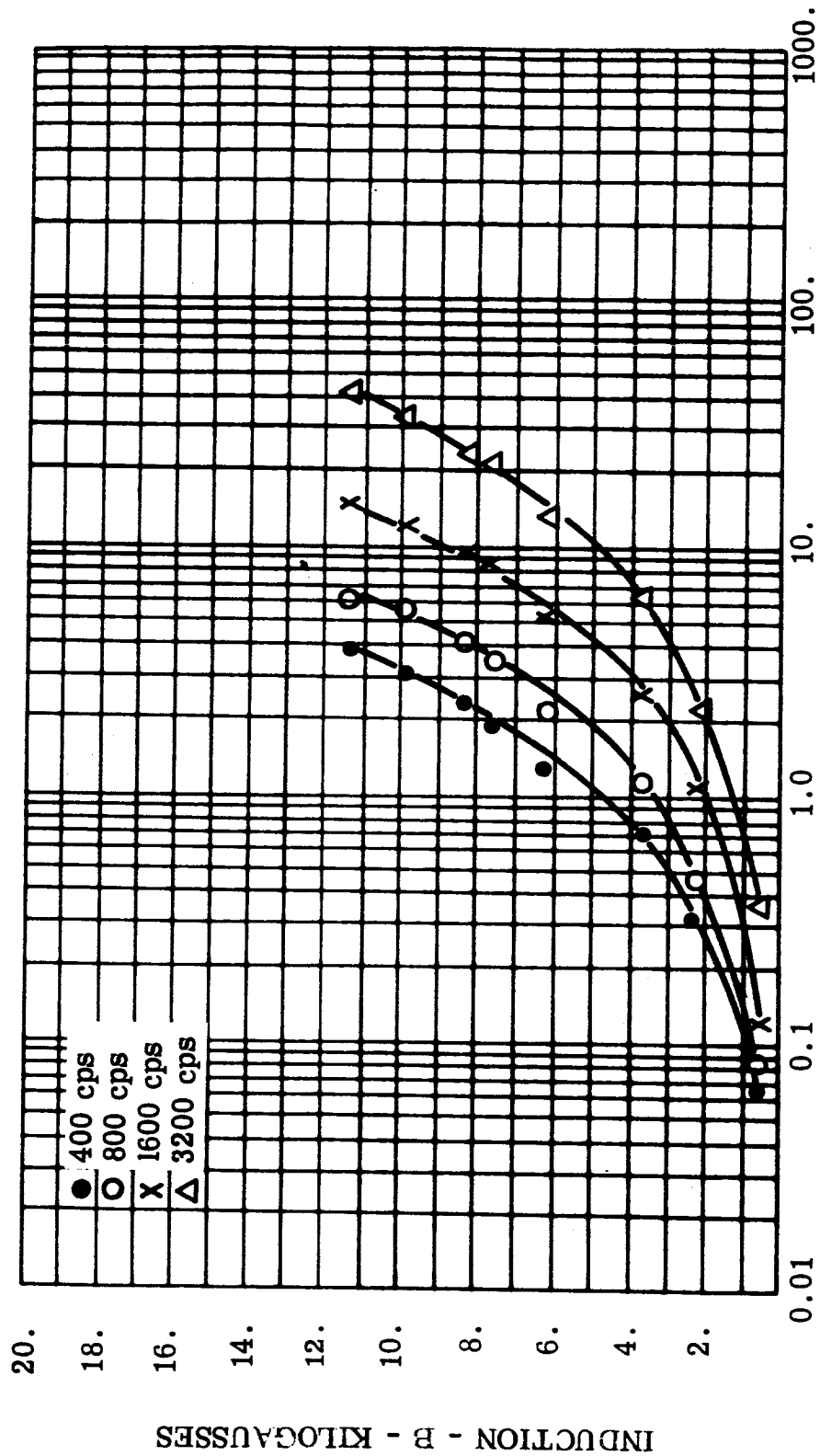
TOTAL CORE LOSS - P_c , sq - WATTS PER POUND

FIGURE 78. P_c , sq - Total Core Loss, 0.004 Inch Hipernik V Toroid, Core 18, Room Ambient



APPARENT POWER - P_a, sq - VOLT-AMPERES PER POUND

FIGURE 79. P_a, sq - Apparent Power, 0.004 Inch Hipernik V Toroid, Core 18, Room Ambient



TOTAL CORE LOSE - P_c , sq - WATTS PER POUND

FIGURE 80. P_c , sq - Total Core Loss, 0.004 Inch Hipernik V Toroid, Core 18, -55°C

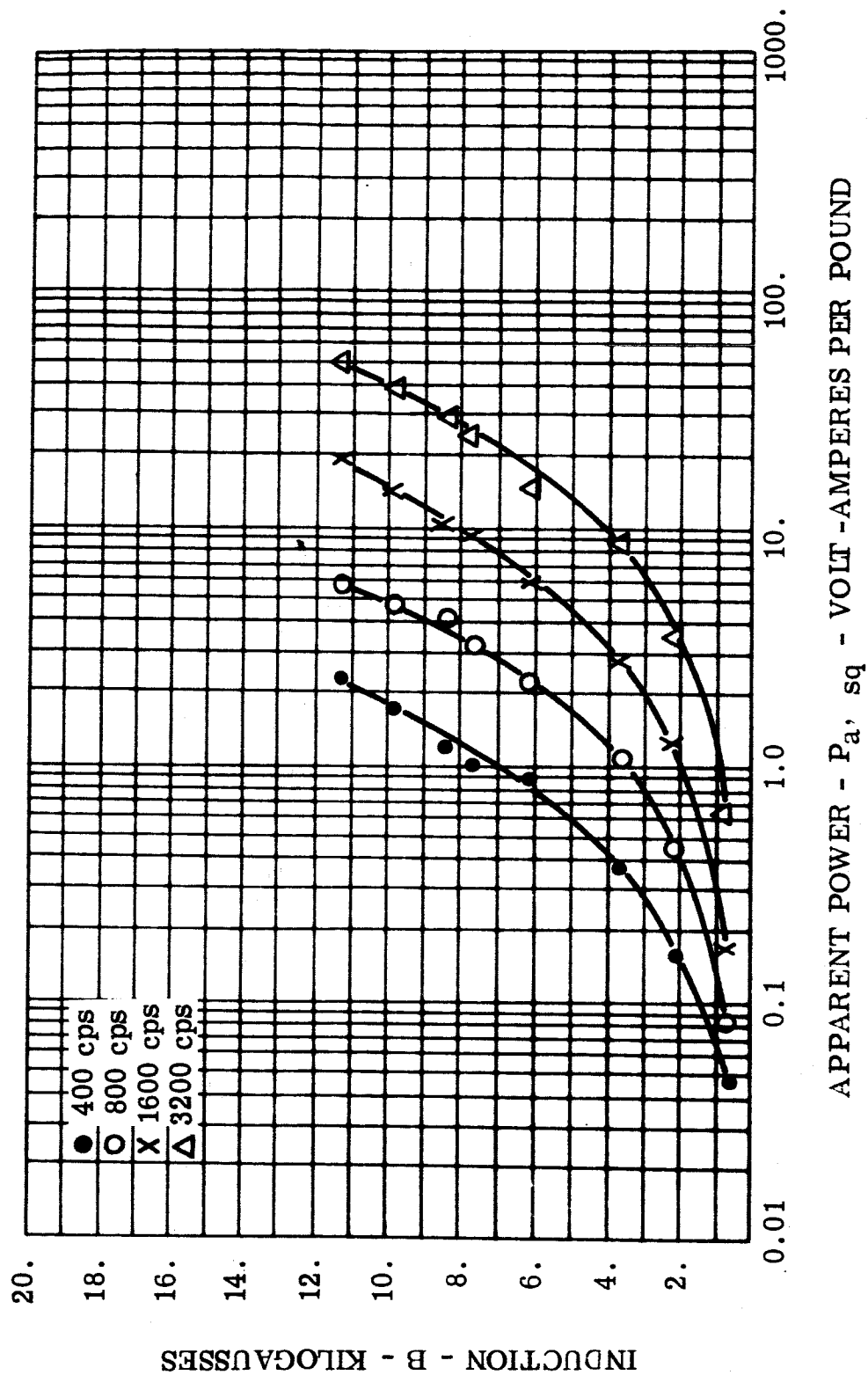


FIGURE 81. P_a, sq - Apparent Power, 0.004 Inch Hipernik V Toroid, Core 18, -55°C

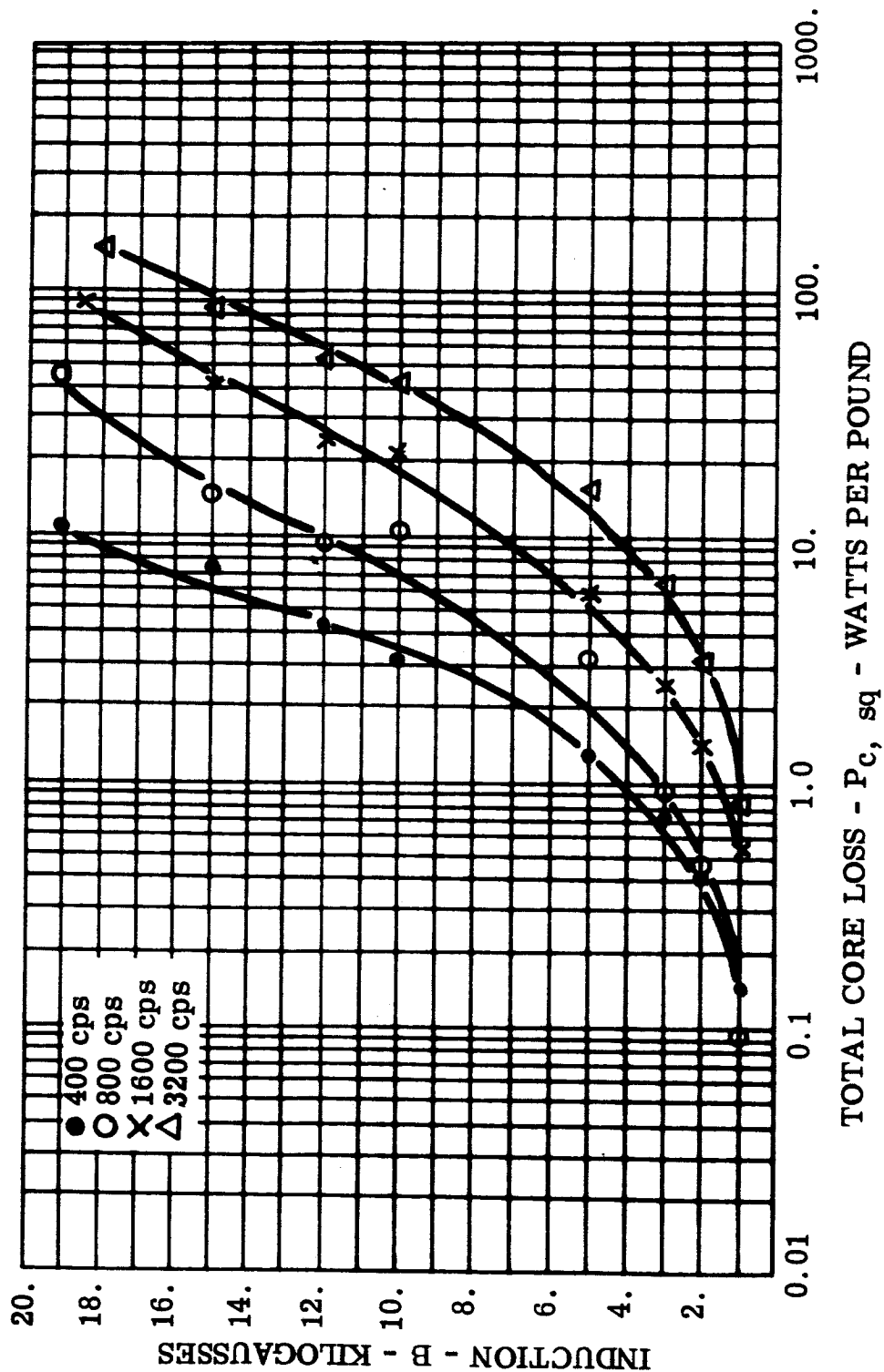


FIGURE 82 $P_{c, sq}$ - Total Core Loss, 0.002 Inch Magnesil Toroid, Core 28, Room Ambient

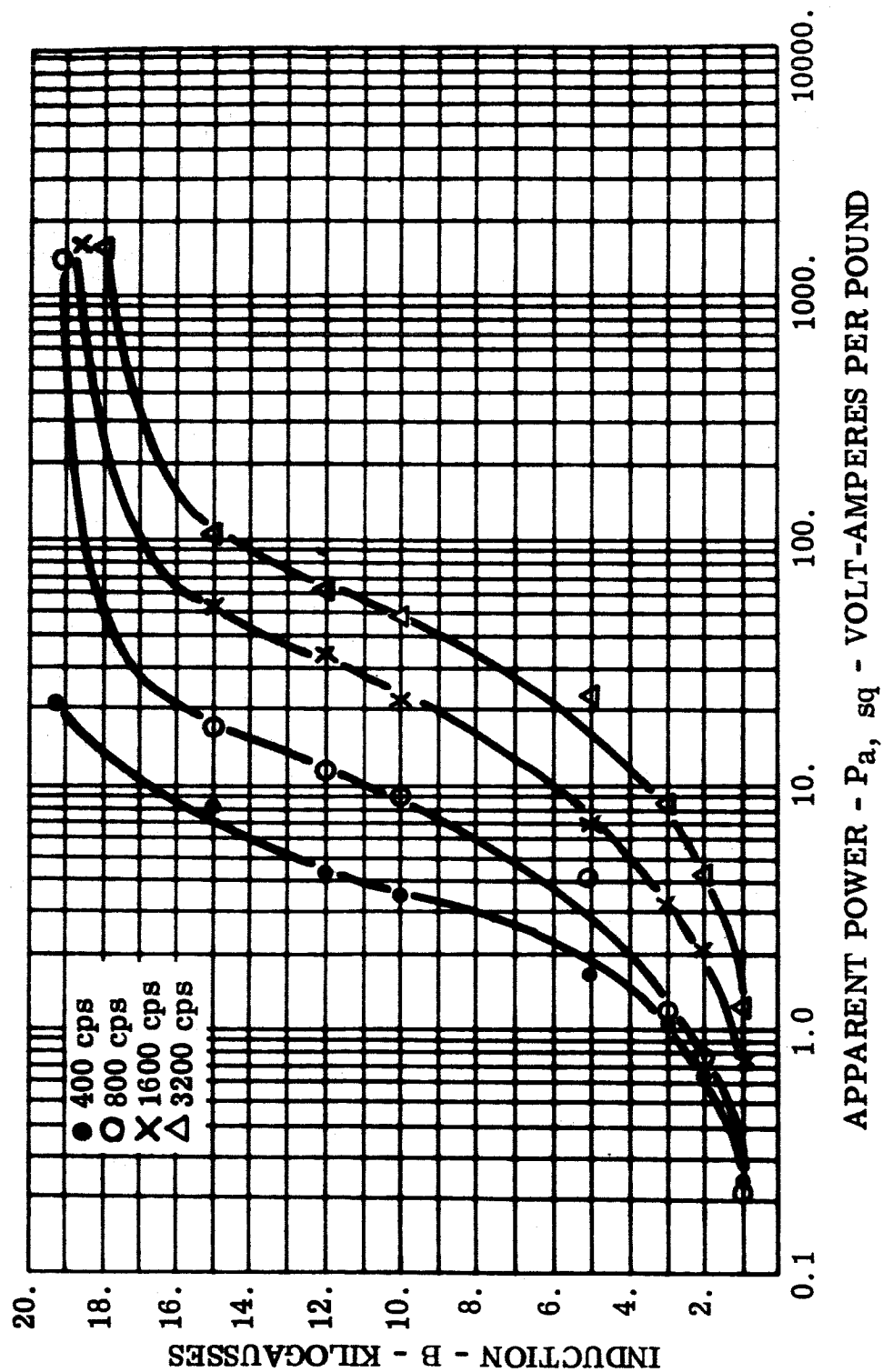


FIGURE 83 P_a, sq - Apparent Power, 0.002 Inch Magnesil Toroid, Core 28, Room Ambient

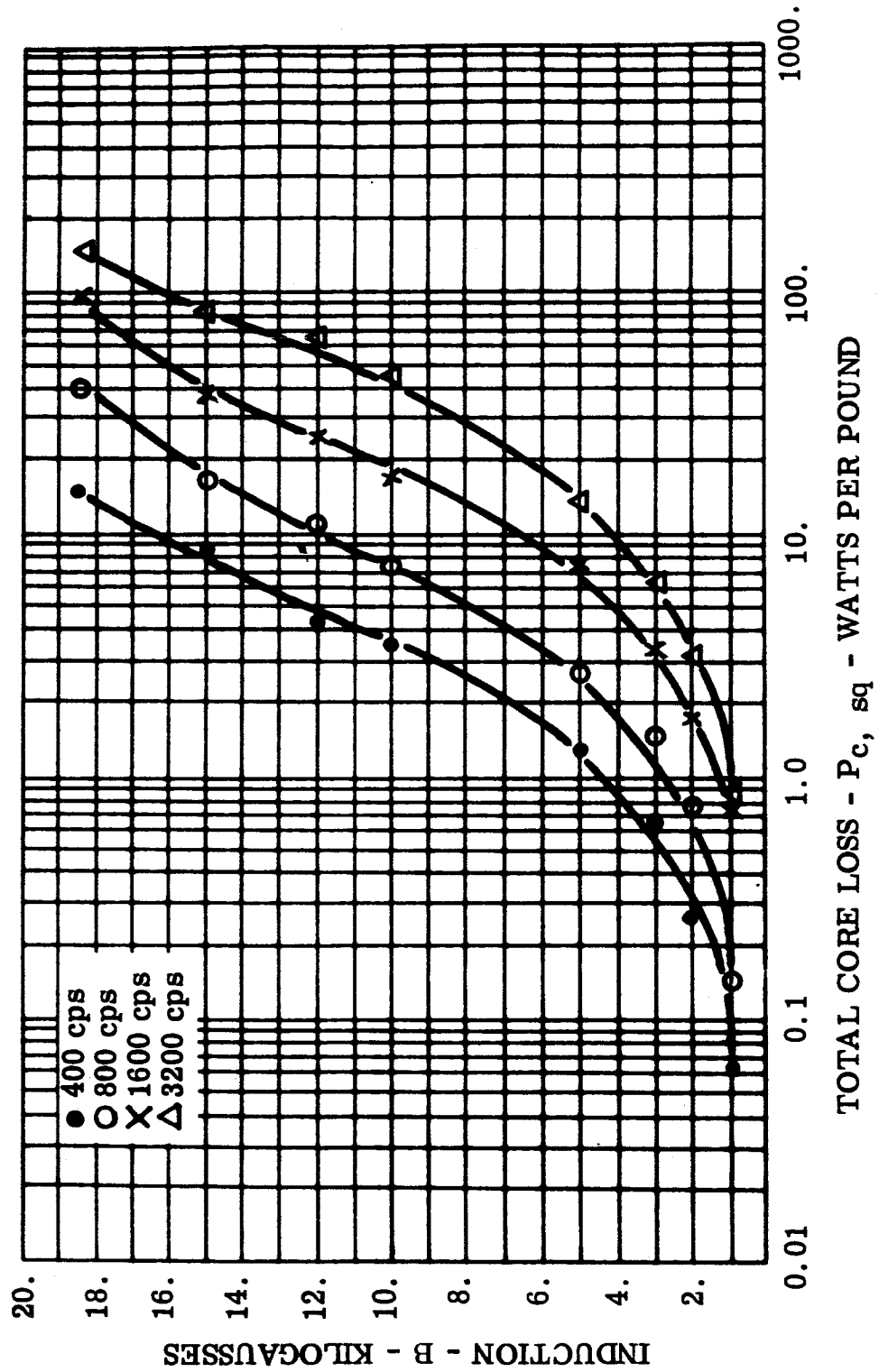


FIGURE 84 $P_{c, sq}$ - Total Core Loss, 0.002 Inch Magnesil Toroid, Core 28, -55°C

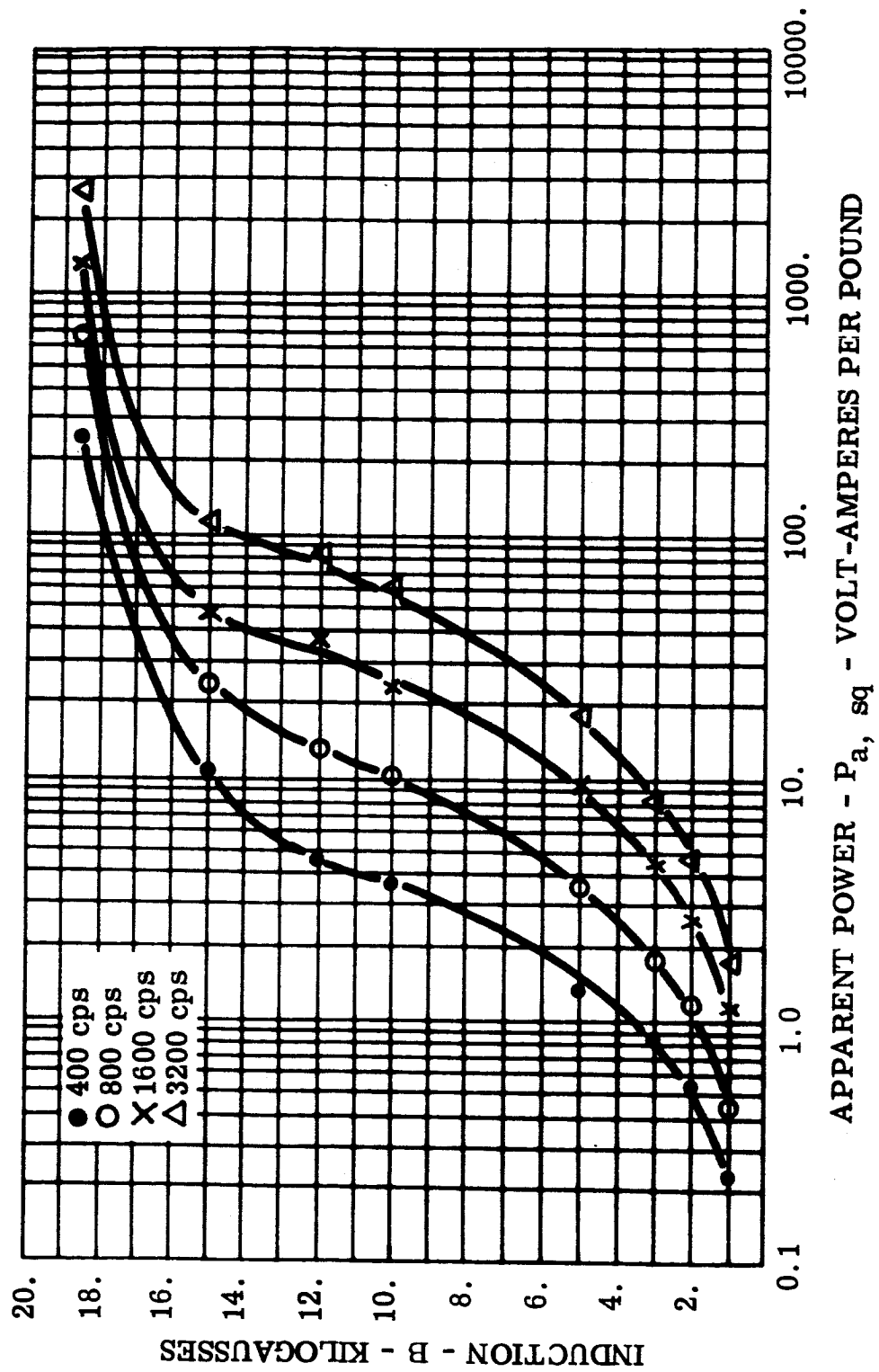


FIGURE 85 P_a , sq - Apparent Power, 0.002 Inch Magnesil Toroid, Core 28, -55°C

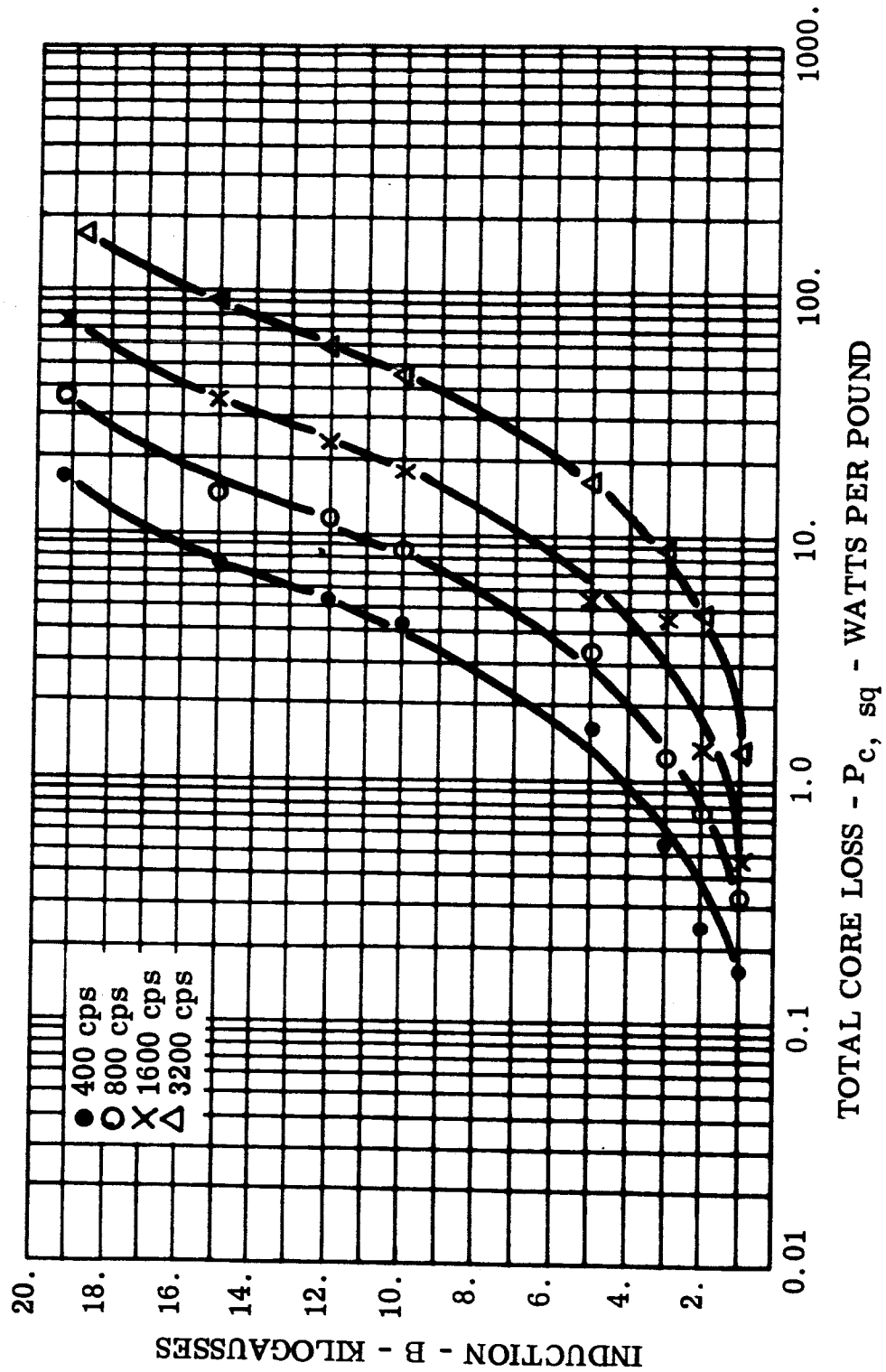


FIGURE 86 $P_{c, sq}$ - Total Core Loss, 0.002 Inch Magnesil Toroid, Core 30,
Room Ambient

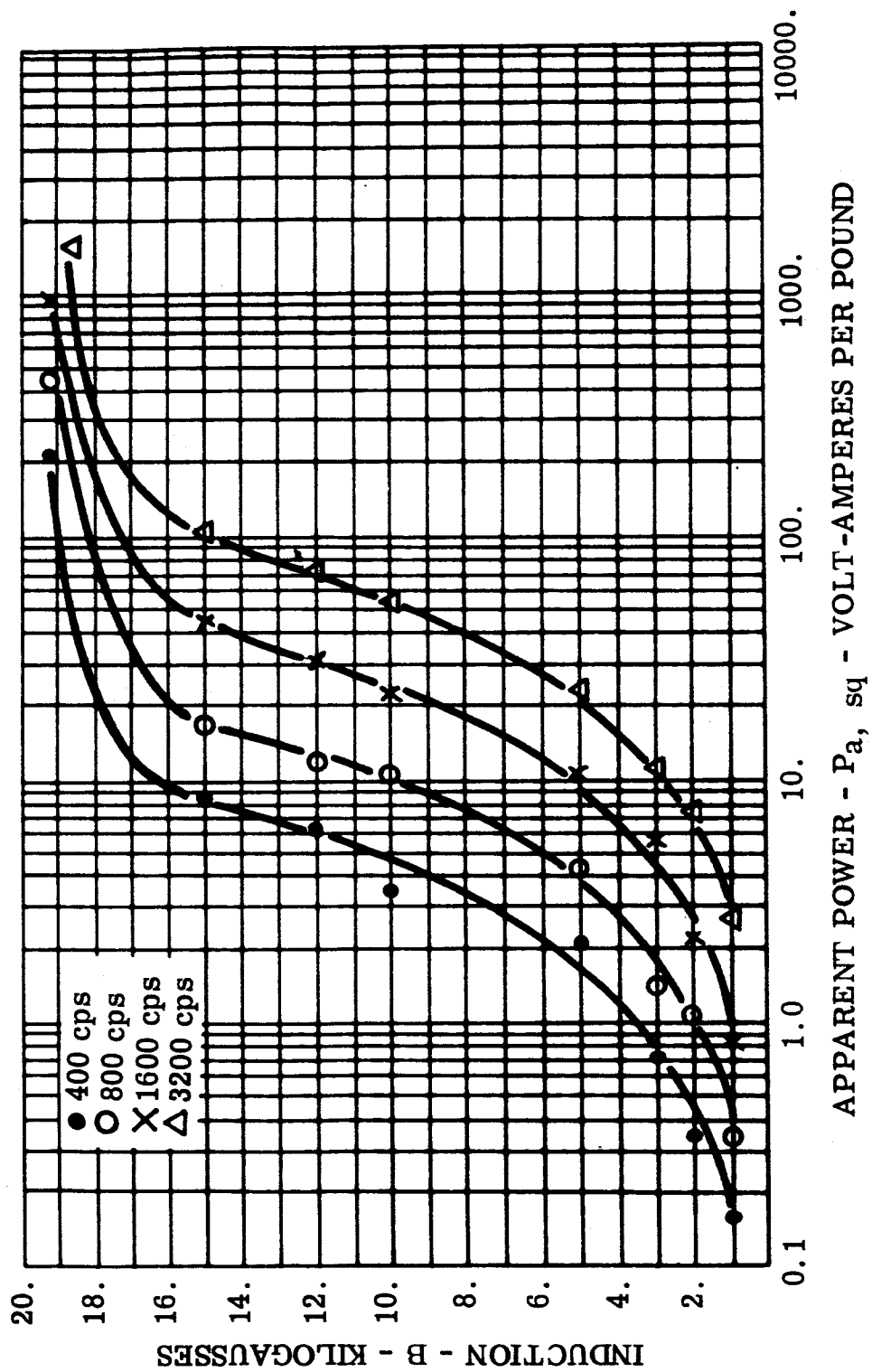


FIGURE 87 $P_{a, sq}$ - Apparent Power, 0.002 Inch Magnesil Toroid, Core 30,
Room Ambient

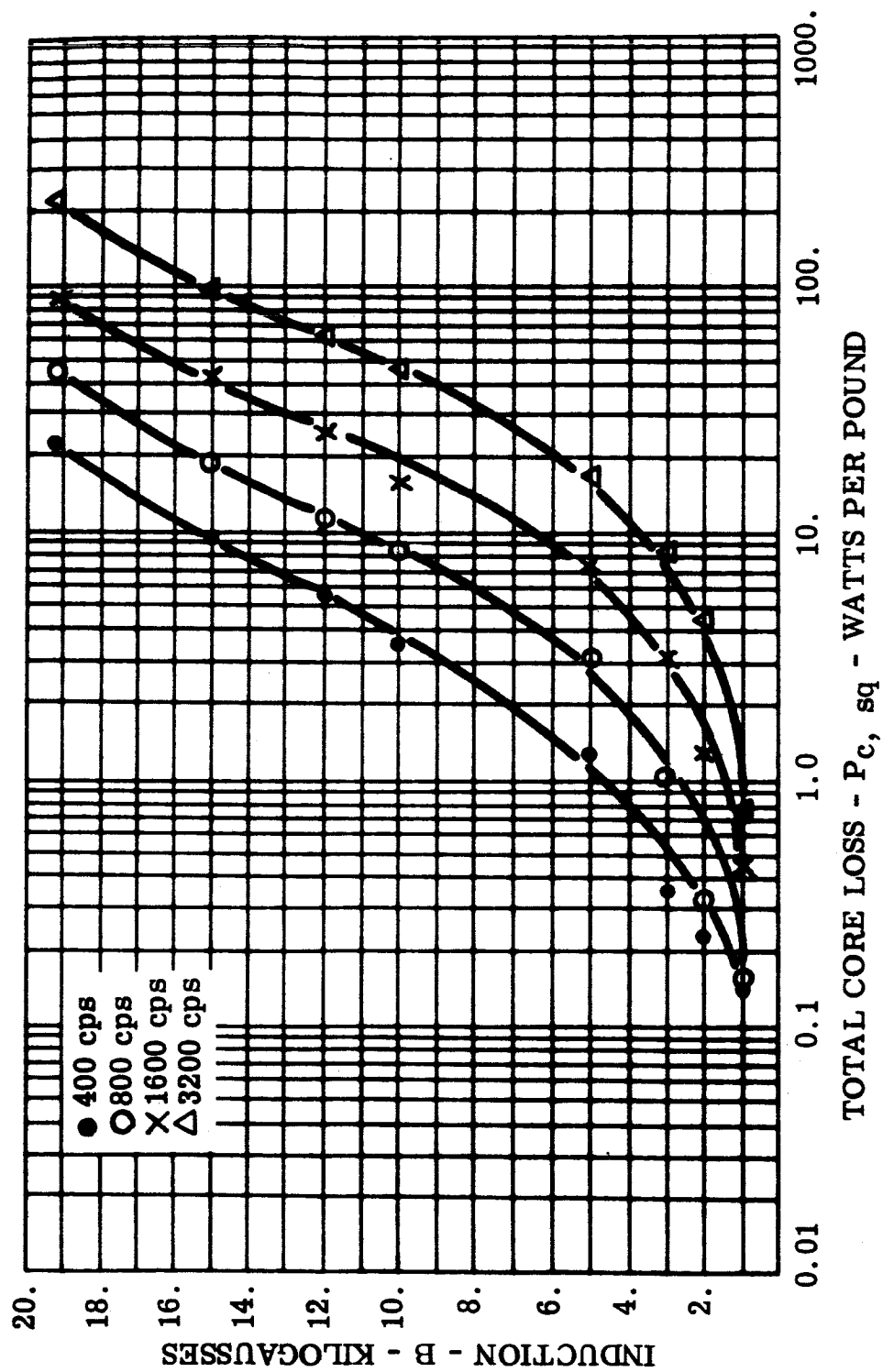


FIGURE 88 $P_{c, sq}$ - Total Core Loss, 0.002 Inch Magnesil Toroid, Core 30, -55°C

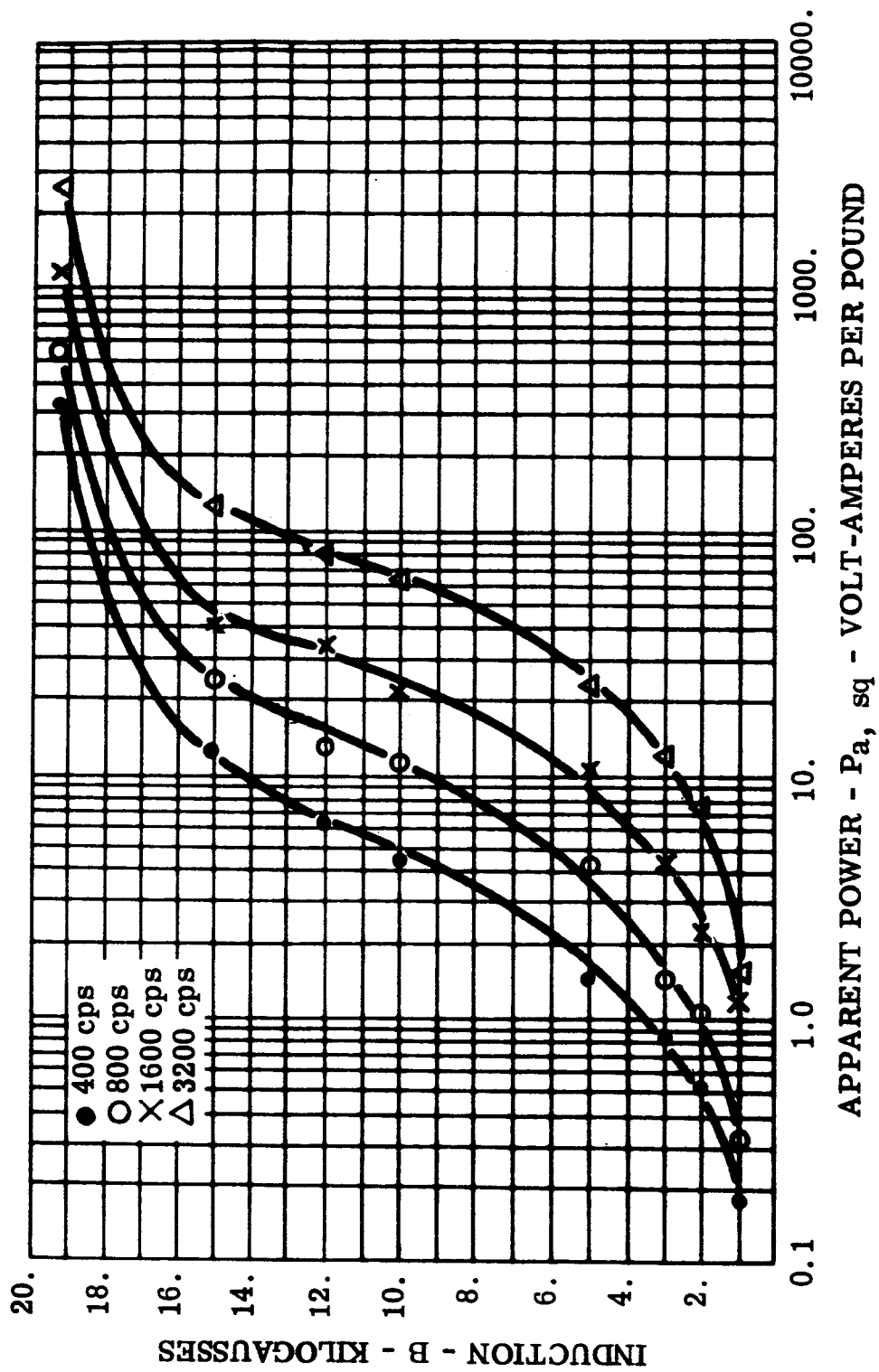


FIGURE 89 P_a , sq - Apparent Power, 0.002 Inch Magnesil Toroid, Core 30, -55°C

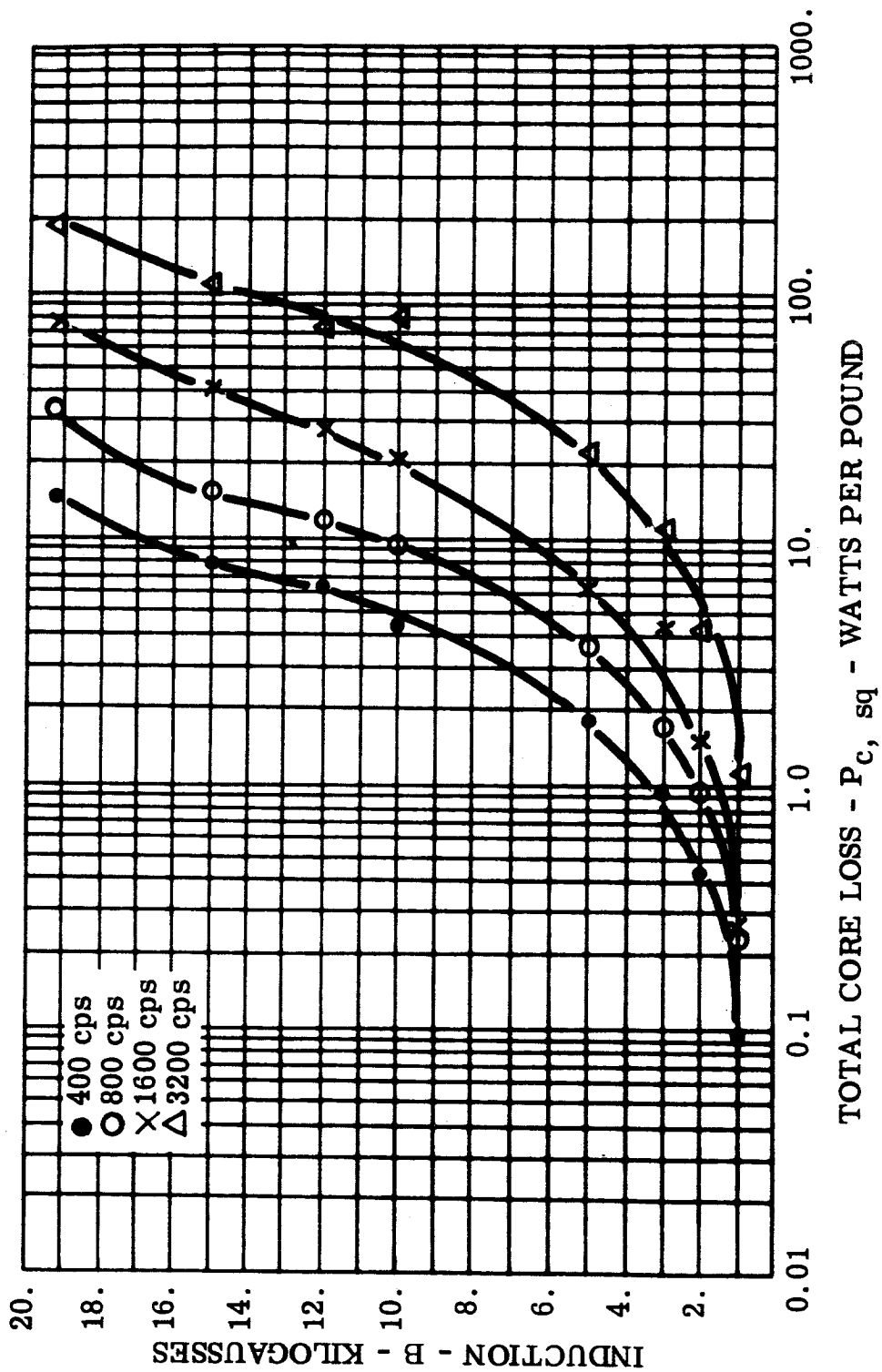
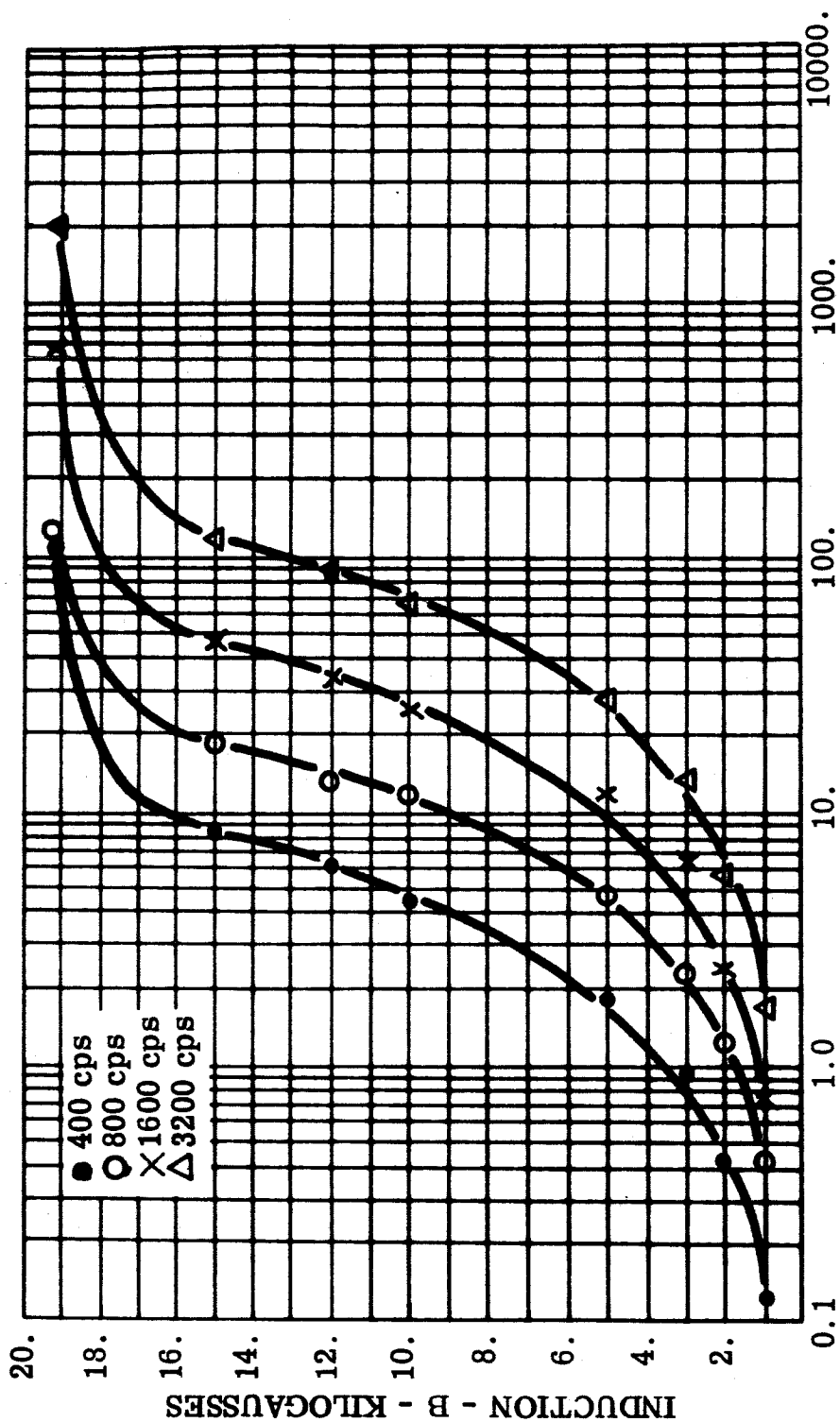


FIGURE 90 $P_{c, sq}$ - Total Core Loss, 0.004 Inch Magnesil Toroid, Core 26,
Room Ambient



APPARENT POWER - P_a, sq - VOLT-AMPERES PER POUND

FIGURE 91 P_a, sq - Apparent Power, 0.004 Inch Magnesil Toroid, Core 26, Room Ambient

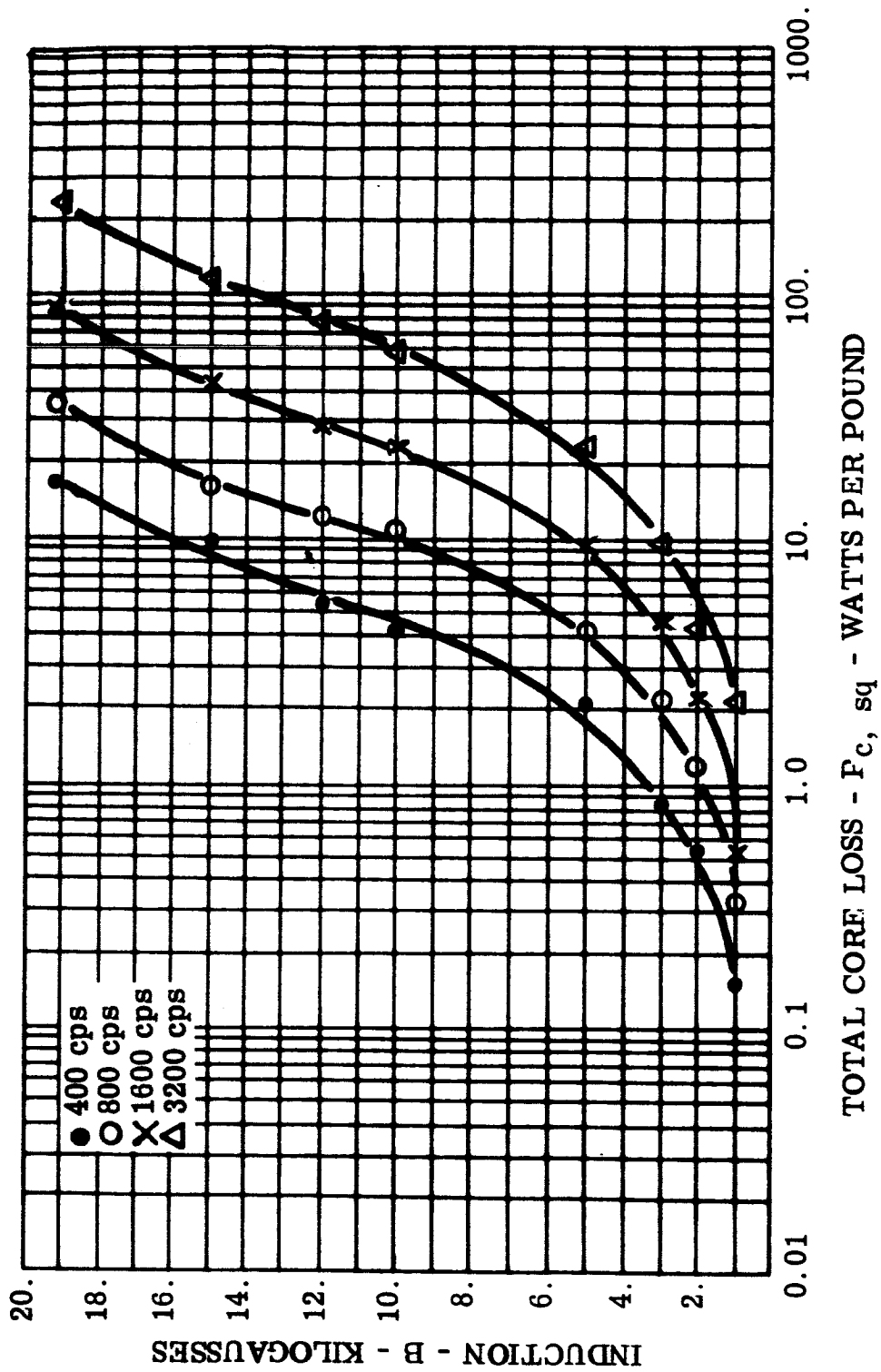


FIGURE 92 $P_{c, sq}$ - Total Core Loss, 0.004 Inch Magnesil Toroid, Core 26, -55°C

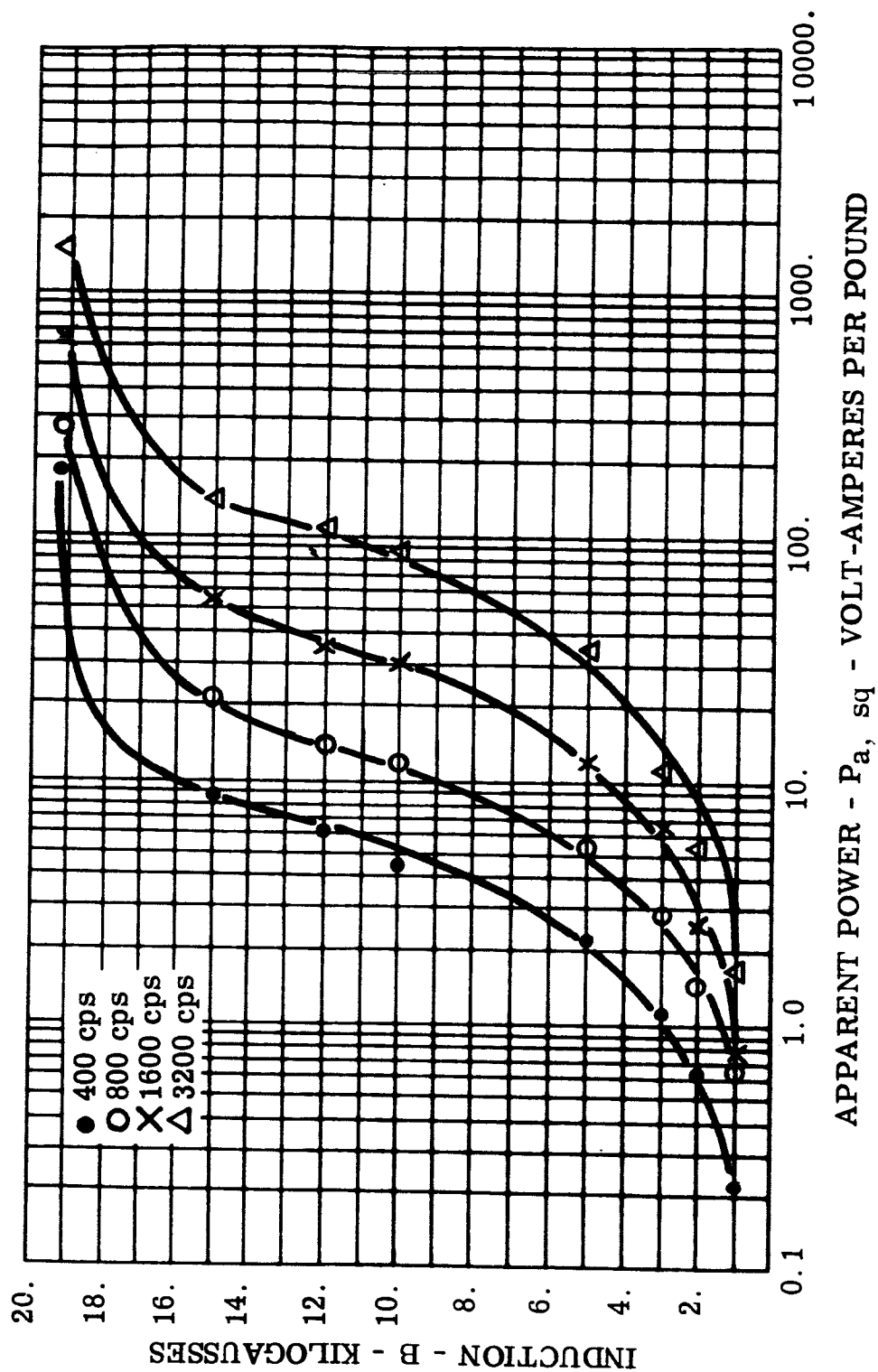


FIGURE 93 $P_{a, sq}$ - Apparent Power, 0.004 Inch Magnasil Toroid, Core 26, -55°C

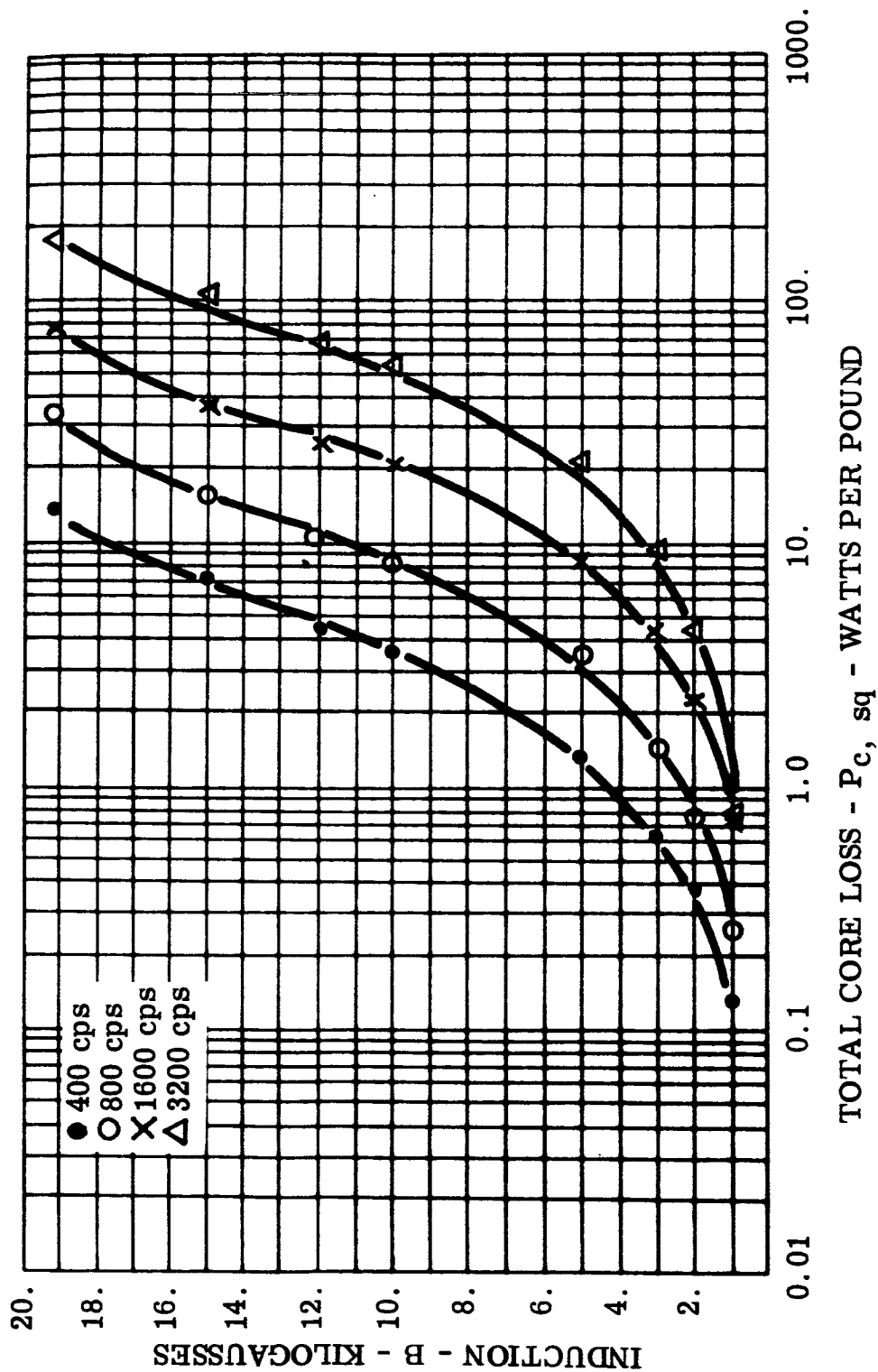


FIGURE 94 $P_{c, sq}$ - Total Core Loss, 0.004 Inch Magnesil Toroid, Core 27, Room Ambient

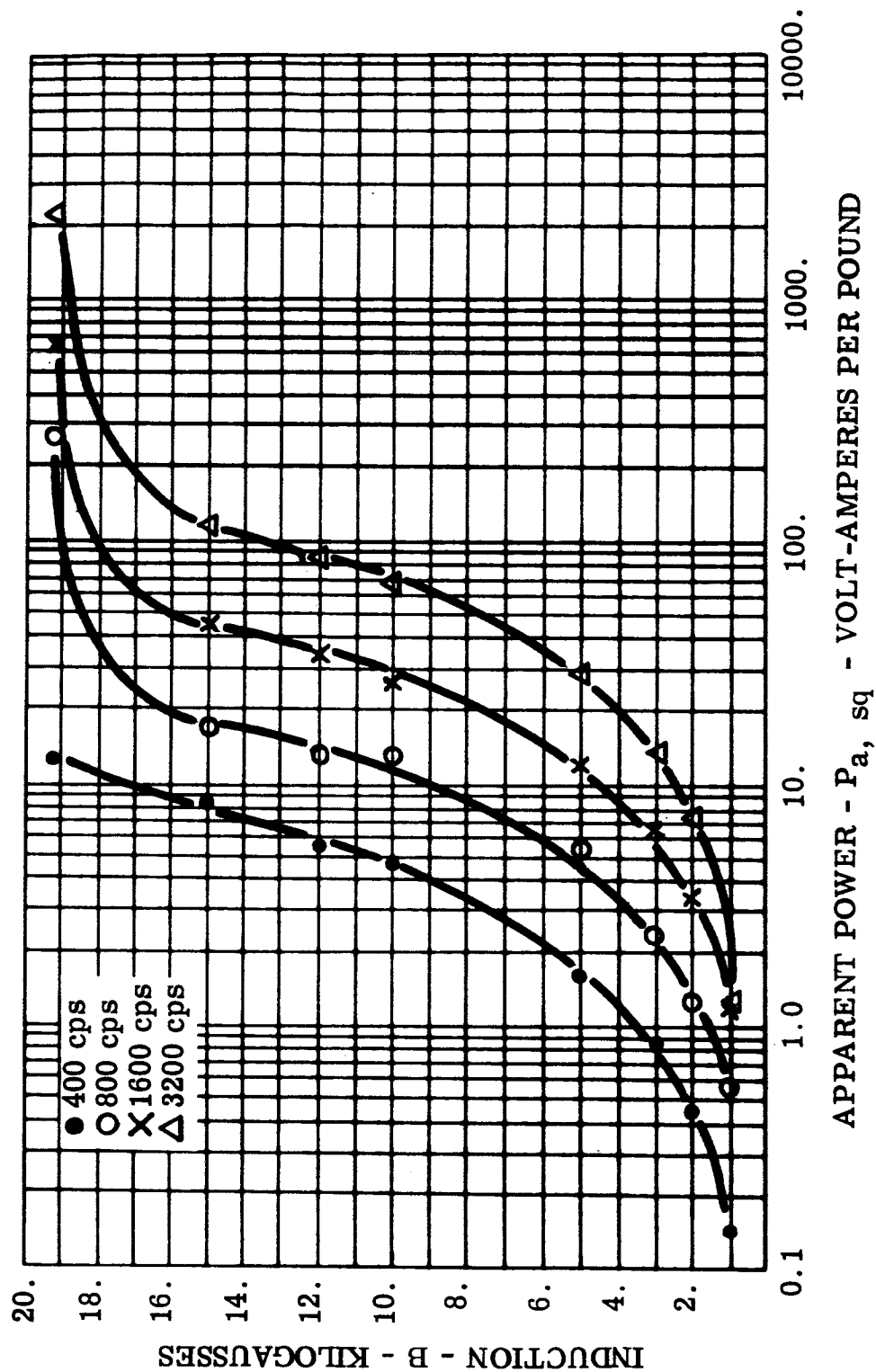


FIGURE 95 P_a, sq - Apparent Power, 0.004 Inch Magnesil Toroid, Core 27,
Room Ambient

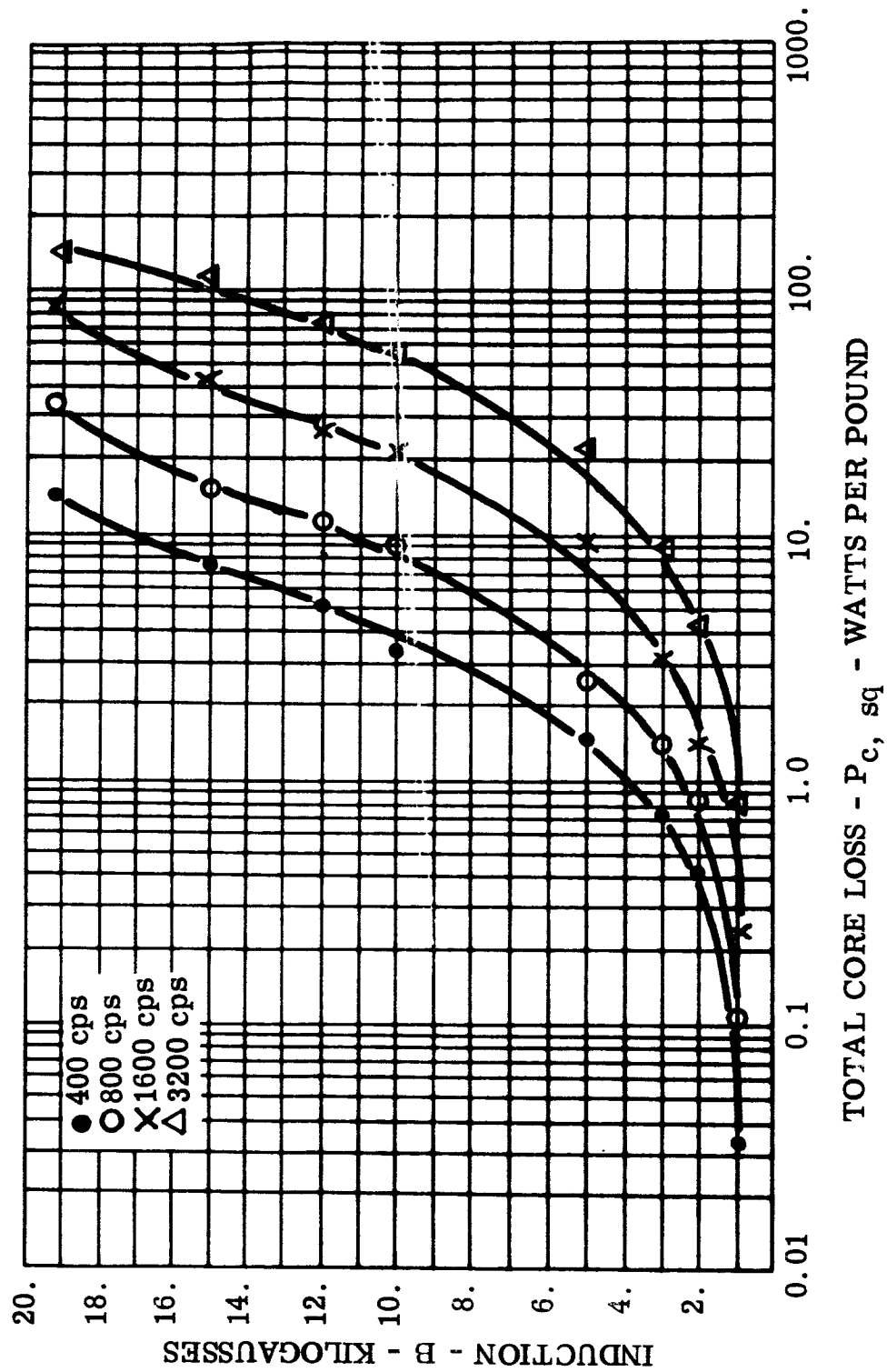


FIGURE 96 $P_{c, sq}$ - Total Core Loss, 0.004 Inch Magnesil Toroid, Core 27, -55°C

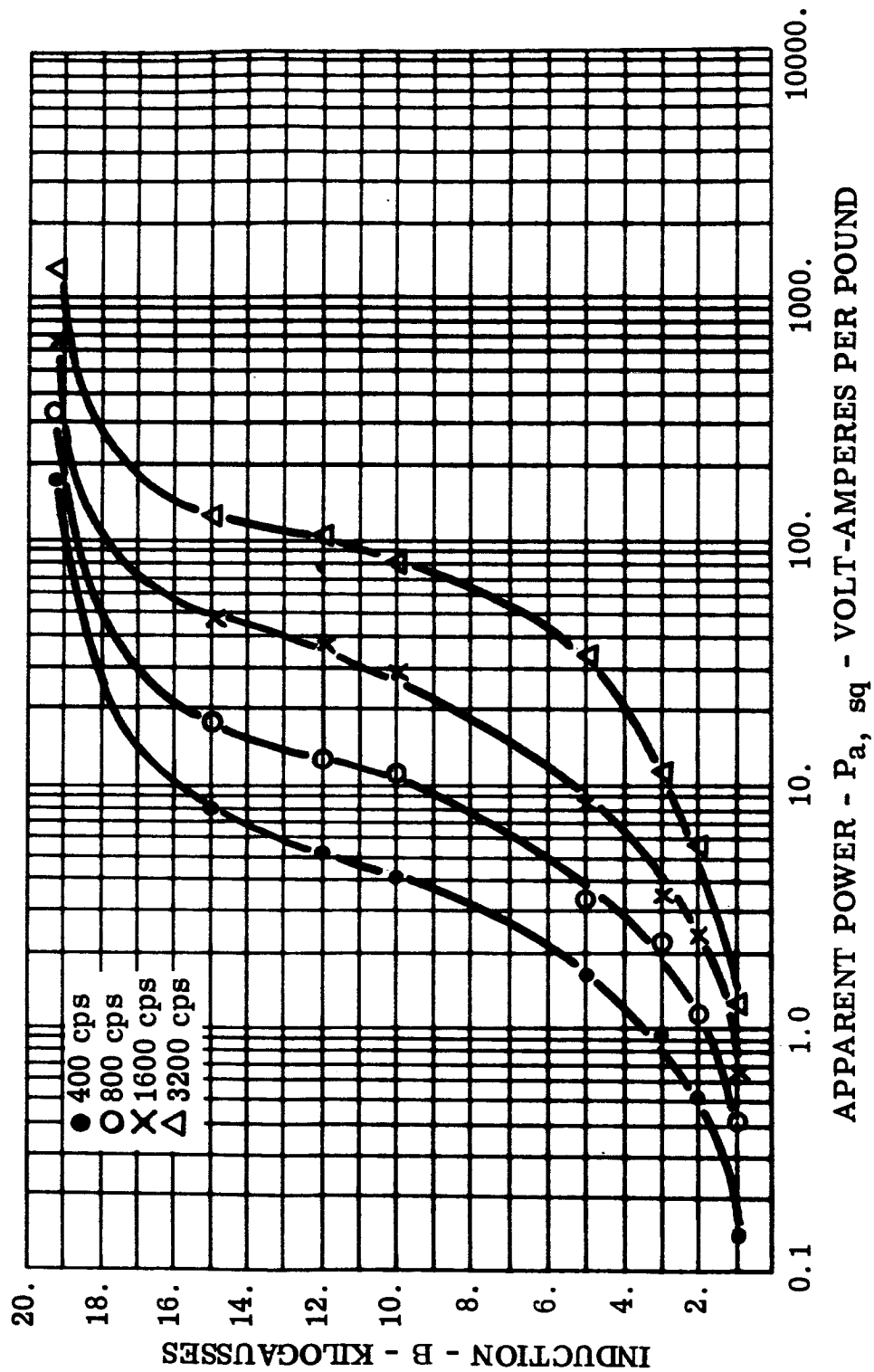


FIGURE 97 $P_{a, sq}$ - Apparent Power, 0.004 Inch Magnesil Toroid, Core 27, -55°C

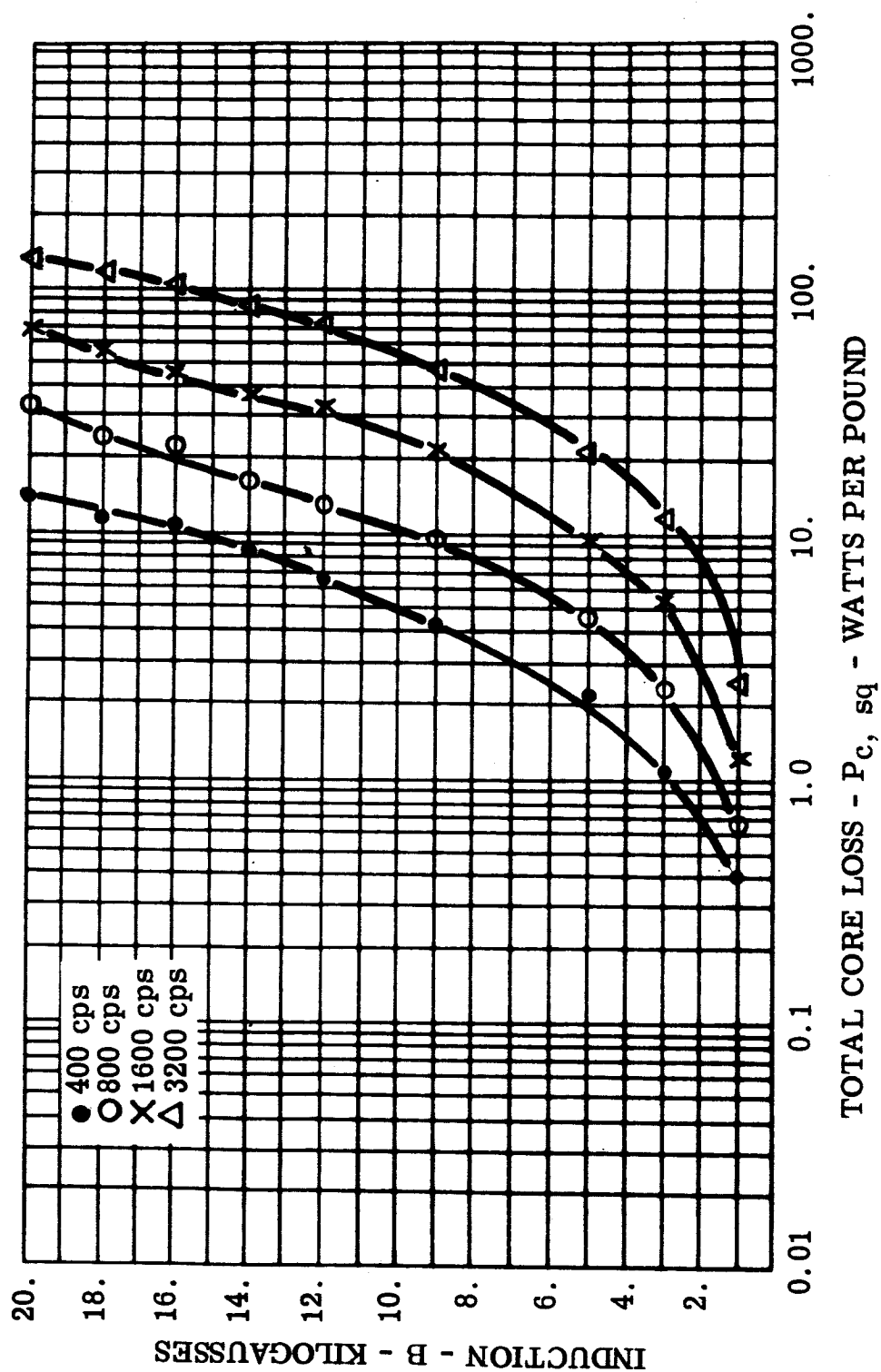


FIGURE 98 $P_{c, sq}$ - Total Core Loss, 0.002 Inch Supermendur Toroid, Core 12,
Magnetic Field Annealed, Room Ambient

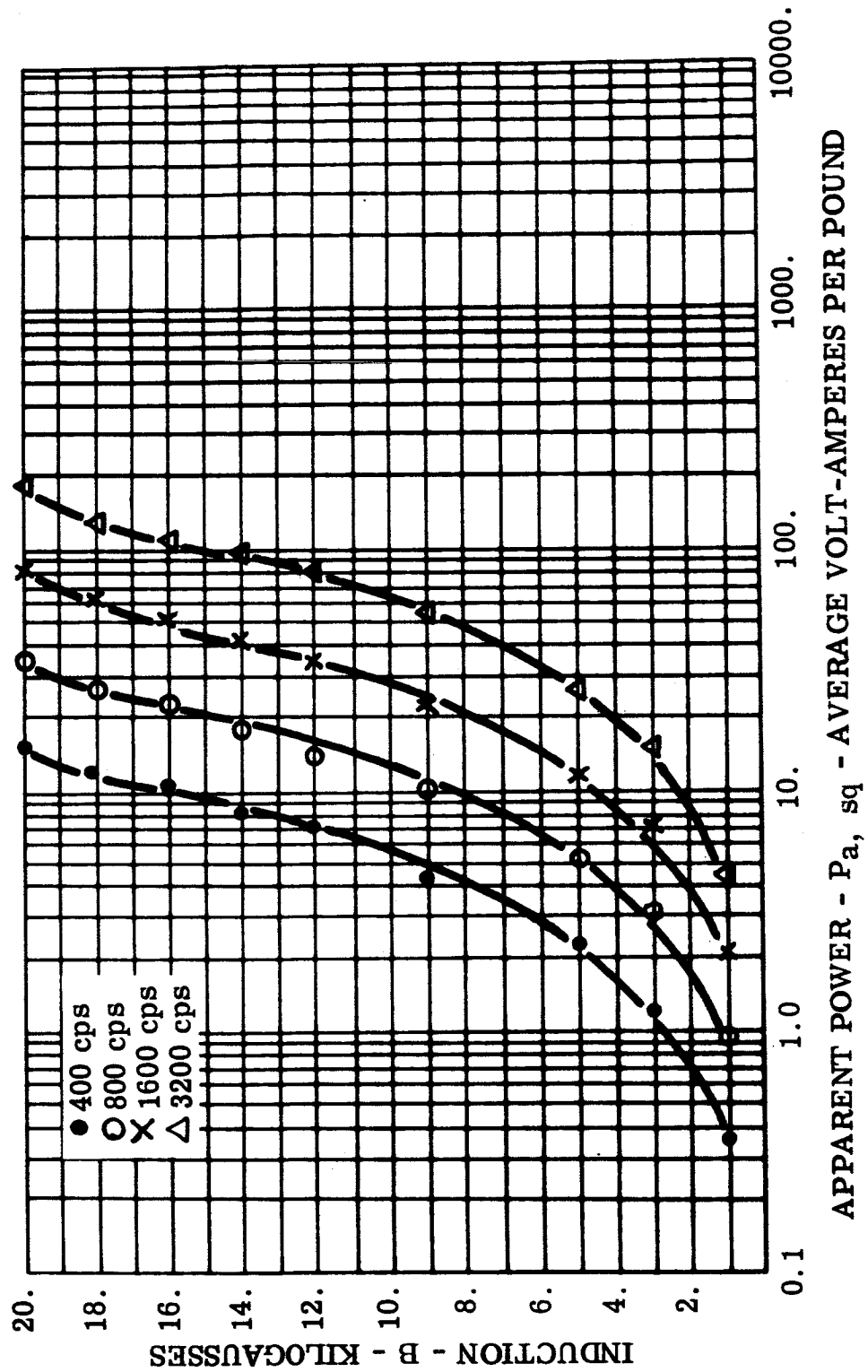


FIGURE 99 $P_{a, sq}$ - Apparent Power, 0.002 Inch Supermendur Toroid, Core 32, Magnetic Field Annealed, Room Ambient

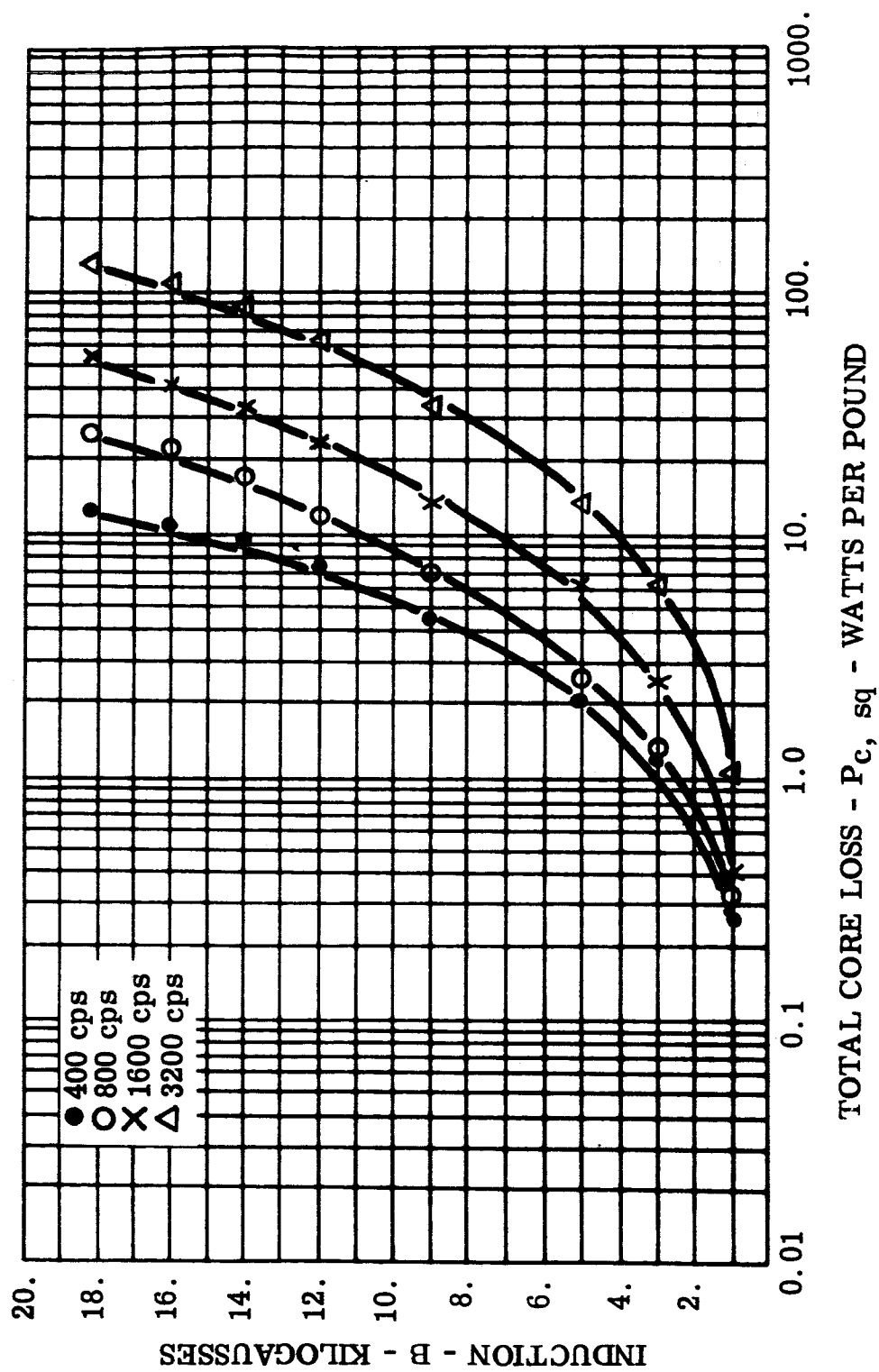


FIGURE 100 $P_{c, sq}$ - Total Core Loss, 0.002 Inch Supermendur Toroid, Core 32, Magnetic Field Annealed, -55°C

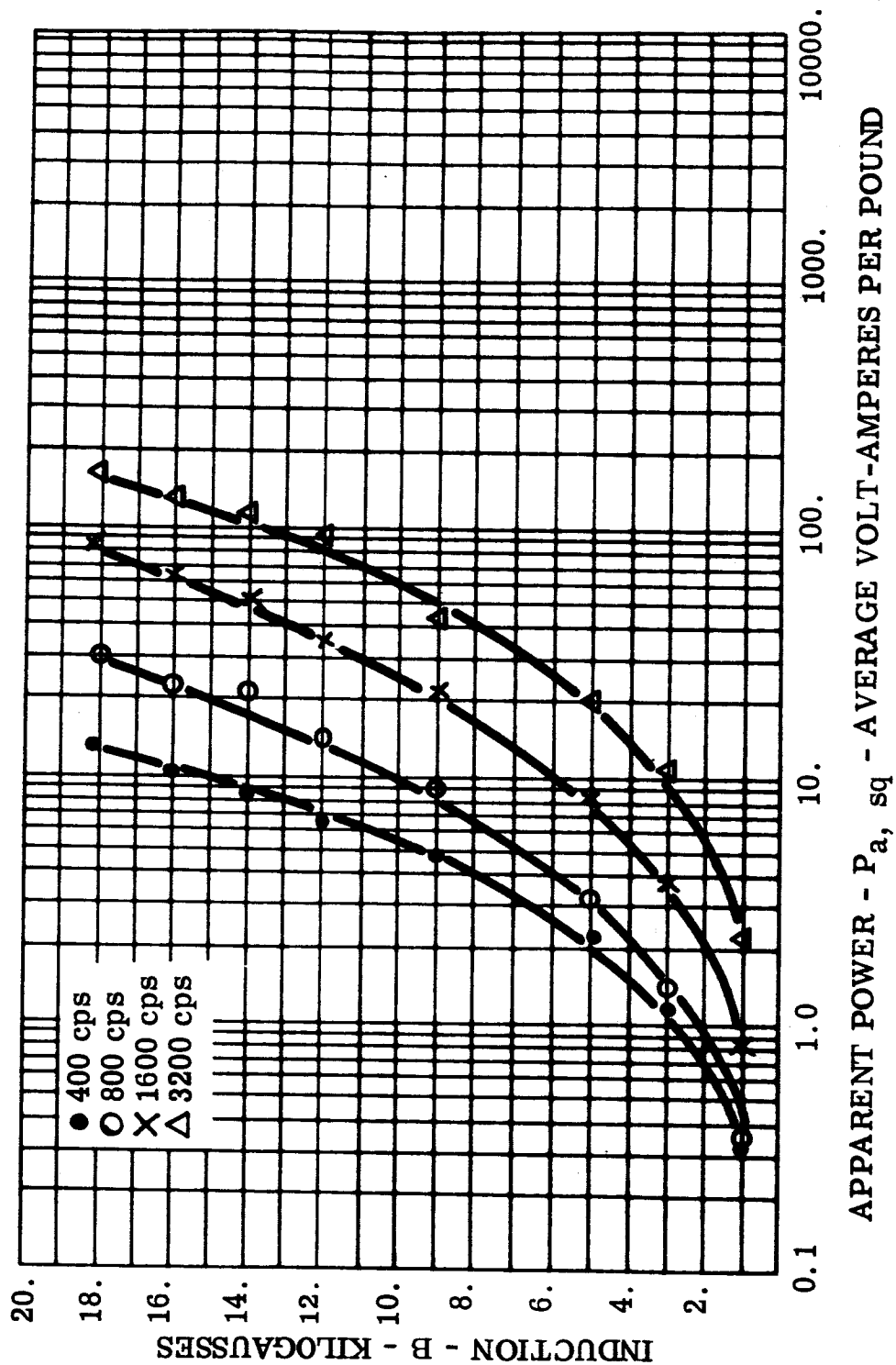


FIGURE 101 $P_{a, sq}$ - Apparent Power, 0.002 Inch Supermendur Toroid, Core 32, Magnetic Field Annealed, -55°C

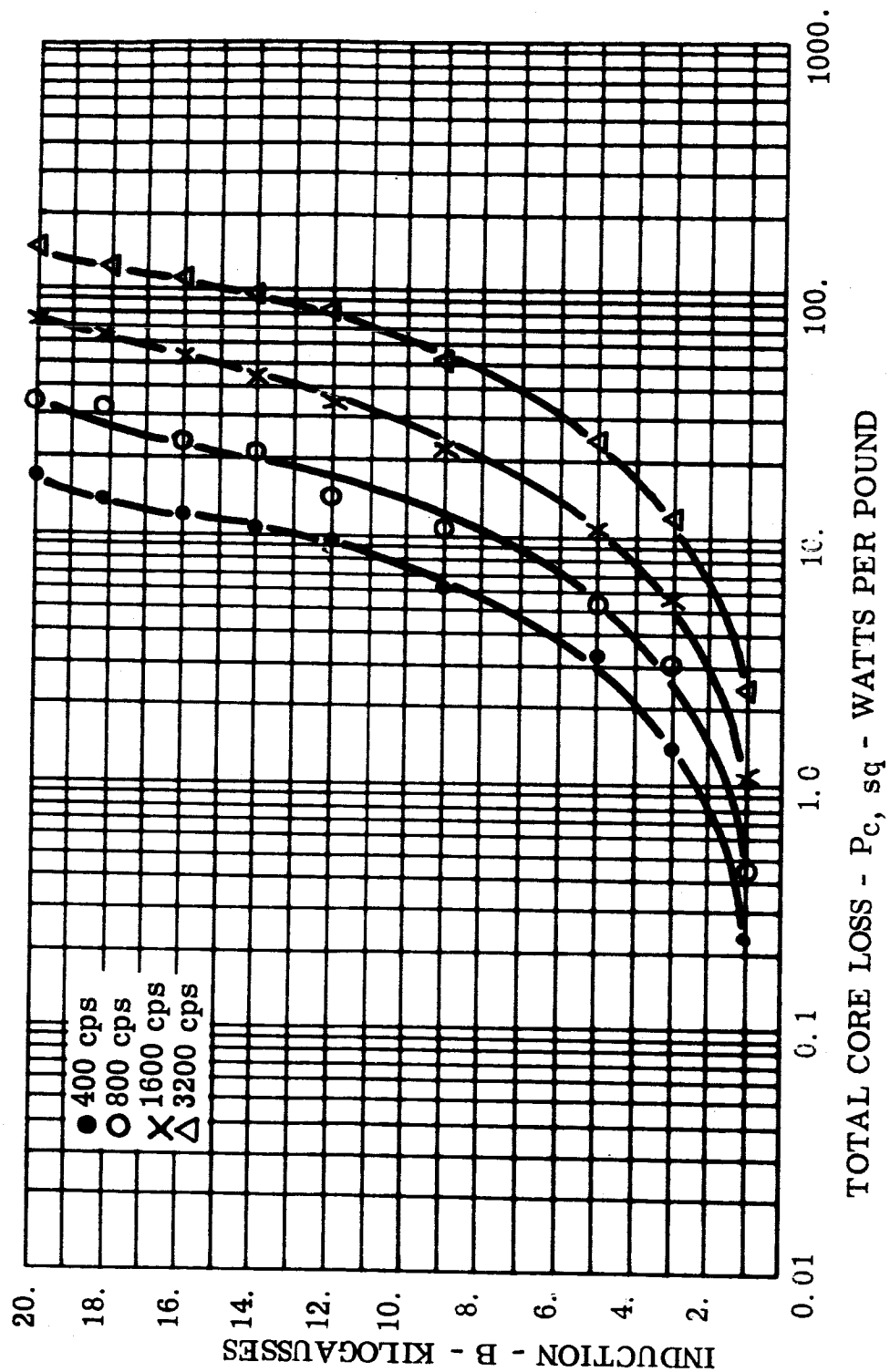


FIGURE 102 $P_{c, sq}$ - Total Core Loss, 0.002 Inch Supermendur Toroid, Core 33, Magnetic Field Annealed, Room Ambient

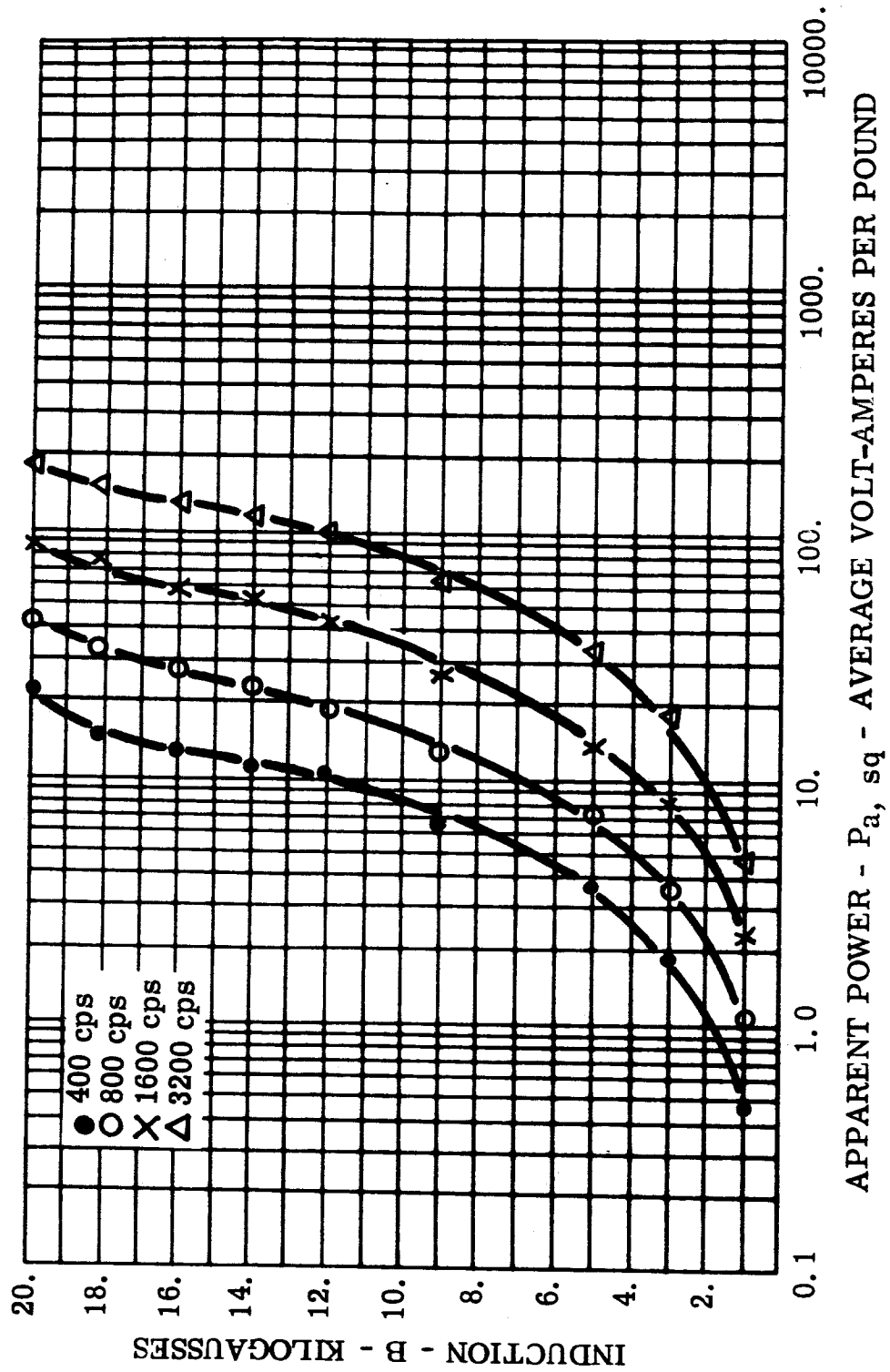


FIGURE 103 P_a, sq - Apparent Power, 0.002 Inch Supermendur Toroid, Core 33,
Magnetic Field Annealed, Room Ambient

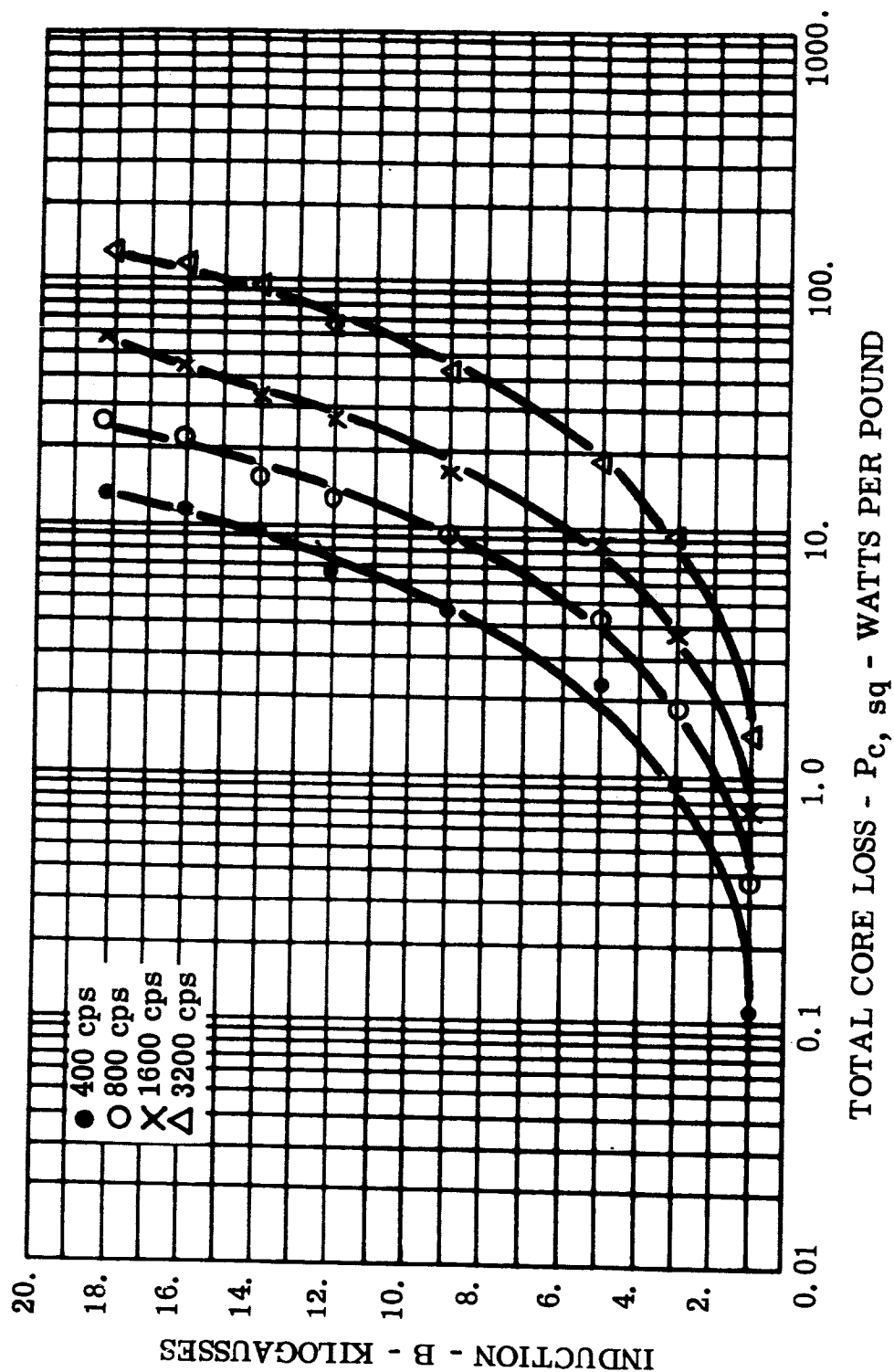
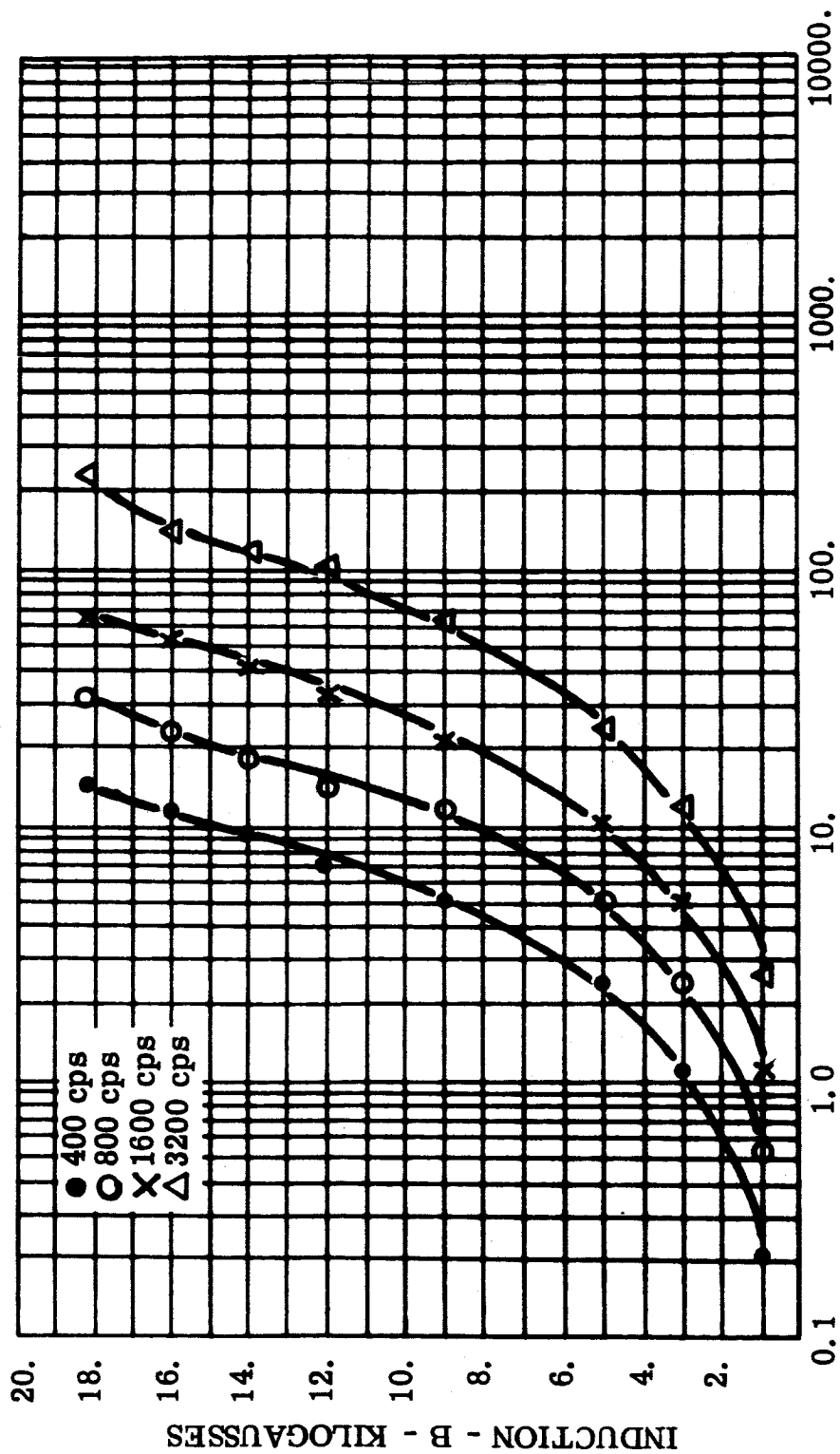


FIGURE 104 P_c , sq - Total Core Loss, 0.002 Inch Supermendur Toroid, Core 33,
Magnetic Field Annealed, -55°C



APPARENT POWER - P_a, sq - AVERAGE VOLT-AMPERES PER POUND

FIGURE 105 P_a, sq - Apparent Power, 0.002 Inch Supermendur Toroid, Core 33,
Magnetic Field Annealed, $-55^{\circ}C$

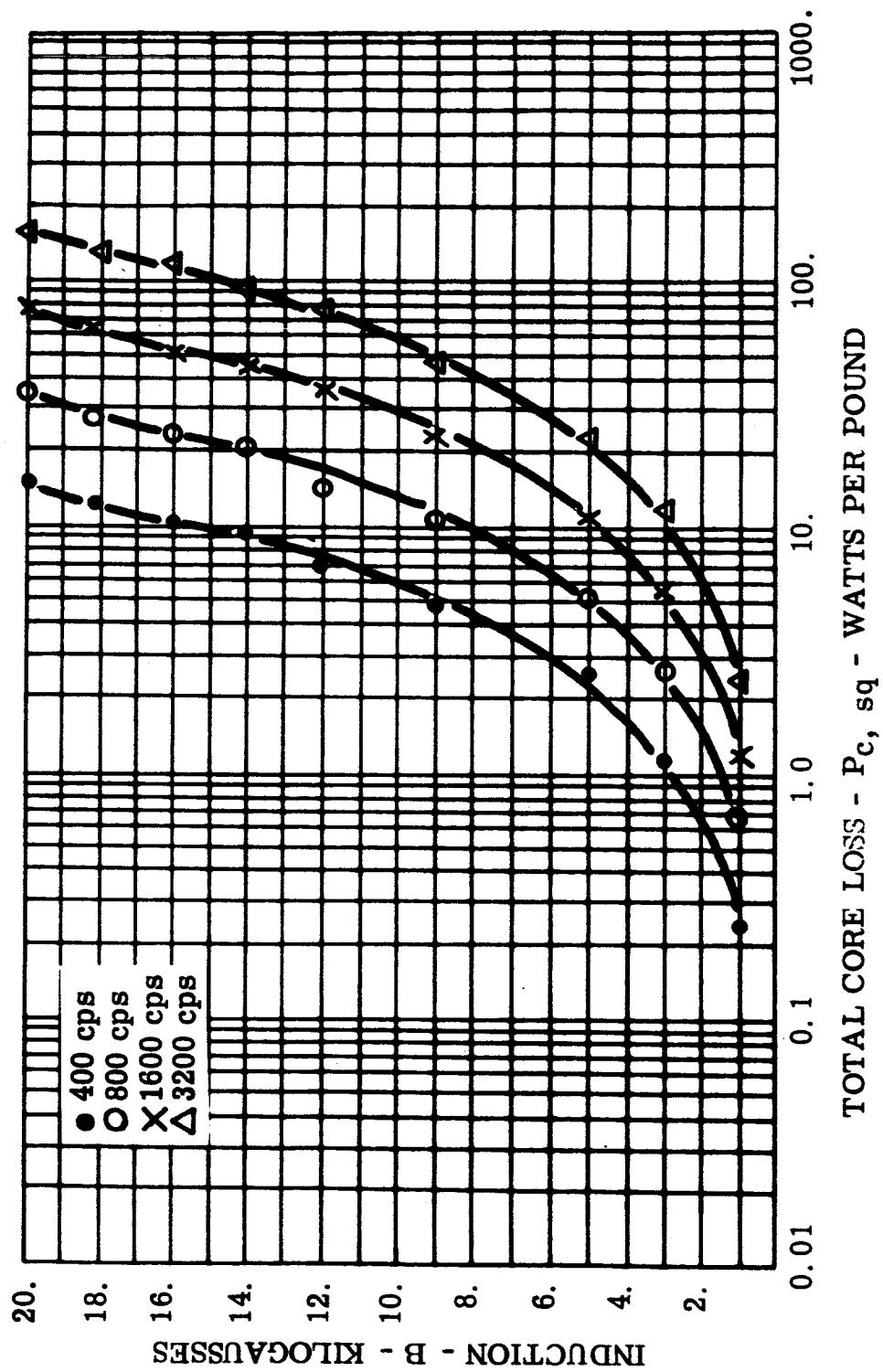


FIGURE 106 P_c , sq - Total Core Loss, 0.002 Inch Supermendur Toroid, Core 34,
Magnetic Field Annealed, Room Ambient

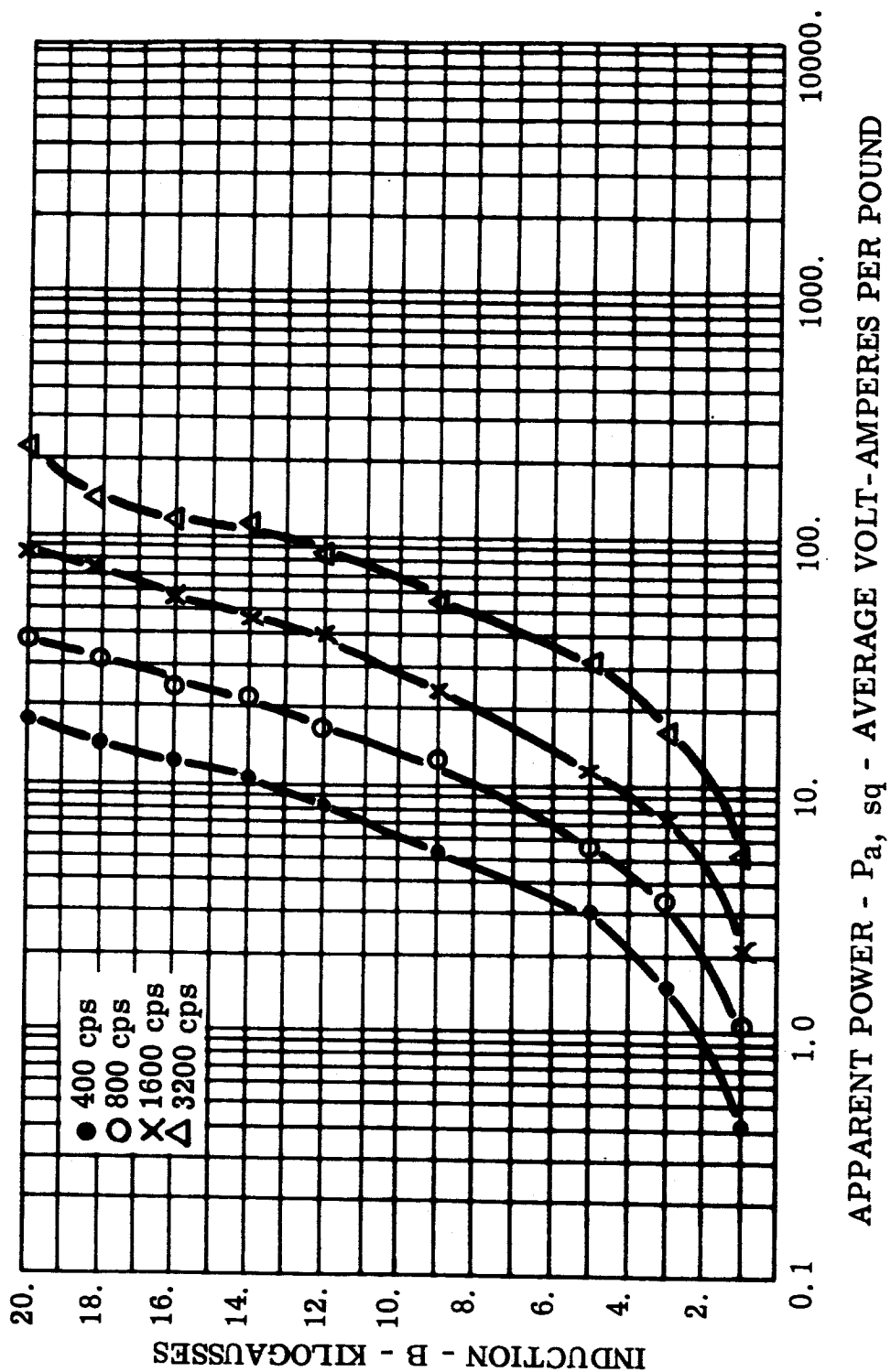


FIGURE 107 P_a , sq - Apparent Power, 0.002 Inch Supermendur Toroid, Core 34,
Magnetic Field Annealed, Room Ambient

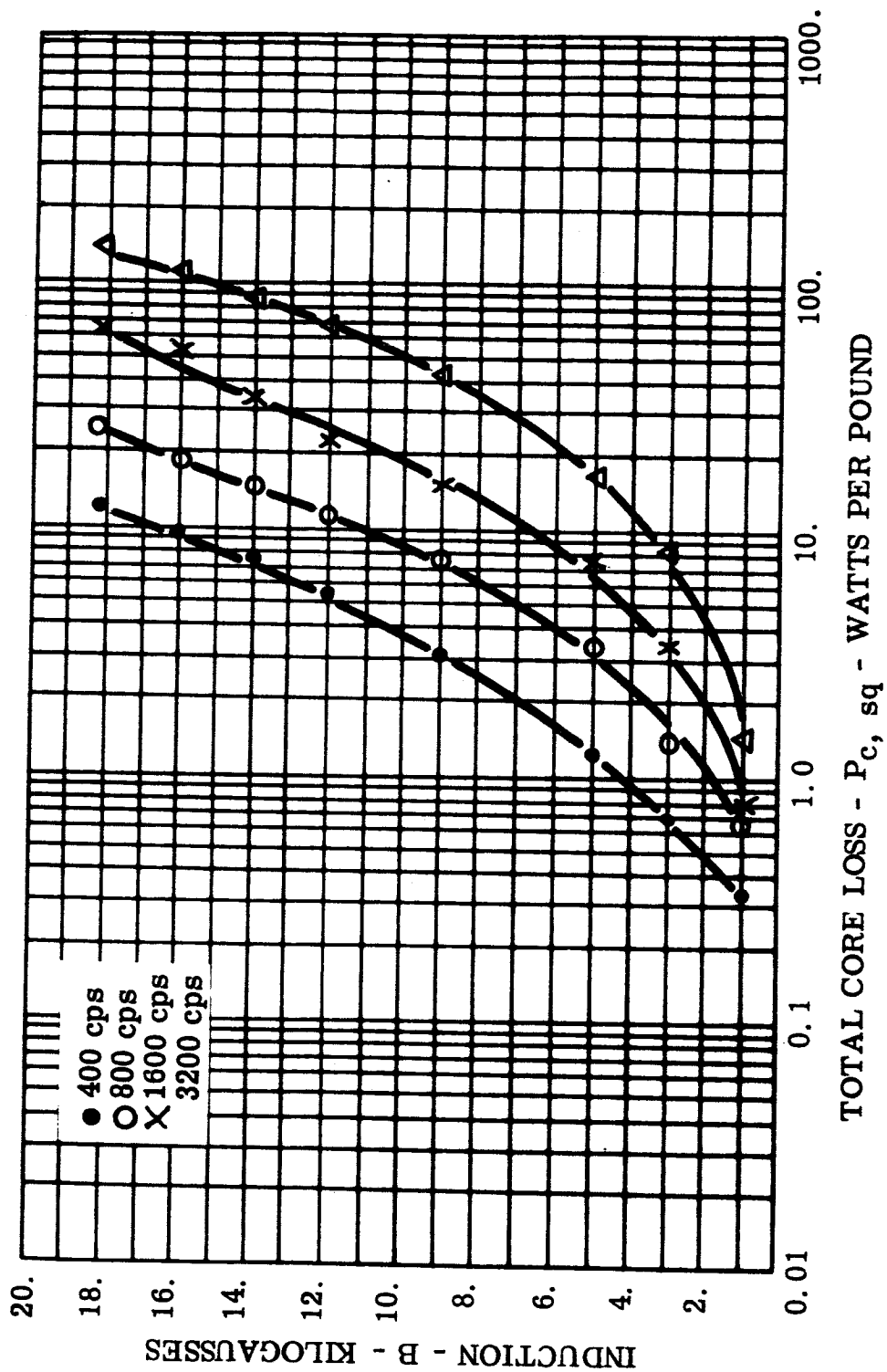


FIGURE 108 $P_{c, sq}$ - Total Core Loss, 0.002 Inch Supermendur Toroid, Core 34,
Magnetic Field Annealed, -55°C

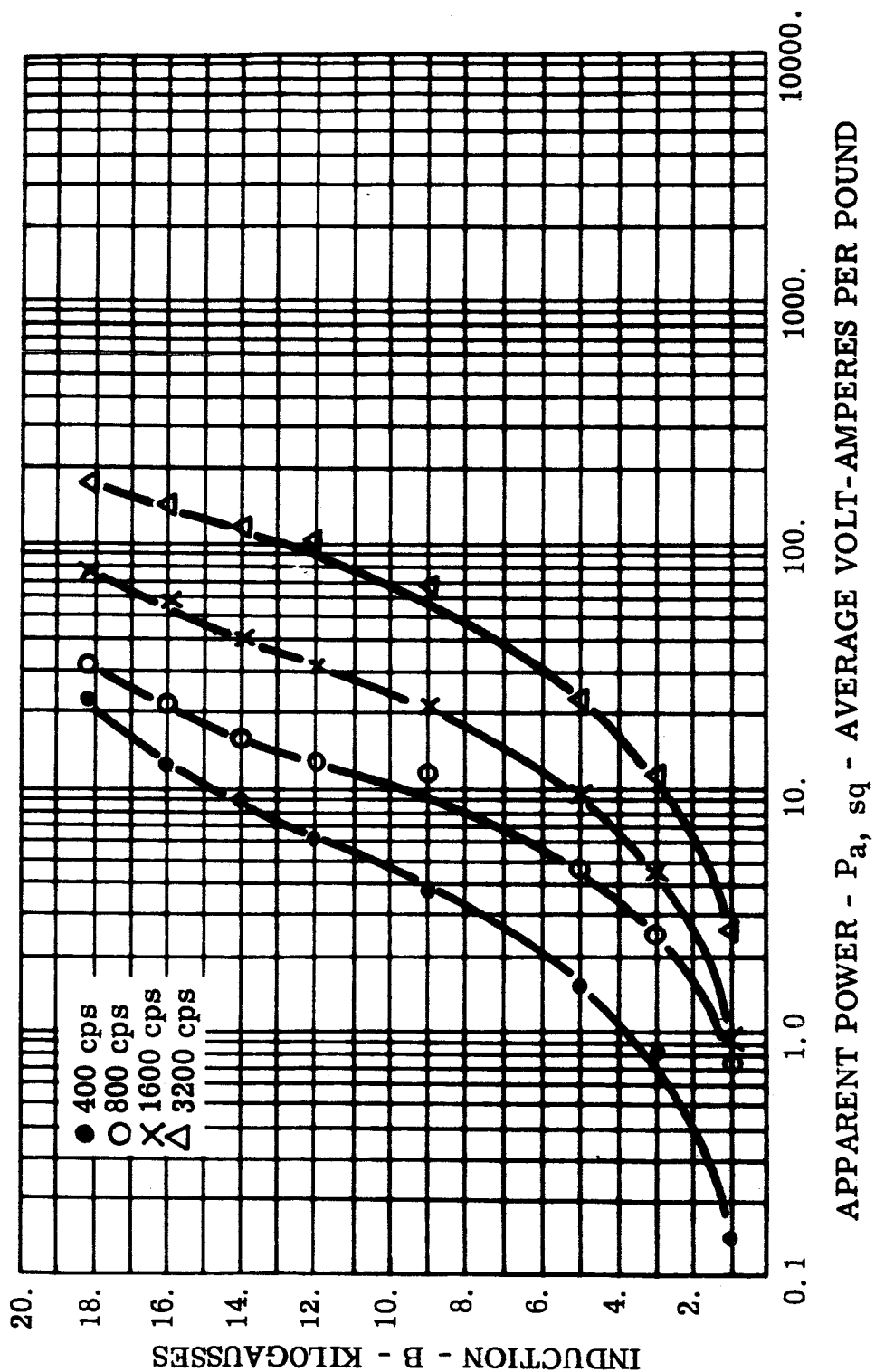


FIGURE 109 P_a, sq - Apparent Power, 0.002 Inch Supermendur Toroid, Core 34, Magnetic Field Annealed, -55°C

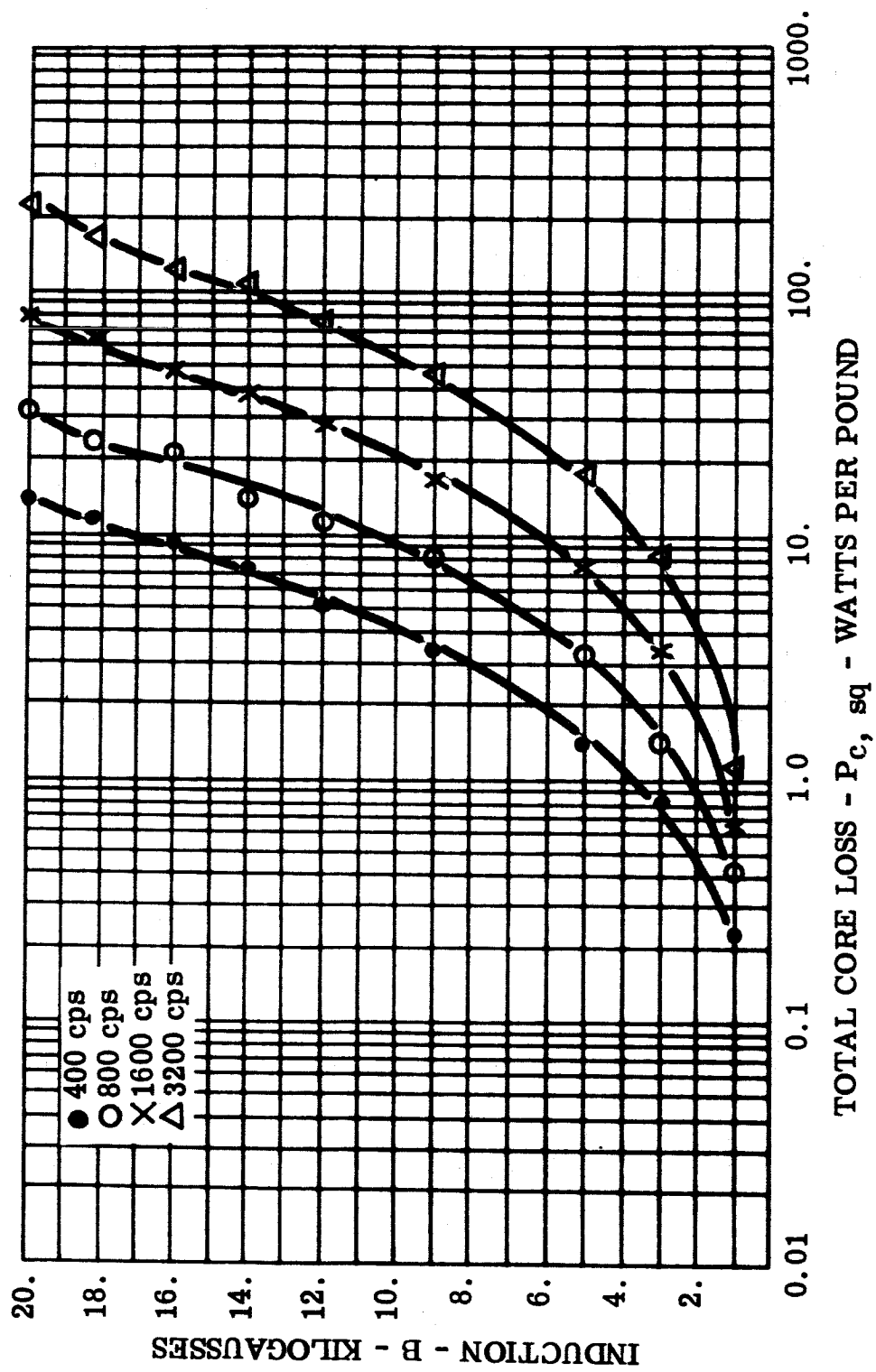


FIGURE 110 P_c , sq - Total Core Loss, 0.004 Inch Supermendur Rowland Ring, Core 35, Magnetic Field Annealed, Room Ambient

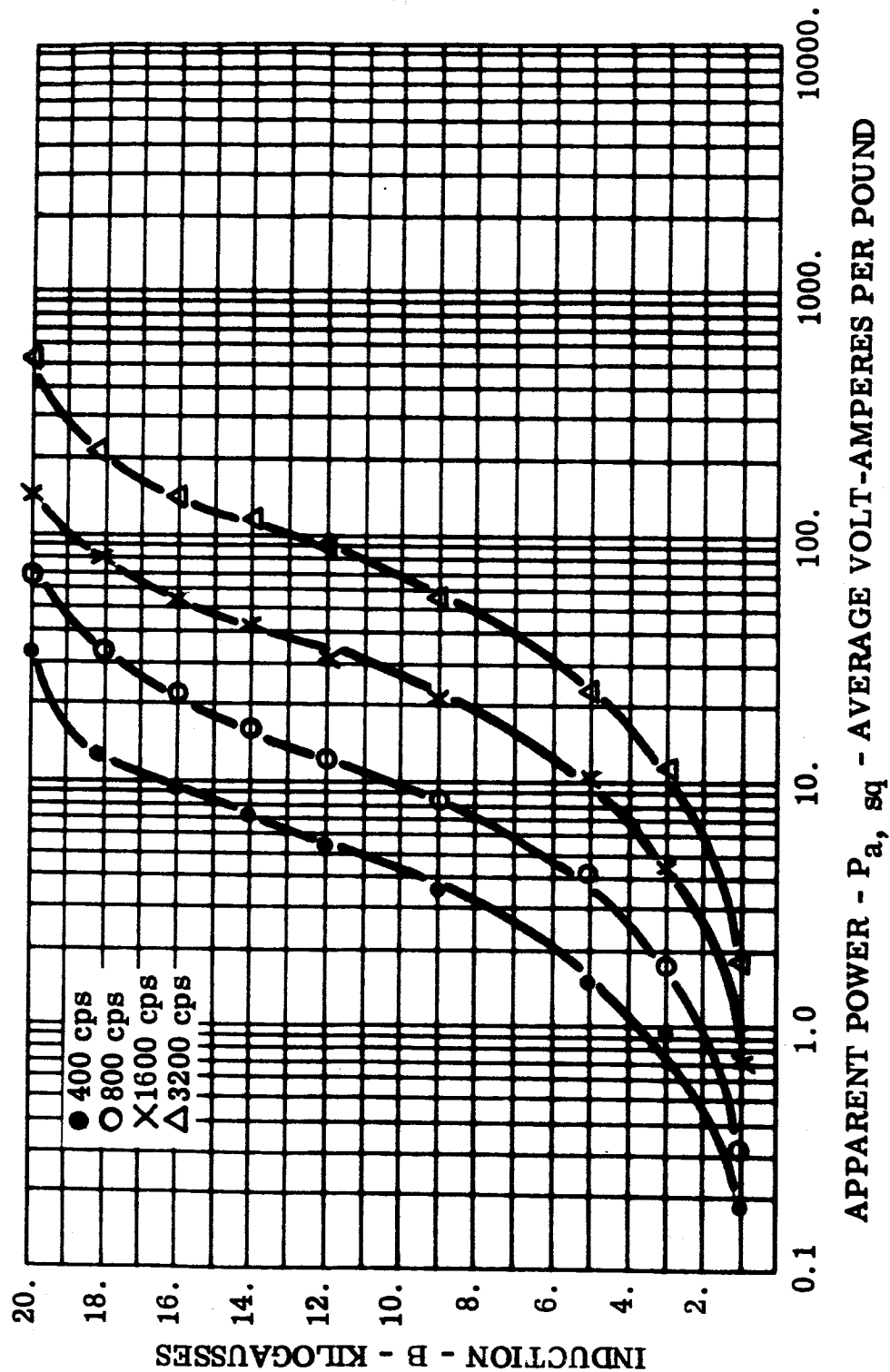


FIGURE 111 P_a, sq - Apparent Power, 0.004 Inch Supermendur Rowland Ring, Core 35, Magnetic Field Annealed, Room Ambient

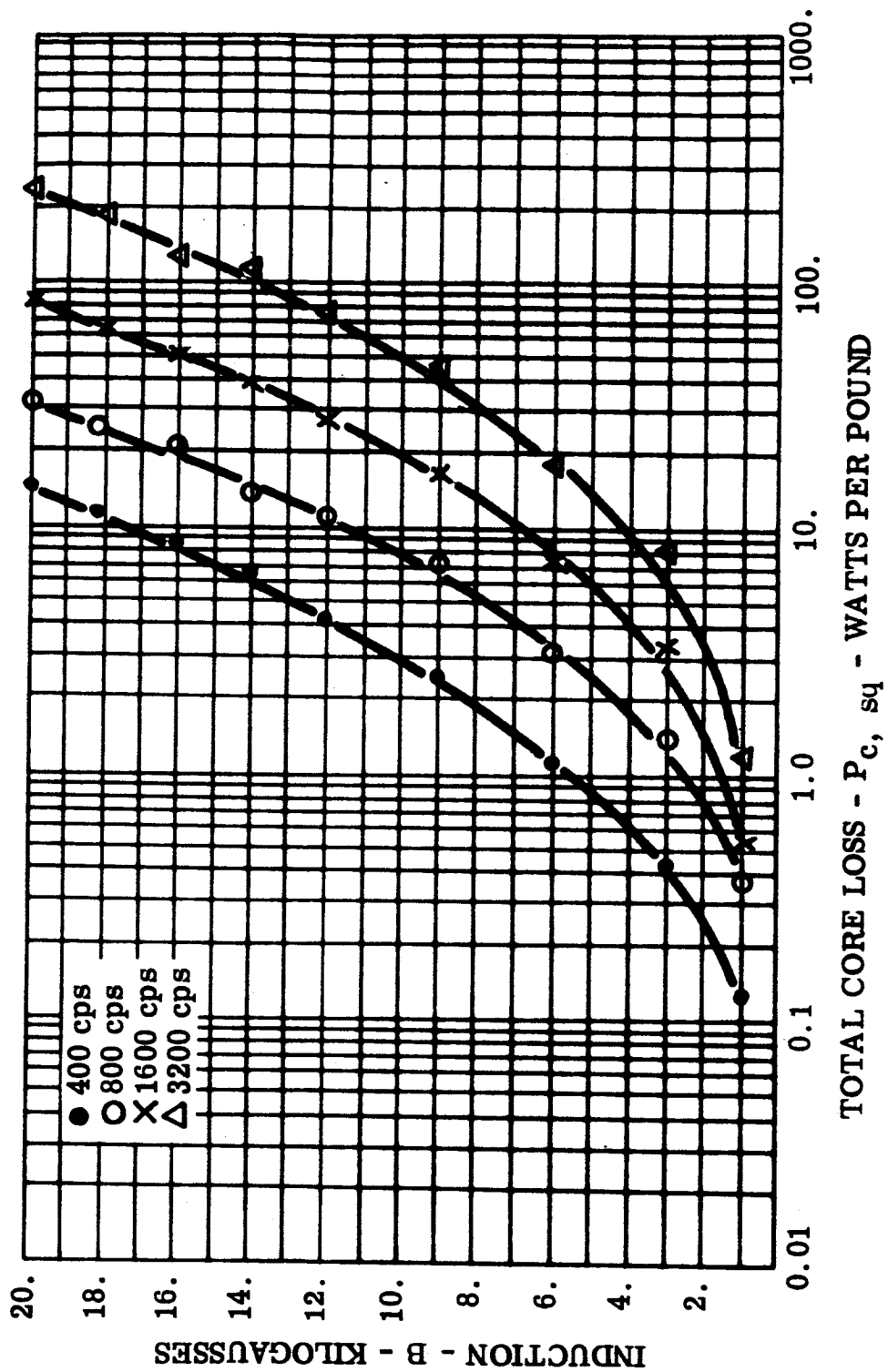


FIGURE 112 $P_{c, sq}$ - Total Core Loss, 0.004 Inch Supermendur Rowland Ring,
Core 35, Magnetic Field Annealed, -55°C

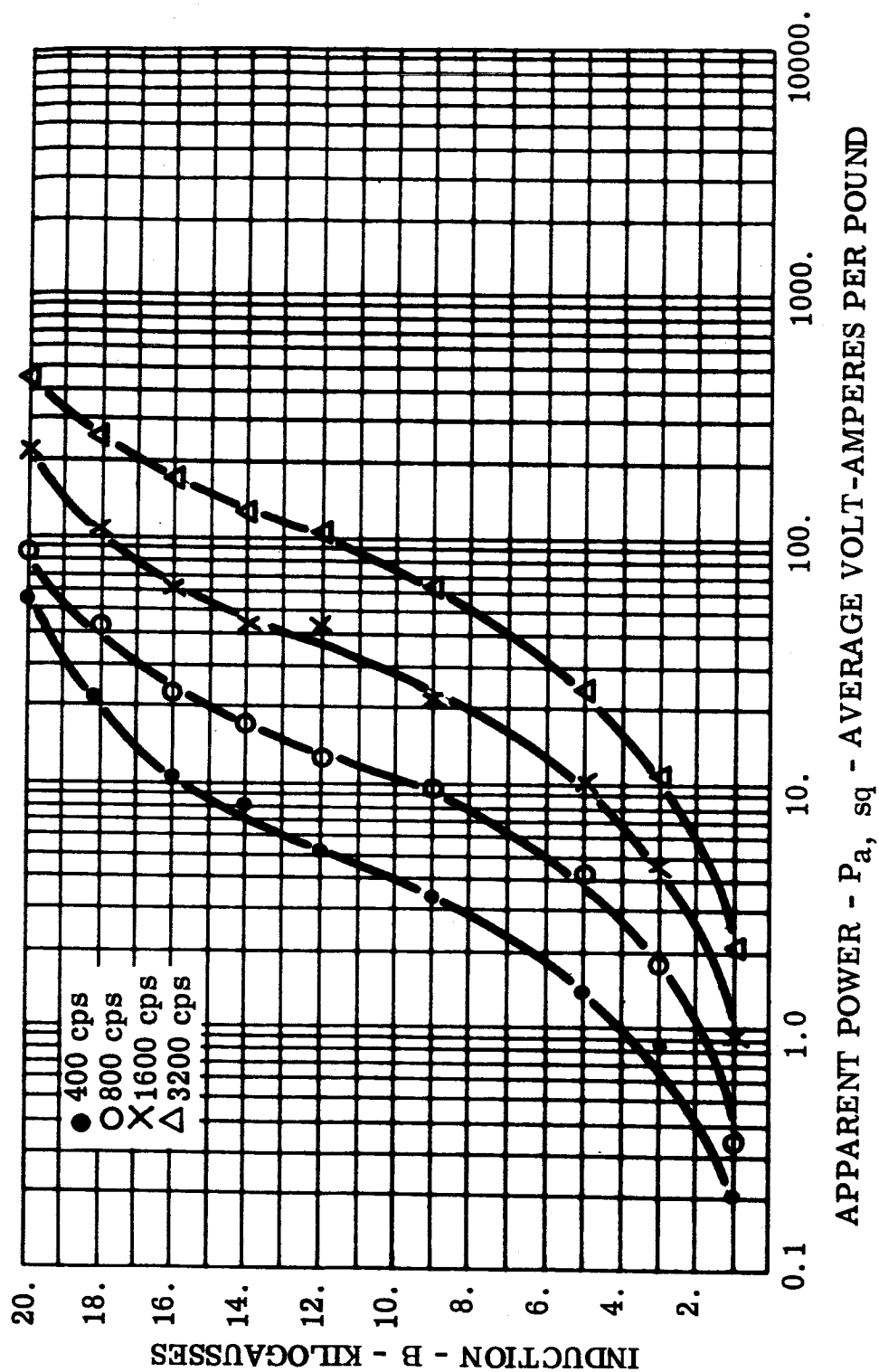


FIGURE 113 P_a, sq - Apparent Power, 0.004 Inch Supermendur Rowland Ring,
Core 35, Magnetic Field Annealed, -55°C

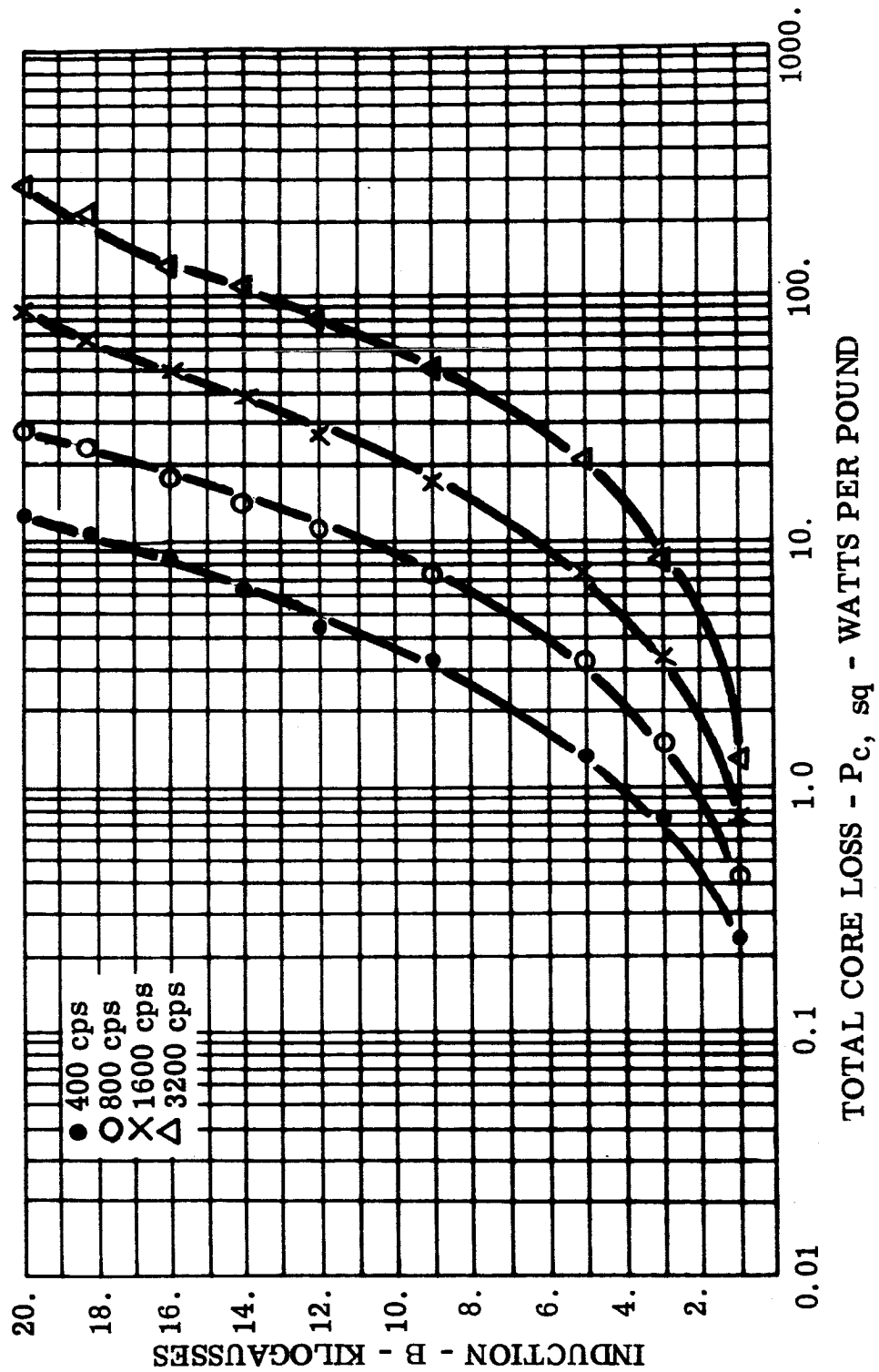


FIGURE 114 P_c , sq - Total Core Loss, 0.004 Inch Supermendur Rowland Ring,
Core 36, Magnetic Field Annealed, Room Ambient

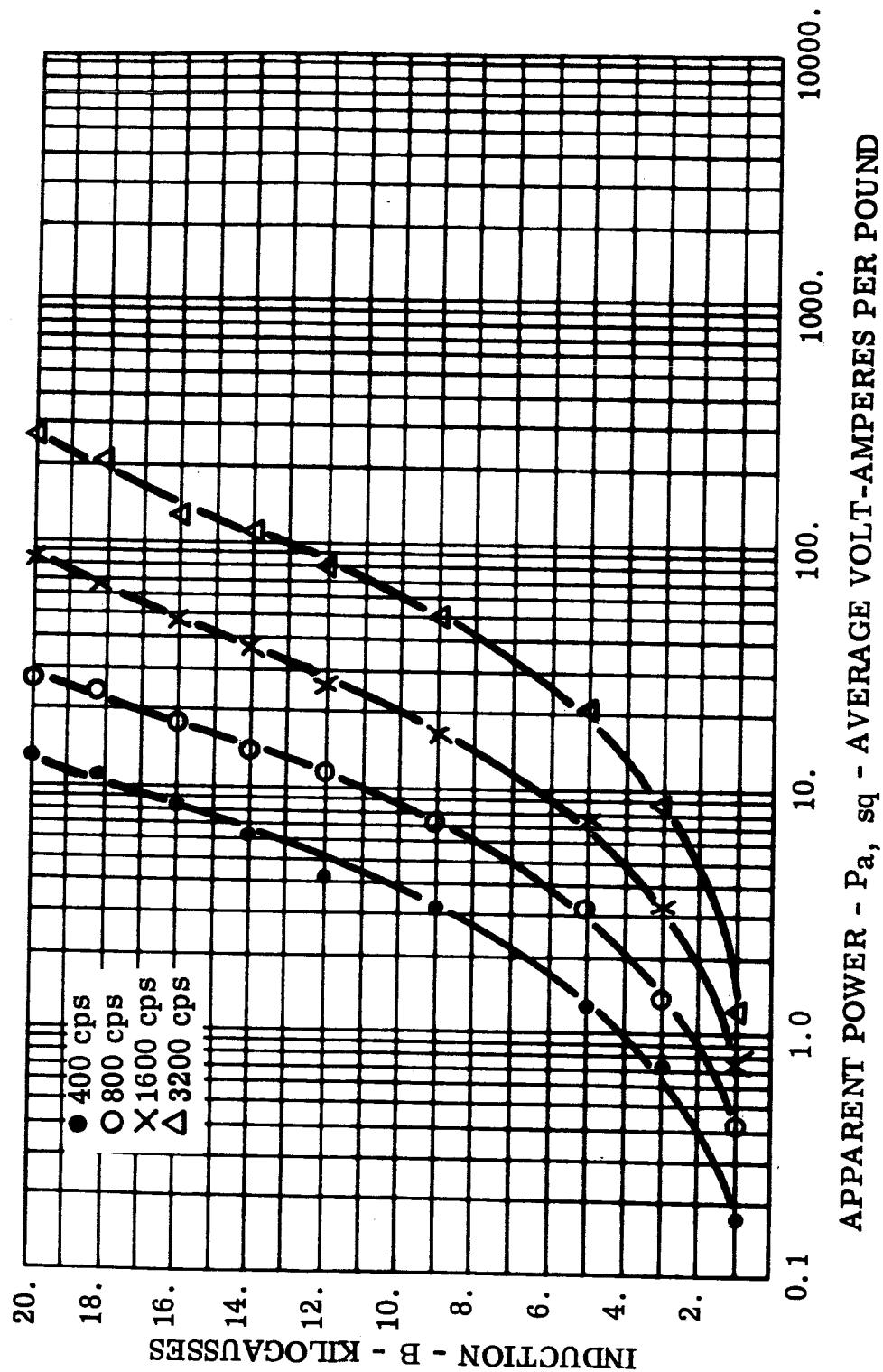


FIGURE 115 P_a, sq - Apparent Power, 0.004 Inch Supermendur Rowland Ring, Core 36, Magnetic Field Annealed, Room Ambient

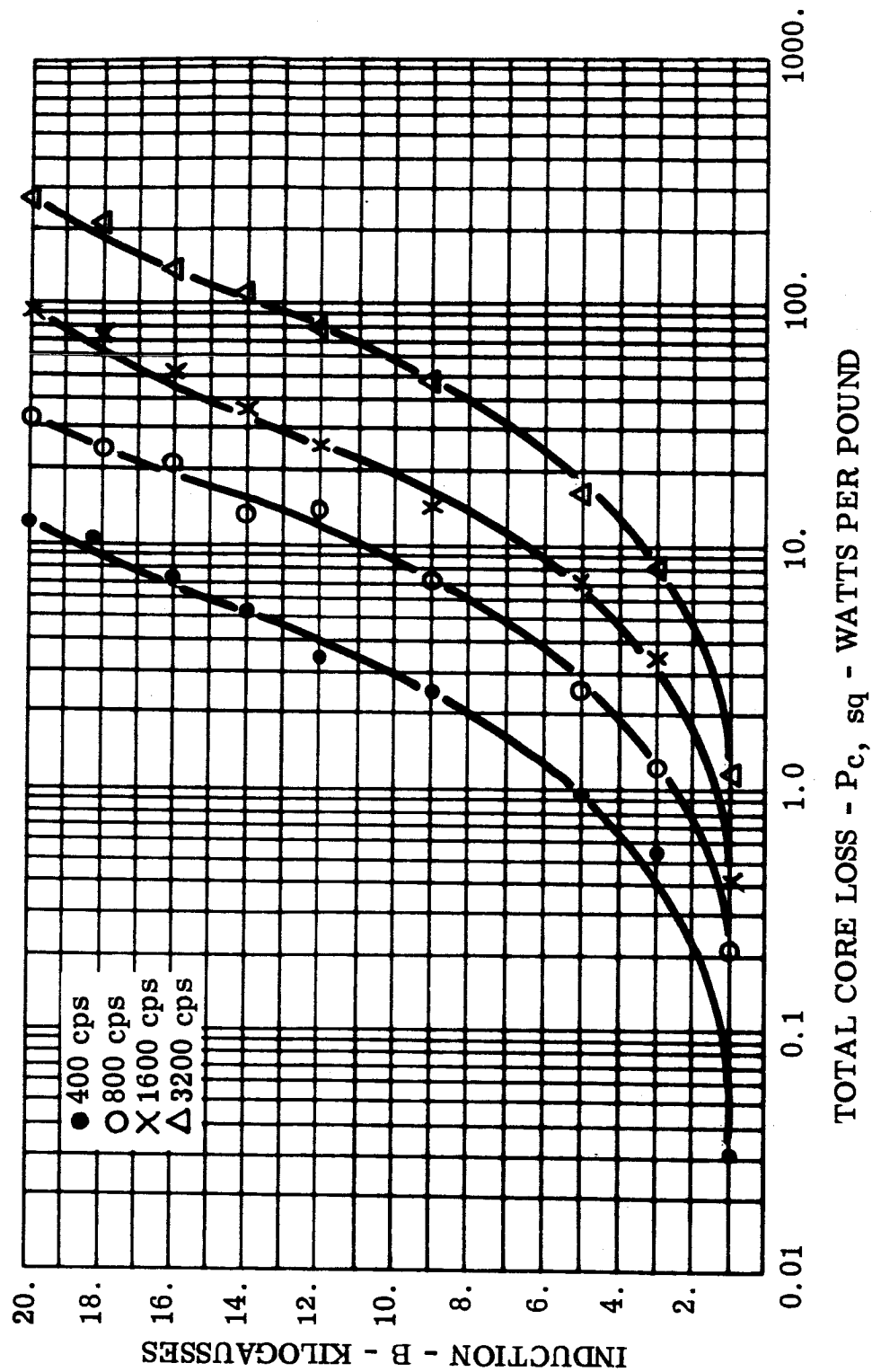


FIGURE 116 P_c , sq - Total Core Loss, 0.004 Inch Supermendur Rowland Ring,
Core 36, Magnetic Field Annealed, -55°C

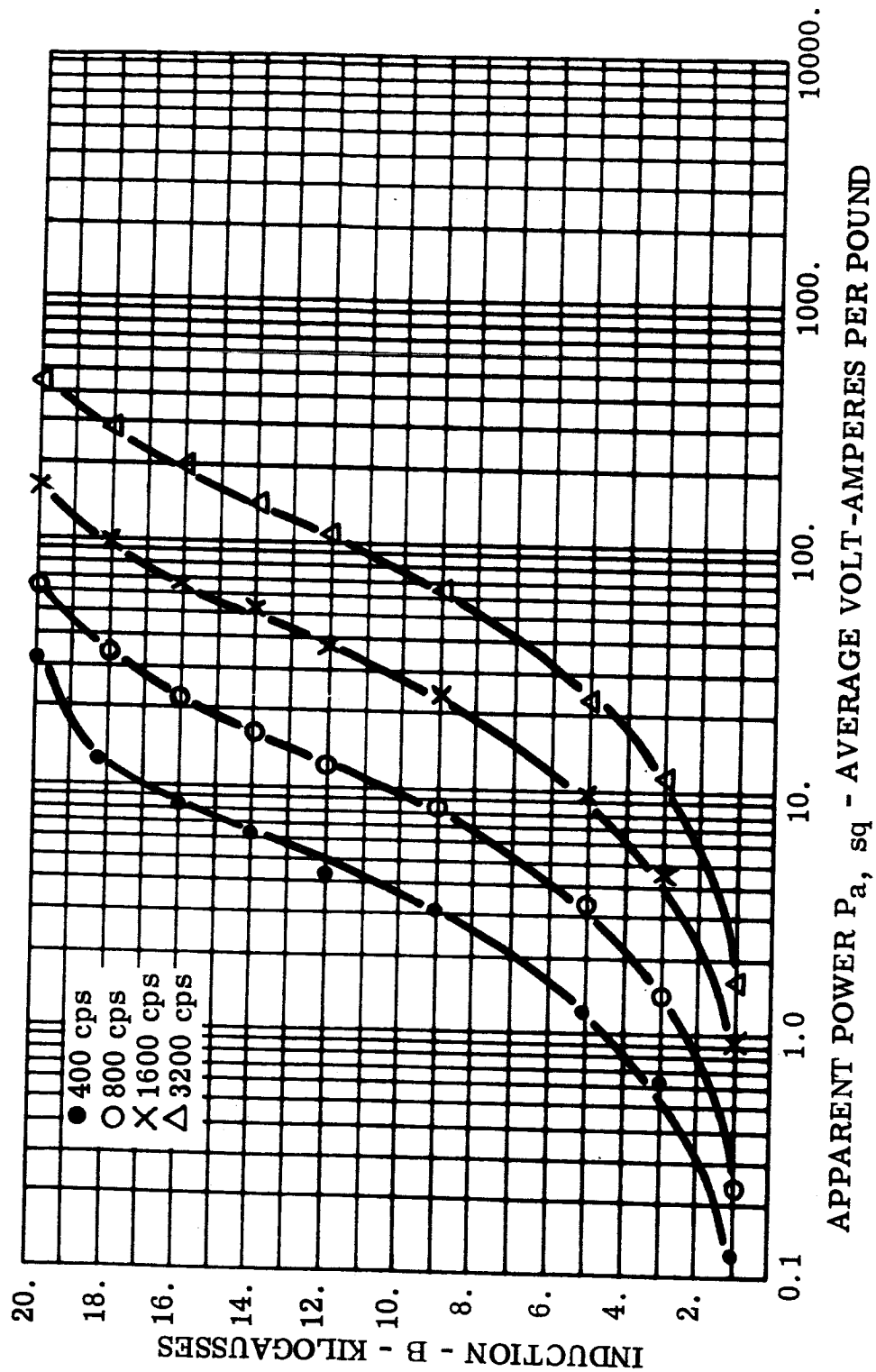


FIGURE 117 $P_{a, sq}$ - Apparent Power, 0.004 Inch Supermendur Rowland Ring,
Core 36, Magnetic Field Annealed, -55°C

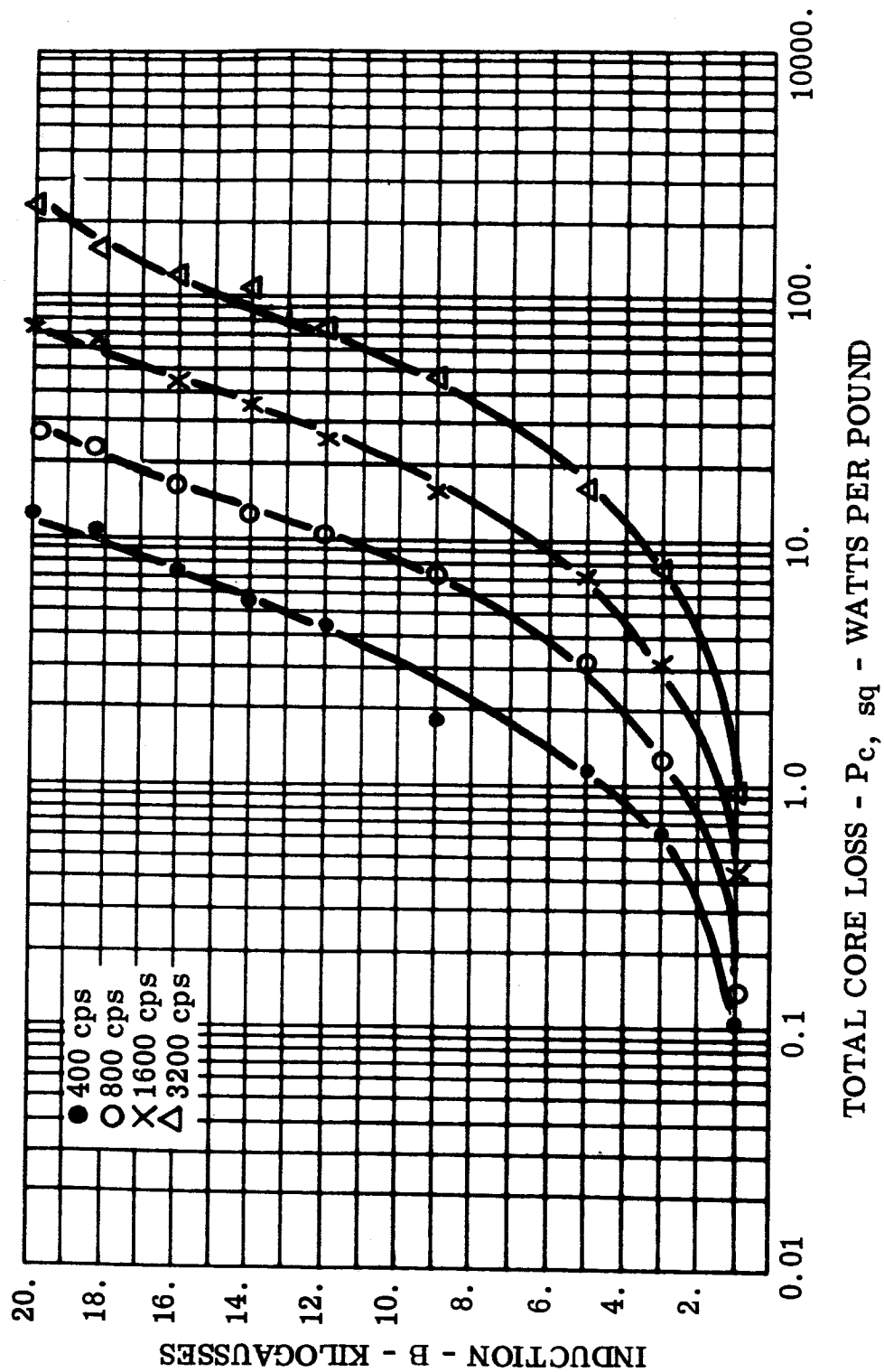
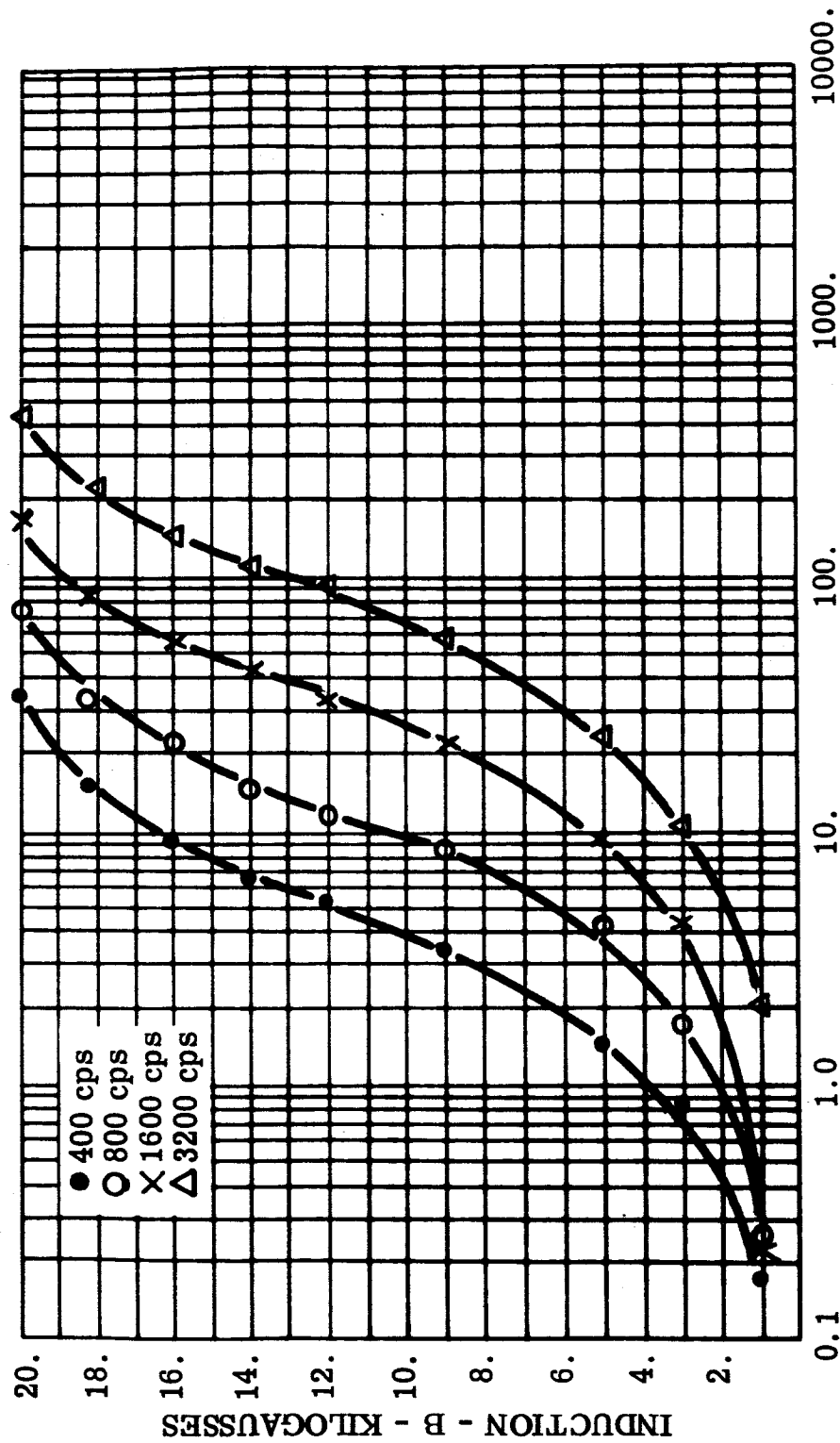


FIGURE 118 $P_{c, sq}$ - Total Core Loss, 0.004 Inch Supermendur Rowland Ring, Core 37, Magnetic Field Annealed, Room Ambient



APPARENT POWER - P_a, sq - AVERAGE VOLT-AMPERES PER POUND

FIGURE 119 P_a, sq - Apparent Power, 0.004 Inch Supermendur Rowland Ring, Core 37, Magnetic Field Annealed, Room Ambient

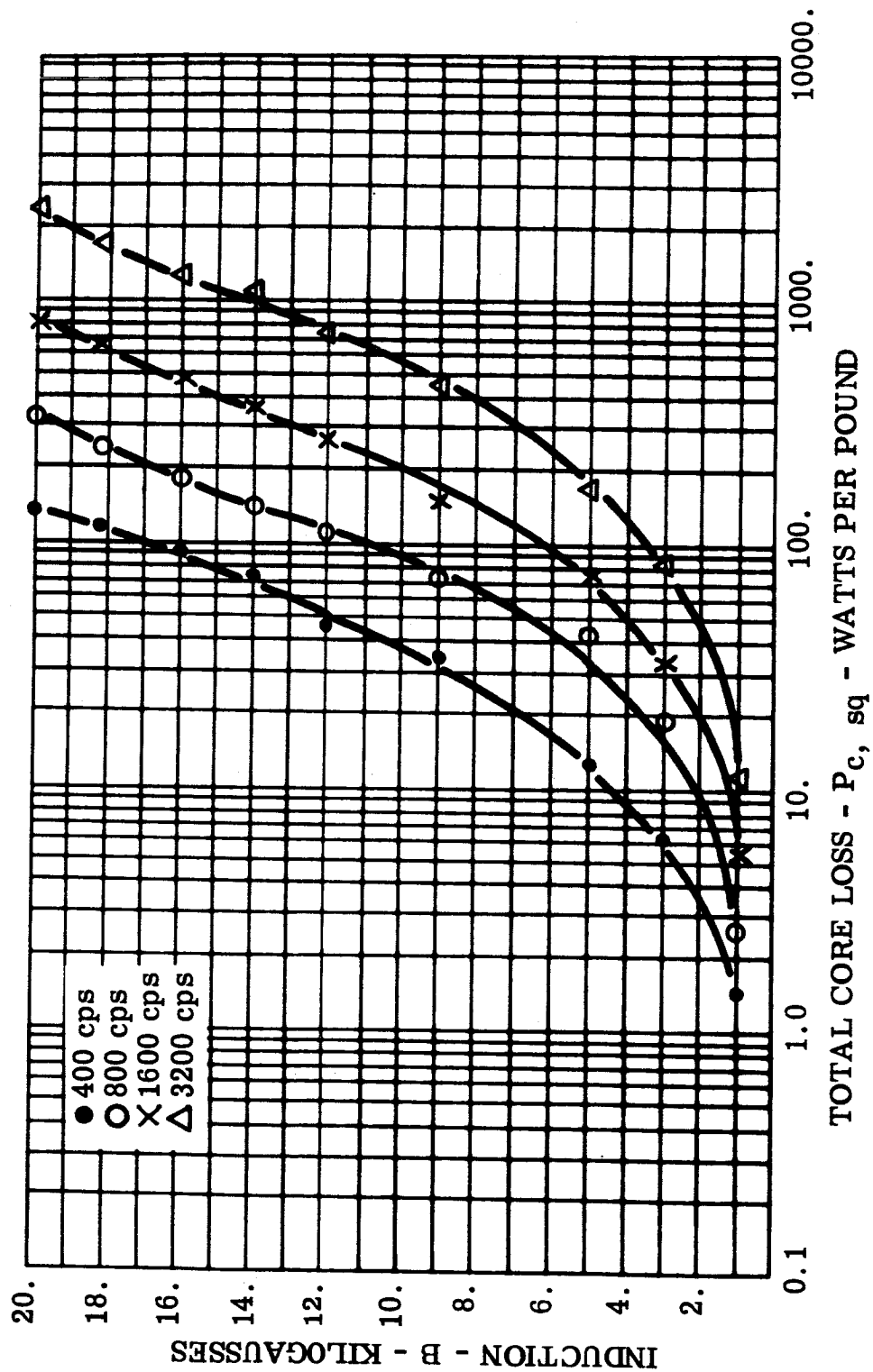


FIGURE 120 P_c , sq - Total Core Loss, 0.004 Inch Supermendur Rowland Ring,
Core 37, Magnetic Field Annealed, -55°C

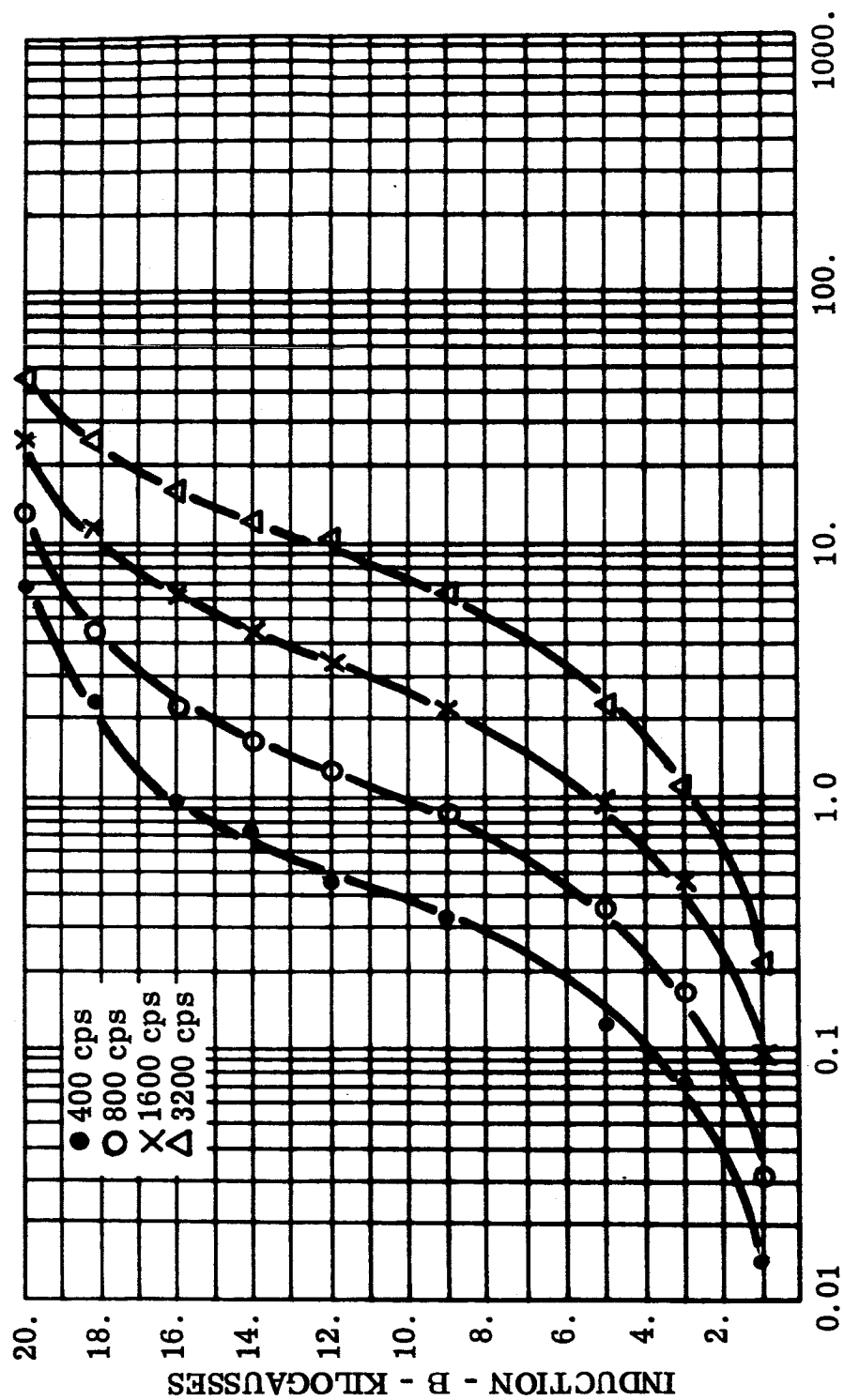


FIGURE 121 P_a , sq - Apparent Power, 0.004 Inch Supermendur Rowland Ring,
Core 37, Magnetic Field Annealed, -55°C

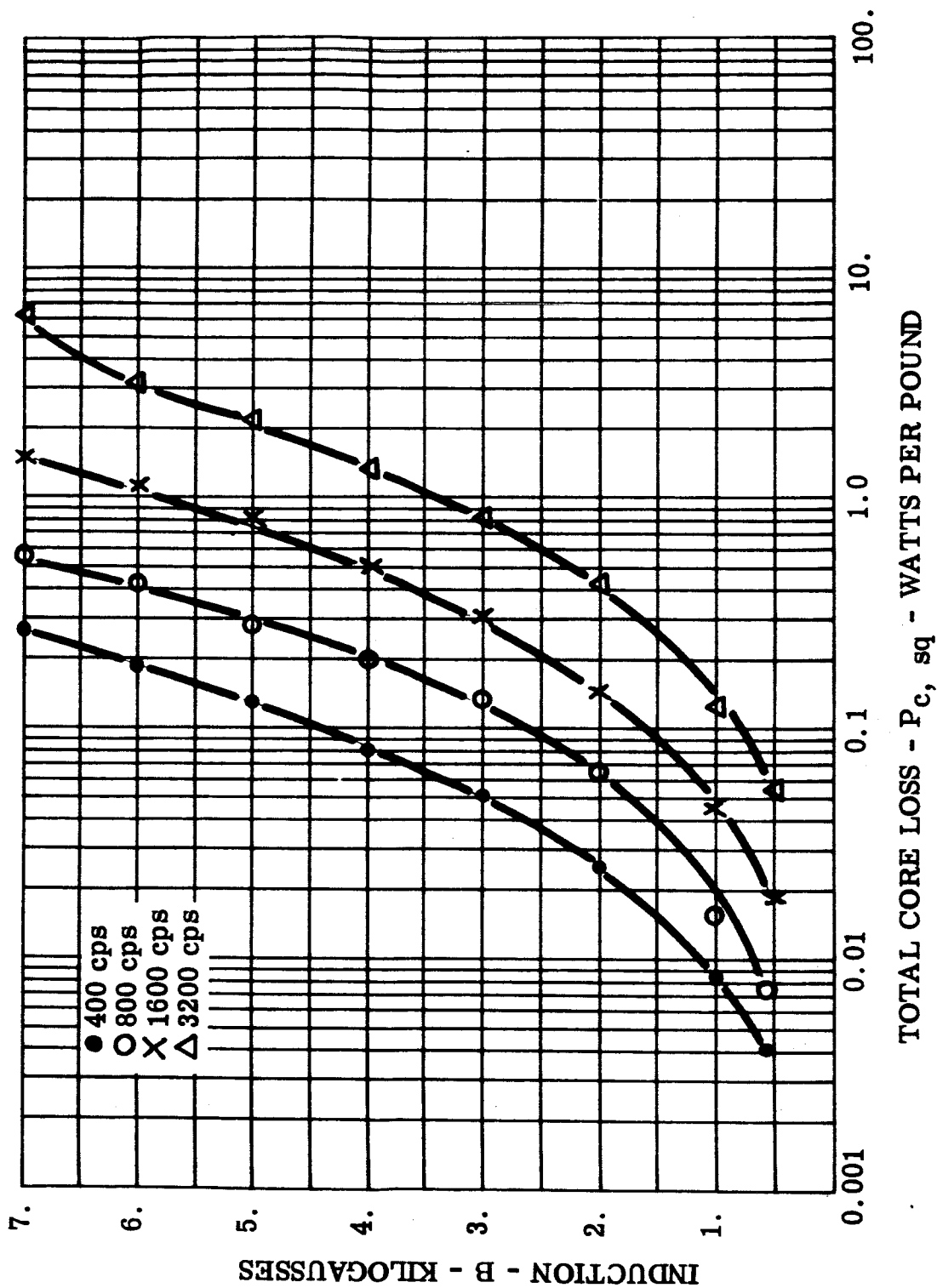
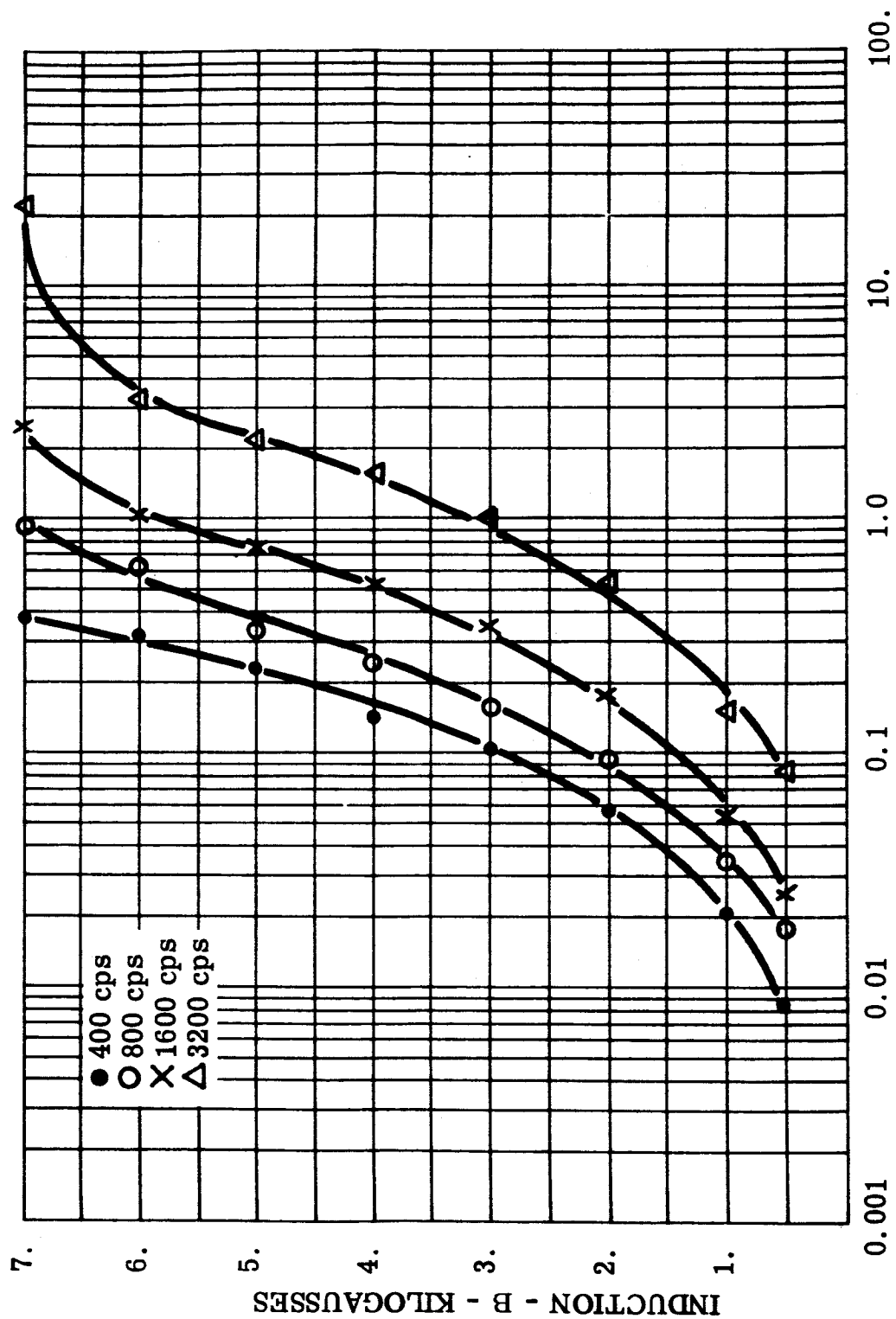


FIGURE 122 $P_{c, sq}$ - Total Core Loss, 0.002 Inch Hy-Ra 80 Toroid, Core 23, Room Ambient



APPARENT POWER - P_a, sq - AVERAGE VOLT-AMPERES PER POUND

FIGURE 123 P_a, sq - Apparent Power, 0.002 Inch Hy-Ra 80 Toroid, Core 23,
Room Ambient

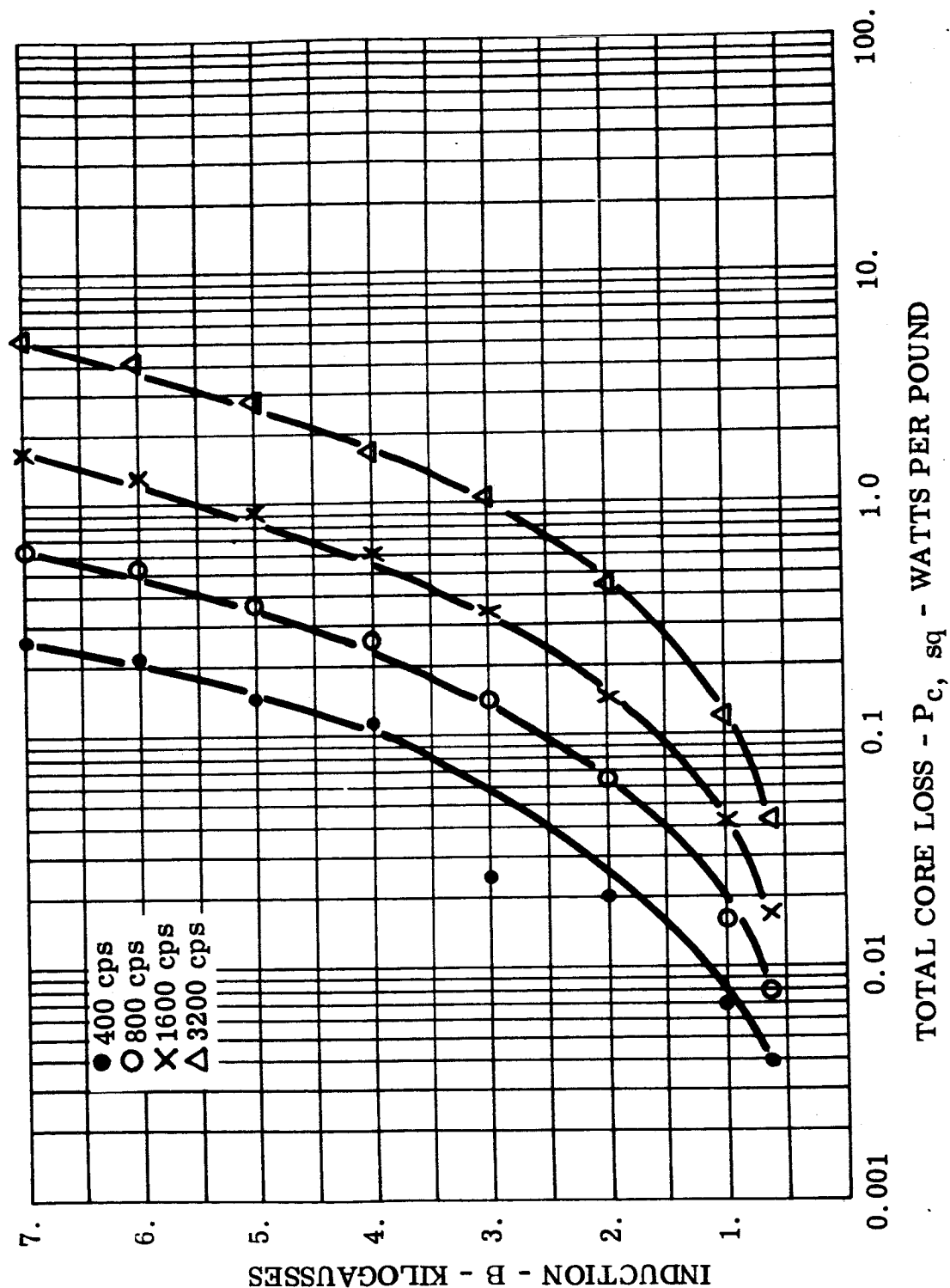
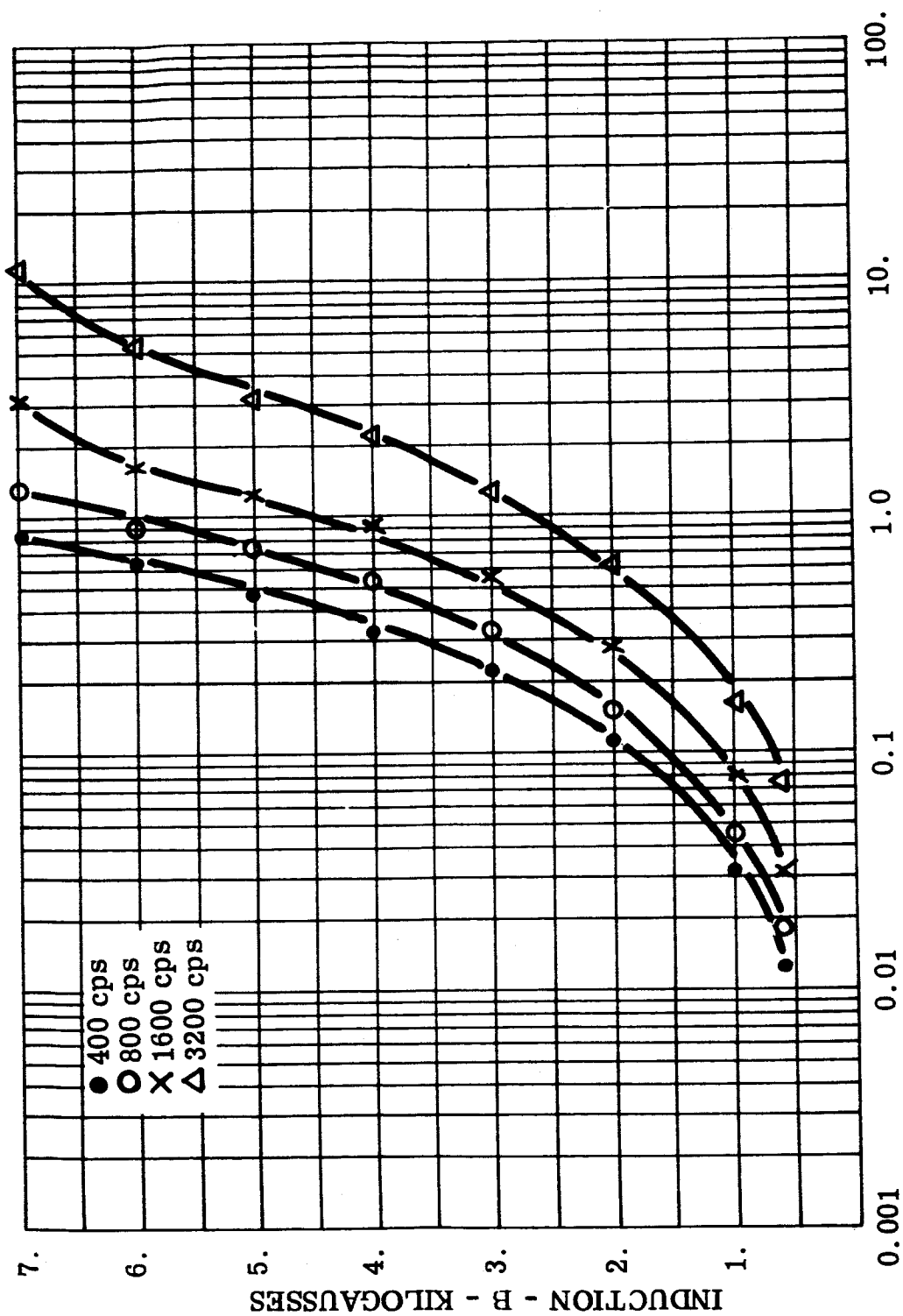


FIGURE 124 $P_{c, sq}$ - Total Core Loss, 0.002 Inch Hy-Ra 80 Toroid, Core 23, -55°C



APPARENT POWER - P_a, sq - VOLT-AMPERES PER POUND

FIGURE 125 P_a, sq - Apparent Power, 0.002 Inch Hy-Ra 80 Toroid, Core 23, -55°C

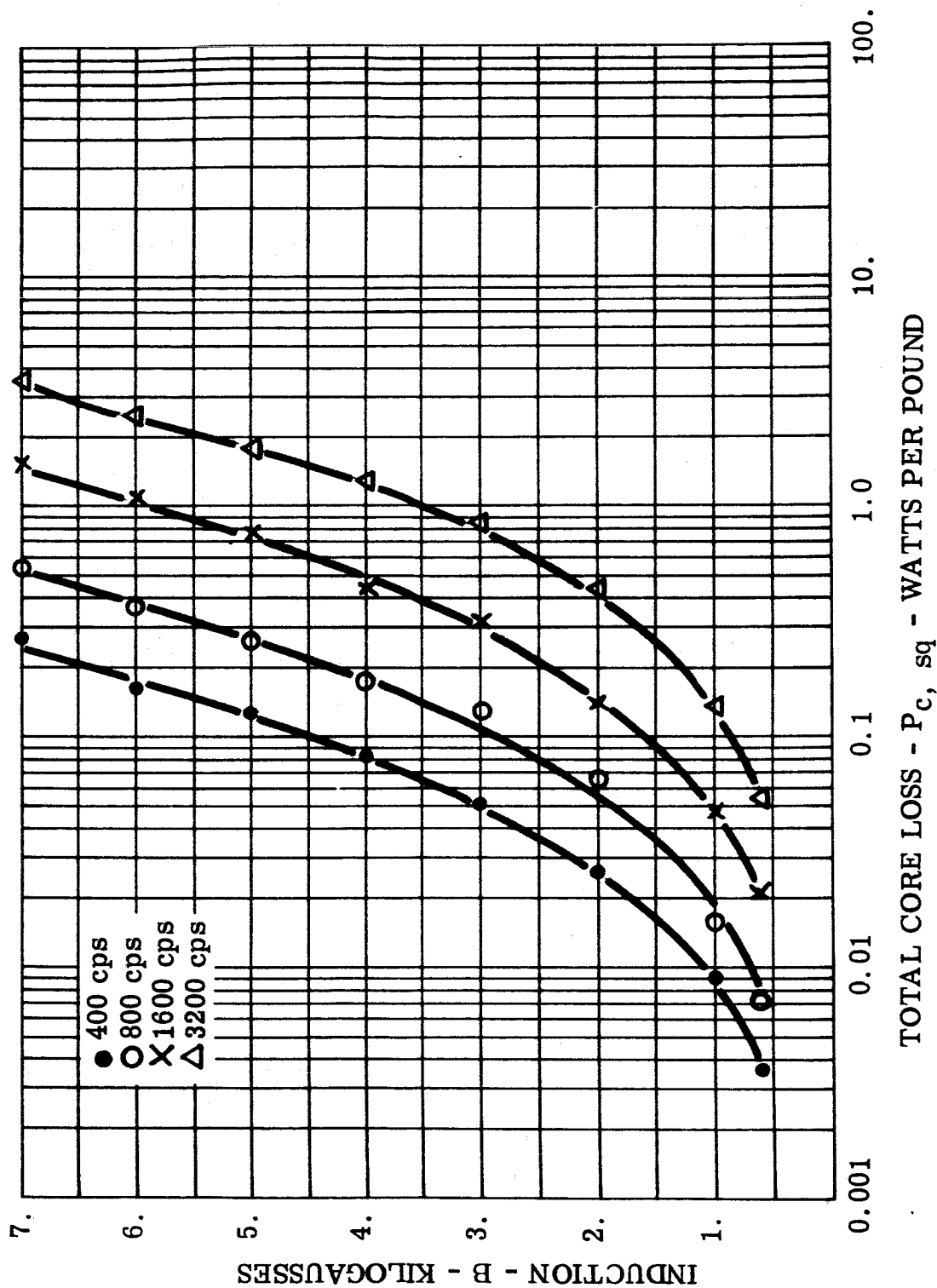
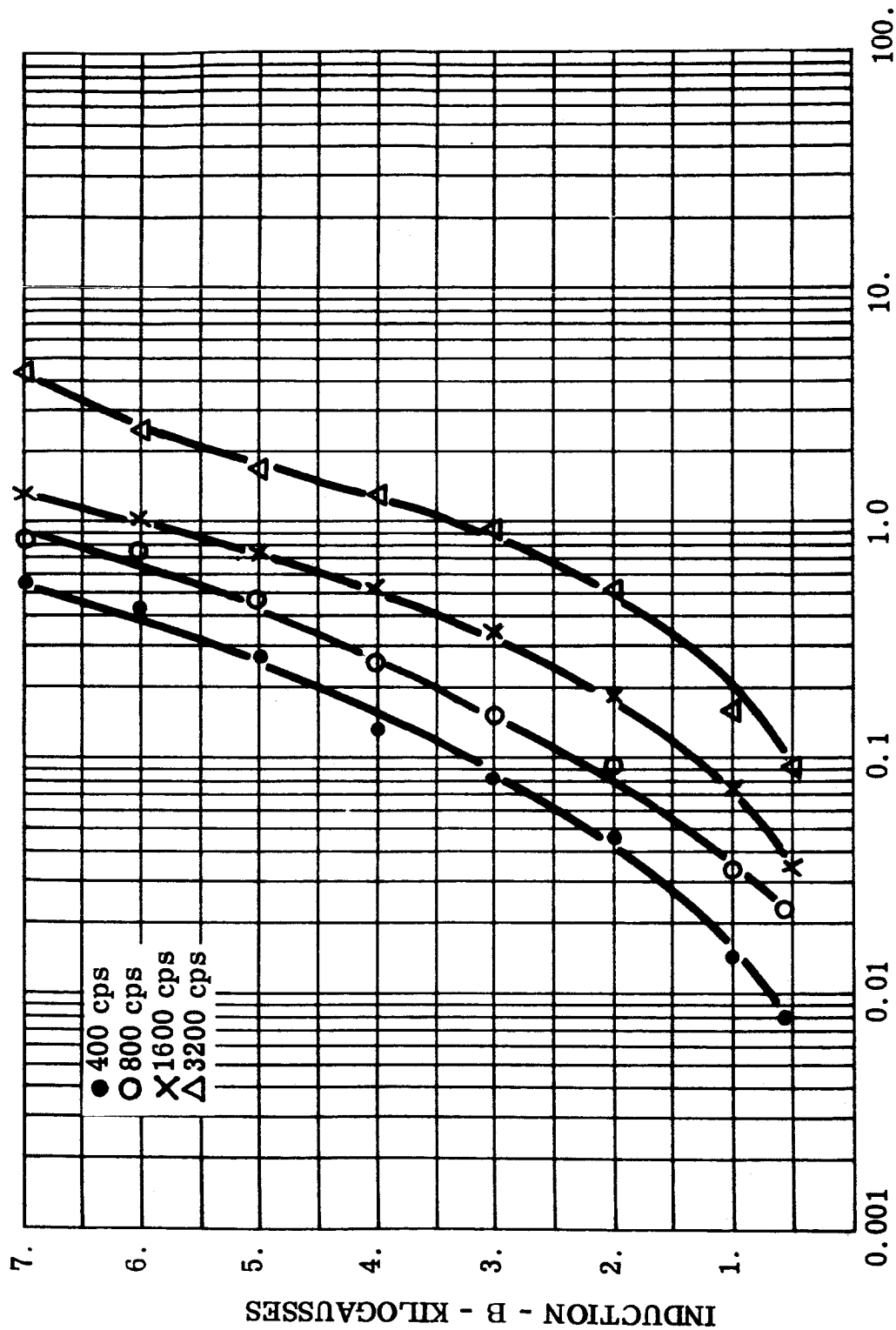


FIGURE 126 $P_{c, sq}$ - Total Core Loss, 0.002 Inch Hy-Ra 80 Toroid, Core 24, Room Ambient



APPARENT POWER - P_a, sq - AVERAGE VOLT-AMPERES PER POUND

FIGURE 127 P_a, sq - Apparent Power, 0.002 Inch Hy-Ra 80 Toroid, Core 24, Room Ambient

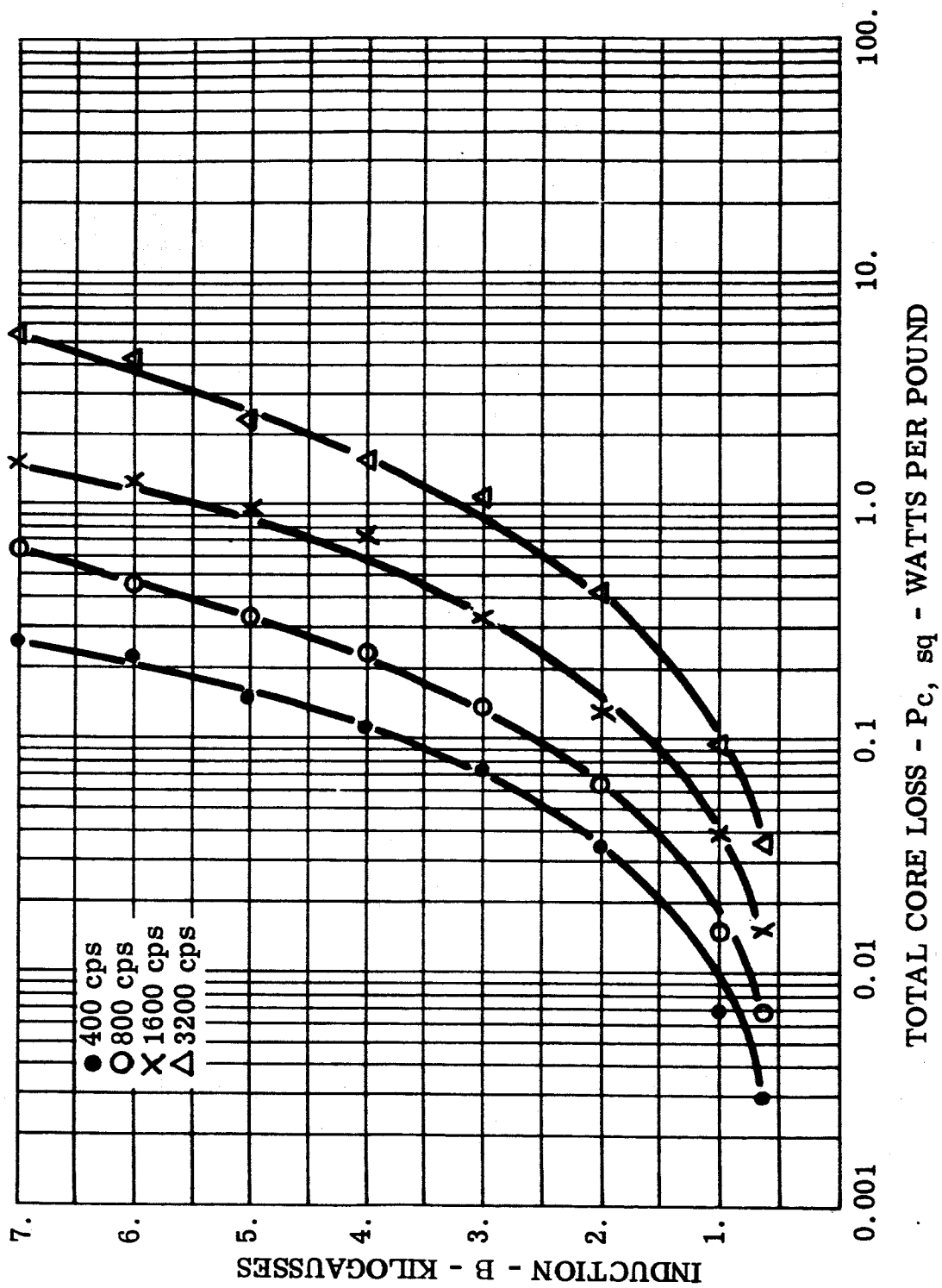


FIGURE 128 $P_{c, sq}$ - Total Core Loss, 0.002 Inch Hy-Ra 80 Toroid, Core 24, -55°C

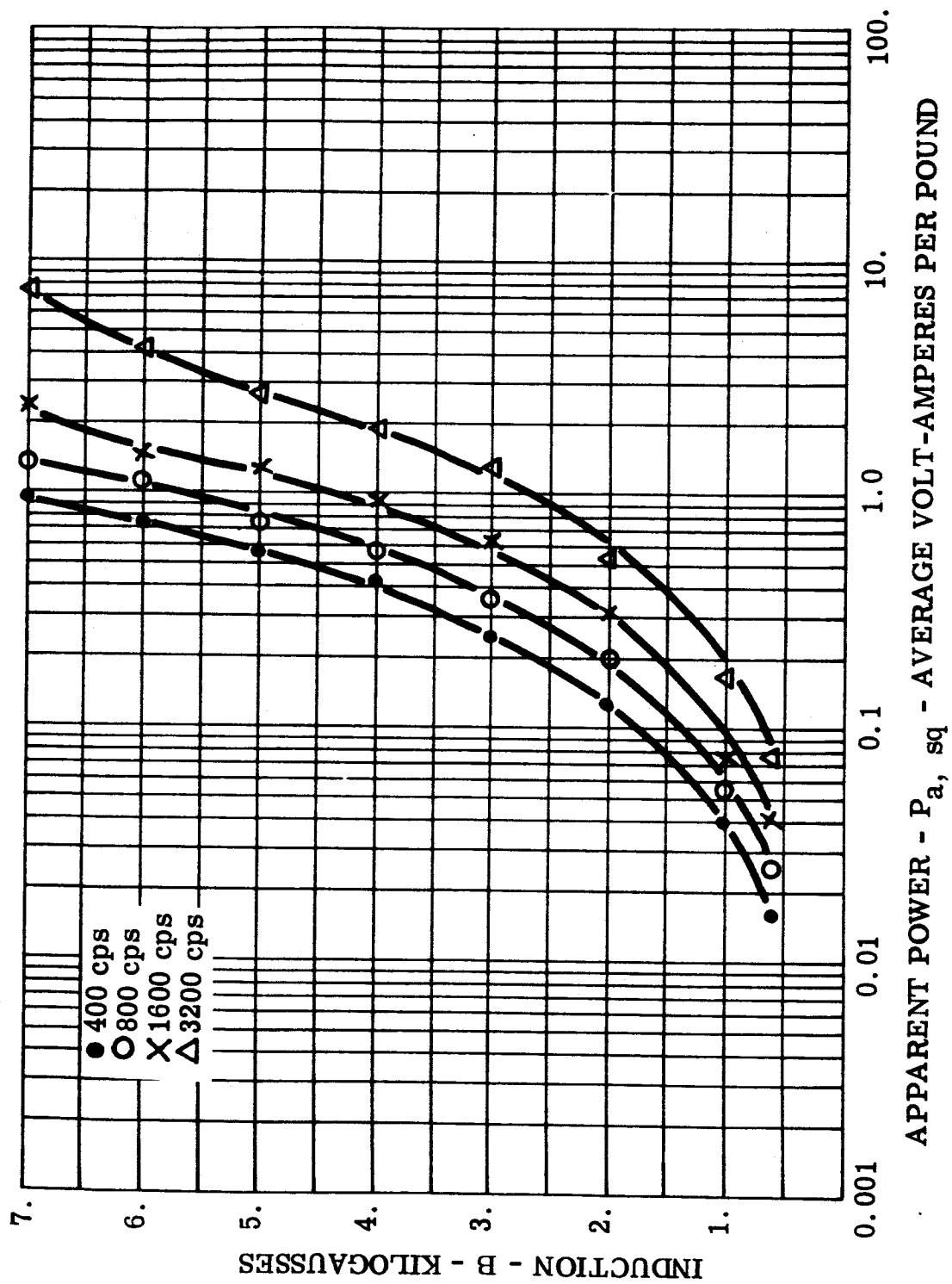


FIGURE 129 P_a, sq - Apparent Power, 0.002 Inch Hy-Ra 80 Toroid, Core 24, -55°C

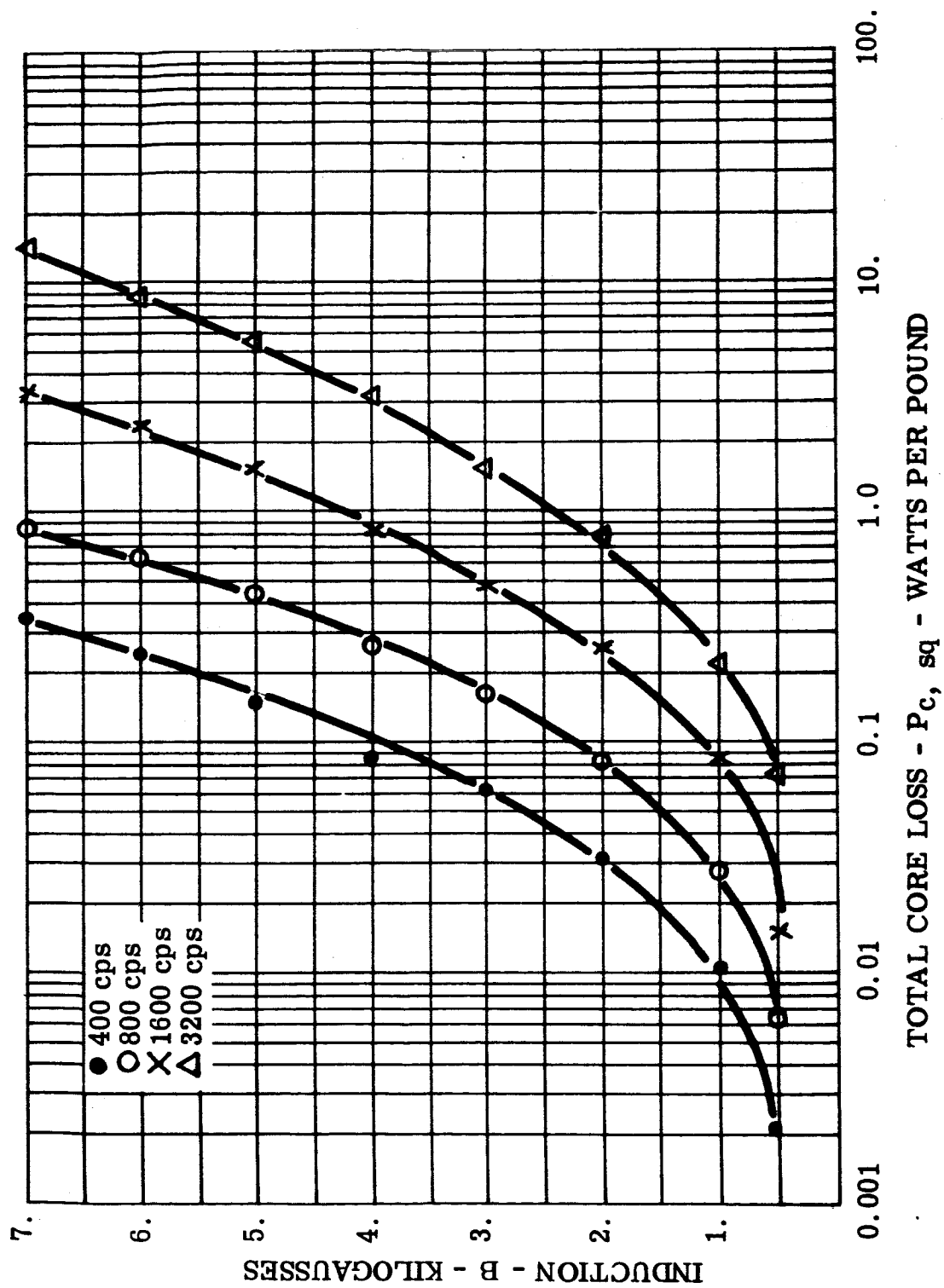
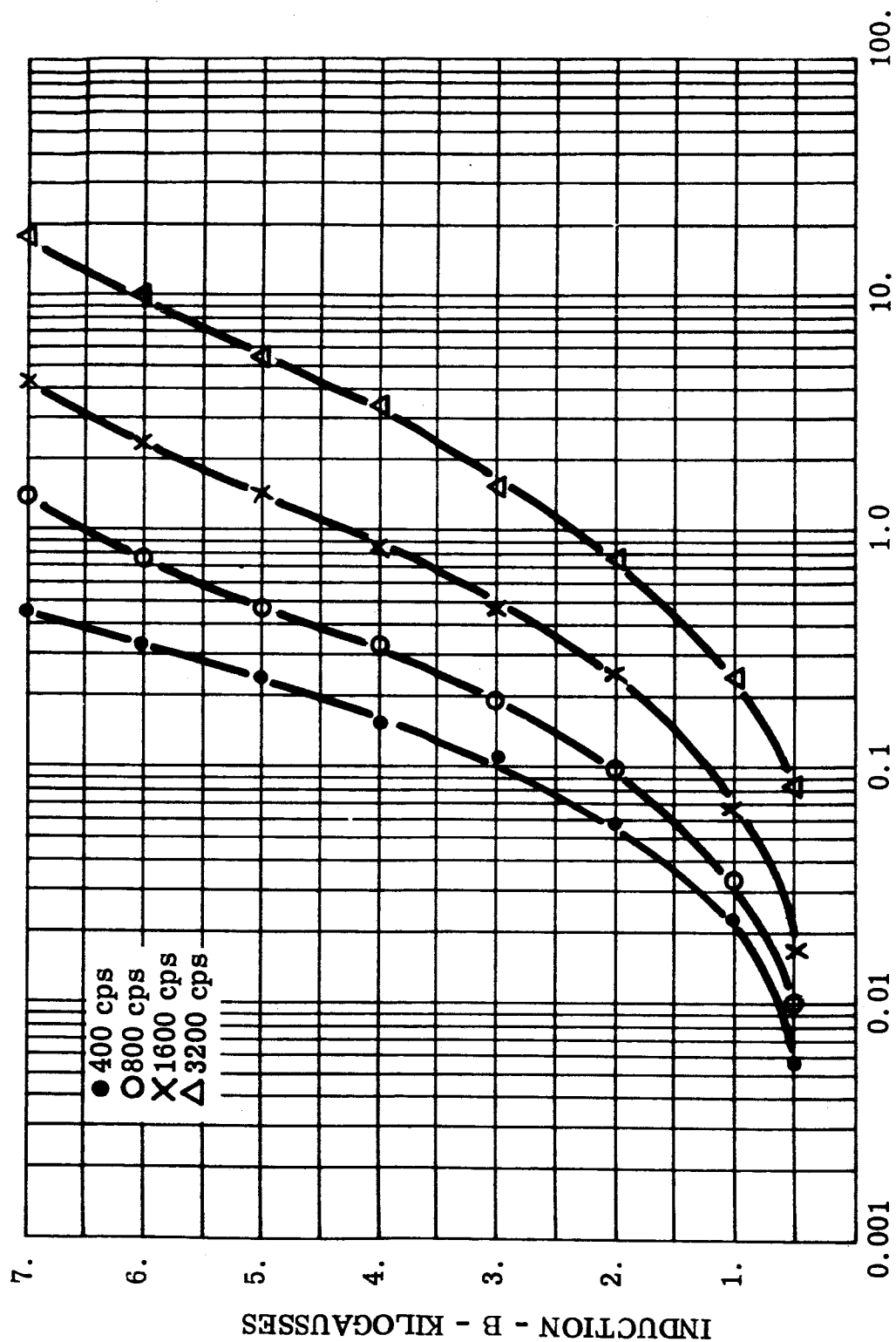
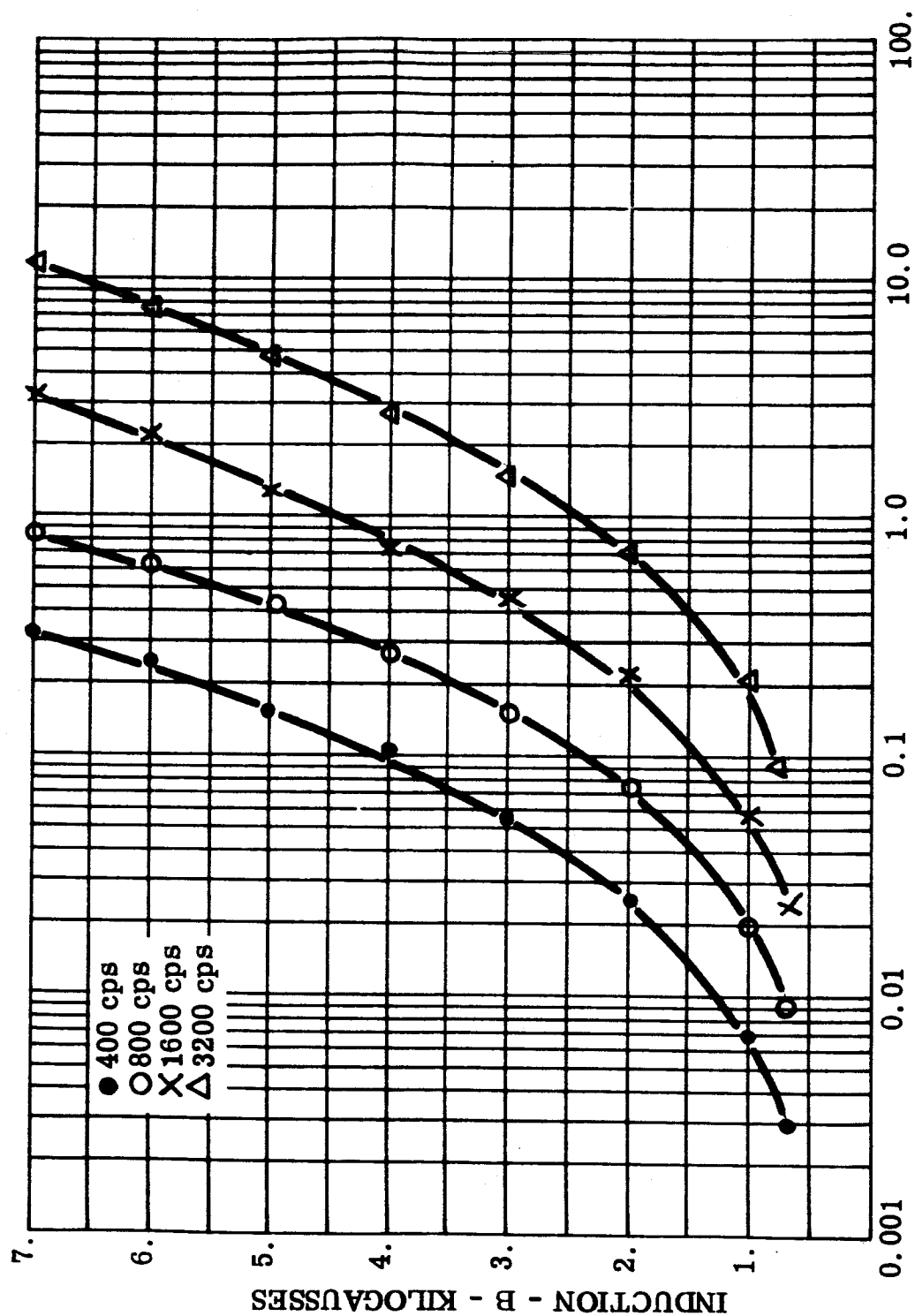


FIGURE 130 $P_{c, sq}$ - Total Core Loss, 0.004 Inch Hy-Ra 80 Toroid, Core 19, Room Ambient



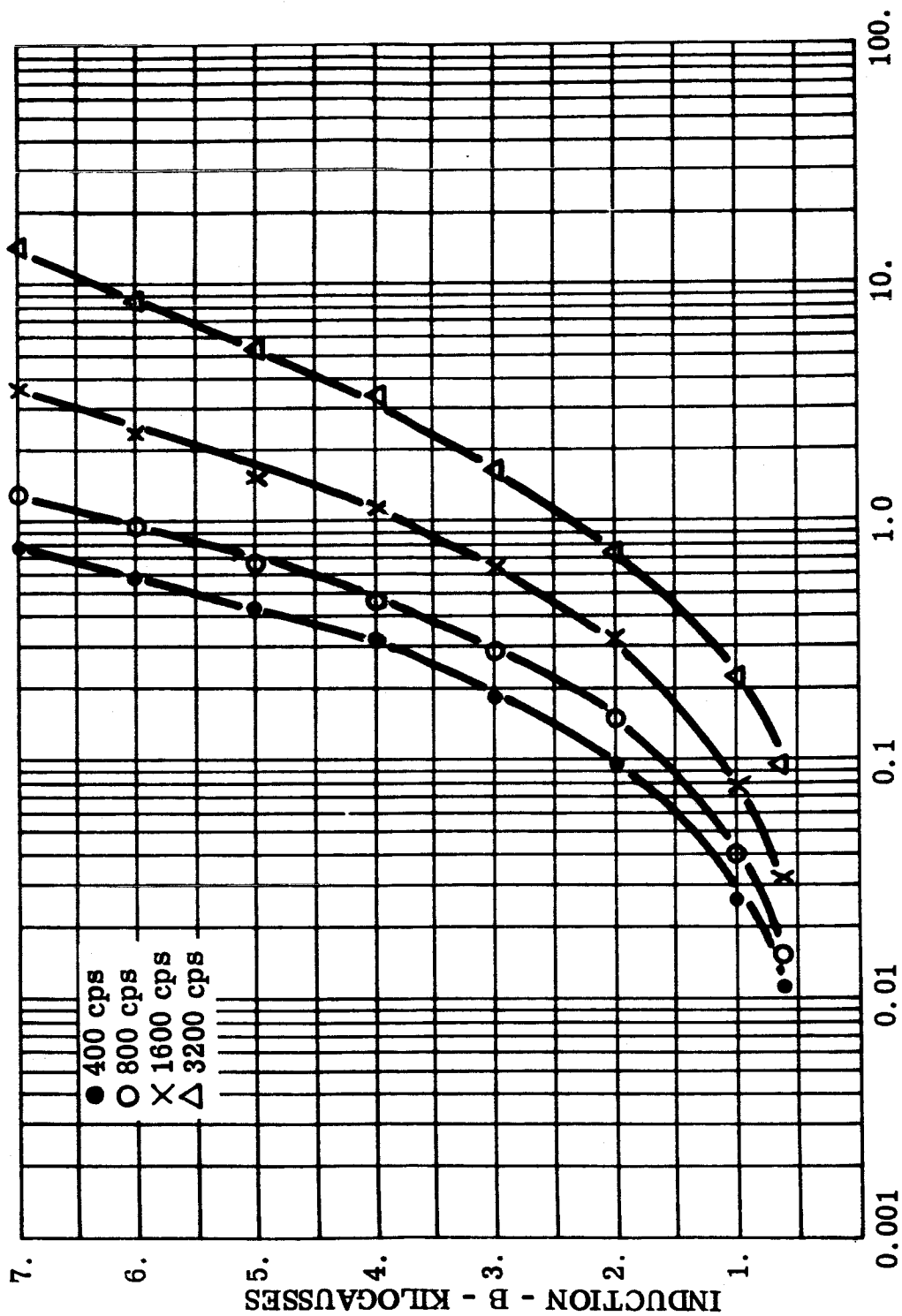
APPARENT POWER - P_a , sq - AVERAGE VOLT-AMPERES PER POUND

FIGURE 131 P_a , sq - Apparent Power, 0.004 Inch Hy-Ra 80 Toroid, Core 19, Room Ambient



TOTAL CORE LOSS - $P_{c, sq}$ - WATTS PER POUND

FIGURE 132 $P_{c, sq}$ - Total Core Loss, 0.004 Inch Hy-Ra 80 Toroid, Core 19, -55°C



APPARENT POWER - P_a , sq - AVERAGE VOLT-AMPERES PER POUND

FIGURE 133 P_a , sq - Apparent Power, 0.004 Inch Hy-Ra 80 Toroid, Core 19, -55°C

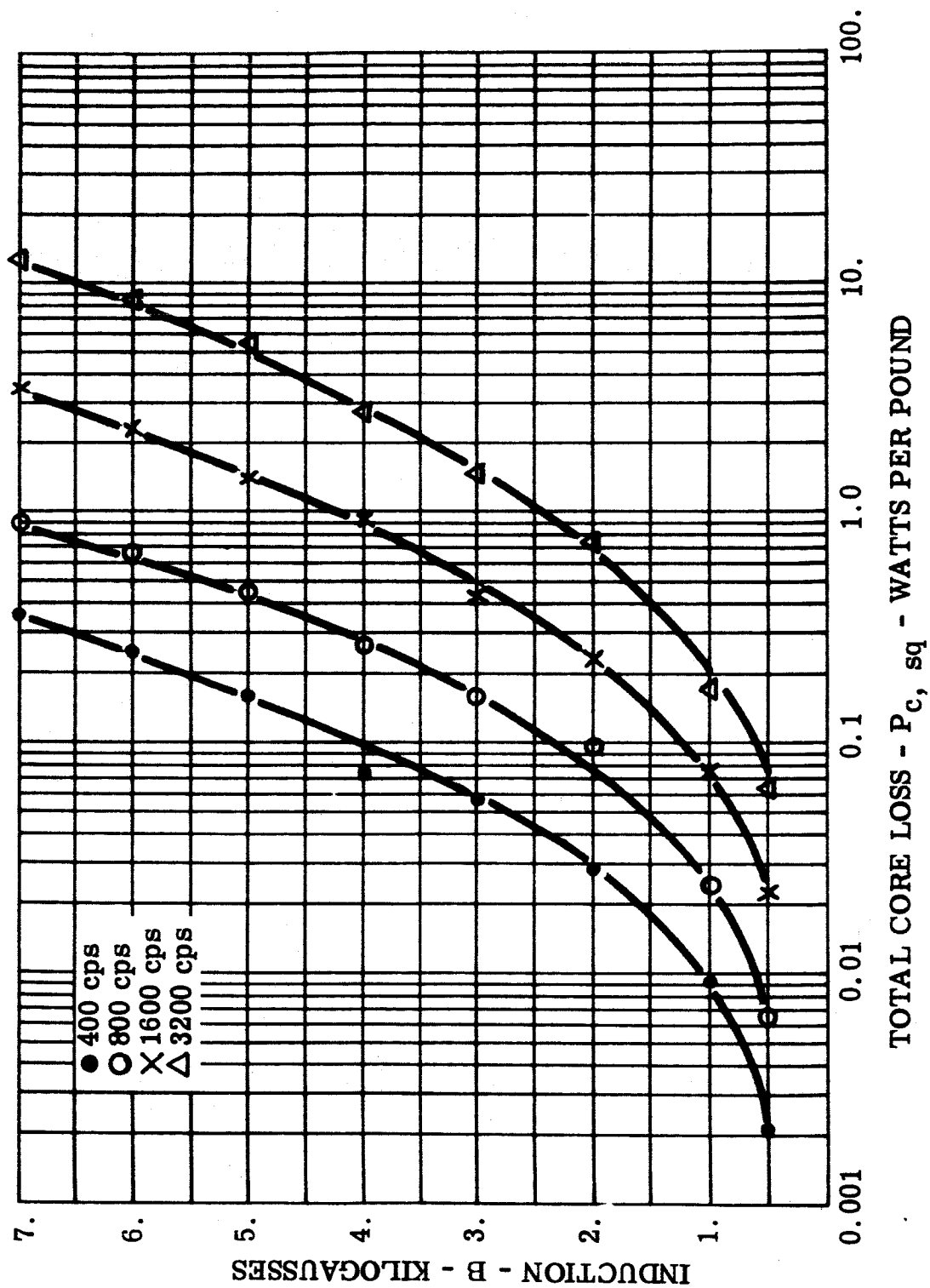


FIGURE 134 $P_{c, sq}$ - Total Core Loss, 0.004 Inch Hy-Ra 80 Toroid, Core 20, Room Ambient

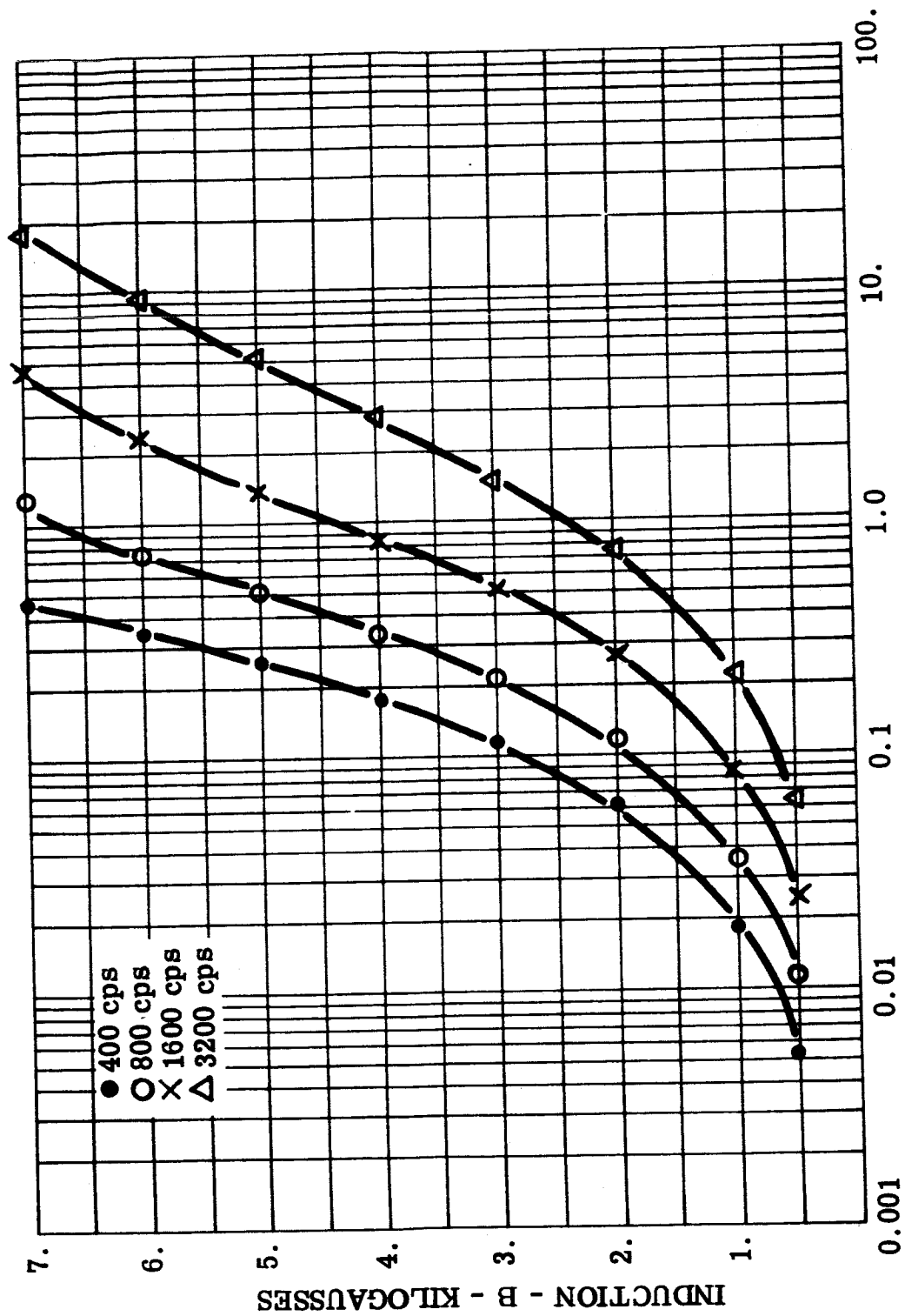


FIGURE 135 P_a , sq - Apparent Power, 0.004 Inch Hy-Ra 80 Toroid, Core 20, Room Ambient

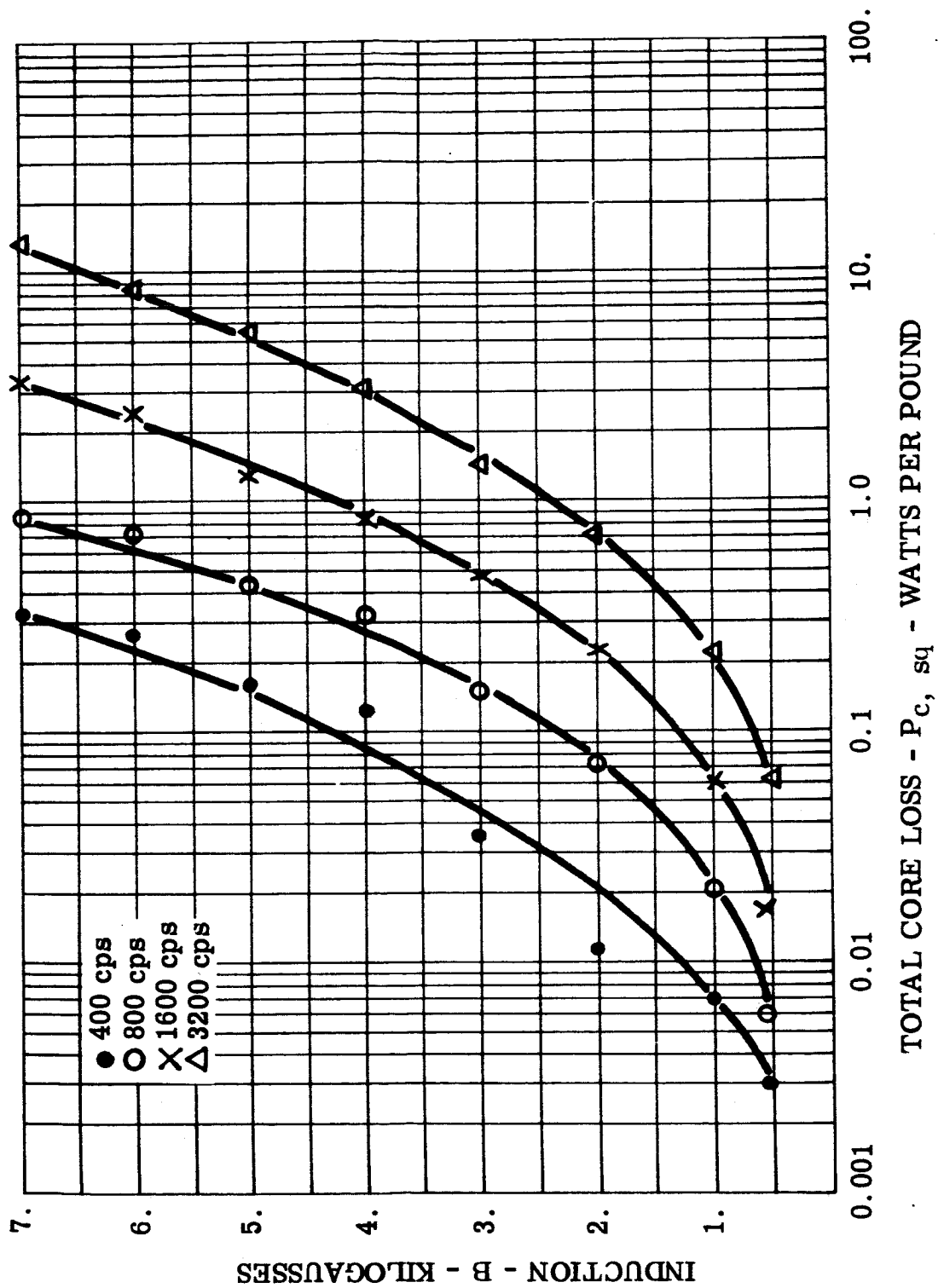


FIGURE 136 $P_{c, sq}$ - Total Core Loss, 0.004 Inch Hy-Ra 80 Toroid, Core 20, -55°C

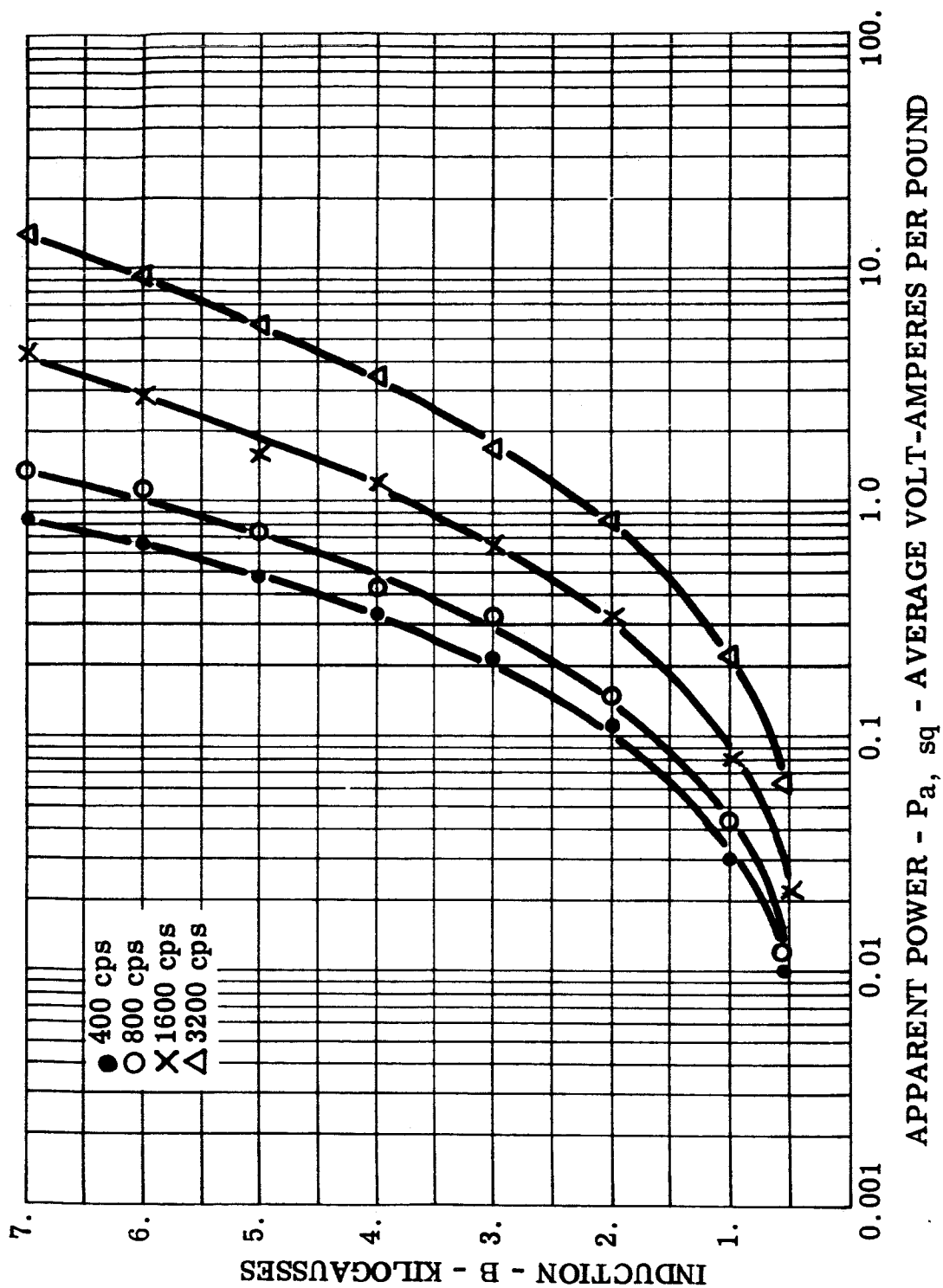


FIGURE 137 $P_{a, sq}$ - Apparent Power, 0.004 Inch Hy-Ra 80 Toroid, Core 20, -55°C

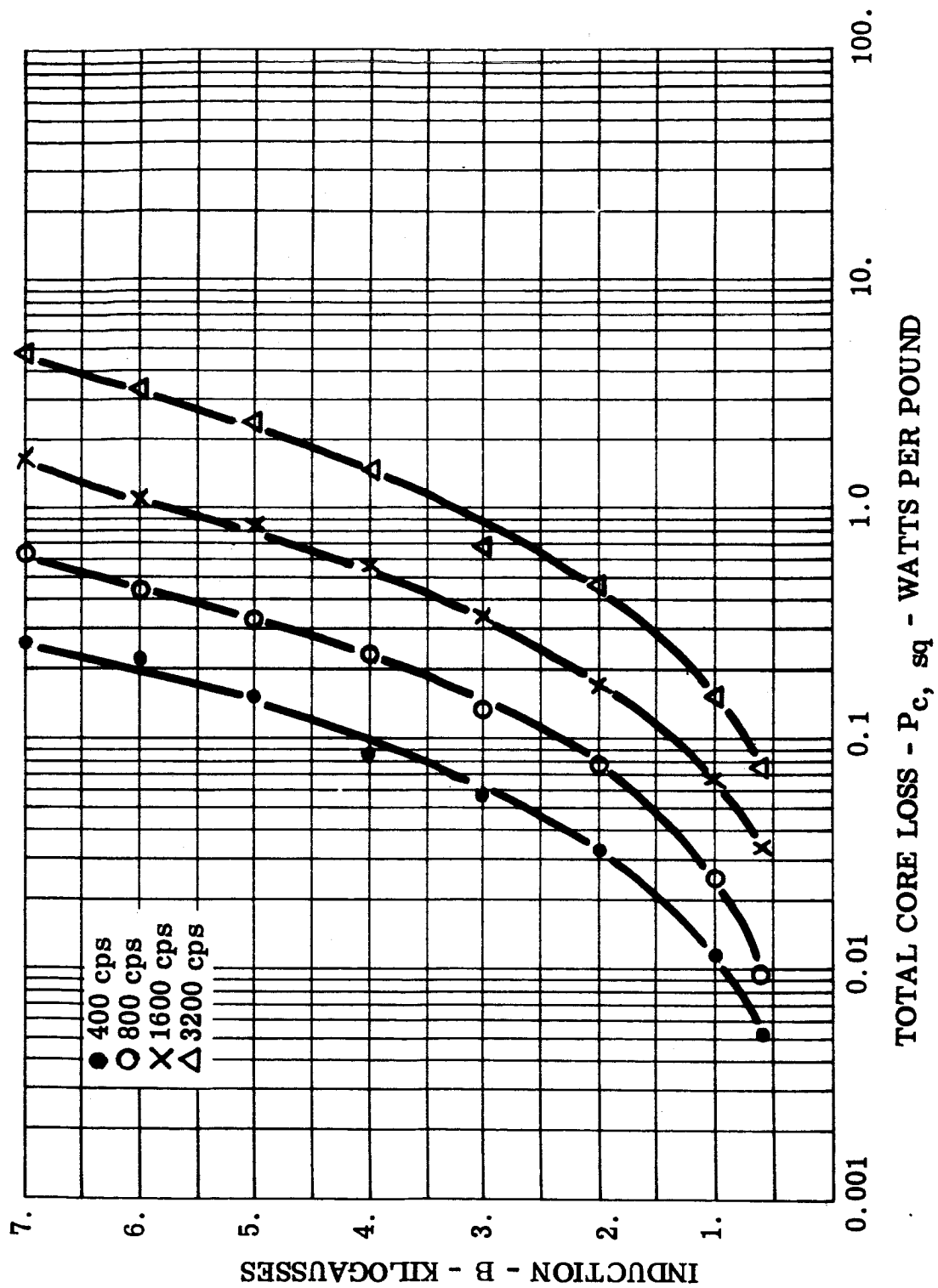
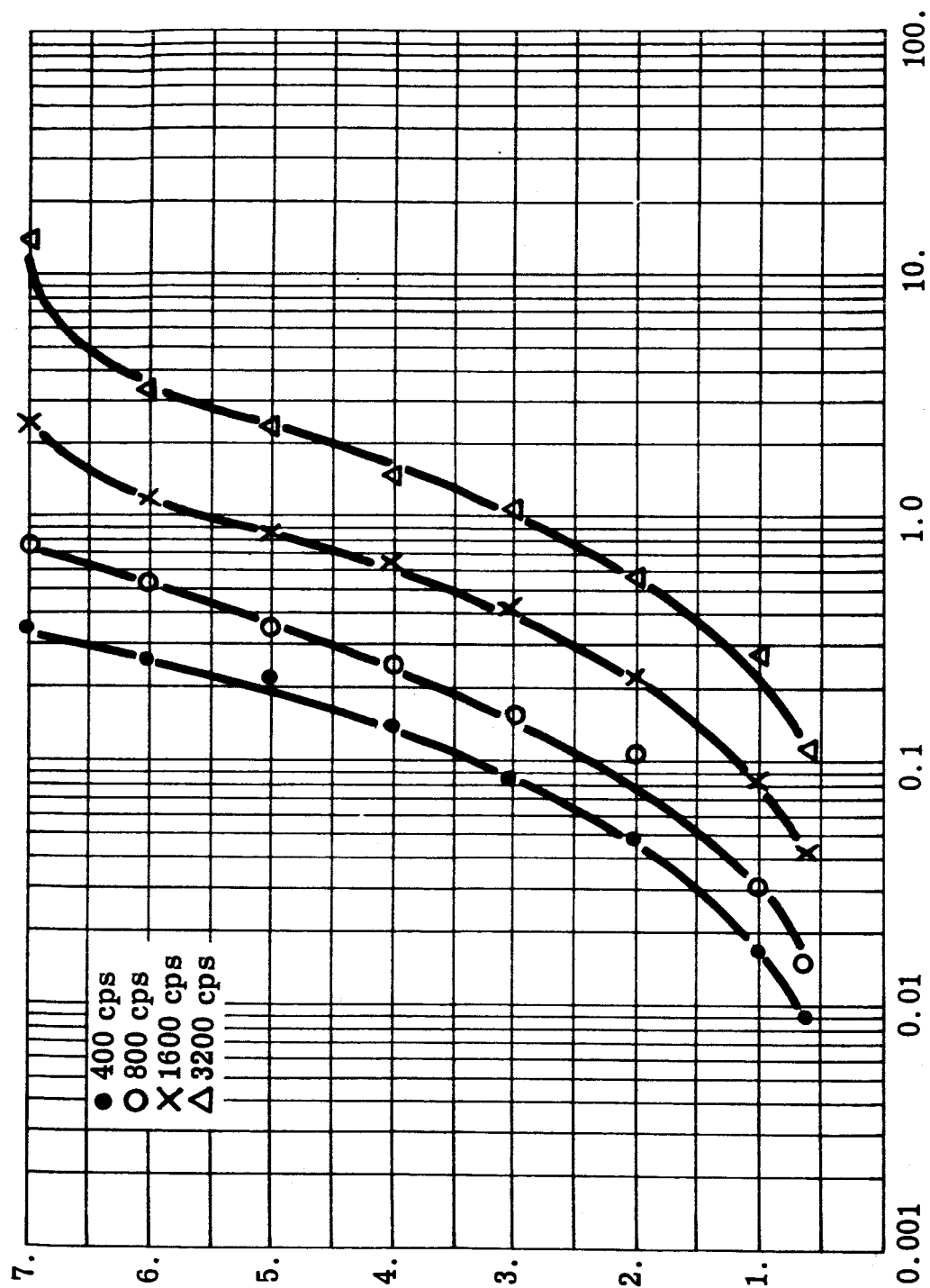


FIGURE 138 $P_{c, sq}$ - Total Core Loss, 0.002 Inch Permalloy 80 Toroid,
Core 2, Room Ambient



APPARENT POWER - P_a , sq - AVERAGE VOLT-AMPERES PER POUND

FIGURE 139 P_a , sq - Apparent Power, 0.002 Inch Permalloy 80 Toroid,
Core 2, Room Ambient

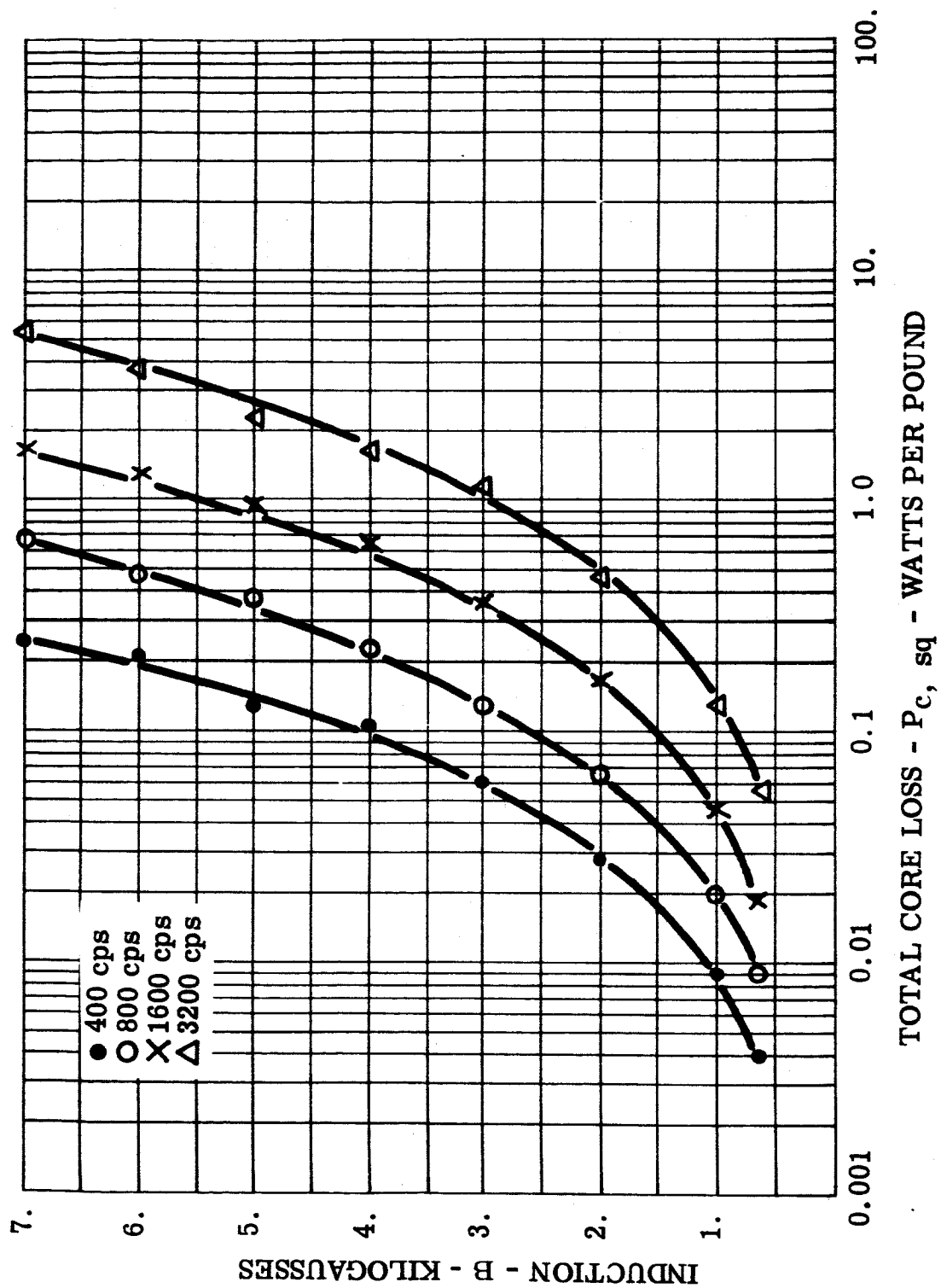


FIGURE 140 P_c , sq - Total Core Loss, 0.002 Inch Permalloy 80 Toroid, Core 2, -55°C

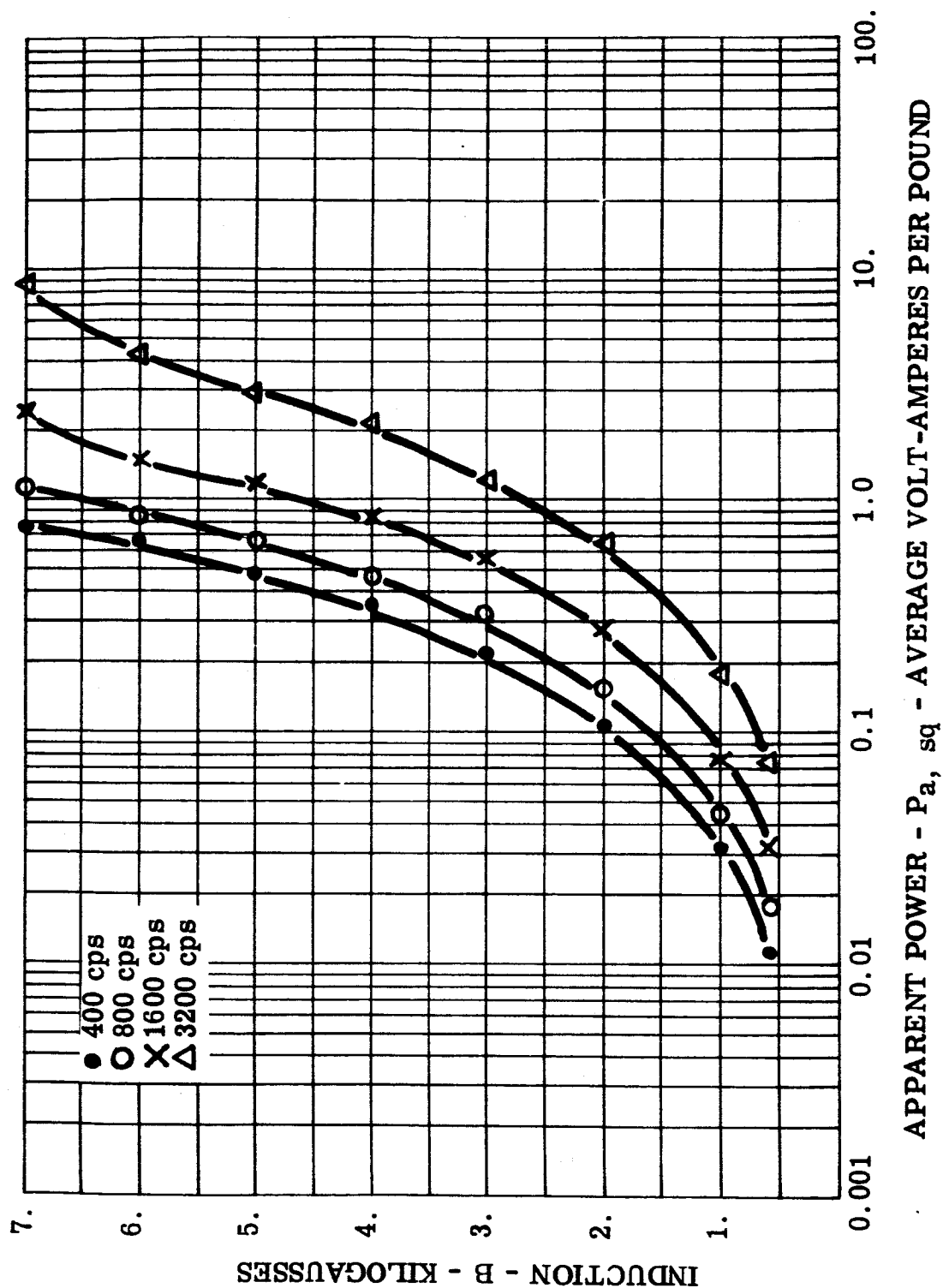


FIGURE 141 P_a, sq - Apparent Power, 0.002 Inch Permalloy 80 Toroid, Core 2, -55°C

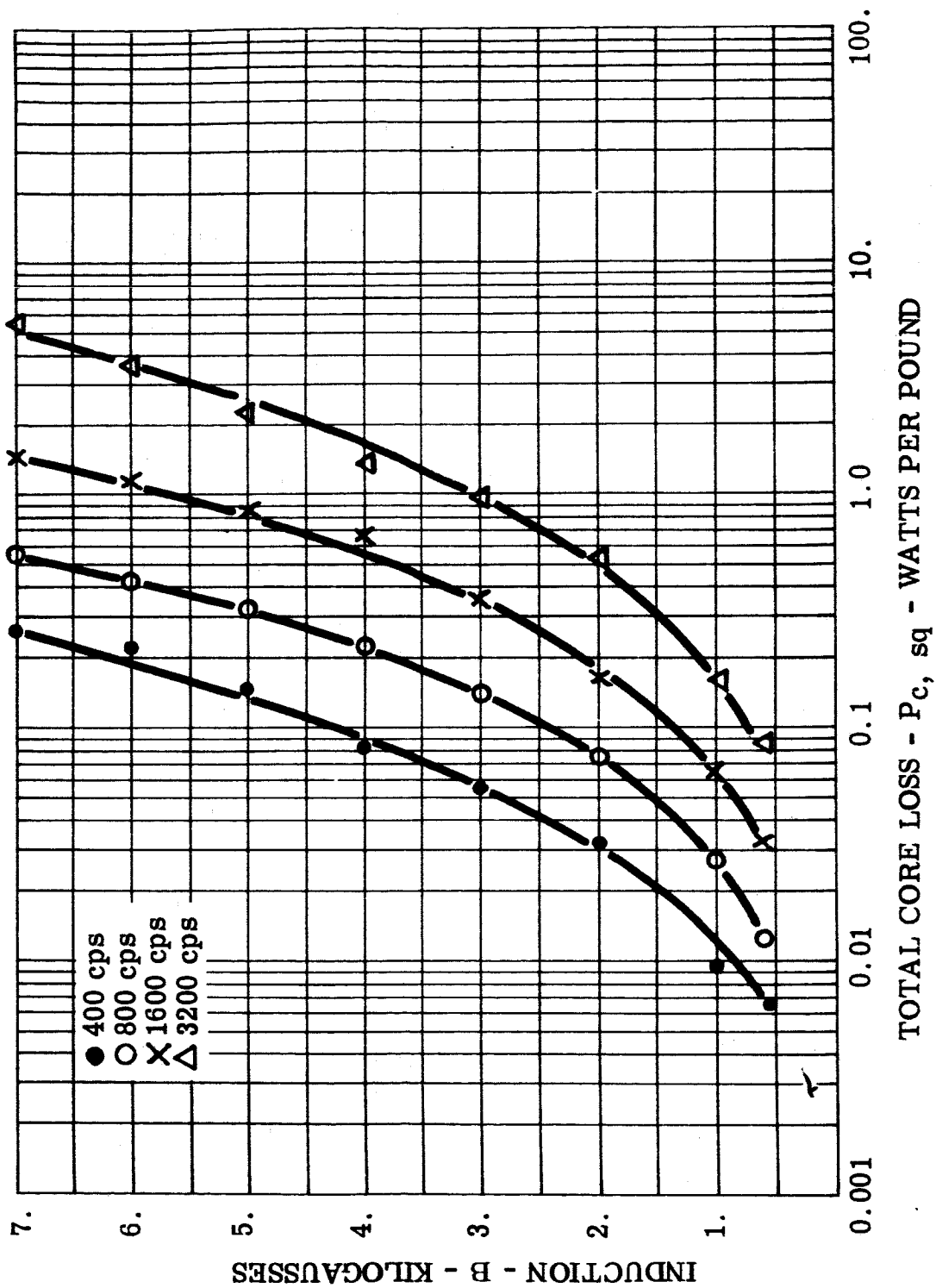
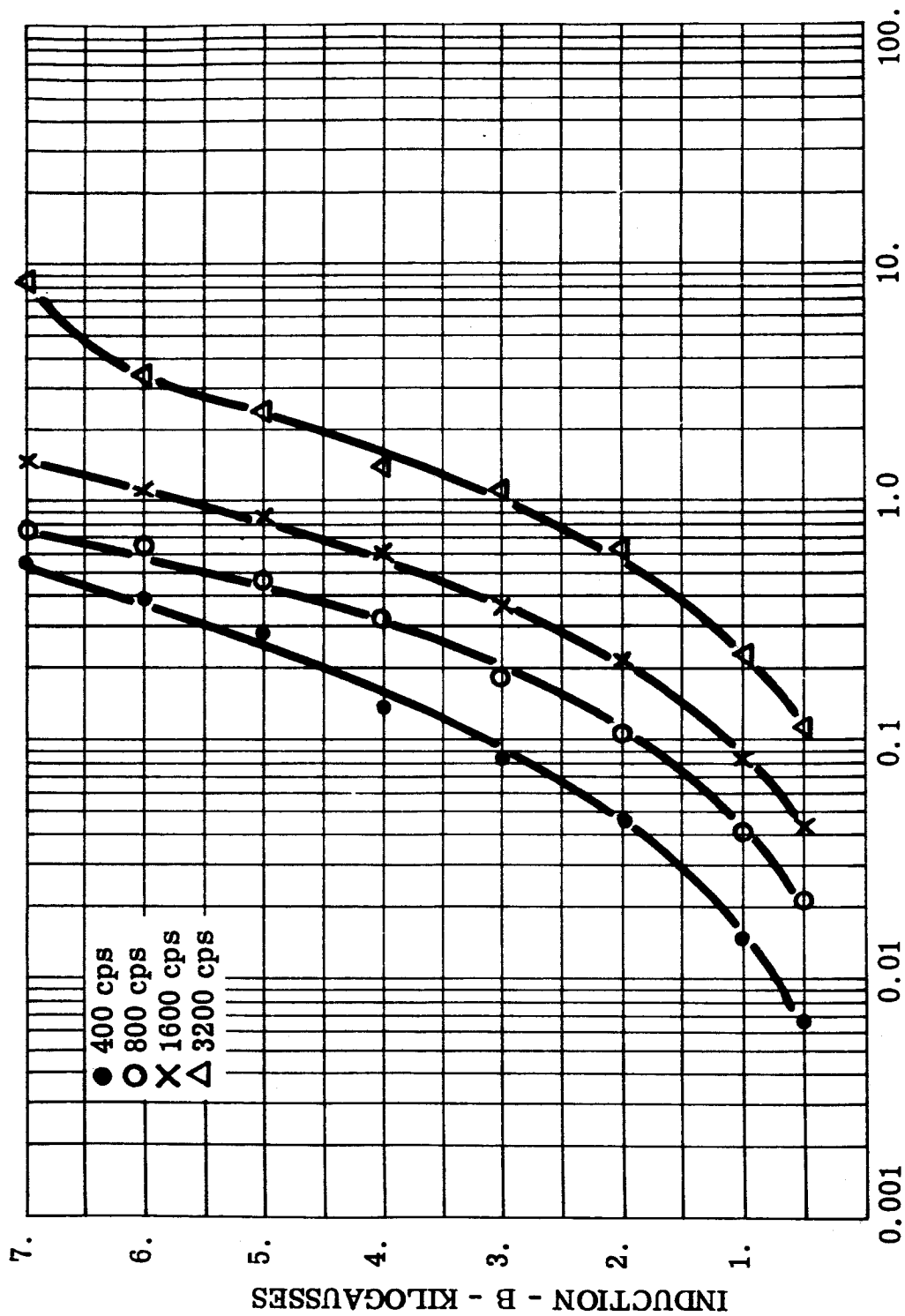


FIGURE 142 P_c , sq - Total Core Loss, 0.002 Inch Permalloy 80 Toroid,
Core 3, Room Ambient



APPARENT POWER - P_a, sq - AVERAGE VOLT-AMPERES PER POUND

FIGURE 143 P_a, sq - Apparent Power, 0.002 Inch Permalloy 80 Toroid,
Core 3, Room Ambient

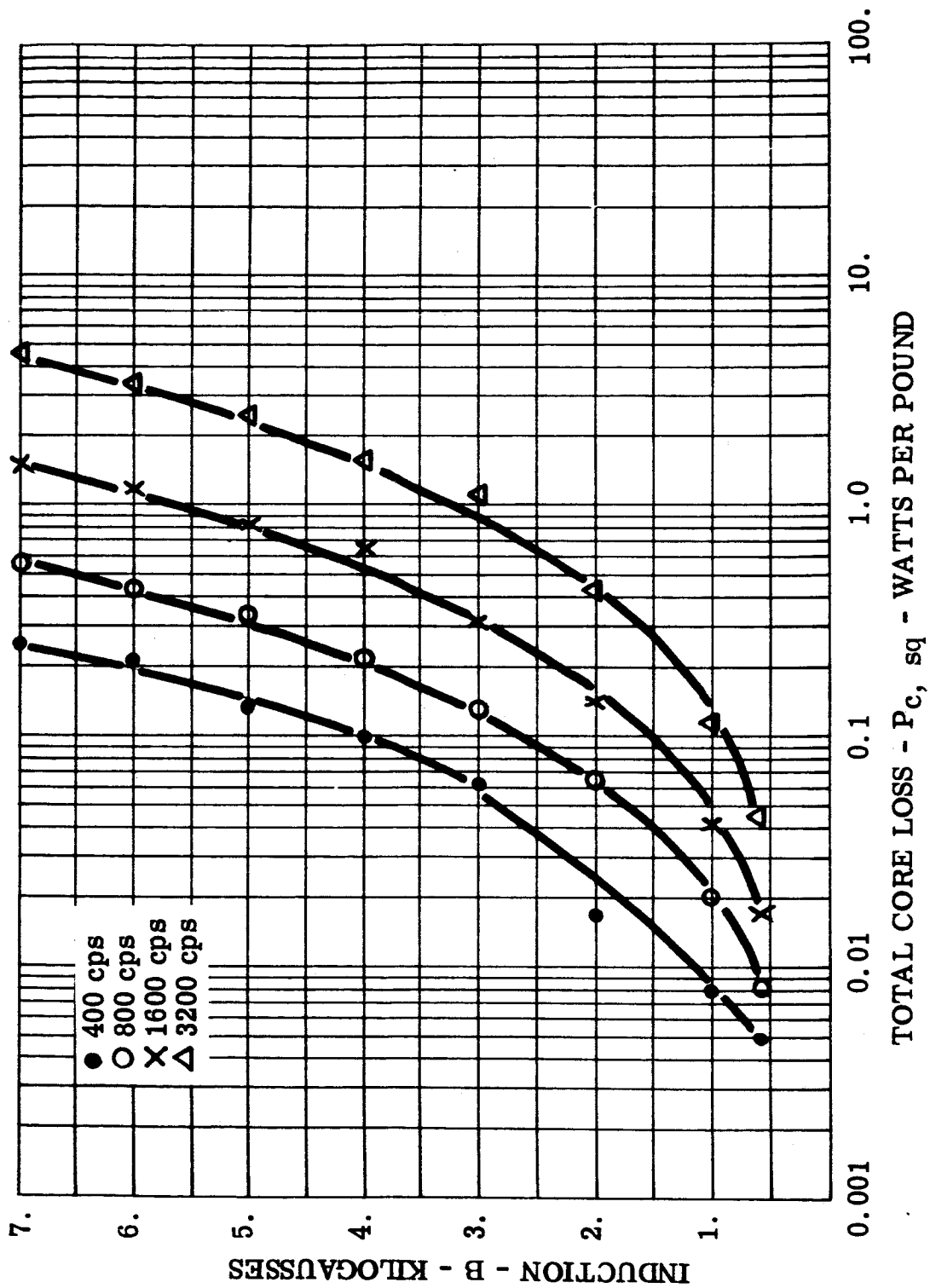
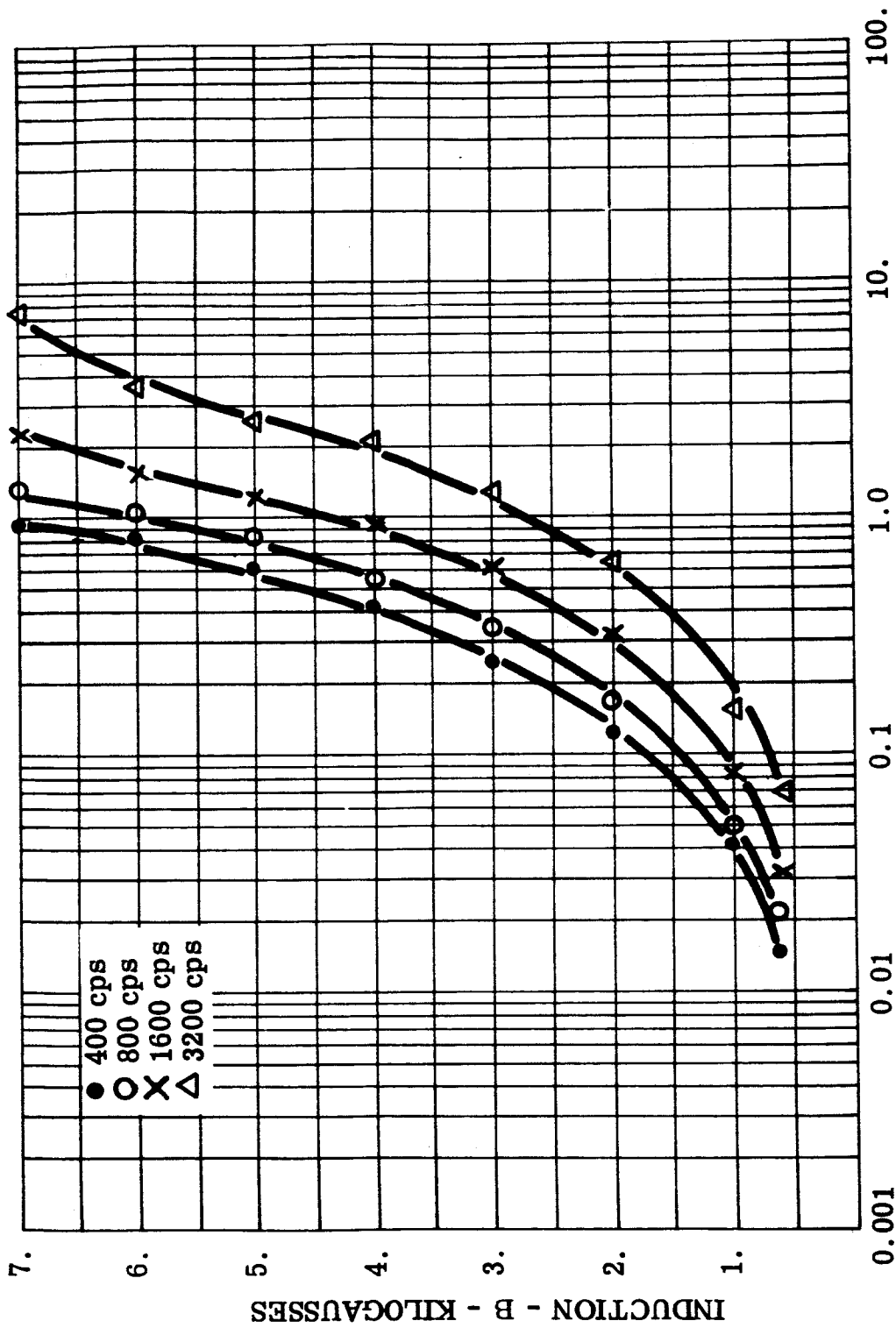


FIGURE 144 $P_{c, sq}$ - Total Core Loss, 0.002 Inch Permalloy 80 Toroid, Core 3, -55°C



APPARENT POWER - $P_{a, sq}$ - AVERAGE VOLT-AMPERES PER POUND

FIGURE 145 $P_{a, sq}$ - Apparent Power, 0.002 Inch Permalloy 80 Toroid, Core 3, -55°C

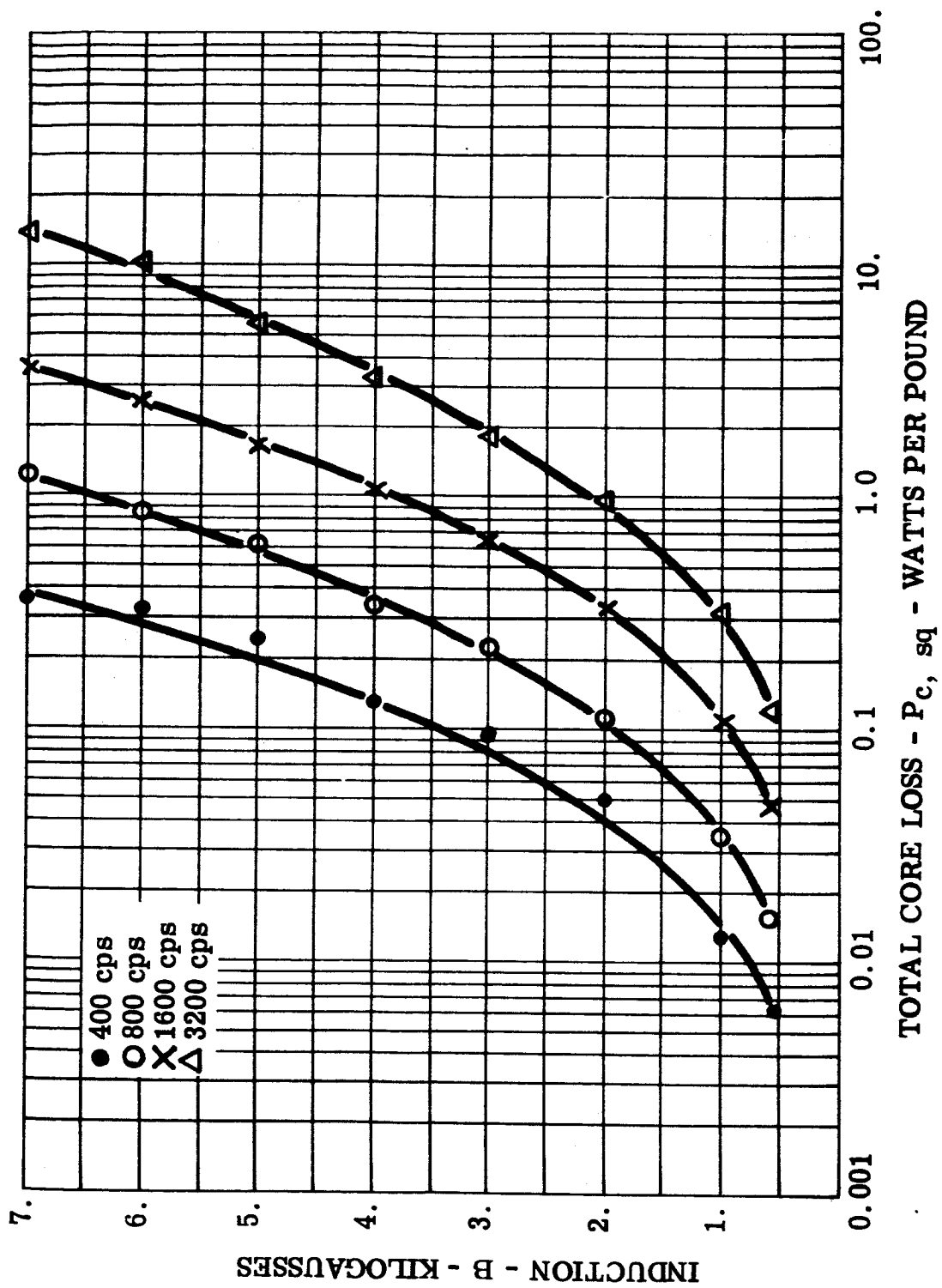


FIGURE 146 $P_{c, sq}$ - Total Core Loss, 0.004 Inch Permalloy 80 Toroid,
Core 5, Room Ambient

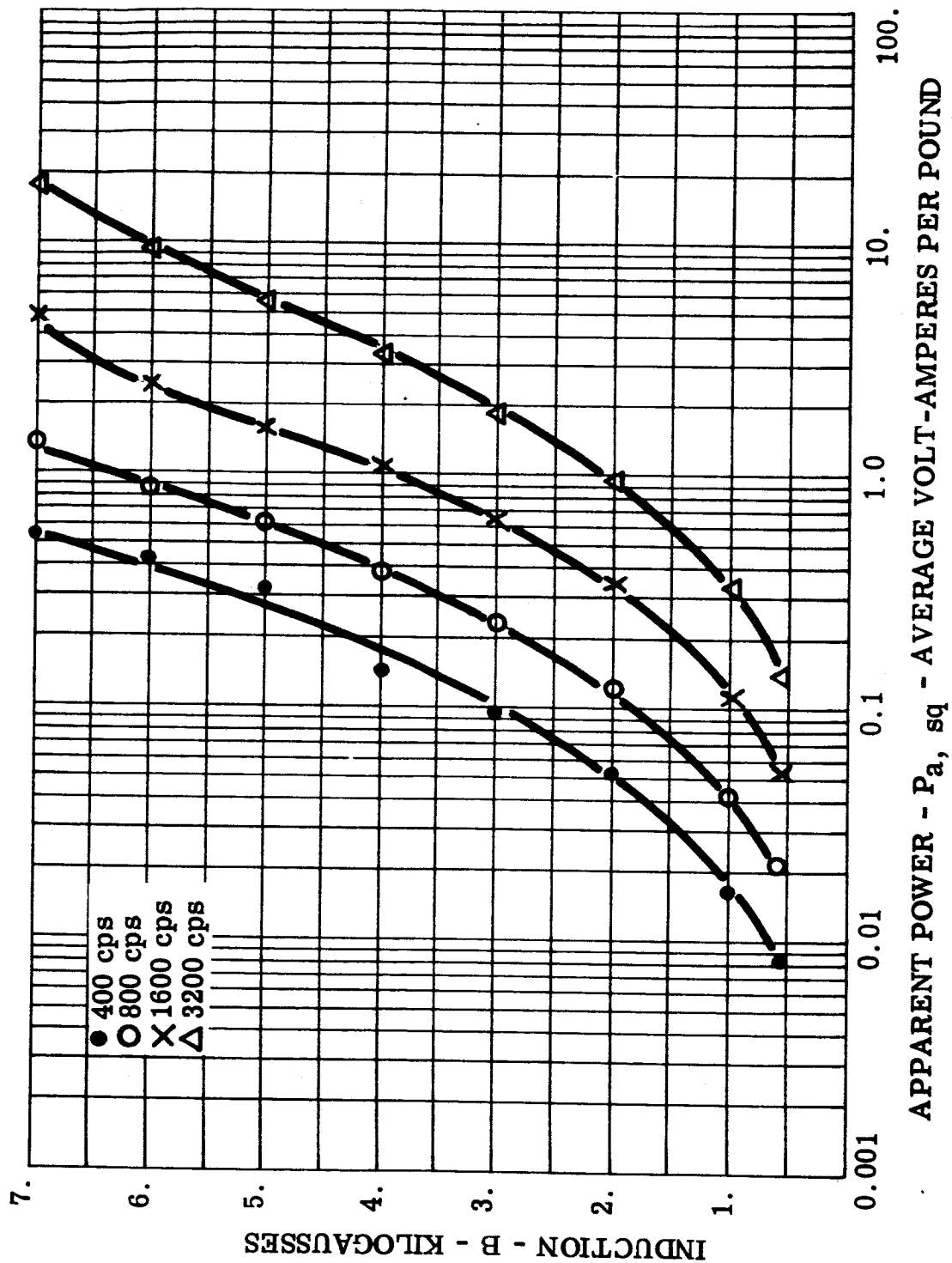


FIGURE 147 P_a, sq - Apparent Power, 0.004 Inch Permalloy 80 Toroid, Core 5, Room Ambient

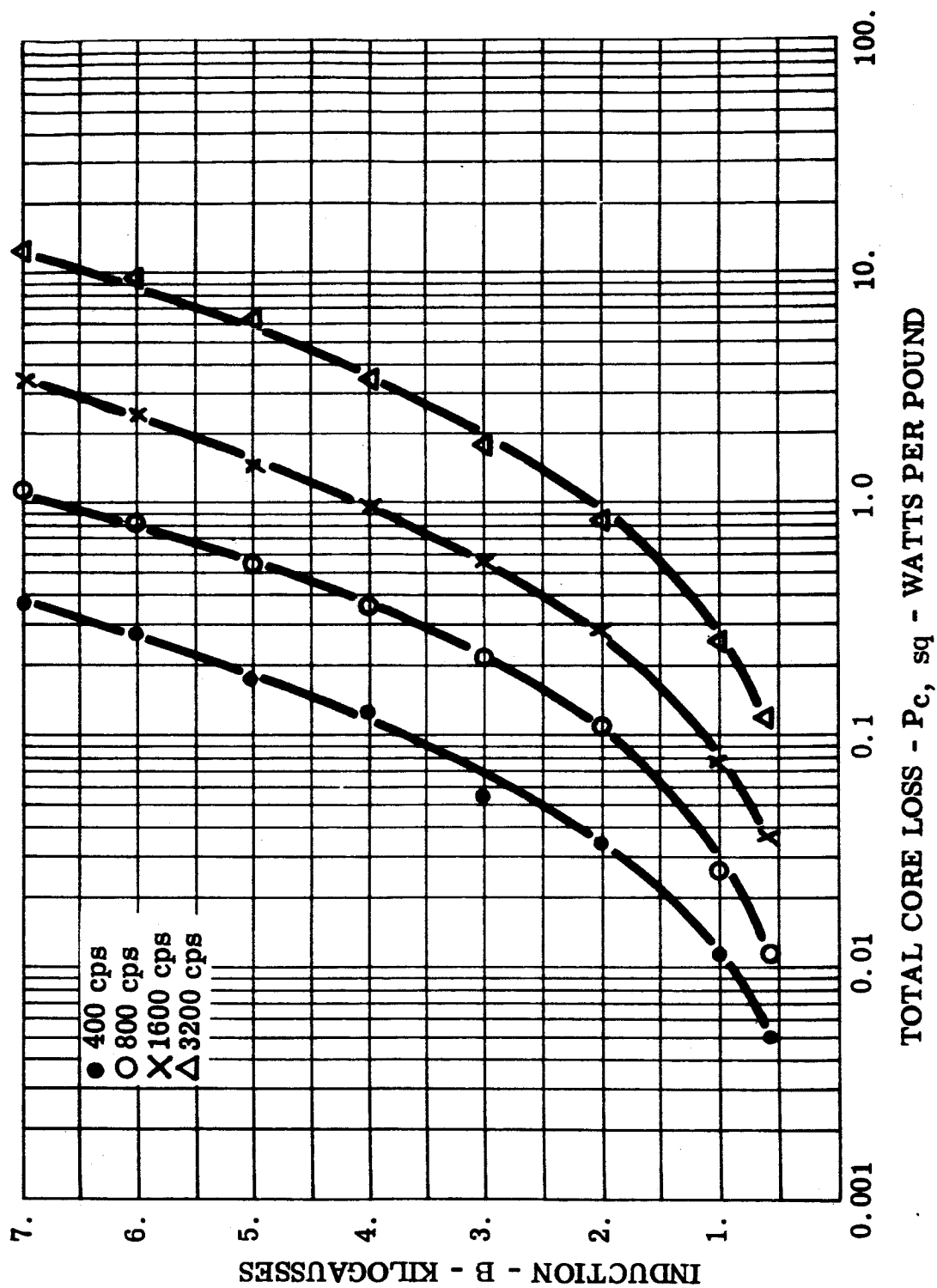
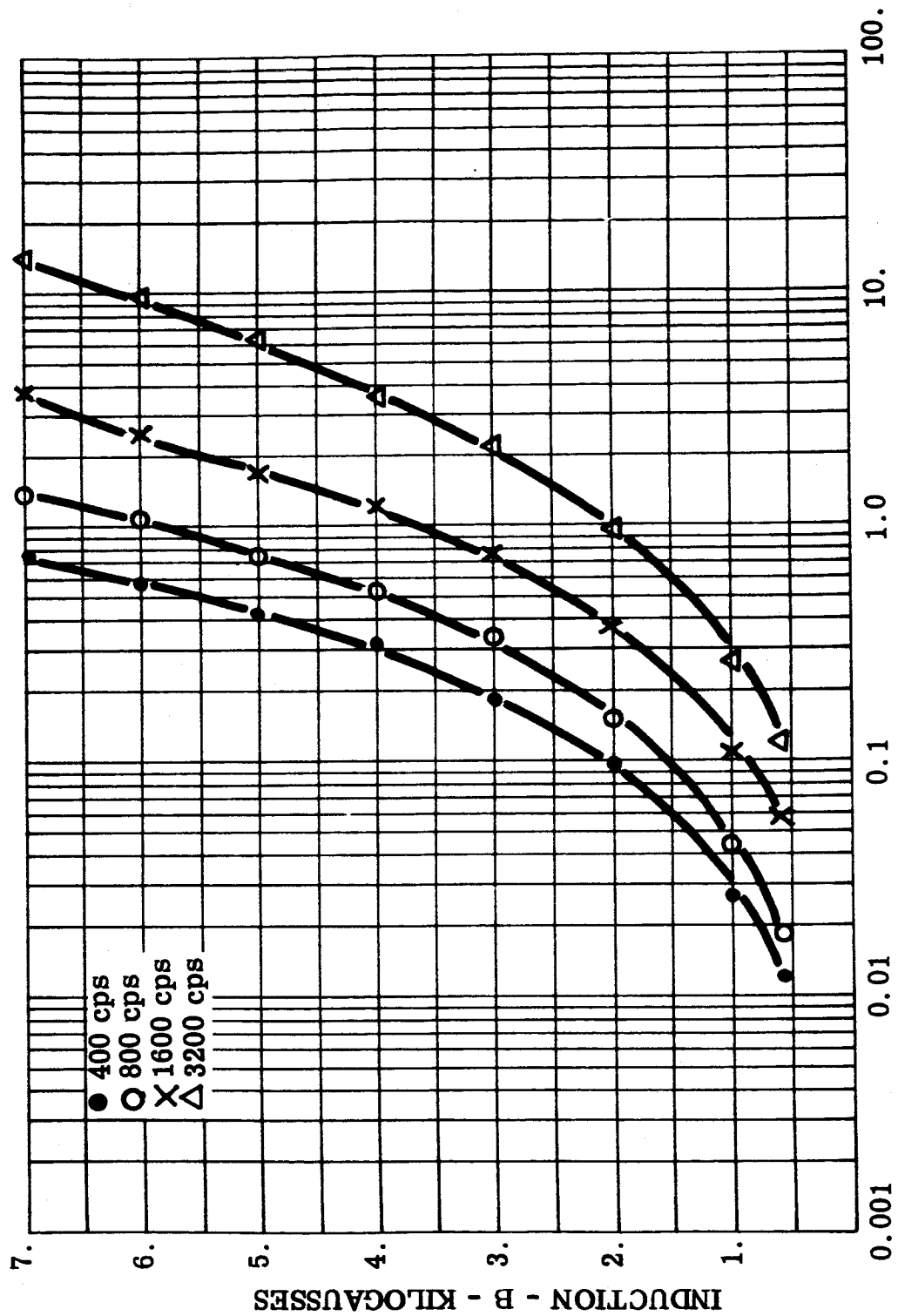


FIGURE 148 $P_{c, sq}$ - Total Core Loss, 0.004 Inch Permalloy 80 Toroid, Core 5, -55°C



APPARENT POWER - P_a , sq - AVERAGE VOLT-AMPERES PER POUND

FIGURE 149 P_a , sq - Apparent Power, 0.004 Inch Permalloy 80 Toroid, Core 5, -55°C

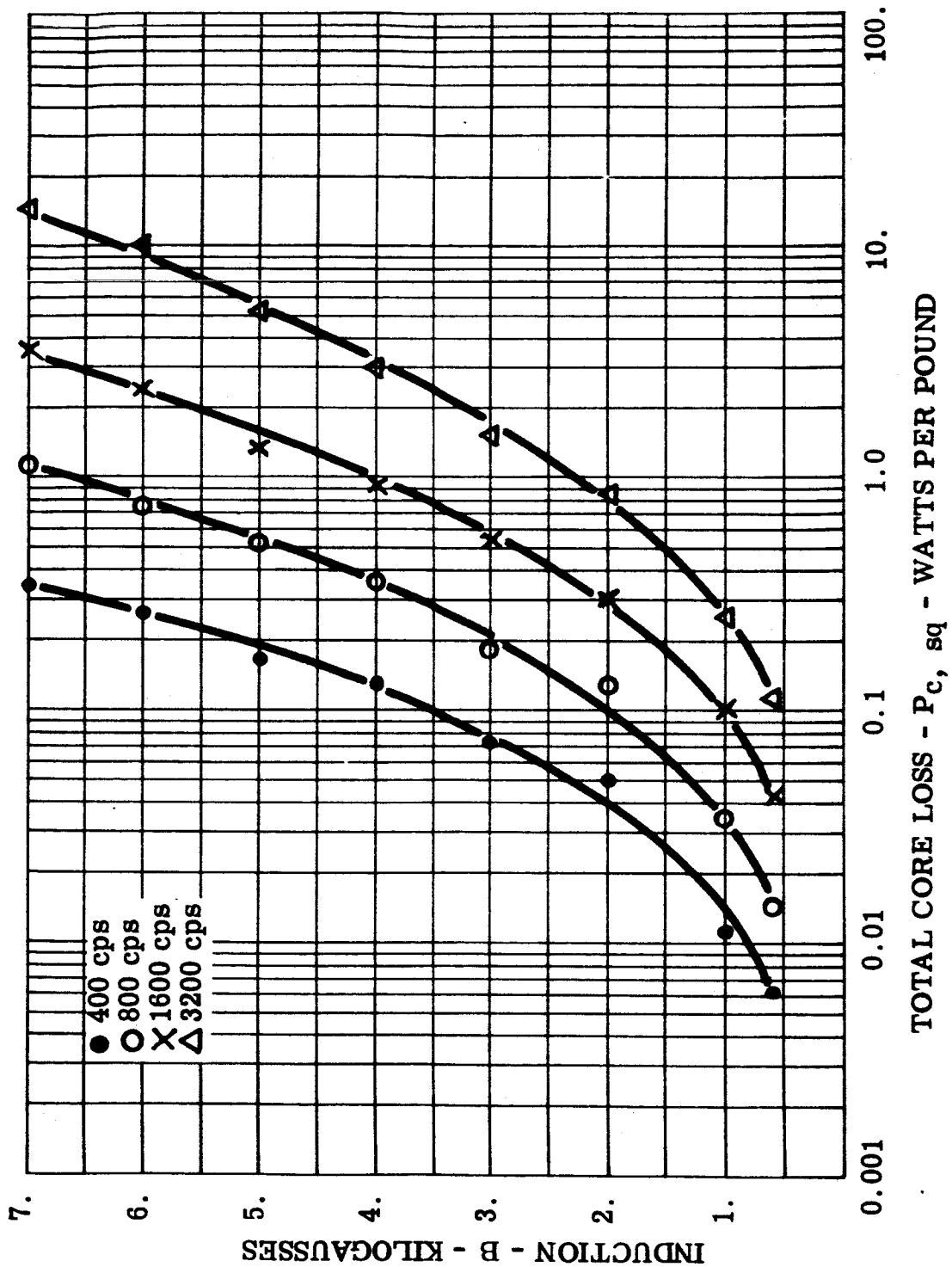
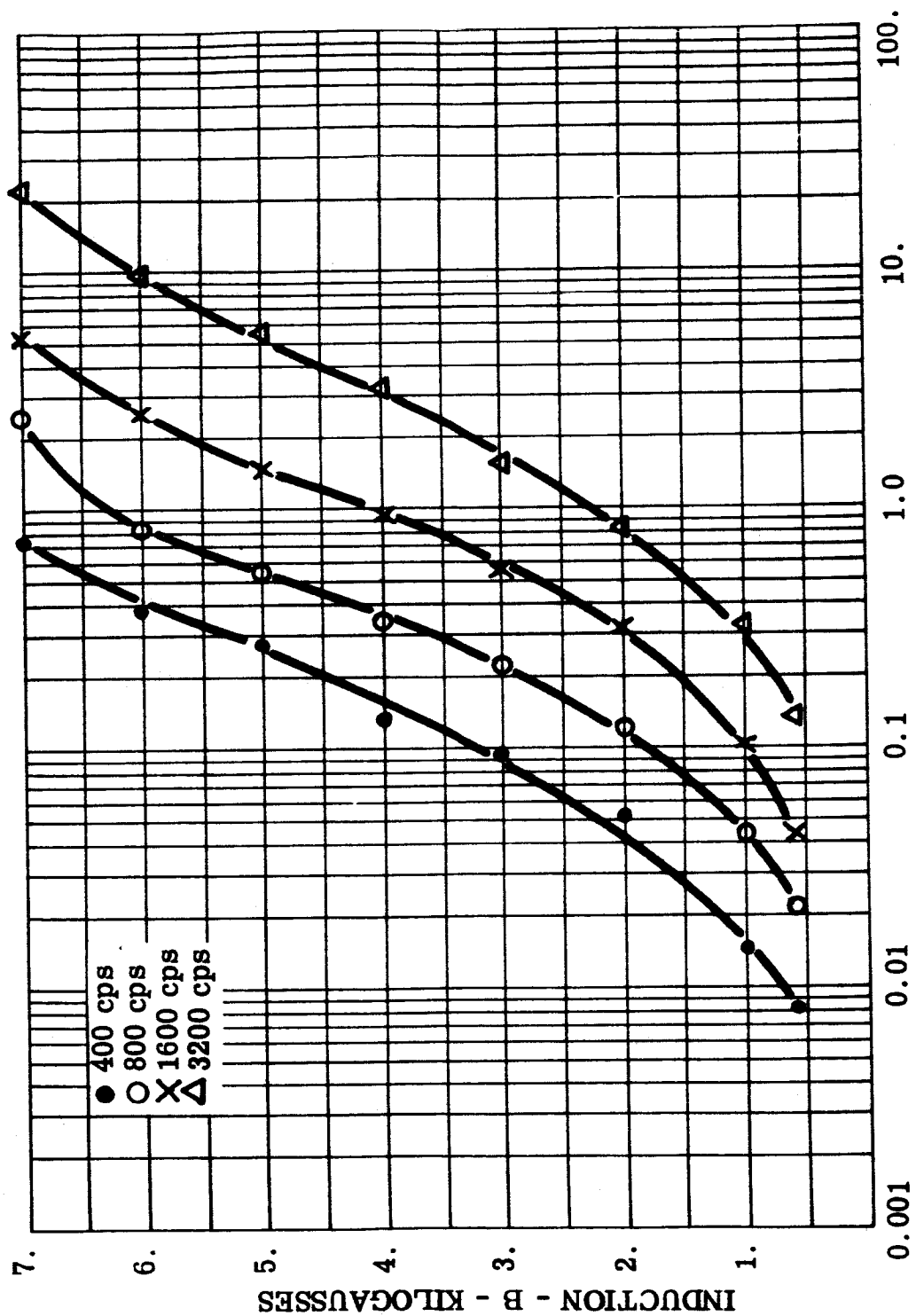


FIGURE 150 P_c , sq - Total Core Loss, 0.004 Inch Permalloy 80 Toroid, Core 6,
Room Ambient



APPARENT POWER - P_a , sq - AVERAGE VOLT-AMPERES PER POUND

FIGURE 151 P_a , sq - Apparent Power, 0.004 Inch Permalloy 80 Toroid, Core 6,
Room Ambient

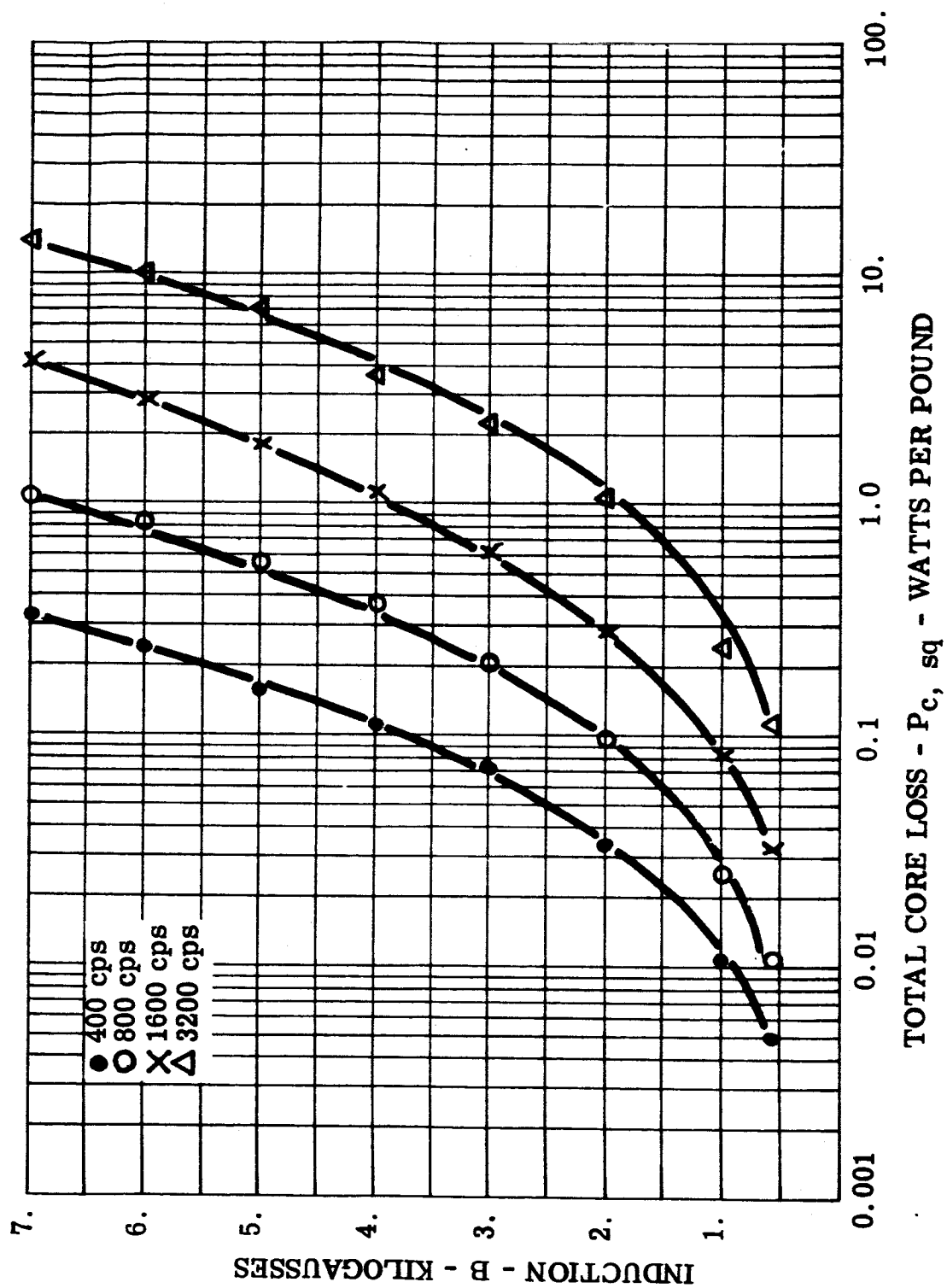
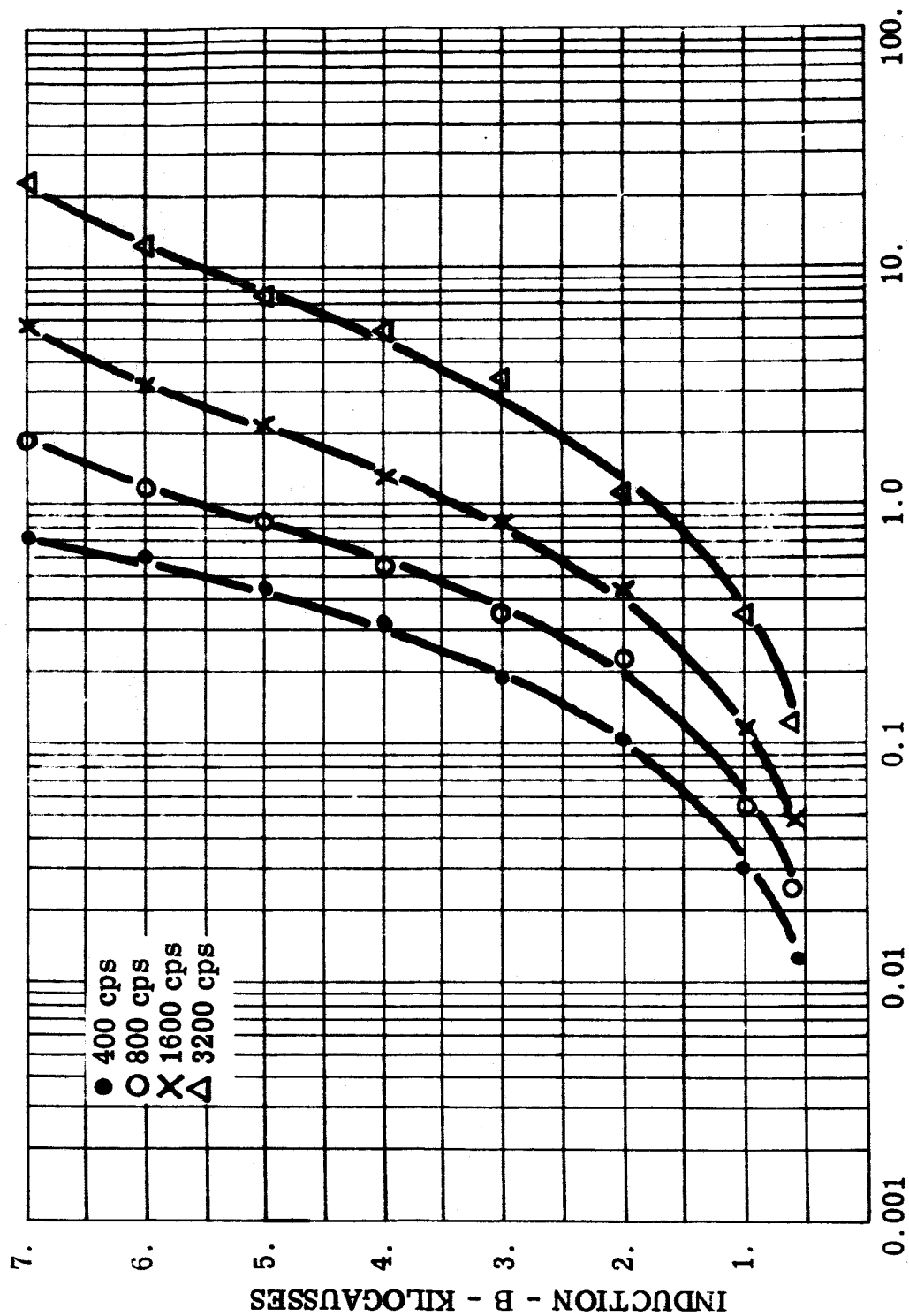


FIGURE 152 $P_{c, sq}$ - Total Core Loss, 0.004 Inch Permalloy 80 Toroid, Core 6, -55°C



APPARENT POWER - $P_{a, sq}$ - AVERAGE VOLT-AMPERES PER POUND

FIGURE 153 $P_{a, sq}$ - Apparent Power, 0.004 Inch Permalloy 80 Toroid, Core 6, -55°C

SECTION VI

APPENDIX A

SYMBOLS AND DEFINITIONS

Symbols and Definitions

PART I

A. Symbols Used in Magnetic Testing

- B - Normal induction, magnetic induction, or magnetic flux density
- B_d - Remanent induction
- B_{dm} - Remanence
- B_m - Maximum induction in a hysteresis loop
- B_r - Residual induction
- B_s - Saturation induction
- H - Magnetizing force, magnetic field strength
- H_c - Coercive force
- H_{cs} - Coercivity
- $P_{a, sq}$ - Apparent power, square wave
- P_c - Total core loss
- $P_{c, sq}$ - Total core loss, square wave
- P_h - Normal hysteresis loss
- P_e - Eddy current loss
- μ - Normal permeability
- μ_{Δ} - Incremental permeability
- μ_m - Maximum permeability
- μ_0 - Initial permeability

B. Definitions of Terms Used in Magnetic Testing

Coercive Force, H_c

The d-c magnetizing force at which the magnetic induction is zero when the material is in a symmetrically cyclically magnetized condition.

Coercivity, H_{cs}

The maximum value of coercive force.

Apparent Power, P_a

The power expended in a magnetic specimen in which there is a cyclically alternation induction, square wave form rather than sinusoidal. (Proposed definition.)

Core Loss (Total), P_c

The power expended in a magnetic specimen in which there is a cyclically alternating induction, normally sinusoidal.

Core Lose (Total), P_c, sq

The product of the average exciting current and the applied average voltage under square wave conditions in an electrical circuit containing reactance. (Proposed definition.)

Eddy Current Loss, Normal, P_e

That portion of the core loss which is due to induced currents circulating in the magnetic material subject to a symmetrically cyclically magnetized excitation.

Hysteresis Loss, Normal, P_h

The power expended in a ferro-magnetic material, as a result of hysteresis when the material is subjected to a symmetrical cyclically magnetized excitation.

Induction, Normal, B

The maximum induction, in a magnetic material that is in a symmetrically magnetized condition.

Induction, Remanent, B_d

The magnetic induction that remains in a magnetic circuit after the removal of an applied magnetomotive force.

Induction, Residual, B_r

The magnetic induction corresponding to zero magnetizing force in a magnetic material that is in a symmetrically cyclically magnetized condition.

Induction, Saturation, B_s

The maximum intrinsic induction possible in a material.

Magnetizing Force (Magnetic Field Strength), H

That magnetic vector quantity at a point in a magnetic field which measures the ability of electric currents or magnetized bodies to produce a magnetic induction at the given point.

Permeability, Incremental, μ_Δ

The ratio of a cyclic change in magnetic induction to the corresponding cyclic change in magnetizing force when the mean induction differs from zero.

Permeability, Initial, μ_0

The limiting value approached by the normal permeability as the applied magnetizing force, H , is reduced to zero.

Permeability, Maximum, μ_m

The maximum value of normal permeability for a given material.

Permeability, Normal, μ

The ratio of the normal induction to the corresponding magnetizing force.

Remanence, B_{dm}

The maximum value of the remanent induction for a given geometry of the magnetic circuit.

PART II

A. Symbols Used in CCFR Testing of Toroidal Magnetic Amplifier Cores.

AT	- Same as H_1
B_m	- Peak induction or peak flux density
$2B_m$	- Maximum flux density swing
B_r	- Residual induction or residual flux density
$B_m - B_r$	- Squareness
$\frac{B_r}{B_m}$	- Squareness ratio
ΔB	- Delta induction or delta flux density
ΔB_0	- Delta induction, fixed
ΔB_1	- Delta induction, fixed
ΔB_2	- Delta induction, fixed
CCFR	- Constant current flux reset
DAT	- Same as ΔH
G	- Gain
H_m	- Peak magnetizing force
H_0	- Magnetizing force, dependent
H_1	- Magnetizing force, dependent
H_2	- Magnetizing force, dependent
ΔH	- Incremental magnetizing force
SAT	- Same as B_m
T	- Same as $\frac{B_r}{B_m}$

B. Definitions Used in CCFR Testing of Toroidal Magnetic Amplifier Cores.

Constant Current Flux Reset, CCFR

This test employs an excitation current consisting of half-wave sine current pulses of sufficient and constant magnitude to drive the core flux into positive saturation. A direct-current magnetizing force of adjustable magnitude is applied to the core so as to reset the magnetic flux away from positive saturation during the intervals between pulses of excitation current. The resultant cyclic flux change is measured by means of a sensitive flux voltmeter connected to a separate pickup winding on the core.

Flux Density Swing, Maximum; $2B_m$

The maximum flux density swing equal to the absolute total value of positive and negative peak induction or $2B_m$. ($2B_m = 2 \text{ SAT}$)

Gain, G

$G = \frac{\Delta B_2 - \Delta B_1}{\Delta H}$, a measure of loop steepness in terms of incremental permeability.

Induction, Delta (Delta Flux Density): ΔB

Delta induction is the change in induction (flux density) when a core is in a cyclically magnetized condition.

Induction, Fixed Delta; ΔB_1 , ΔB_0 , ΔB_2

1. ΔB_1 - delta induction equal to one third of $2B_m$, maximum flux density swing.
2. ΔB_0 - delta induction equal to one half of $2B_m$, maximum flux density swing.
3. ΔB_2 - delta induction equal to two thirds of $2B_m$, maximum flux density swing.

Induction, Residual (Residual Flux Density), B_r

Residual induction is the magnetic induction at which the magnetizing force is zero while the material is cyclically magnetized with a half-wave sinusoidal magnetizing force of a specified peak magnitude (This definition differs from the standard definition which requires symmetrically cyclically magnetized conditions).

Induction, Peak (Peak Flux Density), B_m

Peak induction is the magnetic induction corresponding to the peak applied magnetizing force. The peak induction will usually be slightly less than the saturation. ($B_m = SAT$)

Magnetizing Force, Dependent; H_1 , H_0 , H_2

1. H_1 - The d-c reset magnetizing force required to produce a cyclic change of induction ΔB_1 ($H_1 = AT$)
2. H_0 - The d-c reset magnetizing force required to produce a cyclic change of induction ΔB_0 ($H_0 = AT + 1/2 DAT$)
3. H_2 - The d-c reset magnetizing force required to produce a cyclic change of induction ΔB_2 ($H_2 = AT + DAT$)

Magnetizing Force, Incremental; ΔH

The incremental change in magnetizing force equal to $H_2 - H_1$.
($\Delta H = DAT$)

Magnetizing Force, Peak; H_m

Peak magnetizing force is the maximum value of applied magnetomotive force per mean length of path of the core.

Squareness; $B_m - B_r$

The delta B induction change between the peak induction, B_m , and the residual induction, B_r .

Squareness Ratio; $\frac{B_r}{B_m}$

$$\left[\frac{B_r}{B_m} = 1 - \left(\frac{B_m - B_r}{B_m} \right) = T \right]$$

PART III

General Definitions of Terms

Acoustic

Pertaining to the science of sound.

Aluminum Foil

Thin aluminum material less than 0.006 inch thick.

Aluminum Strip

Aluminum strip is greater than 0.006 inch thick.

Atomic Ordering

Forming a superlattice which is an ordered arrangement of atoms in a solid solution superimposed on the normal solid solution lattice.

Base Line Property

Those initial magnetic, physical or mechanical properties that are normally present at room temperature, i.e. - saturation induction, thermal expansion, tensile strength.

B. C. C.

Body centered cubic structure.

Bloch Wall

The boundary between adjacent domains of different magnetization vectors or anti-parallel electron spins in which the electron spins of each atom in the wall are slowly changed so as to affect the complete change in magnetization vectors between adjacent domains. The Bloch wall width is determined by the individual ferromagnetic material and is a discrete width. The energy of the wall is variable depending upon the angle between adjacent domains and the crystallographic plane of the wall.

Centistoke

A unit of kinematic viscosity.

Critical Temperature

The temperature at which a change in crystal structure, phase or physical properties occurs under constant pressure conditions.

Converter

A device which changes or converts a-c current to d-c current.

Disordered Structure

The crystal structure of a solid solution in which the atoms of different elements are randomly distributed with respect to the available lattice sites.

Domain

A small region, in ferromagnetic materials, where the atomic magnetic moments are all aligned parallel to one another.

Dose (Integrated Flux)

The total radiation exposure to which the specimen has been subjected (expressed as the number of particles per square centimeter).

Double Window Transformer

A transformer built from laminations from which two square openings have been punched.

Doubly Grain-Oriented Silicon Steel

An iron base alloy containing about 3 percent silicon where the phase that is present (α iron) is body centered cubic. The individual re-crystallized grains of this alloy are oriented such that the cube face plane is in the plane of the material and a cube edge direction is parallel to the rolling direction.

F.C.C.

Face centered cubic structure.

Field

The space where an electric or magnetic force is being exerted.

High Vacuum (Space Vacuum)

This term, as used in this report, refers to a vacuum equal to or higher than 10^{-6} torr (mm Hg).

Inverter

A device which changes d-c current to a-c current.

Isotropic

Having the same properties in all directions.

Magnetic Field Annealing (MFA)

Annealing a magnetic material in the presence of a magnetic field so as to align the magnetic domains in a direction parallel to the field.

Magnetostriction

A change in the dimensions of a body when magnetized.

Neutron

One of the elementary particles which, together with the proton, comprises the nucleus of all elements. It has no charge.

Ordering Temperature

The temperature at which atomic ordering of different elements occurs.

Proton

One of the elementary particles which, together with the neutron, comprises the nucleus of all elements. It has a positive charge.

Resistivity, Electrical, P

Electrical resistivity of a material.

Rowland Ring

A continuous ring of magnetic material of uniform radial width and cross-sectional area with no joints or welds. The ratio of its mean diameter to its radial width is ten to one or greater.

Singly Grain-Oriented Silicon Steel

An iron base alloy containing approximately 3-1/4 percent silicon where the phase that is present is body centered cubic α iron.

The individual recrystallized grains of this alloy are oriented in the rolling direction such that the cube edge direction and the rolling direction are parallel. The face diagonal plane is in the plane of the material.

Stress Relief Annealing (SRA)

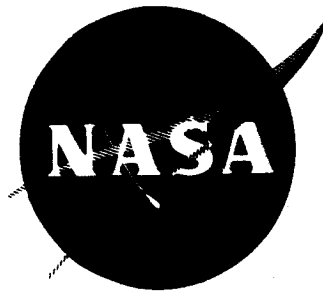
Heating to a suitable temperature, holding long enough to reduce residual stresses and then cooling slowly enough to minimize the development of new residual stresses.

Structure Sensitive Properties

The properties that are structure sensitive in magnetic materials are permeability (μ), coercive force (H_c), and hysteresis loss (P_h). The factors that affect these properties are composition, impurities, strain, temperature, crystal structure and crystal orientation.

Tape

A thin strip of magnetic material a few mils thick which is normally wound into the shape of a round core.



Report No.

NASA-CA-54963

Westinghouse

WAED65.50E

PART. 2
CONTROL AND SYSTEM PROTECTION FOR
PARALLELED STATIC INVERTERS AND CONVERTERS

CONTRACT NO. NAS 3-2792
AMENDMENT NO. 5

EIGHTH QUARTERLY REPORT FOR THE PERIOD
JUNE 1, 1965 TO AUGUST 31, 1965

by

H. B. James
E. F. Swiderski

PREPARED FOR THE NATIONAL AERONAUTICS AND SPACE ADMINISTRATION

Technical Management, NASA-Lewis Research Center
Space Power Systems Division, Francis Gourash



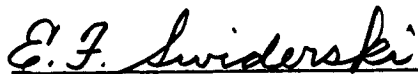
Westinghouse Electric Corporation
AEROSPACE ELECTRICAL DIVISION
LIMA, OHIO

PART 2


CONTROL AND SYSTEM PROTECTION FOR
PARALLELED STATIC INVERTERS AND CONVERTERS


NAS 3-2792, Amendment 5


Prepared by:


E. F. Swiderski
Advanced Program Engineering

Approved by:


R. W. Briggs
Project Manager


H. B. James
Manager, Advanced Programs


N. W. Bucci, Jr.
Engineering Manager
Systems Research & Development

WESTINGHOUSE ELECTRIC CORPORATION
AEROSPACE ELECTRICAL DIVISION
LIMA, OHIO

ABSTRACT

This report describes the static switch work completed during the first quarter of NASA Contract NAS 3-2792, Amendment No. 5.

The initial work on static switching consisted of preparing specifications which were used as guidelines and objectives in the design of direct current and alternating current contactors which are to be integrated into the existing inverter/converter breadboard system.

The investigation and study of power and control circuits, capable of performing the outlined requirements, resulted in the preliminary design of the direct current Inverter Control Contactor/Converter Control Contactor and of the alternating current Load Bus, Load Control and Tie Bus Contactors. Circuit schematics and electrical part lists are provided for these designs.

The selected direct and alternating current contactor power circuit designs resulted after consideration of several different configurations. A discussion on these configurations is presented.

TABLE OF CONTENTS

<u>Section</u>	<u>Page</u>
Abstract	ii
I INTRODUCTION	1
Task V - Modification of Inverter and Converter Systems .	1
A. Paralleled Converter System	1
B. Paralleled Inverter System	2
C. Verification and Demonstration Tests	3
Task VI - Additional Control Protective Concepts	3
A. Static Power Switches	3
B. Annunciator	4
C. Load Programmer	5
D. Tests	5
E. Reliability	5
II GENERAL INFORMATION ON STATIC SWITCHES	6
III STATIC CONTACTOR SPECIFICATIONS	7
A. General Requirements	7
B. Voltage and Current Specifications	10
IV STATIC CONTACTOR DESIGN	13
A. Characteristics of Power Switching Device	13
B. Converter System Contactor Circuit Considerations ..	14
1. D-C Static Contactor with Capacitor Turn-Off ...	14
2. D-C Static Contactor with Capacitor Resonant Circuit Turn-Off	16
3. D-C Static Contactor with Resonant Circuit Turn-Off Capacitor Initially Charged	16
C. Converter System Contactor Description	18
D. Inverter System Contactor Circuit Considerations ...	20
E. Inverter System Contactor Description	24

LIST OF ILLUSTRATIONS

<u>Figure</u>	<u>Title</u>	<u>Page</u>
III-1	Paralleled Inverter/Converter System Block Diagram ..	9
IV-1	D-C Static Contactor With Capacitor Turn-Off	15
IV-2	D-C Static Contactor With Resonant Circuit Turn-Off ...	15
IV-3	D-C Static Contactor With Resonant Circuit Turn-Off Capacitor Initially Charged	17
IV-4	D-C Static Contactor With Resonant Circuit Turn-Off Capacitor Initially Charged	17
IV-5	Converter System Static Contactor Circuit	19
IV-6	Controlled Rectifier A-C Switching Circuits	23
IV-7	Alternating Current Inverter System Static Contactor Circuit	25

LIST OF TABLES

<u>Number</u>	<u>Title</u>	<u>Page</u>
III-1	Converter System Static Contactor Current and Voltage Specification	11
III-2	Inverter System Static Contactor Current and Voltage Specification	12
IV-1	Parts List for Static ICC/CCC	21
IV-1	Parts List for Static ICC/CCC (Cont.)	22
IV-2	Parts List for Inverter System Static LBC, LCC, and TBC	27
IV-2	Parts List for Inverter System Static LBC, LCC, and TBC (Cont.)	28

SECTION I

INTRODUCTION

The major task of the work statement of this contract amendment is the development of controls and system protection for paralleled static inverters and converters for aerospace application. This effort is a continuation of the development carried on under NASA Contract NAS 3-2792 Amendment No. 1. Report No. NASA-CR-54242 covers the major portion of this effort. The first portion of Amendment No. 5 covers modifications and improvements to circuit development which evolved from the earlier work. The specific tasks of Amendment No. 5 are:

Task V - Modification of Inverter and Converter Systems

A. PARALLELED CONVERTER SYSTEMS

1. Redesign the output windings of the Master Royer Oscillator and/or the windings of the converter output load current sensing transducer to limit the unbalance current in the load division protection circuit to within 10-20% (design goal 15%) of the static converter rated current. Adjust the load division protection loop circuit to obtain the gain requirements necessary to limit the load division to the above differential current requirement. In making these modifications, the operating frequency of the Master Royer Oscillator that supplies voltage to the transducer circuits may be increased if necessary to obtain additional sensitivity and gain.
2. Isolate the load division protection circuitry so that when a paralleled operating system is de-energized or changed to isolated system operation, the transition is accomplished without shutting down any of the converters of the system. The circuit modifications to provide this capability are to include but are not to be limited to increasing the signal level and the addition of resistors and semiconductor diodes to each converter.
3. The overcurrent protection circuits are to be modified to eliminate nuisance trips and to provide selective tripping for tie-bus faults and feeder or load bus faults. The circuit modifications are to include but are not to be limited to two overcurrent sensing levels with two corresponding time constants which are to be coordinated with the overvoltage and undervoltage circuits.

Redesign the sensing portion of differential current protection circuit to provide selective isolation of feeder faults within zone one for paralleled system operation. The differential current protection must coordinate with the overcurrent protection circuits to prevent nuisance operations that will reduce the system's capability to supply maximum load.

4. Add mechanical switches to each of the existing converter automatic protection and paralleling breadboards to facilitate manual control of the load division circuits for emergency manual operation of the paralleled converter system.

B. PARALLELED INVERTER SYSTEMS

1. Determine the causes of the frequency instability that occurs when the frequency reference of one inverter fails and/or any inverter is deenergized thereby resulting the shutting down of the other inverters in the paralleled system. The circuits are to be modified to eliminate frequency instability problems in accordance with recommendations based on test results.

2. Provide selective tripping for overcurrents due to load-bus faults. This work shall include performing tests to establish response characteristics and modifying time delay circuits to obtain proper coordination with the established response characteristic.

3. Eliminate nuisance and false tripping caused by noise and other disturbances on the d-c paralleling bus. This work will include but is not to be limited to the following circuit modifications; re-routing critical lead wires, the use of shielded cables, and the use of Zener diodes and negative d-c bias voltages.

4. The differential current protection circuit is to be modified to provide protection against line to line faults. The circuit modification is to include but is not to be limited to the addition of two additional current transformers to permit sensing and controlling the currents in each phase of the three phase inverters.

5. Modify the current transformers in the load division current loop circuits for both the load division control and load division protection circuits to eliminate the necessity of short circuiting the load division transformer terminals by means of auxiliary contacts on the main contactor. This modification is to include but is not to be limited to the addition of transistor controlled d-c bias currents and bias windings, which saturate the transformer cores, thereby effectively disconnecting the transformers from the loop circuits.

C. VERIFICATION AND DEMONSTRATION TESTS

1. Existing breadboarded units, i.e., inverter/converter breadboards and inverter/converter automatic paralleling and protective circuit breadboards developed are to be tested in paralleled inverter/converter systems. The purpose of these tests is to verify and demonstrate that the above modifications have conclusively corrected the described deficiencies and have not degraded the performance characteristics of the paralleled inverter/converter systems. Tests are to be performed and data obtained for operating conditions, loading conditions, and only the necessary fault conditions to verify and demonstrate satisfactory operation.

A complete topical report is in preparation at this time and will be issued upon conclusion of systems testing. It will not be covered separately in this quarterly report.

The remainder of this contract (Task VI) covers development of static switches and an annunciator circuit, along with a load programmer study.

The specific tasks of the second half of Amendment No. 5 are:

Task VI - Additional Control and Protection Concepts

A. STATIC POWER SWITCHES

1. Replace all contactors and manual load switches used in the automatic paralleled inverter/converter breadboard systems with static solid state semiconductor switching devices.

The static switches will use silicon controlled-rectifiers which will be capable of interrupting 200 percent load and 250 percent short circuit current after a time period which is identical to the "fault times" used in the present inverter/converter system. The static switches shall not degrade present capabilities and operating characteristics with regard to the reliability and response of the existing paralleled inverter/converter systems. As a design objective the static switches will approach the efficiency and weight of comparable conventional contactors.

2. Scaling techniques are to be applied to the static switches and associated circuitry designs to determine and recommend the types and ratings of static switches and associated circuitry for operation in inverters and converters rated at 1.0, 5.0, 10.0 kilowatts. Power frequency is 400 cycles. Output voltages are to be the same as for the present inverters and converters.

There will be a discussion in the topical report covering inverter/converter input static switch component weight, efficiency, complexity, and reliability versus input voltage.

B. ANNUNCIATOR

1. Design a visual annunciator system to indicate operating mode, static switch position, and the nature of faults for a two channel converter/inverter power system. The following information will be displayed for each channel.

a. Operating Mode

- (1) Paralleled
- (2) Isolated
- (3) Manual

A lamp will be lighted when either condition exists.

b. Static Switches - A lamp will be lighted when each associated static switch is energized. There shall be a separate lamp for each static switch.

c. Fault Indication - Each fault sensed by the control and protection circuits for the inverter/converter power supplier will be used to light a lamp. There shall be a separate lamp for each sensing function.

2. Extension of the annunciator to an n-channel (greater than two) system will be discussed as part of the topical report.

3. Fault indications shall be operational during the paralleled and isolated modes but not during manual operation.

4. The circuit components shall be all static devices where applicable but relays may be used if necessary in specific applications and with the prior approval of the NASA Project Manager.

5. It shall be a design objective that the annunciator design be the same for the inverter and converter power system.

6. A breadboard unit will be constructed to demonstrate performance of the inverter/converter annunciator in a two-channel paralleled inverter/converter system. Simulated signals may be used to operate the annunciator during preliminary phases.

C. LOAD PROGRAMMER

Perform an analysis to determine the requirements for a general type load programmer that can be adapted to load profiles with four load priorities for paralleled inverter and converter systems of power ratings from 1 to 10 kw including the power rating of the present breadboarded systems. The following programmer functions are recommended for inclusion in the analysis, but the analysis is not to be limited to, or by, these functions:

1. Monitor total system load and load sharing to determine and accomplish the best load distribution among the paralleled units.
2. Establish an adjustable load priority system to be applicable to various load profiles and for those fault conditions, so that under fault conditions the programmer will tend to maintain a continuous flow of power in accordance with the load priority selected.
3. The programmer is to be capable of anticipating overload and possible faults or failures of critical components in the system and to provide remedial corrective action, i.e., power cut-back, power redistribution, or the shutdown and scram of either loading or power inverter/converter units to alleviate the anticipated fault condition. The anticipatory circuits may operate on the basis of thermal, power, voltage, and current measurements.

D. TESTS

1. The breadboarded inverter/converter paralleled systems are to be tested and demonstrated in conjunction with the static power switches and the annunciator systems. Sufficient data is to be obtained and recorded to verify satisfactory operation under various loading, abnormal operation, and fault conditions.

E. RELIABILITY

1. Prepare reliability estimates for automatic paralleled and protected inverter and converter systems operating in conjunction with static power switches and the annunciator system.

In accordance with established work schedules, the major portion of this part of the contract, performed through the first quarter, has been devoted to the study and design of static switches. The remaining report will be devoted to this area only.

SECTION II

GENERAL INFORMATION ON STATIC SWITCHES

Mechanical contactors have been used in aircraft and missile electrical system applications and the electrical industry in general for many years. These electromagnetic contactors with their moving mechanical contacts possess certain inherent limitations as circuit interrupters. These limitations, generally speaking, include susceptibility to contact contamination and pitting resulting from use in hostile environments associated with inductive system parameters. In severe environments of mechanical shock and vibration and low pressures of a vacuum the design of the electromechanical contactor becomes demanding. When requirements of fast response, repeated cycling, minimum contact bounce, long life, and high reliability are included these specifications become difficult to attain with mechanical contactors.

The semiconductor controllable switching devices, with associated circuitry, have made it possible to duplicate the electromagnetic contactor action without the use of moving parts. The application of these switching devices into a static contactor can provide the features which make the mechanical contactor design difficult or altogether impossible. Therefore, use of static contactors can eliminate some of the principal disadvantages of electric power control accomplished with mechanical switchgear.

Although the potential features of the static contactor are impressive it also has some shortcomings. The primary disadvantages of the static contactor, compared to its electromagnetic counterpart, are the higher contact voltage drops, the need for special attention to semiconductor device cooling and the lack of comparable fault capacity for a comparable size and weight. Generally speaking, the static contactors can be expected to be less efficient, weigh more, and occupy a greater volume than the mechanical contactors. Also, in its open condition, the static contactor does not provide complete electrical isolation between the line and load as obtained by an electromagnetic contactor where the circuit is mechanically interrupted. A leakage current will flow which may be from a few microamperes to several milliamperes depending on the characteristics and rating of the selected switching device.

SECTION III

STATIC CONTACTOR SPECIFICATIONS

A. GENERAL REQUIREMENTS

It is the primary purpose of this program to demonstrate the feasibility of using static contactors to replace the mechanical contactors used in the static inverter/converter electric power system developed on NASA Contract NAS3-2792. Solid-state devices such as transistors, controlled rectifiers, and gate-controlled switches can be used as the electric power conducting contact in the design of static contactors. The semiconductor power device selected for the contactors in this program is the silicon controlled rectifier because it is available with the highest voltage and current ratings of the usable devices and because it will permit implementation at the least cost.

To provide the initial basis for the design of the static contactors some fundamental requirements and specifications will be considered. These are presented below and shall be used as design objectives and guidelines.

1. The static contactors will provide maximum impedance in the open condition and minimum impedance when closed.
2. The contactors will provide a snap on and off action similar to mechanical switchgear.
3. Electric isolation will be provided between the actuating signal and the load.
4. Contactor operation will provide the ability to re-cycle on a fault and be opened after receiving the appropriate signal.
5. After the contactor has been opened because of a system fault, reclosure will not result automatically.
6. The introduction of static contactors in the system will not degrade system performance or produce effects which result in new problems or incompatibilities.
7. The contactors will be required to function and meet the fault test conditions considered in the inverter/converter electric power system developed on NASA Contract NAS3-2792.

8. The contactors will be designed for operation at atmospheric pressure and room ambient temperature. No other environmental factors will be considered and only electrical tests will be performed. Electrical components shall remain within their temperature capabilities by free convection and radiation cooling.

To identify the mechanical contactors and switches to be replaced with static contactors, a simplified block diagram of the existing inverter/converter electric power system is shown in Figure III-1. In the existing system, the Inverter Control Contactor (ICC)/Converter Control Contactor (CCC), the Load Bus Contactor (LBC), and the Tie Bus Contactor (TBC) are electromagnetic devices which are opened or closed by electric signals. The block in Figure III-1 shown as the LCC is presently a knife switch which is operated manually. A manually operated switch was used in this system location because in the earlier NAS3-2792 contract, secondary load protection and its immediate associated considerations were deferred.

The design philosophy of control and protection for the present electrical power system applies to a number of N paralleled inverter/converter subsystems but for demonstration purposes has been limited to the two subsystems. The application of static contactors to this system will use these same considerations.

Generally, faults can appear in any location of an electrical power system from the energy source to the end point of load utilization. Consequently, the contactors must be rated accordingly. In single or isolated subsystem operation, the ICC/CCC, LBC, and LCC are rated for a one per unit steady state load capacity, plus normal overloads, with a fault capability as determined by the inverter/converter current limiting characteristic. In the general case of the paralleled inverter/converter system, the LBC, LCC, and TBC must be rated to permit the conduction of current from the overall paralleled system for faults which occur within the subsystem. The fault power ratings of these contactors, therefore, are a function of the number of paralleled subsystems, with the LBC and TBC rated identically to account for a fault which may result such as at point A in Figure III-1.

The fault power rating of the LCC, in paralleled system operation, is greater than the LBC and TBC because of faults which could occur at point B in Figure III-1, resulting in current from its associated power source and the overall system through the TBC. The rating of the ICC/CCC is the same for parallel operation as it is for single subsystem operation.

Faults and fault protection in the existing system were restricted, during earlier contract work, to the inverter/converter output side. In addition, with the use of a knife switch in the LCC location, faults essentially were not considered between the switch and the load and protection was not provided to

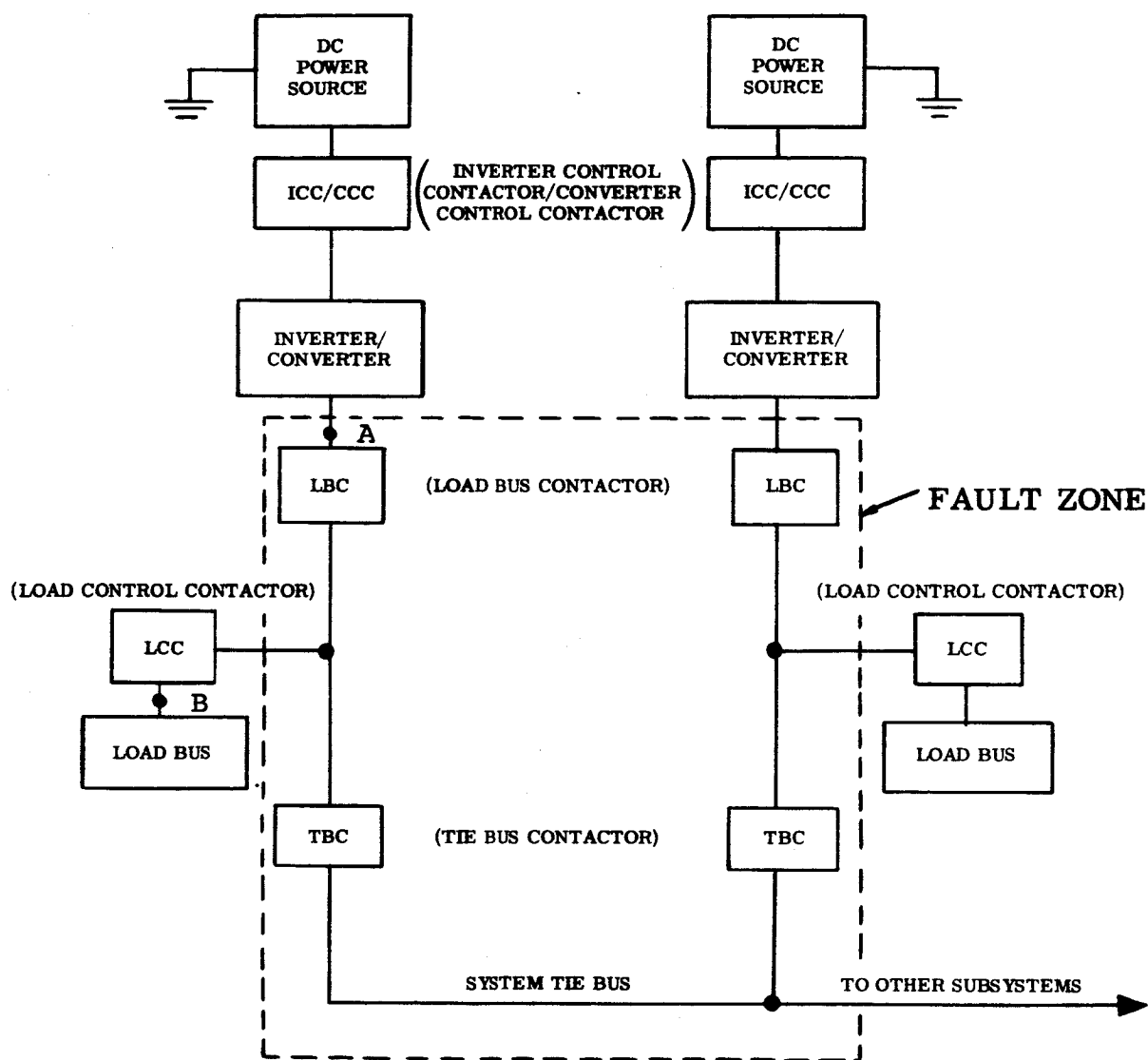


FIGURE III-1. Paralleled Inverter/Converter System Block Diagram

isolate the load from the subsystem. Therefore, the static contactor for this program will be designed for faults which will be limited to a zone from the output side of the inverter/converter to the system tie bus and up to the inverter/converter side of the LCC. This fault zone is shown enclosed by dotted lines in Figure III-1.

In the given two inverter/converter subsystem the power ratings of all the contactors considered are the same for parallel system operation as for single subsystem operation. Therefore, the static contactor power ratings for the LBC, LCC and the TBC, for this two parallel inverter/converter program, are equal and with the exception of the converter system TBC are identical to each other in their respective systems. The difference between the converter system TBC and the identical designs of the converter LBC and LCC is that the TBC must provide for bilateral power transfer while the LBC and LCC are designed for unilateral power transfer. Although all three of the contactors, on the converter output, will use the same electrical components, the TBC will use an additional silicon controlled rectifier contact, with its control circuitry, to permit the flow of power from the paralleled output bus to its associated subsystem load.

In the general case, the converter LBC should also provide bilateral power transfer, similar to its electromechanical counterpart, for fault clearing such as point A in Figure III-1. The present converter system differential protection circuit sensitivity however, dictates that the LBC should be unilateral to provide the desired system isolation for faults which occur at this location. Unilateral power transfer was provided with the mechanical contactor, for purposes of expediency, with a series blocking diode in the power circuit. With unilateral power transfer provided by the static LBC, the series blocking diode can be removed.

B. VOLTAGE AND CURRENT SPECIFICATIONS

The inverter/converter normal system voltages and currents and the system abnormal currents which the static contactors must withstand and open are shown in Tables III-1 and III-2. The design philosophy regarding the silicon controlled rectifier contact current is to provide a steady state capability of two times rated inverter/converter system current and 250 percent short-circuit current. The contactor design selection for a short-circuit capability of 250 percent, with fault times in excess of those necessary for integrated system protection, is compatible with the inverter/converter steady-state current design limitation of 150 percent.

The controlled rectifier contact voltage will be rated for a minimum of two times the highest voltage it is likely to see during operation.

**TABLE III-1. Converter System Static Contactor
Current and Voltage Specification**

	<u>CCC</u>	<u>LBC</u>	<u>TBC</u>	<u>LCC</u>
System Rated Voltage (volts, avg.)	28±2	153±5	153±5	153±5
System Rated Current (amps., avg.)	40 (a)	4.9	4.9	4.9
Normal Overload Current, 125% 5 Minutes (amps., avg.)	50	6.13	6.13	6.13
Maximum Short Circuit Current Steady State, 150% (amps., avg.)	60	7.35	7.35	7.35
Maximum Duration Short Circuit Current (milliseconds)	600	600	175	----
Maximum Peak Transient Current (amps.)	312 (b)	24 (b)	24 (b)	24 (b)
Design-System Rated Current, 200% (amps. avg.)	80	9.8	9.8	9.8
Design-Short Circuit Current, Steady State, 250% (amps., avg.)	100	12.3	12.3	12.3
Design-Short Circuit Time (milliseconds)	1000	1000	1000	1000

(a) - This value taken at 26 volts input from Parallel Inverter and Converter Operation and Improvements in Transformers Contract NAS3-2792, Third Quarterly, Figure 30.

(b) - These values calculated from isolated converter system fault test oscillograms with direct line to ground faults in converter output.

**TABLE III-2. Inverter System Static Contactor
Current and Voltage Specification**

	<u>ICC</u> (a)	<u>LBC</u>	<u>TBC</u>	<u>LCC</u>
System Rated Voltage (volts, L-N, rms, 400 cps)	28±2	115±6	115±6	115±6
System Rated Current (amps, line, rms, 400 cps)	40	2.18	2.18	2.18
Normal Overload Current, 125% 5 minutes (amps., rms)	50	2.73	2.73	2.73
Maximum Short Circuit Current Steady State, 150% (amps., rms)	60	3.27	3.27	3.27
Maximum Duration Short Circuit Current (milliseconds)	215	215	175	----
Maximum Peak Transient Current (amps.)	312 (b)	(c)	(c)	(c)
Design-System Rated Current, 200% (amps., rms)	80	4.36	4.36	4.36
Design-Short Circuit Current, Steady State, 250% (amps., rms)	100	5.45	5.45	5.45
Design-Short Circuit Time (milliseconds)	1000	500	500	500

- (a) - The ICC requirements are identical to those for the CCC given in Table III-1. The currents and voltages for the ICC therefore, are average values with exception of the transient current which is a peak value.
- (b) - This value calculated from isolated converter system fault test oscillogram with direct line to ground fault in converter output.
- (c) - Test data not presently available. To be determined during future system tests.

SECTION IV

STATIC CONTACTOR DESIGN

Fundamentally the static contactor is made up of two parts, a power circuit and a control circuit. The power circuit, consisting of a switching device, permits the conduction of current from the source to the load when activated. The control circuit provides the necessary turn-on and turn-off requirements upon response from input signals. The input signals are provided when the following conditions exist:

1. Current is demanded at the load
2. Current is no longer required by the load, and
3. When abnormal electric power system operation prevails in a protected zone.

Although other electrical components are capable of a switching action, the contactor designs for this program have been limited to the silicon controlled rectifier. The following discussion presents the characteristics of this device.

A. CHARACTERISTICS OF POWER SWITCHING DEVICE

The qualities exhibited by the silicon controlled rectifier include extremely high forward and reverse blocking voltages which are in excess of 1300 volts with typical peak leakage currents of 2 microamperes to 10 milliamperes at a junction temperature of 25°C. The higher voltage rated controlled rectifier devices have lower leakage currents for a given forward current rating.

Voltage transients in the forward direction, and to some extent in the reverse direction, that exceed the rated blocking voltage are protected by the inherent characteristics of the device. Overvoltage in the forward direction will cause the device to break down into the conducting state, and if the rate of change of current and peak current is limited, the device suffers no ill effects. These quantities can be controlled in practical circuits. The circuit, however, must withstand this breakdown conduction.

The main destruction mechanism of a controlled rectifier is excessive current density in the forward direction. This is tempered with the relatively high short time overcurrent ratings of the device, typically 5 to 8 times the peak rated repetitive current rating of the device.

The silicon controlled rectifier is capable of being turned on with a 1 to 10 microsecond pulse. Turnoff time is 5 to 25 microseconds. The device has a 1 to 1.5 volt forward drop and a maximum junction temperature rating of 125°C.

The major disadvantage of the controlled rectifier is its recovery mechanism. The device is controlled by its gate lead when it is required to switch from a blocking to conducting state, but the gate lead no longer has control when the controlled rectifier is conducting.

The direct current contactors of this application must use forced commutation means to regain the blocking state while the alternating current contactors can rely on natural commutation. The forced commutation process requires high surges of energy in the power circuits, as provided by reactive energy storage elements. Thus, the controlled rectifier turn off components tend to be large and bulky.

B. CONVERTER SYSTEM CONTACTOR CIRCUIT CONSIDERATIONS

The design of the converter system static contactors requires consideration of a direct current system only. The following is a discussion of the power circuit configurations investigated for this program.

1. D-C Static Contactor With Capacitor Turn-OFF

A fundamental contactor circuit which uses capacitor forced commutation turn off of the controlled rectifier contact is shown in Figure IV-1. The operation of this circuit is as follows. Supply voltage V is applied to the load by application of a turn-on signal from gate to cathode of silicon controlled rectifier SCR1. With SCR1 conducting, capacitor C is charged to the supply voltage, less the voltage drop across SCR1, through resistor R. The left plate of the capacitor is charged with a positive polarity. To turn SCR1 off, removing the voltage from across the load, SCR2 is turned on. This connects the negative side of capacitor C to the anode of SCR1. This reverse biases SCR1 momentarily resulting in turn off. Capacitor C now becomes charged to essentially supply voltage with a positive polarity on its right plate. Controlled rectifier SCR2 continues to conduct at minimum current through R. When SCR1 is turned on again, with a signal from gate to cathode, the circuit reverts to its original state with SCR2 turned off after being reverse biased by capacitor C.

The disadvantage of this circuit is that, momentarily, two times supply voltage is applied across the load when SCR1 is commutated. This is undesirable since twice the present voltage would be applied across the inverter switching transistors of the existing inverter/converter with this circuit used for the ICC/CCC.

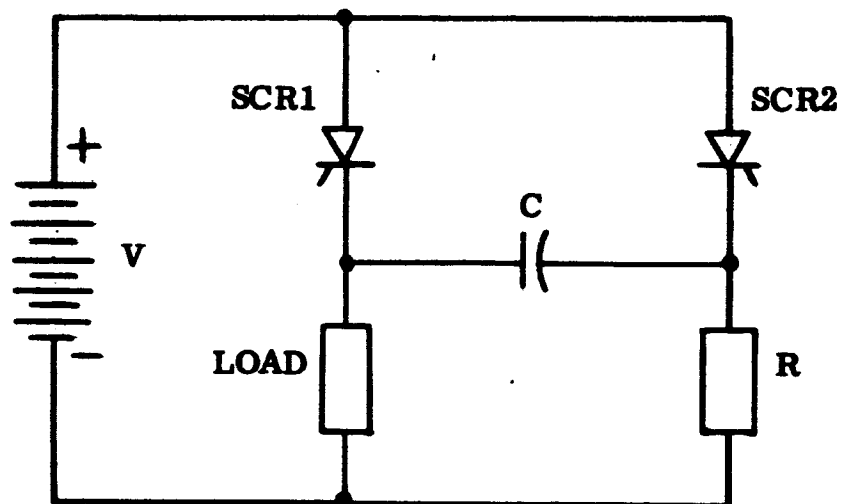


FIGURE IV-1. D-C Static Contactor With Capacitor Turn-Off

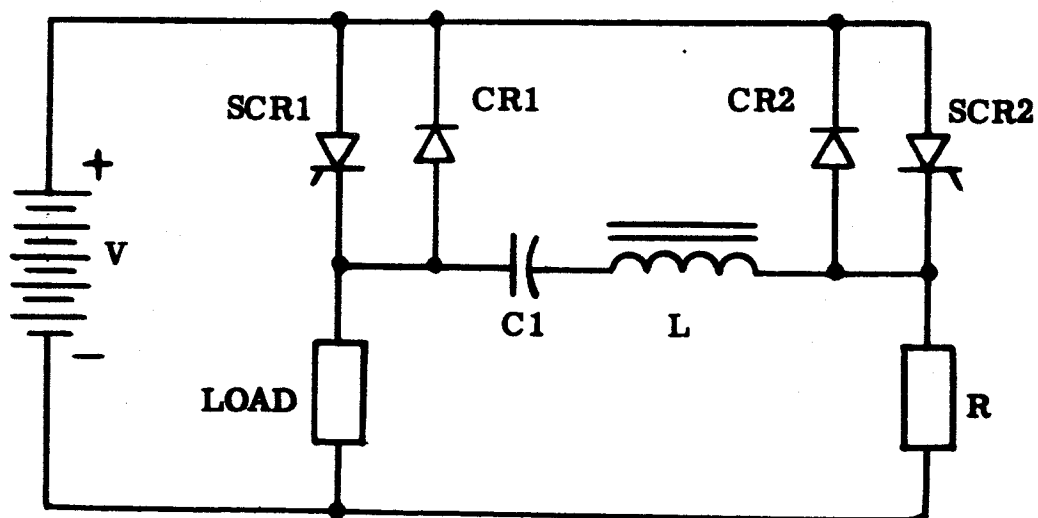


FIGURE IV-2. D-C Static Contactor With Resonant Circuit Turn-Off

2. D-C Static Contactor With Resonant Circuit Turn-Off

A contactor power circuit which eliminates the load voltage rise objection of Figure IV-1 is shown in Figure IV-2. With exception of the addition of inductor L and diodes CR1 and CR2, the circuit configuration of Figure IV-1 and IV-2 are identical.

The circuit operates as follows: With SCR1 conducting, voltage is applied to the load and capacitor C1 is charged to the supply voltage V less the voltage drop across SCR1. The left plate of the capacitor, therefore, is at a positive polarity. To turn SCR1 off, SCR2 is turned on. This provides a path for C1 to discharge resonantly through SCR1 or CR1, SCR2 and L. The discharge current is one alternation of a sine wave. Until the capacitor discharge sine wave current reaches the magnitude of the load current, the effect of the discharge is to reduce the current through SCR1. When the capacitor current reaches and exceeds the original value of SCR1 load current, the excess current flows through CR1, reverse biasing SCR1, turning it off. Capacitor C1 now completes its charge to the supply voltage, less the SCR2 voltage drop, with a positive polarity on the right plate. The capacitor cannot discharge again because CR1 and SCR1 are blocking. Controlled rectifier SCR2 continues to conduct through resistor R. To revert to the original state, with SCR1 conducting, SCR1 is turned on and capacitor C1 discharges through L, SCR2 or CR2, and SCR1. This turns SCR2 off, and SCR1 conducts current to the load.

The objection to this circuit, as presented, is its inability to open when closed onto a short circuit. When a system short-circuit fault occurs, the converter output voltage will droop and essentially attains a zero value because of the current limiting characteristic of the inverter/converter. Should this fault persist after the contactor has been opened the first time, the contactor will not open again if it is closed. The reason for this is that with the immediate depression of the converter output voltage to essentially zero, the capacitor C1 cannot become charged. Although SCR2 can be turned on, by the appropriate signal, SCR1 cannot be turned off and therefore will continue to conduct until it or some other system equipment is destroyed by fault current.

Two contactor circuits capable of overcoming this discrepancy are discussed as follows.

3. D-C Static Contactor With Resonant Circuit Turn-Off Capacitor Initially Charged

Contactor circuits of Figure IV-3 and Figure IV-4 provide a means of initially charging commutating capacitor C1 prior to the time SCR1 is turned on. Figure IV-3 is the same as Figure IV-2 with the exception that SCR3 has been added to the power circuit in series with SCR1 and

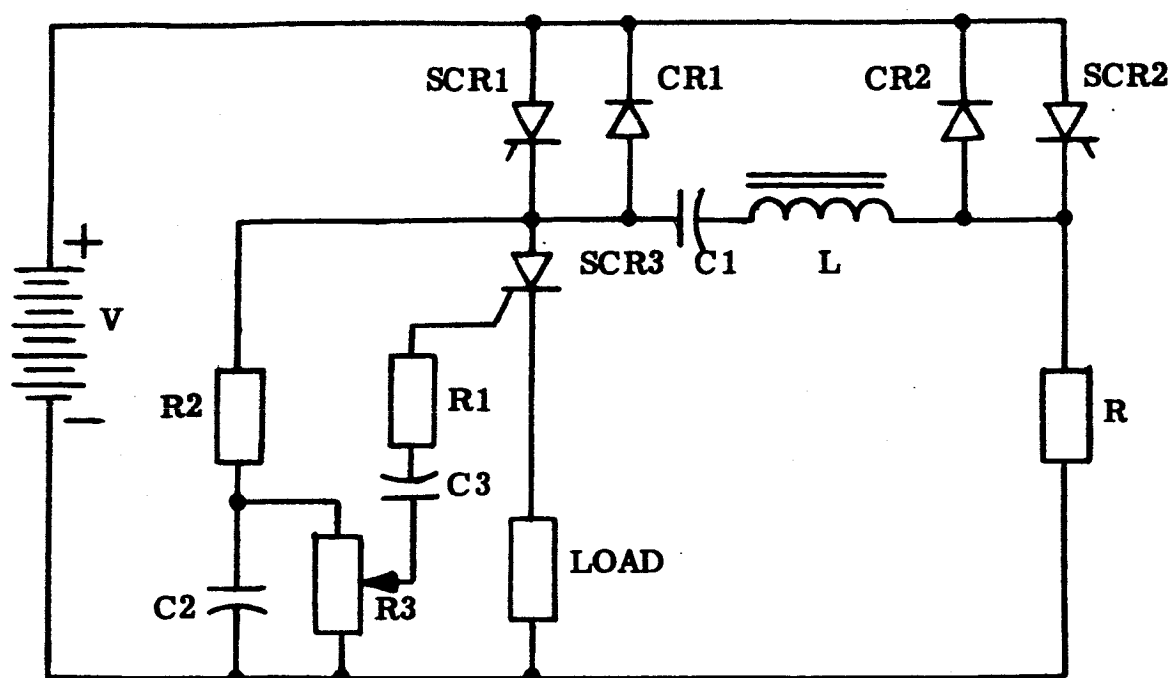


FIGURE IV-3. D-C Static Contactor With Resonant Circuit Turn-Off
Capacitor Initially Charged

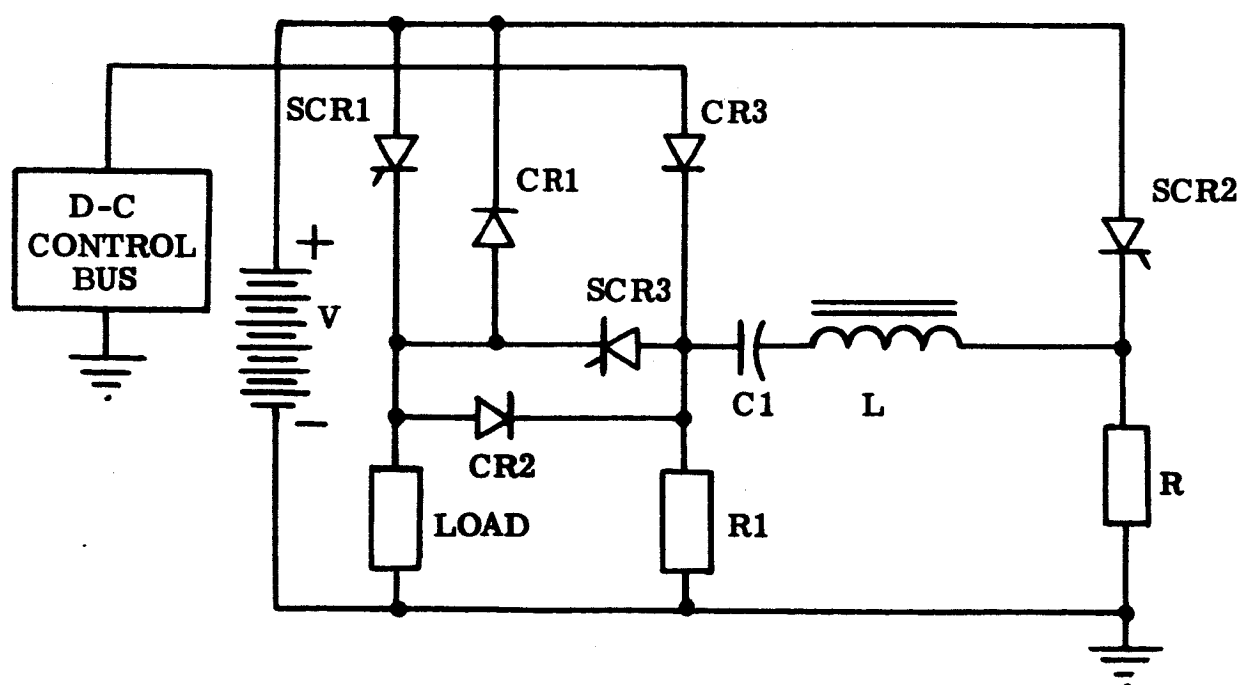


FIGURE IV-4. D-C Static Contactor With Resonant Circuit Turn-Off
Capacitor Initially Charged

the load. When SCR1 is turned on, it will charge capacitor C1 through L and R. After a time delay, which is a function of R2 and C2, SCR3 turns on applying voltage to the load. Controlled rectifier SCR1 turn-off occurs as discussed for the circuit of Figure IV-2. Controlled rectifier SCR3 turns off naturally when the current through it decreases below the holding current because of SCR1 turning off.

The disadvantage of this circuit is the increase in steady state power losses to twice that of Figure IV-2. For this reason, this circuit will not be discussed further.

The power circuit selected for the ICC/CCC, shown in Figure IV-4, is basically that of Figure IV-2. Its operation is as follows. With SCR2 and SCR3 off, capacitor C1 is charged through CR3, L, and R from the d-c control bus when a momentary turn-on signal is provided for SCR1. Capacitor C1 completes its charge, with its left plate positive, before SCR1 is turned on because of a time delay in the SCR1 gate to cathode control circuit. If the contactor has not closed on a short circuit, the voltage across the load will be normal and the initial charge on capacitor C1 will be maintained by conduction of diode CR2. Without diode CR2 capacitor C1 could, with extensive load operation, lose its initial charge through self leakage.

To turn SCR1 off, because of a fault or normal system shutdown, turn-on signals are provided simultaneously to SCR2 and SCR3. The turn-off operation is then the same as discussed for Figure IV-2. Controlled rectifier SCR2 continues to conduct minimum current through R. Controlled rectifier SCR3 turns off naturally after C1 charging current ceases. The capacitor is now charged with its right plate at a positive polarity. This charge is maintained through the high resistance path provided by R1. To return to the original condition, with SCR1 conducting, SCR1 is turned on. Prior to SCR1 turning on, a d-c control bus voltage of 26 to 30 volts is connected in series, through CR3, with C1, L and R. The instantaneous potential at the cathode of SCR2 then becomes the sum of the control bus voltage and the voltage across capacitor C1. This reverse biases SCR2, resulting in turn-off.

C. CONVERTER SYSTEM CONTACTOR DESCRIPTION

The complete circuit schematic for the ICC/CCC, is shown in Figure IV-5. Free wheeling diode CR4 has been added across the load side terminals L1 and L2 of the contactor to provide a path for circulating inductive currents when the contactor is opened. The electrical component and circuit selection for the LBC and LCC will be identical to each other but will not be identical to the ICC/CCC. The control circuit components for the LBC and LCC may be identical to the ICC/CCC; the power circuit parts will differ, however, because of the larger current rating of the ICC/CCC and the difference in

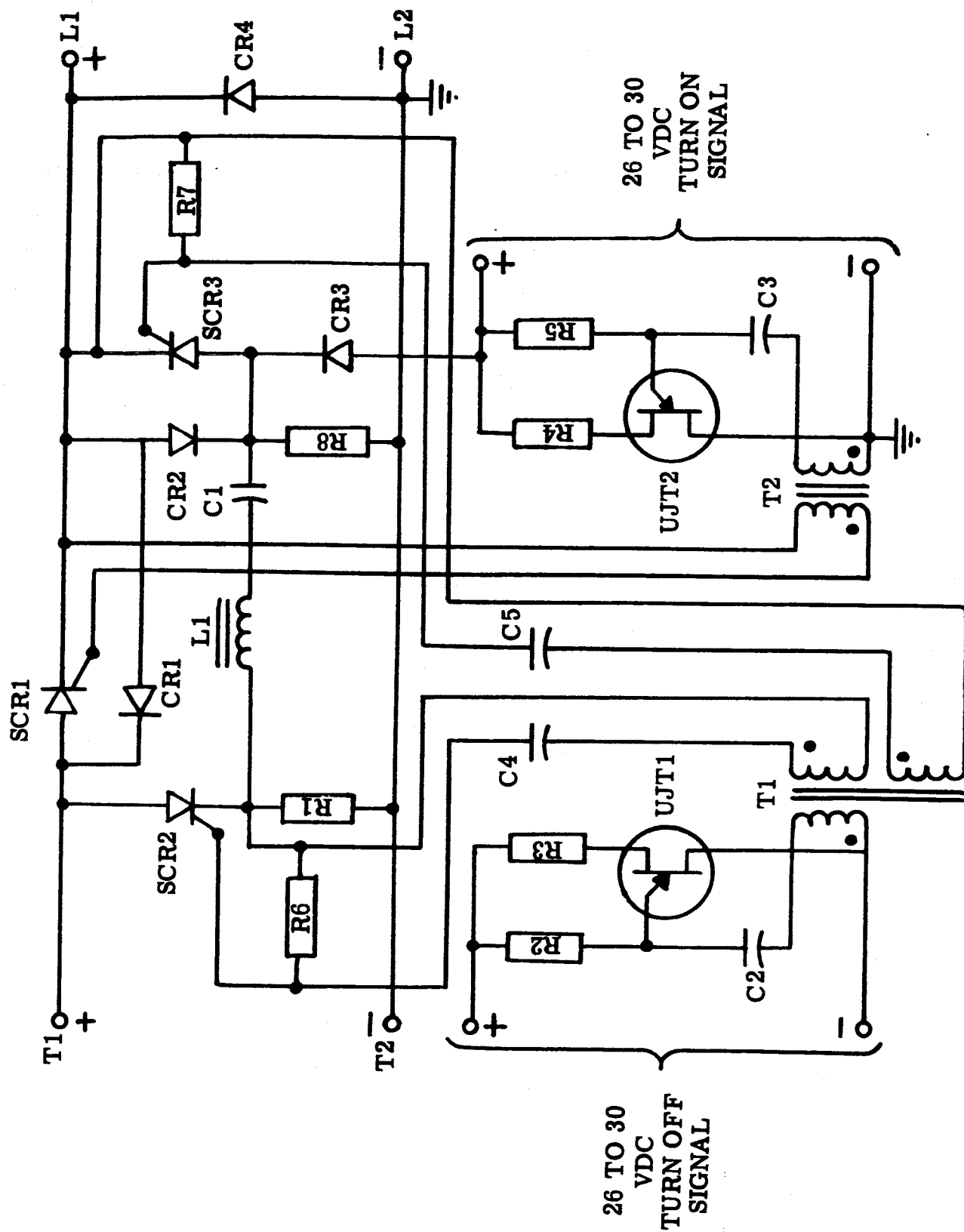


FIGURE IV-5. Converter System Static Contactor Circuit

circuit configuration. The TBC, providing bilateral current conduction, will use the electrical parts of the LBC and LCC.

Since the operation of the power circuit was described in Section IV. B. 3., the following discussion will be limited to the description of the control circuits. In addition, because the control circuits for turn-on and turn-off are basically the same, only the turn-on circuit will be discussed. The principal difference between the two control circuits is in the pulse transformers which show a single secondary for the turn-on configuration and two isolated secondary windings for the turn-off configuration.

The control circuits consist of unijunction transistors operating in a relaxation oscillator mode. With the input to the turn-on circuit momentarily connected to the direct voltage control bus, capacitor C3 starts to charge through resistor R5. After a time delay, which has permitted C1 to become charged through diode CR3, the voltage across C3 reaches a potential which causes the unijunction transistor UJT2 to conduct through the emitter to base 1 circuit. This provides a pulse to transformer T2 which causes SCR1 to conduct. The controlled rectifier gate pulse continues until the discharge of capacitor C3 reaches a reduced voltage which causes UJT2 to cut off. Capacitor C3 is then charged again to a potential which causes UJT2 to conduct. The cycle is repeated and will continue as long as an input signal is provided. When the control circuit is initially energized, the current through the pulse transformer is in a direction which places a reverse voltage on the gate to cathode of SCR1.

The design of the Inverter Control Contactor/Converter Control Contactor (ICC/CCC) has been completed according to the circuit configuration of Figure IV-5. The parts list for this design is presented in Table IV-1.

D. INVERTER SYSTEM CONTACTOR CIRCUIT CONSIDERATIONS

There are several possible power contact arrangements which can be used to make an alternating current static contactor with controlled rectifiers alone or in combination with diodes. Figure IV-6 illustrates these configurations showing a single phase arrangement only for each representation. The selected circuit will be made up in a three phase configuration for the contactors of this program.

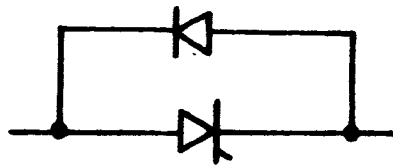
The circuits of Figure IV-6 (a), (c), and (d) offer inverse voltage protection to the controlled rectifiers inherently through the use of diodes. In the forward direction voltage transients of sufficient magnitude could cause forward random or intermittent breakdown conduction unless adequately protected by auxiliary components or the controlled rectifiers are selected with forward voltage breakdown ratings in excess of the transients. On the other hand, if the voltage and associated current transients are not in excess of the maximum SCR ratings, and if the load circuit can withstand the

TABLE IV-1. Parts List for Static ICC/CCC

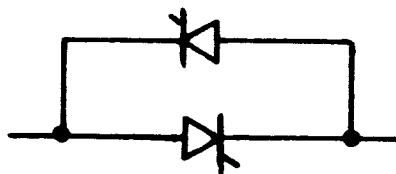
<u>Identification</u>	<u>Part Number</u>	<u>Qty/Contactor</u>
Resistors		
R1 100 ohms $\pm 1/2\%$, 25W	19C8220-21	1
R2, 8 10K ohms $\pm 5\%$, 0.5W	909C790-10	2
R3, 4 2 in parallel-200 ohm $\pm 2\%$, 2W	19C7558-4	4
R5 51K ohms $\pm 5\%$, 0.5W	909C790-38	1
R6, 7 1K ohm	909C790-91	2
Capacitors		
C1 100 μ fd, 200 VDC	G.E. Cat. No. 28F1103	1
C2 0.22 μ fd $\pm 5\%$, 200 VDC	908D109-18	1
C3 1.0 μ fd $\pm 5\%$, 200 VDC	908C109-2	1
C4, 5 0.1 μ fd $\pm 5\%$, 200 VDC	908D109-14	2
Diodes		
CR1, 4 12A, 100V	Type 1N1200A	1
CR2, 3 1.6A, 200V	Type 1N1220A	2
Unijunction Transistors		
UJT1, 2 2N2646	909C808-7	2

TABLE IV-1. Parts List for Static ICC/CCC (Cont.)

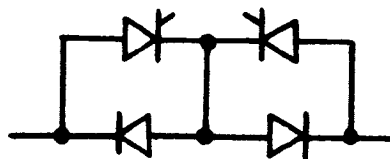
<u>Identification</u>	<u>Part Number</u>	<u>Qty/Contactor</u>
Silicon Controlled Rectifiers		
SCR1 110A RMS, 100V	G.E. Type C55A	1
SCR2, SCR3 35A, RMS, 150V	Type 2N684	2
Pulse Transformers		
T1	Sprague 35ZM930	1
T2	Pulse Engrg. Inc. 2231	1
Inductor		
L1 3 μ h	(W) EM K5-0001	1



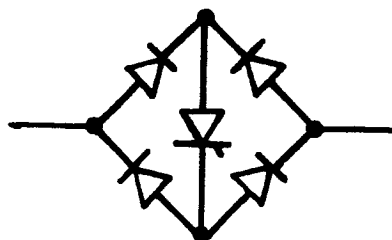
(a) SCR With Paralleled Diode



(b) SCR's Paralleled Back-to-Back



(c) SCR's In Series Opposition With Paralleled Diodes



(d) SCR Within Diode Bridge

FIGURE IV-6. Controlled Rectifier A-C Switching Circuits
WAED65. 50E-23

breakdown conduction transient, the controlled rectifiers will not be damaged by this conduction and circuit operation should not be impaired. The disadvantage of the configurations of Figure IV-6(c) and (d) is the multiple series forward voltage drop of the two and three semiconductor devices, respectively, with their associated power losses. These circuits, therefore, will not be considered for this program.

The circuit configuration of Figure IV-6(a), although offering the advantage of reduced SCR gate control complexity, is not applicable to loads with a grounded neutral since half wave rectification would result. Therefore, the controlled rectifier contact arrangement to be used in this application is that of Figure IV-6(b). With currently available controlled rectifier reverse voltage ratings, inverse voltage transients should not be a problem with this selected circuit.

The use of controlled rectifiers in alternating current applications, unlike that of application in direct current circuits, does not require energy storage turn-off components. Controlled rectifiers used in an alternating current circuit will cease to conduct naturally on the first current zero after the removal of the gate to cathode signal. It therefore becomes necessary for the control circuit to provide a gate signal to the controlled rectifiers each time the alternating phase sequence provides a condition with the anode potential more positive than the cathode. To eliminate the possibility of phase control, it also becomes necessary for the gate signal to be available as soon as the anode polarity starts positive. This signal must be of sufficient duration to permit the anode current to become greater than the SCR holding current. This condition must be provided with inductive loads where the current lags its respective voltage.

E. INVERTER SYSTEM CONTACTOR DESCRIPTION

The direct current ICC/CCC, which is common to both the converter and inverter systems, was described in Section IV.C. and therefore will not be discussed further in this section.

The complete circuit schematic for the alternating current LBC, LCC, and TBC is shown in Figure IV-7. These contactors will use the same electrical components since their power ratings are identical. The operation of this circuit is as follows.

The power circuit static contacts consisting of controlled rectifiers SCR1 through SCR6 are connected back-to-back in pairs, in series with the three power lines between the power source and the load. With the d-c control bus energized with a potential of 22 to 30 volts, a regulated voltage of 15 volts is provided by resistor R31 and zener diode CR21. This regulated voltage is applied to a Royer Oscillator. The controlled rectifier gate drives are supplied by this free running oscillator which provides electrical isolation between the contactor control and power circuits. The oscillator, which has

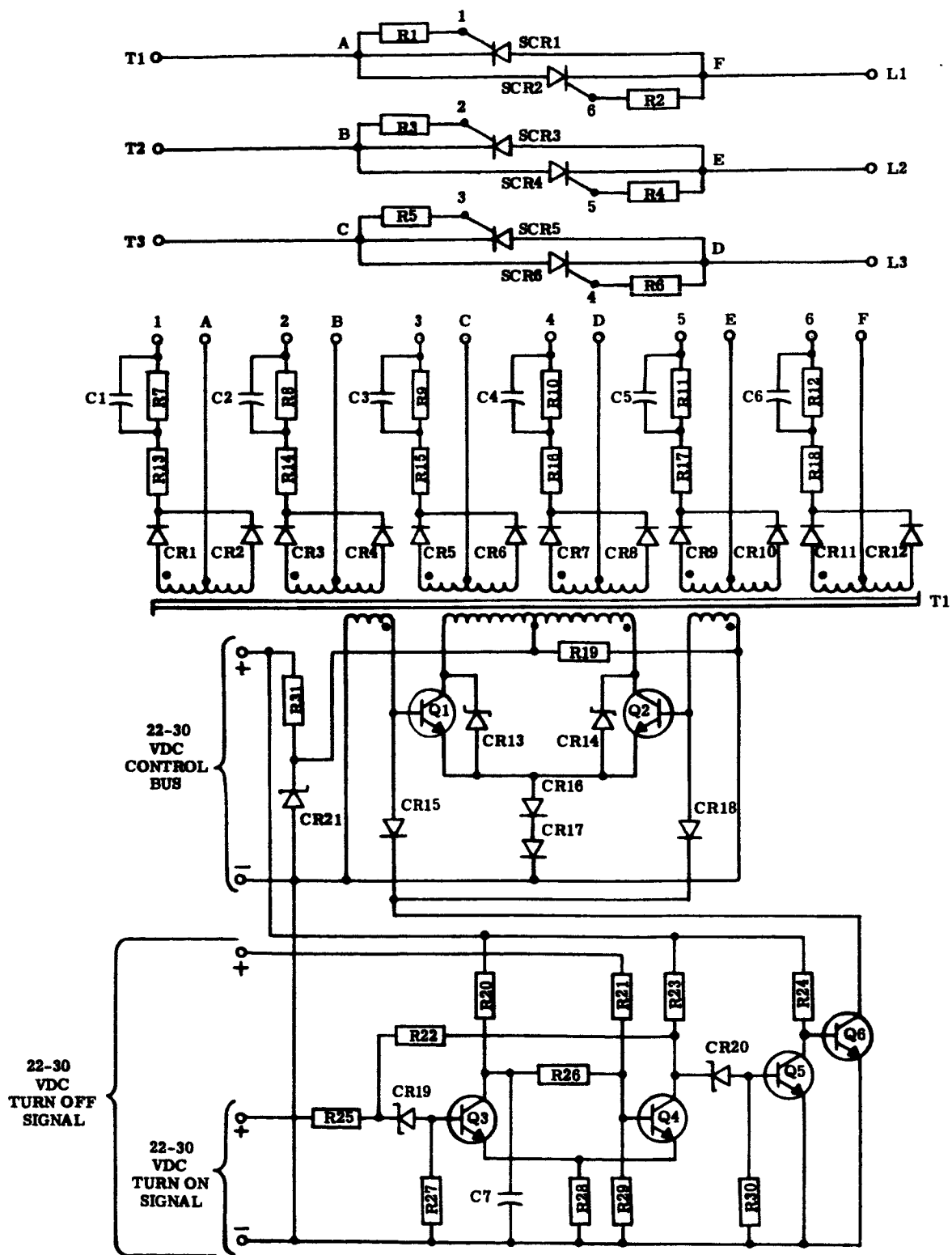


FIGURE IV-7. Alternating Current Inverter System Static Contactor Circuit

been described in the literature, is made up of transistors Q1 and Q2, saturating transformer T1, voltage spike suppression diodes CR13 and CR14, feedback winding diodes CR16 and CR17, and starting resistor R19.

Isolated signals, resulting from the rectified oscillator square waves, gate the controlled rectifiers from six separate windings using rectifier diodes CR1 through CR12, current limiting resistors R7 through R18, and wave form shaping capacitors C1 through C6. With the oscillator running and line voltage applied, the static contactor will be closed. When the oscillator is shut down, gate signals are not provided to the controlled rectifiers SCR1 through SCR6 therefore, conduction ceases, line current is blocked, and the contactor is open.

The control logic for the contactors consists of a bistable Schmitt trigger which is composed of resistors R20, R23, R26, R28, and R29, capacitor C7 and transistors Q3 and Q4. When control bus voltage is first applied to the contactor, transistor Q4 conducts through resistors R23 and R28, after being forward biased from base to emitter by a voltage provided by resistors R20, R26 and R29. With Q4 on transistor Q5 will be off, and transistor Q6 will be on. Transistor Q6 with diodes CR15 and CR18 short circuit CR16 and CR17 and the base to emitters of the oscillator transistors Q1 and Q2. This causes the oscillator to remain in a shutdown condition and consequently the contactor is open.

When a turn-on signal is applied, transistor Q3 is forward biased through resistors R25 and R27 and zener diode CR19. With transistor Q3 conducting, Q4 is turned off. This results in Q5 turning on since it is forward biased through resistors R23 and R30 and zener diode CR20; consequently Q6 turns off, causing the oscillator to run and the contactor to close. Since the turn-on signal is applied momentarily, feedback resistor R22 is provided to maintain transistor Q3 of the Schmitt trigger conducting.

When a turn-off signal is applied, because of normal system shutdown or a system fault, transistor Q4 turns on after being forward biased through resistors R21 and R29. Transistor Q3 and Q5 will turn off and Q6 is turned on since it becomes forward biased from base to emitter through resistor R24. With Q6 conducting, oscillator operation ceases and the contactor is open. The contactor will remain opened until it is closed by a turn-on signal.

The design of the inverter system alternating current LBC, LCC, and TBC has been completed according to the circuit configuration of Figure IV-7. The parts list for these designs is presented in Table IV-2.

TABLE IV-2. Parts List for Inverter System Static LBC, LCC, and TBC

<u>Identification</u>		<u>Part Number</u>	<u>Qty/ Contactor</u>
Resistors			
R1, 2, 3, 4, 5, 6	100 ohm \pm 5%, 0.5W	909C790-1	6
R7, 8, 9, 10, 11, 12	2 in Ser. 15 \pm 5%, 0.5W	909C790-15	12
R13, 14, 15, 16, 17, 18	10 ohm \pm 5%, 0.5W	909C790-66	6
R19	100 ohm \pm 1%, 5W	21C9972-9	1
R20	20 K \pm 5%, 0.5W	909C790-37	1
R21	43 K \pm 5%, 0.5W	909C790-44	1
R22	41 K $\left\{ \begin{array}{l} 39K \pm 5\%, 0.5W \\ 2 K \pm 5\%, 0.5W \end{array} \right.$	909C790-12	1
		909C790-20	1
R23	10 K \pm 5%, 0.5W	909C790-10	1
R24	2.6 K $\left\{ \begin{array}{l} 1K \pm 10\%, 0.5W \\ 1.6K \pm 5\%, 0.5W \end{array} \right.$	909C790-91	1
		909C790-96	1
R25	51 K \pm 5%, 0.5W	909C790-38	1
R26	24 K \pm 5%, 0.5W	909C790-23	1
R27	47 K \pm 5%, 0.5W	909C790-40	1
R28	470 ohm \pm 5%, 0.5W	909C790-65	1
R29	13 K \pm 5%, 0.5W	909C790-25	1
R30	47 K \pm 5%, 0.5W	909C790-40	1
R31	10 ohm \pm 1%, 50W	19C8414-15	1
Capacitors			
C1, 2, 3, 4, 5, 6	0.5 μ fd \pm 5%, 200 VDC	908D088-21	6
C7	0.22 μ fd \pm 10%, 200 VDC	908D088-28	1

TABLE IV-2. Parts List for Inverter System Static LBC, LCC, and TBC (Cont.)

<u>Identification</u>		<u>Part Number</u>	<u>Qty/ Contactor</u>
Diodes			
CR1 thru CR12	IN645, 400 Ma at 25°C, 225 V	906D976-1	12
CR13, 14	33V, 3W	Unitrode Type UZ733	2
CR15, CR18	IN645, 400 Ma at 25°C, 225V	906D976-1	2
CR16, CR17	IN1202A, 12A, 200V	906D609-10	2
CR19, CR20	8.2V + 5% at 50 μ a, 400 MW	938D392-7	2
CR21	15V, 50W	Motorola 50M15Z	1
Transistors			
Q1, Q2	2N3442, 10A, 140V	929A091-1	2
Q3, 4, 5, 6	2N2102, 1A, 80V	914F298-2	4
Silicon Controlled Rectifiers			
SCR1 thru SCR6	35A, RMS, 800V	Type 2N692	6
Transformer		(W) T1	1

DISTRIBUTION LIST

Eighth Quarterly Technical Report

One copy to be sent to each addressee, unless otherwise indicated. Note that more than one addressee may be shown for the same address.

National Aeronautics & Space Administration
Lewis Research Center
21000 Brookpark Road
Cleveland, Ohio (44135)

Attn: B. Lubarsky MS 500-201	(1)
George Mandal MS 5-5	(1)
J. P. Quitter MS 500-109	(1)
C. S. Corcoran, Jr. MS 500-201	(1)
E. A. Koutnik MS 500-201	(1)
A. C. Herr MS 77-1	(1)
F. Gourash MS 500-201	(3)
Alice Dill MS 5-5	(1)
Dorothy Morris MS 3-7	(2)
John E. Dilley MS 500-309	(1)
V. R. Lalli MS 500-203	(1)
R. R. Miller MS 500-202	(1)
H. A. Shumaker MS 500-201	(1)
Bernard L. Sater MS 54-3	(1)
Russell Shattuck MS 21-5	(1)
J. J. Weber MS 3-19	(1)
V. F. Hlavin MS 3-14 -- (Final and Topical Reports Only).	
---*---	

National Aeronautics & Space Administration
Goddard Space Flight Center
Greenbelt, Maryland

Attn: F. C. Yagerhofer	(1)
Joseph M. Sherfey	(1)
William M. Tucker	(1)
E. R. Pasciutti	(1)
W. R. Cherry	(1)
---*---	

DISTRIBUTION LIST (CON'T.)

National Aeronautics & Space Administration
Marshall Space Flight Center
Huntsville, Alabama

Attn: James C. Taylor (M-ASTR-R) (1)
Richard Boehme (M-ASTR-EC) (1)

---*---

National Aeronautics & Space Administration
Manned Spacecraft Center
Houston, Texas

Attn: A. B. Eickmeir (SEDD) (1)
F. Eastman (1)

---*---

National Aeronautics & Space Administration
4th and Maryland Avenue, S. W.
Washington 25, D. C. (20546)

Attn: James R. Miles, Sr. (SL) (1)
P. T. Maxwell (RNW) (1)
A. M. Greg Andrus (ST-2) (1)
James J. Lynch (RNP) (1)
M. J. Krasnican (MAT) (1)

---*---

Naval Research Laboratory
Washington 25, D. C.

Attn: B. J. Wilson (Code 5230) (1)

---*---

Bureau of Naval Weapons
Department of the Navy
Washington 25, D. C. (20546)

Attn: Milton Knight (Code RAEE-511) (1)

---*---

Jet Propulsion Laboratory
4800 Oak Grove Drive
Pasadena, California

Attn: Aldon Schloss (1)

---*---

DISTRIBUTION LIST (CONT.)

**Diamond Ordnance Fuze Laboratories
Connecticut Avenue & Van Ness Street, N. W.
Washington, D. C.**

Attn: R. B. Goodrich (Branch 940) (1)
--*--

**U. S. Army Research & Development Laboratory
Energy Conversion Branch
Fort Monmouth, New Jersey**

Attn: H. J. Byrnes (SIGRA/SL-PSP) (1)
--*--

**Engineers Research & Development Laboratory
Electrical Power Branch
Fort Belvoir, Virginia**

Attn: Ralph E. Hopkins (1)
--*--

**Aeronautical Systems Division
Wright-Patterson Air Force Base
Dayton, Ohio**

Attn: Capt. W. E. Dudley-ASRMFP-3 (1)
Don Mortell (APIP-3) (1)
--*--

**University of Pennsylvania
Power Information Center
Moore School Building
200 South 33rd Street
Philadelphia 4, Pennsylvania (1)**
--*--

**Duke University
College of Engineering
Department of Electrical Engineering
Durham, North Carolina**

Attn: T. G. Wilson (1)
--*--

DISTRIBUTION LIST (CON'T.)

**National Aeronautics & Space Administration
Scientific and Technical Information Facility
Post Office Box 33
College Park, Maryland**

Attn: NASA Representative

(1)

--*--

**AiResearch Division
Garrett Corporation
Cleveland Office
20545 Center Ridge Road
Cleveland 16, Ohio**

Attn: W. K. Thorson

(1)

--*--

**Westinghouse Electric Corporation
Aerospace Electrical Division
Lima, Ohio**

Attn: Address Kernick

(1)

--*--

**General Electric Company
Specialty Control Dept.
Waynesboro, Virginia**

Attn: Mr. Lloyd Saunders

(1)

--*--

**Lear-Siegler, Incorporated
Power Equipment Division
Post Office Box 6719
Cleveland 1, Ohio**

Attn: Mr. Robert Saslaw

(2)

--*--

**The Bendix Corporation
Bendix Systems Division
Ann Arbor, Michigan**

Attn: K. A. More

(1)

--*--

DISTRIBUTION LIST (CON'T.)

**The Bendix Corporation
Red Bank Division
1900 Hulman Building
Dayton, Ohio**

**Attn: R. N. Earnshaw
---*---**

(1)

**VARO, Incorporated
2201 Walnut Street
Garland, Texas**

**Attn: J. H. Jordan
---*---**

(1)

**Wright - Patterson Air Force Base
AFAPL (APIP-30)
Ohio**

**Attn: Paul R. Bertheaud
---*---**

(1)

**G. M. Defense Research Lab.
General Motors Corporation
Santa Barbara, California**

**Attn: T. M. Corry
---*---**

(1)

**General Dynamics Astronautics
Dept. 963-2
5001 Kearney Villa Road
San Diego, California**

**Attn: R. Schaelchlin
---*---**

(1)

**University of Virginia
Thornton Hall
Charlottesville, Virginia**

**Attn: A. R. Kuhlthau, Director,
Research Laboratories for
the Engineering Sciences
---*---**

(1)

DISTRIBUTION LIST (CON'T.)

**Prestolite
Toledo, Ohio**

**Attn: J. F. Caney
---*---**

(1)

**General Electric Company
Space Power and Propulsion System
Bldg. 701 - Room 120 (N8)
Evendale, Ohio**

**Attn: Russell N. Edwards
---*---**

(2)

**Thompson Ramo Wooldridge, Inc.
7209 Platt Ave.
Cleveland, Ohio**

**Attn: J. E. Murray
---*---**

(1)

**The Martin Company
Post Office Box 988
Baltimore, Maryland (21203)**

**Attn: F. C. McGintey MS 844
---*---**

(1)

**Solid State Controls, Inc.
8580 North High Street
Worthington, Ohio (43085)**

**Attn: Lee Garrett
---*---**

(1)

**Hamilton Standard Division
United Aircraft Corporation
Broadbrook, Connecticut (06016)**

**Attn: Ernest Levy
---*---**

(1)

DISTRIBUTION LIST (CONT.)

Department of the Navy
Bureau of Ships
Washington, D. C. (20546)

Attn: Chief, Bureau of Ships
9620/2-1
Ser. 660K-4866
--*--

(1)

U. S. Army Engineer Research & Development Lab.
Fort Belvoir, Virginia (22066)

Attn: SMCFB-EB
--*--

(1)

Mrs. Ruth R. McCullough, Supervisor
Technical Information Center
Westinghouse Electric Corporation
Friendship International Airport
Box 1693
Baltimore, Maryland (21203)
--*--

(1)

Electro-Optical Systems
300 North Halstead Street
Pasadena, California (91107)

Attn: Jack Davis
--*--

(1)

Aerospace Corporation
Post Office Box 95085
Los Angeles, California (90045)

Attn: Library Technical Documents Group
--*--

(2)

Lockheed Missiles and Space Company
Medium Space Vehicles Programs
Dept. 91-35, Bldg. 519
Post Office Box 504
Sunnyvale, California (94088)

Attn: J. A. Mascovich
--*--

(1)

DISTRIBUTION LIST (CON'T.)

Lockheed Missiles and Space Company
Dept. 50/52 Bldg. 102
Post Office Box 504
Sunnyvale, California (94088)

(1)

--*--

AiResearch Manufacturing Company
Post Office Box 5217
Phoenix, Arizona (85010)

Attn: Mrs. S. F. Makenzie, Librarian

(1)

--*--

Lear Siegler, Inc.
632 Tinton Avenue
New York, New York, (10055)

Attn: J. Rambusek

(1)

--*--

Gulton Industries, Inc.
Engineered Magnetics Division
13041 Cerise Avenue
Hawthorne, California (90250)

Attn: Burton J. McComb

(1)

--*--

NASA-Electronics Research Center
575 Technology Lane
Cambridge, Massachusetts (02139)

Attn: Dr. Fred L. Niemann
Albert Canal

(1)

(1)

--*--

NASA-Ames Research Center
Moffett Field, California (94035)

Attn: James Swain

(1)

--*--

DISTRIBUTION LIST (CON'T.)

**The Garrett Corporation
333 West First Street
Dayton, Ohio (45402)**

Attn: Don Elbert

--*--

(1)

**AVCO-Everett Research Laboratory
2385 Revere Beach Parkway
Everett, Massachusetts, (02149)**

Attn: Ann Marie Napolitana, Library Assistant

--*--

(1)